CHARACTERIZATION OF COLD FLOW PROPERTIES OF BIODIESEL TRANSESTERIFIED FROM WASTE FRYING OIL

A THESIS SUBMITTED TO THE GRADUATE
SCHOOL OF APPLIED SCIENCES
OF
NEAR EAST UNIVERSITY

by
FİLİZ AL SHANABLEH

In Partial Fulfilment of the Requirements
for Degree of Doctor of Philosophy
in
Mechanical Engineering

NICOSIA, 2017

FİLİZ ALSHANABLEH
CHARACTERIZATION OF COLD FLOW PROPERTIES OF BIODIESEL
TRANSESTERIFIED FROM WASTE FRYING OIL
NEU
2017

CHARACTERIZATION OF COLD FLOW PROPERTIES OF BIODIESEL TRANSESTERIFIED FROM WASTE FRYING OIL

A THESIS SUBMITTED TO THE GRADUATE
SCHOOL OF APPLIED SCIENCES
OF
NEAR EAST UNIVERSITY

by
FİLİZ AL SHANABLEH

In Partial Fulfilment of the Requirements
for Degree of Doctor of Philosophy
in
Mechanical Engineering

NICOSIA, 2017

Filiz AL SHANABLEH: CHARACTERIZATION OF COLD FLOW PROPERTIES OF BIODIESEL TRANSESTERIFIED FROM WASTE FRYING OIL

Approval of Director of Graduate School of
Applied Sciences

Prof. Dr. Nadire ÇAVUŞ

We certify this thesis is satisfactory for the award of the degree of Doctor of Philosophy in Mechanical Engineering

Examining Committee in Charge:

Prof. Dr. Mahmut A. SAVAŞ	Committee Chairman, Co-Supervisor, Department of Mechanical Engineering, NEU
Prof. Dr. Şenol BEKTAŞ	Department of Electrical and Electronics Engineering, NEU
Prof. Dr. Özgür ÖZERDEM	Department of Electrical and Electronics Engineering, LAU
Assoc. Prof. Dr. Murat FAHRİOĞLU	Department of Electrical and Electronics Engineering, Director of Renewable Energy Research Group, METU-NCC
Assist. Prof. Dr. Ali EVCİL	Supervisor, Department of Mechanical Engineering, NEU

I hereby declare that, all the information in this document has been obtained and presented in accordance with academic rules and ethical conduct. I also declare that, as required by these rules and conduct, I have fully cited and referenced all material and results that are not original to this work.

Name, Last Name : Filiz AL SHANABLEH

Signature :

Date: 27/12/2017

ACKNOWLEDGEMENTS

This thesis becomes a reality with the kind support, encouragement and help of many individuals. I am grateful to all of them.

Foremost, my sincere gratitude to my thesis co-supervisor Prof. Dr. Mahmut A. Savaş for his invaluable advices, guidance, encouragement and tolerance throughout this study, he has taught me more than I could ever give him praise for here. I am also very grateful to my thesis supervisor Assist. Prof. Dr. Ali Evcil for his supporting guidance, positive motivation and elucidating instructions all the time. They are precious role models not only teaching to be visionary and humble scientists and also being a dedicated teachers.

My special thanks to the Vice-President of Near East University Prof. Dr. Şenol Bektaş for his endless support throughout the years.

I am very much indebted to my dear friends Engr. Sema and Muzaffer Kaya not only for their priceless technical support but also for their precious friendship and profound support.

I am grateful to my parents whose love, support and guidance are with me in whatever I pursue. They are ultimate role models of living honest and fruitful life.

And last, but not least, all my grateful thanks and all my deepest love goes to my family. I wish to thank to my husband Assist. Prof. Dr. Tayseer Al Shanableh for his endless patience and support. I would like to thank to my beloved children Muhammed, Nur, Yasemin and Nazira for their unrequited love, patience, encouragement, support and belief in myself which made it possible this long journey. They are my true joy and my inner treasure.

To my beloved children…

“Never stop fighting until you arrived at your destined place –that is, the unique you. Have an aim in life, continuously acquire knowledge, work hard, and have perseverance to realize the great life.”

A. P. J. Abdul Kalam

ABSTRACT

Biodiesel is one of the most popular alternatives as a diesel fuel, due to its suitability for the conventional diesel engines with minimum or no modifications, as well as in blends with petroleum diesel. Biodiesel can be produced by transesterification from edible or non-edible oil/fat which are renewable in nature, hence biodiesel itself is categorized as a renewable energy sources. The use of waste frying oil is an effective way of reducing the cost of raw material in biodiesel production. Perhaps, a more important aspect is the environmental benefits.

In the present work, waste frying oil and refined canola oil were used as feedstock for biodiesel production. The two approaches employed in biodiesel production were conventional base-catalyzed and more recently supercritical methanol transesterification techniques. An original batch type reactor was designed and manufactured to overcome the extreme conditions of high temperatures and pressures in supercritical methanol transesterification. It appeared that the supercritical transesterification was advantageous over the base catalyzed one and eliminated the necessity for feedstock preparation and also reduced the time for reaction and purification processes.

Thirteen different parameters including Cold Flow Properties (CFP), i.e. cloud point, cold filter plugging point, and pour point, of the biodiesel samples produced were tested following the relevant ASTM and EN standards. It was noted that the biodiesels transesterified from waste and refined oils exhibited no considerable differences in their CFP temperatures.

Estimation of CFP temperatures based on the fatty acid composition of a feedstock can reduce the experimental effort to produce a biodiesel suitable for a regional climate. In an attempt for this, prediction models were developed using artificial neural network. The model developed revealed that CFP of biodiesel were influenced primarily by saturation or unsaturation of fatty acid components.

The so-called computer-aided cooling curve analysis employed in metal casting industry was modified and applied to the current biodiesel samples in order to estimate the solid fractions at the three CFP temperatures. The results suggested that the current approach may be considered as a potential tool to estimate rapidly the CFP temperatures and the corresponding solid fractions.

Keywords: Biodiesel; cold flow properties; base-catalyzed transesterification; supercritical methanol transesterification; artificial neural networks; cooling curve analysis

ÖZET

Biyodizel mevcut petrol dizel bazlı yakıtların yerini alabilecek veya her oranda harmanlanabilecek bir yakıttır. Biyodizel, bitkisel veya hayvansal bazlı tüm yağlardan transesterifikasyon ile üretilebilir. Bu nedenle, biyodizel yenilenebilir bir enerji kaynağıdır. Biyodizel üretiminde atık kızartma yağlarından yararlanılması, en büyük girdi olan hammadde maliyetini düşürmenin yanı sıra çevresel fayda sağlamaktadır.

Mevcut çalışmada, biyodizel atık kızartma yağı ve rafine kanola yağı kullanılarak baz katalizör ve süperkritik metanol transesterifikasyon teknikleriyle üretilmiştir. Süperkritik yöntemde karşılaşılan yüksek sıcaklık ve basınç koşullarının üstesinden gelmek üzere özgün bir reaktör tasarlanmış ve imal edilmiştir. Süperkritik transesterifikasyonun, baz katalizör ile yapılan uygulamaya kıyasla, hammaddenin ön hazırlığını ortadan kaldırdığı, reaksiyon ve saflaştırma işlemlerinin sürelerininin kısalttığı anlaşılmıştır.

Üretilen biyodizel numunelerinin, bulutlanma noktası, soğukta filtre tıkama noktası ve akma noktası ile tarif edilen Soğuk Akış Özellikleri (CFP) dahil olmak üzere on üç farklı özelliği ilgili ASTM ve EN standartlarını takip ederek test edilmiştir. Atık yağlardan ve taze rafine yağlardan transesterifiye edilen biyodizellerin CFP sıcaklıklarında önemli farklılıklar gözlenmemiştir. Hammaddelerin yağ asidi bileşimine dayalı CFP sıcaklıklarının tahmini, bölge iklim koşullarına uygun bir biyodizel üretmek için deneysel çabayı azaltabilir. Bu nedenle, çalışma kapsamında yapay sinir ağı kullanılarak tahmin modelleri geliştirilmiştir. Elde edilen modeller, biyodizel CFP'sinin öncelikle yağ asidi bileşenlerinin doymuşluğu veya doymamışlığı durumundan etkilendiğini ortaya koymuştur.

Üç farklı CFP sıcaklığında sıvı-katı karışımındaki katı oranını hesaplamak amacıyla, metal döküm endüstrisinde kullanılan bilgisayar destekli soğuma eğrisi analizi mevcut biyodizel numunelerine uyarlanmıştır. Bu yöntem ile her üç CFP sıcaklığını ve bu sıcaklıklardaki katı oranlarını süratli biçimde belirlemenin mümkün olduğu anlaşılmıştır. Böylelikle, yüksek donma eğilimli bir biyozidel numunesi de süratli biçimde değerlendirilebilir.

Anahtar Sözcükler: Biyodizel; soğuk akış özellikleri; baz-katalizörlü transesterifikasyon; superkritik methanol transesterifikasyon; yapay sinir ağları; soğutma eğrisi analizi

TABLE OF CONTENTS

CHAPTER 1: INTRODUCTION

CHAPTER 2: LITERATURE REVIEW

CHAPTER 3: EXPERIMENTAL PRODUCTION OF BIODIESEL VIA BASE CATALYZED TRANSESTERIFICATION AND OPTIMIZATION OF PROCESS PARAMETERS USING TAGUCHI METHOD

CHAPTER 4: DESIGN AND MANUFACTURE OF AN EXPERIMENTAL REACTOR FOR PRODUCTION OF BIODIESEL VIA SUPERCRITICAL METHANOL

CHAPTER 5: PREDICTION OF COLD FLOW PROPERTIES OF BIODIESEL USING NEURAL NETWORKS

CHAPTER 6: VARIATION OF SOLID FRACTION WITH COLD FLOW PROPERTIES OF BIODIESEL

CHAPTER 7: CONCLUSIONS AND RECOMMENDATIONS

LIST OF TABLES

LIST OF FIGURES

LIST OF ABBREVIATIONS

ANN:	Artificial Neural Networks
ASTM:	American Society for Testing and Materials
BD:	Biodiesel
CA-CCA:	Computer Aided Cooling Curve Analysis
CN:	Cetane Number
CP:	Cloud Point
CFPP:	Cold Filter Plugging Point
EN:	European Norms
FA:	Fatty Acid
FAME:	Fatty Acid Methyl Ester
FFA:	Free Fatty Acid
GC:	Gas Chromatography
MLR:	Multiple Linear Regressions
MSE:	Mean Square Error
MUFA:	Mono Unsaturated Fatty Acid
PD:	Petroleum Diesel
PP:	Pour Point
PUFA:	Poly Unsaturated Fatty Acid
RCO:	Refined Canola Oil
RCOME:	Refined Canola Oil Methyl Ester
RFO:	Refined Frying Oil
RFOME:	Refined Frying Oil Methyl Ester
RMSE:	Root Mean Square Error
SCM:	Supercritical Methanol
SE:	Standard error of prediction

SFA:	Saturated Fatty Acid
SVO:	Straight Vegetable Oil
TS:	Turkish Standards
ULSD:	Ultra Low Sulfur Diesel
WCO:	Waste Canola Oil
WCOME:	Waste Canola Oil Methyl Ester
WFO:	Waste Frying Oil
WFOME:	Waste Frying Oil Methyl Ester

CHAPTER 1
INTRODUCTION

1.1 Framework

The energy demand across the world is increasing steadily due to rapid population growth and desire for improved living standards. The major concerns in energy production are the protection of environment and the conservation of non-renewable energy resources. These require alternative development of the sources of energy as substitutes for traditional fossil fuels. In liquid fuels, biodiesel (BD) is one of the most popular alternatives due to its suitability for the conventional diesel engines with minimum or no modifications, as well as in blends with petroleum diesel (PD). BD has been traditionally derived from edible or non-edible oil/fat which are renewable in nature (Acaroğlu 2007, Sharma et al 2007, Balat and Balat 2008, Shahid and Jamal 2008). Highly viscous oils/fats are commonly converted into less viscous BD by transesterification. In the transesterification process which can be catalyzed by a base, acid or enzyme, oil/fat is reacted with an alcohol to yield fatty acid methyl esters (FAME), i.e. BD, and a glycerol co-product which has a commercial value. The base-catalyzed transesterification (Encinar et al., 2002) is considered to be the most promising route for lowering viscosity.

The fuels are at the top of the imports list in the TRNC and is a major drawback in terms of the economic growth of the country. The total import of fuels and LPG is about the twice of the whole exports of the country. TRNC imported 192.8 million dollars of petroleum based fuel in 2012 between January and November, this corresponds to the 12.3 % of the total imports (TRCR, 2012). Among all other fuels that have been imported diesel fuels alone, with 51.7 % market share, ranking number one (GPO, 2010). BD fuel from domestic sources can reduce significantly the petroleum imports of the country.

Vegetable oil is the most common feedstock for BD production, however it makes-up about 75% of the total cost the BD production process (Phan and Phan, 2008; Öğüt and Oğuz, 2006). The production of BD from vegetable oil has been debated also due the use of fertile land to crop oilseeds which reduces the land available for food crops. The result is an increase in food prices and making food scarce all around the world. Hence, the use of waste frying oil (WFO) instead of virgin vegetable oil is desirable to reduce not only the raw material cost but also in terms of a number of environmental issues. The cost of waste oil is estimated to be less than half the price of virgin oil (Encinar et al., 2002), e.g. reported as US$ 0.22 per liter in Brasil (Araujo et al., 2010) and is still free in the TRNC. In addition, the utilization of WFO reduces the environmental pollution.

Growth of population and increasing food consumption have increased accumulation of WFO from households, restaurants, hotels, schools and industrial sources. This is a growing problem not only in TRNC but also all around the world. Being an island, the situation appears to be more serious in Cyprus as compared to the mainland. The WFO poured down the sinks and drains, causes problems for sewage treatment plants increasing the depuration costs. The municipalities often collect WFO from schools, restaurants, hotels and industrial sources then, dump it into a waste disposal area without sewage treatment. This poses a detrimental environmental effect on soil, rivers and sea, and eventually on the living matter. In fact, WFO is a valuable residue and can be considered as a potential raw material for soap manufacturing, energy production by means of anaerobic digestion, thermal cracking and more recently for BD fuel production (Phan and Phan, 2008; Sabudak and Yıldız, 2010; Araujo et al., 2010; Zhang et al., 2003; Encinar et al.,2002; Maceiras et al., 2009). The European Parliament banned the use of WFO in the manufacture of animal food in 2004. The same ban has been in effect in Turkey since 2005. Hence, WFO can be utilized as a raw material primarily in BD production.

Although it is a valuable waste and can be a major feedstock for BD production, there are no major organizations either, private or state that collect WFO in the TRNC. In the TRNC, according to State Planning Organization Report 2012, about 5 million liters (4.5 thousand tons) of vegetable oils (mainly sunflower oil) is consumed every year as food products of which almost all is imported from abroad and 1.2 million liters (1.1 thousand tons) of WFO piles up each year. However, a very small portion of the WFO has been reclaimed and reused. Until now the waste frying oil is often flushed down the drains. The result of an informal survey (Evcil et al., 2010; AlShanableh et al., 2011; AlShanableh et al., 2012), given in Figure 1.1, in prior to the experimental work revealed that the university cafeterias can be a major source of WFO. The smallest amount of waste oil is accumulated in kebab houses. While about 85 % of the virgin oil that was consumed could be recovered as waste in the university campus and in fast food restaurants, this value drops to 35 % for kebap houses. As a result, on average 67 % of vegetable oil/fat that was consumed could be recovered as waste oil from a typical food establishment in TRNC.

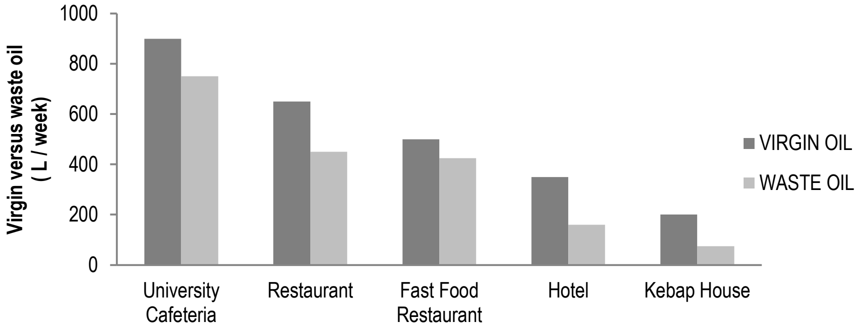

Figure 1.1 : Average accumulation of virgin and waste oil in liters per week for typical food establishments in North Cyprus

The use of BD does not only provide advantages of being renewable fuel over PD, but also offers other advantages such as, less CO hence, lower exhaust emissions (Zhang et al., 2003); higher flash point (~150°C) means less volatility and safer for storage and transportation; higher cetane number that results better ignition in engine (Knothe, 1997); better lubricity that reduces engine wear and extends engine life (Hoekman et al., 2012). Despite its advantages, there are some challenges about BD fuel, as it has higher viscosity, lower volumetric heating value compared to PD fuel, and its cold flow properties (CFP) is a major drawbacks. The tendency of a PD fuel to gel or solidify in cold weather is well known. BD starts to gel at higher temperatures than PD and its cold flow characteristics are very poor.

The major international biodiesel standards are EN (European Norms) 14214 and ASTM (American Society for Testing and Materials) D6751. In all specifications, the tendency of a fuel to gel or solidify at low temperatures is characterized by their Cold Flow Properties (CFP), i.e., Cloud Point (CP), Cold Filter Plugging Point (CFPP) and Pour Point (PP). They directly determine the usage of fuel according to the climatic conditions of a particular region. Since biodiesel freezes at higher temperatures than diesel fuel, determination of its CFP and their improvement are major challenges (Altun and Lapurerta, 2014; Giraldo et al., 2013; Jin et al., 2010; Anwar and Garforth, 2016; Wang et al., 2014; Rasimoğlu and Temur, 2014). The CP is the temperature at which a cloud of wax crystals first becomes visible when the fuel is cooled under conditions addressed by ASTM D2500 or EN 23015. It may be considered approximately as the beginning of fuel freezing. The PP is described in ASTM D97 and ISO 3016 as the temperature at which wax crystallization becomes sufficient to gel the fuel. It is not the end of solidification, but is the lowest temperature at which the fuel can flow. In ASTM D6371 and EN 116, the CFPP is defined as the temperature at which the crystals grow and begin to adhere to each other, therefore plugging the diesel filters. It directly affects the diesel engine performance in winter. The CP is the highest temperature used for the characterization of cold flow and the PP is the lowest. The CFPP is usually between CP and PP. The CP is the only cold flow property that is considered in ASTM D6751 standard whereas PP and CFPP rather than CP are taken into account in EN 14214 standard.

1.2 Objectives and Outline of the Thesis

The experimental and numerical research activities realized within the current PhD thesis can be highlighted as follows:

- Utilization of experimental production of BD mainly from WFO via base-catalyzed transesterification reaction.
- Optimization of process parameters of base-catalyzed transesterification by Taguchi method.
- Characterization of the fuel properties of BD produced by base-catalyzed transesterification following the ASTM and EN specifications.
- Investigation on the improvement of the CFP of the WFO-based BD by blending canola oil- based BD and PD.
- Design of a reactor for construction and utilization for production of BD by supercritical method.
- Prediction of the CFP of the BD using chemical composition of feedstock by numerical methods such as multiple linear regression and artificial neural networks.
- Examination of the cold flow behavior of BD produced from WFO during solidification by employing the computer-aided cooling curve analysis.

CHAPTER 2

LITERATURE REVIEW

The number of research work related to BD based on a literature survey in Science Direct with papers, abstracts and patents included has grown exponentially in recent years as shown in Figure 2.1. About 15 % of these studies are related to CFP of BD.

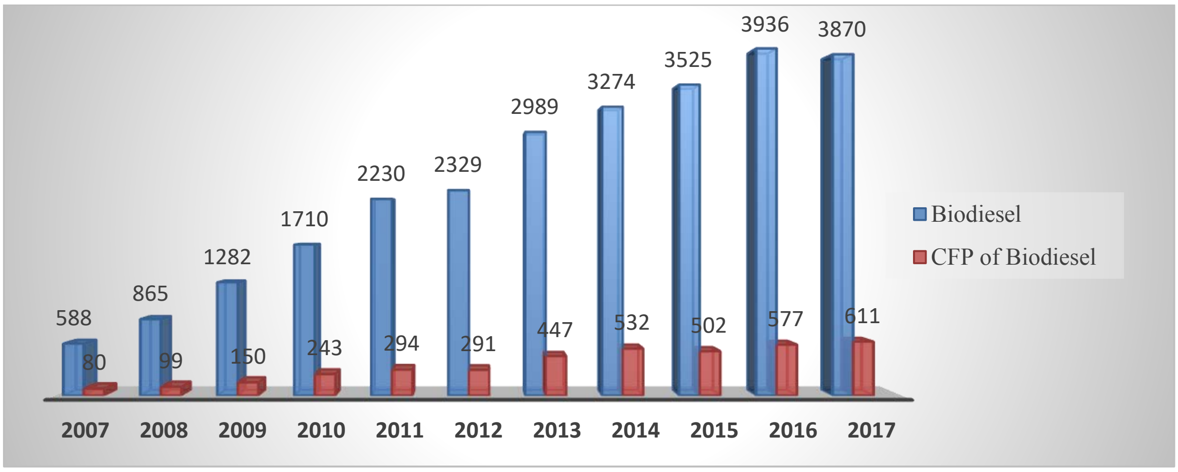

Figure 2.1: Number of publications per year since 2007 related to “biodiesel” and “CFP of biodiesel” theme

In 1893, Rudolf Diesel invented a diesel engine that could work with vegetable oil, and in 1911, he operated that engine using peanut oil at the World’s Fair in Paris. Shortly thereafter, the availability of low-cost fossil fuels led to the modification of diesel engines. The vegetable oil was more viscous than that of the PD fuels created performance problems with modified diesel engines. Since then, only in emergency situations, vegetable oils replaced petroleum fuels and first trials for conversion of vegetable oil alkyl esters were carried out in France in 1940s (Ma and Hanna, 1999). During that time, original diesel engine that was designed to work with highly viscous vegetable oil was modified and optimized to work based on a thinner fuel that was PD by the petroleum companies. Up to this date, this modification of the engine introduced compatibility problems because of highly viscous, lipid-based diesel fuels. In the early 1980s, fluctuation in oil prices and the reality that oil was not a renewable energy source encored extensive research work on fats and oils to replace PD. Since early 1990s, vegetable oils were started to be converted to mono alkyl esters called BD, to reduce those problems.

2.1 Diesel Fuels

Diesel fuel is any liquid fuel that can be burnt in diesel engines, the most popular of which is PD that is obtained by distillation of crude oil. Renewable alternatives of PD are BD, biomass to liquid or gas to liquid diesel. Different international standards have been established and implemented to detect fuel quality, and these standards have been revised frequently. In 1991, Standard Specification for Diesel Fuel Oils was passed in ASTM as D975 and in 2001, D6751 for BD was passed. The European Union eventually has established the first diesel fuel specification in 1993 as EN 590 and as EN 14214 in 2003 for BD standard. The two standards define various fuel properties to satisfy acceptable engine performance and storage and also transportation safety rather than the feedstock.

2.1.1 Petroleum diesel

PD is the primary diesel engine fuel that has been used as light and heavy duty vehicle fuel. Besides, it is also being burnt for heating and electricity generation purposes. PD is mainly composed of 64 % aliphatic hydrocarbons (C_nH_{2n+2} ; n=1 to 20), 35% aromatic hydrocarbons (C_5H_{5-Y}) and approximately 1-2% olefin hydrocarbons (C_nH_{2n}). PD usually called middle distillate and obtained via fractional distillation of crude petroleum between temperatures 200 °C and 350 °C at atmospheric pressure, that is lighter and less dense than industrial fuels, but heavier and denser than gasoline (ASTDR, 1995). However, the composition varies resulting from different refining and blending processes. The PD has a chemical formula on average $C_{12}H_{23}$, and C atoms range from 10 to 15.

Any fuel, before being used as diesel fuel must meet the specification according the ASTM D975 Standard. This specification covers seven grades (such as Grade 1D, 2D, 4D) of PD suitable for various types of diesel engines. Some requirements for PD which are all performance-based demands are summarized in Table 2.1.

Table 2.1: Some requirements for PD (ASTM D975)

Property	Grade No. 1-D	Grade No. 2-D	Grade No. 4-D
Flash point °C, min	38	52	55
Water and sediment, % vol, max.	0.05	0.05	0.50
Distillation temp., °C, 90%, max.	288	338	--
Kinematic Viscosity, mm^2/s at 40°C, min-max	1.3-2.4	1.9-4.1	5.5-24.0
Ramsbottom carbon residue, 10%, %mass, max.	0.15	0.35	--
Ash, % mass, max.	0.01	0.01	
Sulfur, % mass, max	0.50	0.50	
Copper strip corrosion, max 3 hours at 50°C	No. 3	No. 3	--
Cetane Number, min.	40	40	30

2.1.2 Straight vegetable oil

Straight vegetable oils (SVO), composed of mostly, 98 % triglycerides (that contain FA) and small amounts of mono- and diglycerides (Figure 2.2), also known as triglycerides (Demirbaş and Kara, 2006). Triglycerides are composed of esters of three fatty acids (FA) and one glycerol (Balat, 2007).

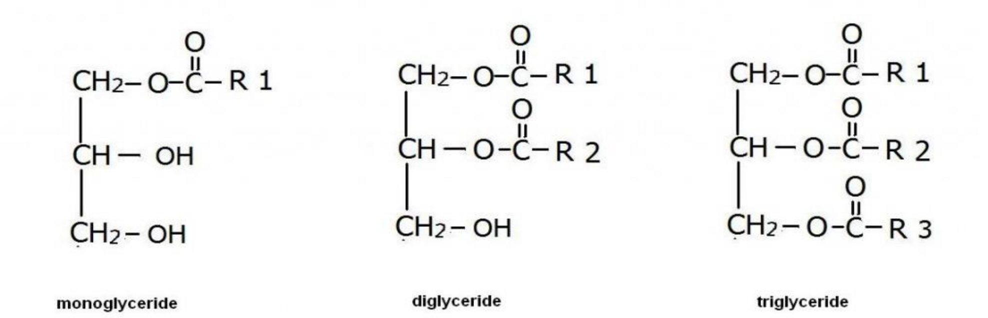

Figure 2.2: Chemical structure of monoglyceride, diglyceride and triglyceride

Vegetable oils differ from one to another according to types of FA which are also vary from one to another in their carbon chain length and in the type of C-C bonding (Tippayawong et al., 2002). Three types of FA may be present in vegetable oils namely, SFA (saturated fatty acids) such as palmitic (C16:0) and stearic (C18:0) acids which have only single bonds in their carbon chain, MUFA (mono-unsaturated fatty acids) such as palmitoleic (C16:1) and oleic (C18:1) acids have one double bond, whereas PUFA (poly-unsaturated fatty acids) such as linoleic (C18:2) and linolenic (C18:3) acids have two or three double bonds in their carbon chain. Due to high level of saturation, SFA have higher melting points when compared to MUFA and PUFA, therefore SFA freezes earlier at cold temperatures. Table

2.2 shows the chemical formula and structure of various FA present in SVO and also some of their relavant physical properties.

Table 2.2: Chemical structure and some physical properties of common fatty acids

Name of Fatty Acid	Structure (xx:y)*	Formula	Molecular Mass (g/mol)	Density at 25°C (g/cm^3)	Melting Point (°C)
Caprylic	8:0	$C_8H_{16}O_2$	144.21	0.910	16.7
Capric	10:0	$C_{10}H_{20}O_2$	172.27	0.893	31.6
Lauric	12:0	$C_{12}H_{24}O_2$	200.32	1.007	43.8
Mystric	14:0	$C_{14}H_{28}O_2$	228.38	0.99	54.4
Palmitic	16:0	$C_{16}H_{32}O_2$	256.43	0.852	62.9
Palmitoleic	16:1	$C_{16}H_{30}O_2$	254.41	0.894	-0.1
Stearic	18:0	$C_{18}H_{36}O_2$	284.48	0.94	69.3
Oleic	18:1	$C_{18}H_{34}O_2$	282.47	0.895	13.5
Linoleic	18:2	$C_{18}H_{32}O_2$	280.45	0.9	-5
Linolenic	18:3	$C_{18}H_{30}O_2$	278.44	0.916	-16.5
Arachidic	20:0	$C_{20}H_{40}O_2$	312.54	0.824	75.5
Gondoeic	20:1	$C_{20}H_{38}O_2$	310.5	0.883	23.5
Behenic	22:0	$C_{22}H_{44}O_2$	340.59	0.822	80
Erucic	22:1	$C_{22}H_{42}O_2$	338.58	0.860	33.8
Lignoceric	24:0	$C_{24}H_{48}O_2$	368.63	0.802	84.2

*(xx:y) xx indicates number of carbon atom in fatty acid and y is number of double bounds

Several studies have shown that SVO can be utilized as alternative fuel in diesel engines, i.e., hazelnut (Çetin and Yüksel, 2007), sunflower (Bruwer et al., 1980; Özaktaş, 2000), rapeseed (Nwafor and Rice, 1996; Labeckas and Slavinskas, 2006), cottonseed (Rakopoulos, 2007), used frying vegetable oil (Zaher, 2003), palm oil (Sapau et al., 1996; El-Awad and Yusaf, 2004), jojoba (Huzayyin et al., 2004), and Jatropha curcas (Pramanik, 2003).

Substantial amounts of oxygen in SVO molecules make it heavier than the hydrocarbon origin PD molecules which results in some differences in fuel properties (Goering et al., 1982). Fuel-related properties of some SVO are listed in Table 2.3. The viscosity of the SVO, which can be 10-20 times higher than that of the PD (2.7 mm^2/s at 38 ^{o}C), is the main problem that prevents its use in diesel engines (Tippayawong, 2002; Demirbaş and Kara, 2006). Wang et al. (2006) reported that high viscosity of SVO is due to its large molecular mass which causes problems in injection and atomization system of the engine. Other problems due to the use of SVO in diesel engines can be summarized as; high acidity, high FFA, gum formation, polymerization during storage and combustion, carbon deposition.

Table 2.3: The fuel-related properties of some SVO (Srivastava and Prasad, 1999)

Vegetable Oil	Kinematic Viscocity at 38°C (mm^2/s)	Cetane Number	Heating Value (MJ/kg)	Cloud Point (°C)	Pour Point (°C)	Flash Point (°C)	Density (kg/L)	Carbon Residue (wt %)
Babassu	30.3	38.0	-	20.0	-	150	0.9460	-
Corn	34.9	37.6	39.5	-1	-40	277	0.9095	0.24
Cottonseed	33.5	41.8	39.5	1.7	-15	234	0.9148	0.24
Linseed	27.2	34.6	39.3	1.7	-15	241	0.9236	0.22
Palm	39.6	42.0	-	31	-	267	0.9180	-
Peanut	39.6	41.8	39.8	12.8	-6.7	271	0.9036	0.24
Rapeseed	37.0	37.6	39.7	-4	-31.7	246	0.9115	0.30
Safflower	31.3	41.3	39.5	18.3	-6.7	260	0.9144	0.25
Sesame	35.5	40.2	39.3	-4	-9.4	260	0.9133	0.25
Soybean	32.6	37.9	39.6	-4	-12.2	254	0.9138	0.27
Sunflower	33.9	37.1	39.6	7.2	-15	274	0.9161	0.23

Heating values of SVO are about 10 % less than that of PD (about 45 MJ/kg) because of its oxygen content. The flash points of SVOs are very high (above 200°C) that provides them suitable storage conditions, but volatility and cetane numbers are similar to that of PD. One of the challenge for the use of SVO is their CFP, the CP, CFPP and PP of them are higher than that of PD.

2.1.3 Derivatives of vegetable oil

There are four different approaches which are commonly investigated to overcome the main problems with substituting SVO for PD such as high viscosities, low volatilities and polyunsaturated character (Demirbaş, 2008, Srivastava and Prashad, 2000): dilution with hydrocarbons (blending), microemulsions with short chain alcohols, pyrolysis (thermal cracking) and transesterification.

SVO can be diluted to be used as diesel fuel by mixing directly with PD or organic solvent and/or ethanol. The dilution of sunflower oil and high oleic safflower oil with diesel fuels were carried out by Ziejewski et al., (1983) and Özaktaş (2000), both researchers observed satisfactory reduction in viscosity around 5 cSt at 40°C. But use of this blend for long period in the diesel engines were not recommended due to severe injector nozzle choking, sticking and thickening of lubricant. Schwab et al., (1987) showed that the fuel properties of diluted oils were mostly affected by degree of unsaturation. The higher the degree of unsaturation of oil (such as sunflower oil) the higher the oxidation and the polymerization in the various sections of the diesel engine.

Microemulsion is a mixture of oil, water, surfactant, and co-surfactant which is thermodynamically stable (Schwab et al., 1987; Demirbaş and Kara, 2006). The resulting fuel is more suitable than SVO for operation in diesel engines. Goering et al., (1982) found that emulsifying of soybean oil with ethanol and 1-butanol in different ratios functioned similar to diesel fuel. The cheapest vegetable oil-originated diesel fuel could be prepared by blending of soybean oil, methanol, 2-octanol, and a cetane enhancer (Knothe et al., 1997). Fernandes et al., (2006) received a patent by adding water surfactant in microemulsion of diesel oil with vegetable oil. Besides, this fuel increases the engine performance, it maintains the criteria set for toxicity as for environment specifications.

The pyrolysis of SVO was described by Fukuda et al. (2001) as decomposing of triglyceride molecules into alkanes, alkenes, carboxylic acids and aromatic compounds by thermal energy application. Different SVOs produce different type of pyrolysis oil in terms of composition. The pyrolysis oils are similar to PD in structural composition, moreover this method has significant advantages over other methods such as feedstock flexibility, lower processing costs (Stumborg et al., 1996). Plants used for conventional petroleum refining industry could also be used for pyrolysis since both require similar technology.

Transesterification is the dislocation of glycerol from an ester by another alcohol that is also called alcoholysis (Otera, 1993). Resultant mixture contains the fatty acid alkyl esters (known as BD) and are attractive as alternative diesel fuels. Among other methods, this method has been used widely to lower the viscosity of SVO. A review of the current knowledge on the topic is given in the following sections.

2.2 Biodiesel Production by Transesterification

BD has been defined as the monoalkyl esters of long-chain fatty acids derived from renewable feedstock’s that must satisfy the requirements of ASTM D6751 (Krawczyk, 1996). BD can be considered as a possible alternative substitute or extender of PD and the two can be blended in any proportion (Alptekin and Çanakçı, 2009). The transesterification reaction can be shown by the general equation:

$$\text{Triglycerides} + \text{Monohydric Alcohol} \rightleftarrows \text{Monoalkylesters} + \text{Glycerol} \qquad (2.1)$$

Raw materials used to produce BD, transesterification processes and the effect of various parameters on BD yield will be discussed in the following sections.

2.2.1 Feedstock utilized in biodiesel production

The primary raw materials for BD production are oils or fats which are chemically classifed as triglycerides. Choosing a suitable oils or fats for BD production is determined mainly on the availability of the feedstock. At present, the main oilseeds used in extracting vegetable oil are mostly sunflower and rapeseed seeds in Turkey (Öğüt and Oğuz, 2006) and Greece (Panoutsou et al., 2008), and soybean seeds in US (Zhang et al., 2003). The cost of BD produced from vegetable oil is about 1.5 times of the PD. Vegetable oil makes-up about 75% of the total cost of BD production (Phan and Phan, 2008; Öğüt and Oğuz, 2006). The production of BD from vegetable oil has been debated also due to the use of fertile land to crop oilseeds which reduces the land available for food crops. The result is an increase in food prices and making food scarce all around the world. Hence, the use of WFO instead of virgin vegetable oil is desirable to reduce not only the raw material cost but also in terms of a number of environmental issues. The cost of WFO is estimated to be less than half the price of virgin oil (Encinar et al., 2007), e.g. reported as US$ 0.22 per liter in Brasil (Araujo et al., 2010) and is still free in TRNC. In addition, the utilization of WFO reduces the environmental pollution.

Another reactant in the transesterification process is the short chain alcohols such as methanol, ethanol, propanol, and butanol and of which methanol is the most commonly used. Water content is the key quality factor for alcohols in transesterification process that reduces BD yield by forming soap as a side reaction. It also boosts up catalyst consumption costs. The short chain alcohols are hygroscopic that are capable of absorbing water. Whereas higher alcohols form azeotropes with water which means that alcohol and water have similar boiling points. Even though methanol is more toxic, it is the most possible candidate for BD production because it is less hygroscopic and does not form azeotropes with water.

Use of ethanol and butanol makes BD completely bio-based (Qureshi et al., 2008) and also ethanol is less costly than methanol in across the world (Van Gerpen et al., 2004). Table 2.4 below gives a list of properties of common alcohols for BD production.

Table 2.4: Properties of C_1-C_4 alcohols (Rapaka., 2012)

Alcohol	Molecular Weight	Boiling Point (°C)	Melting Point (°C)	Density (g/cm^3)
Methanol	32.04	65	-93.9	0.791
Ethanol	46.06	78.5	-117.3	0.783
1-Propanol	60.09	92.4	126.5	0.803
2-Propanol	60.09	87.4	-89.5	0.786
1-Butanol	74.12	117.2	-	0.809
2-Butanol	74.12	99.5	-	0.808

The selection of a suitable catalyst is a key parameter for designing a sustainable transesterification process. Many researches have been done until to date using homogeneous, heterogeneous and enzymatic catalysts. Among these approaches, the base-catalyzed transesterification (Encinar et al., 2007; Steinbach, 2007) is considered to be the most promising route for lowering viscosity, because of their availability, cost-effectiveness and low reaction temperatures. A comparison of homogenous and heterogeneous catalysts being used in transesterification reaction can be seen in Table 2.5.

Table 2.5: A comparison of catalysts in the transesterification reaction

Catalyst	**Examples**	**Advantages**	**Disadvantages**
Homogeneous Base	NaOH, KOH, $NaOCH_3$	Mild reaction conditions, high conversion and faster reaction rate	Sensitive to FFA and water content (soap formation), difficult catalyst separation
Homogeneous Acid	H_2SO_4, HCl	Insensitive to FFA	Slow reaction rate, high alcohol requirement and reaction temperature, sensitive to water content, difficult purification
Heterogeneous Base	CaO, Zeolite	Mild reaction conditions	Sensitive to FFA and water content, catalyst leaching, high alcohol and high temperature and pressure
Heterogeneous Acid	Ion exchange resins and zirconium oxide	Insensitive to FFA, easy catalyst separation, reusable	Slow reaction rate, high alcohol requirement and high reaction temperature
Enzymes	Lipases	No by-product generation, mild reaction conditions, insensitive to FFA	High cost, slow reaction rates, low yield and enzyme deactivation

2.2.2 Transesterification process for biodiesel production

The transesterification reaction mechanism involves three sequential, reversible reactions chain; the triglycerides are converted step wise to diglycerides, monoglycerides and finally glycerol. At the end of each step one mole of alkyl ester ($R'COOR_1$) is produced as illustrated in the Figure 2.3.

$$\begin{array}{c}
Triglyceride(TG) + R'OH \overset{Catalyst}{\Longleftrightarrow} Diglyceride\ (DG) + R'COOR_1 \\
Diglyceride(DG) + R'OH \overset{Catalyst}{\Longleftrightarrow} Monoglyceride\ (MG) + R'COOR_2 \\
Monoglyceride(MG)\ + R'OH \overset{Catalyst}{\Longleftrightarrow} Glycerol\ (GL) + R'COOR_3
\end{array}$$

Figure 2.3: Transesterification reaction mechanism (US Patent: US7851643, 2010)

R_1, R_2 and R_3 represent fatty acid groups which are initially attached to the fat or oil molecules (triglyceride) while *R'OH* denotes monohydric alcohol such as methanol. The overall tranesterification reaction can be represented by the following chemical equation;

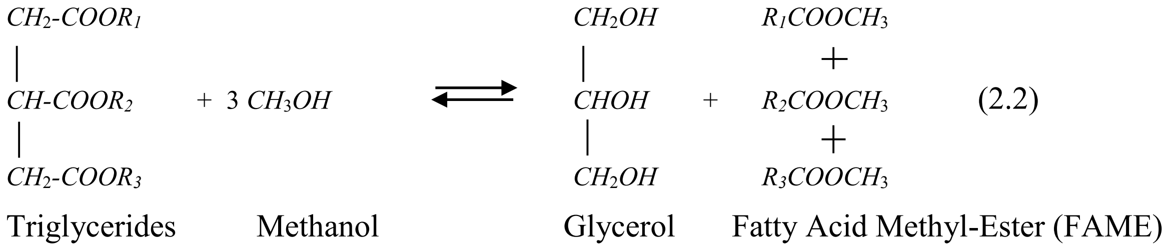

$$\begin{array}{lccccc}
CH_2\text{-}COOR_1 & & & CH_2OH & & R_1COOCH_3 \\
| & & & | & & + \\
CH\text{-}COOR_2 & + 3\ CH_3OH & \rightleftharpoons & CHOH & + & R_2COOCH_3 \\
| & & & | & & + \\
CH_2\text{-}COOR_3 & & & CH_2OH & & R_3COOCH_3 \\
\text{Triglycerides} & \text{Methanol} & & \text{Glycerol} & & \text{Fatty Acid Methyl-Ester (FAME)}
\end{array} \quad (2.2)$$

Complete conversion of one mole of triglycerides and three moles of methanol produces three moles of FAME (BD) and one mole of glycerol. The transesterification reaction cannot proceed easily without using catalyst or supercritical conditions. The most important factor in determining the catalyst type is the properties of the raw material such as water and FFA content. The catalytic and non-catalytic transesterifications will be summarized in the following sections.

2.2.2.1 Base-catalyzed transesterification

To speed up the transesterification process homogeneous or heterogeneous base catalysts can be used, such as metal alkoxides (Schwab et al., 1987, Freedman et al., 1986), and hydroxides (Meher et al., 2006), as well as Na_2CO_3 or K_2CO_3 (Korytkowska 2001). NaOH and KOH are the most commonly used base catalysts for commercial preparation of BD. The classic base-catalyzed transesterification reaction conditions prescribed by Freedman et al. (1986) include a 1:6 oil to alcohol molar ratio of methanol and 1.0 wt % of NaOH as catalyst at 60°C under 1 atm reacts for 1 hour to produce the fatty acid methyl esters (FAME; BD) and glycerol.

Base catalyst provides short reaction time and reasonable reaction temperature and pressure, however the oil contains significant amounts of FFA i.e. higher than 3 % hardly converted into BD but to soap (Sharma and Singh, 2007). Soap inhibits the isolation of the BD from glycerin, and wash water (Çanakçı and VanGerpen., 2003). Moreover, removal of base catalysts, specifically homogeneous ones, is a technically difficult, time consuming and cost effective process (Demirbaş, 2003).

2.2.2.2 Acid-catalyzed transesterification

High FFA content in the feedstock requires acid-catalyzed transesterification process using acids such as sulfuric, hydrochloric, and sulfonic acids (Goff et al., 2004, Lopez et al., 2005). Acid-catalyzed transesterification is preferred over base-catalyzed one because it ensures high conversion efficiency in oils with high FFA. But compared to base-catalyzed reactions, requirement of high alcohol-to-oil molar ratios and relatively slower reaction rate makes it not favored to produce BD (Zhang et al., 2003).

Even when the raw material with high FFA is to be converted to BD with base catalyst, first treatment must be the acid-catalyzed transesterification. This two-step transesterification is essential if FFA content of the feedstock oil is greater than 3 wt % (Sharma and Singh, 2007). First step involves reaction of FFA in the feedstock with alcohol to form fatty acid alkyl ester and water under acid-catalyzed condition, this is referred as esterification. The next step results in complete conversion of triglyceride to fatty acid alkyl ester and glycerol by the base catalyst. It has been noted by Cardoso et al. (2008) that acid catalysis is more suitable with low quality feedstock which has high FFAs and moisture levels.

2.2.2.3 Enzymatic-catalyzed transesterification

Compared with conventional base-catalyzed transesterification, enzymatic-catalyzed one offers a more environmental friendly alternative (Noureddini et al., 2005). Balat and Balat (2008) used different types of enzymes to break down lipids (triglycerides) as catalyst for transesterification process such as Candida, Pseudomonas cepacia, Candida rugasa, Rhizomucor miehei and immobilized lipases and they have found that all these have advantages in comparison to acid/base- catalyzed transesterification. Enzymatic-catalyzed transesterification overcome the difficulties of high FFA and water content of low quality feedstock and conversion to BD higher than 90 % (Watanabe, 2000; Casimir et al., 2007).

The enzyme-catalyzed process requires longer reaction time than the conventional methods because alcohol use for transesterification inhibits the activity of lipases. So, reaction usually occurs within three steps with 1:1 oil to alcohol ratio and each steps requires 4 to 40 h, or more (Zhang et al., 2003). Besides the lipase-catalyzed processes are chemically clean and have modest reaction conditions, another disadvantage of them is their high cost (Van Gerpen et al., 2004; Royon et al., 2007).

2.2.2.4 Non-catalytic supercritical transesterification

The supercritical fluid (SCF) term is used for a substance which has pressure and temperature above its critical point. Behavior of molecules of supercritical state are specific, they move faster as gases but denser as liquids, these make them chemically more reactive. For transesterification reactions SCF are alcohols which become non-polar solvents above their critical points and they easily dissolve non-polar oils/fats. Since chemical reactivity of supercritical alcohol increases, they are more likely to form homogeneous phases with oils/fats. Type of SCF are chosen related to the thermophysical properties of the solvent and reaction temperature and pressure. The most common SCF for transesterification reaction is supercritical methanol (SCM) as mentioned by Demirbaş (2003).

Saka and Kusdiana (2001) have demonstrated first catalyst-free BD production by employing SCM as shown Figure 2.4. The optimum reaction conditions were reported as 1:42 rapeseed oil to methanol molar ratio at 350 ^{o}C, 43 MPa using SCM and it took only 240 s to complete transesterification reaction (Kusdiana and Saka., 2004).

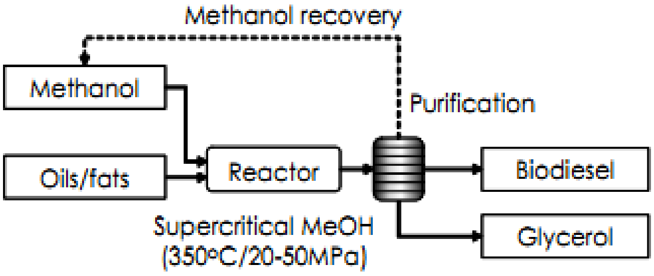

Figure 2.4: Flow diagram of one-step SCM method for BD production

Presence of water in oil/fat or in alcohol has negative effects on methyl ester conversion in conventional catalytic transesterification since it reacts with FFA causing soap formation and reduces catalyst effectiveness. On the contrary, water helps to produce methyl esters in SCM method. Figure 2.5 shows the difference between catalytic methods and non-catalytic SCM methods in relation to the effect of water and FFA content on yields of methyl esters.

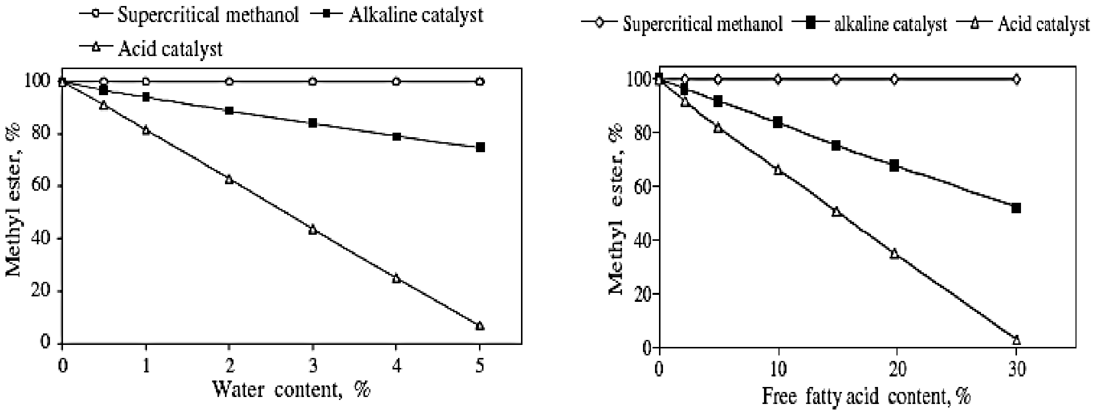

Figure 2.5: Methyl ester yields as a function of water and FFA content in catalytic and non-catalytic transesterifications (Demirbaş, 2003)

Although numerous advantages are provided by the supercritical method, there are also some disadvantages such that high heating and cooling costs, high methanol recovery cost due to high methanol/oil ratios and high reactor construction cost, because of extreme reaction conditions special alloys (e.g., Inconel and Hustelloy) are required for the reactor to avoid its corrosion. Milder reaction conditions were achieved by Saka-Dadan process that was a two-step SCM (Saka et al., 2006) as shown in Figure 2.6.

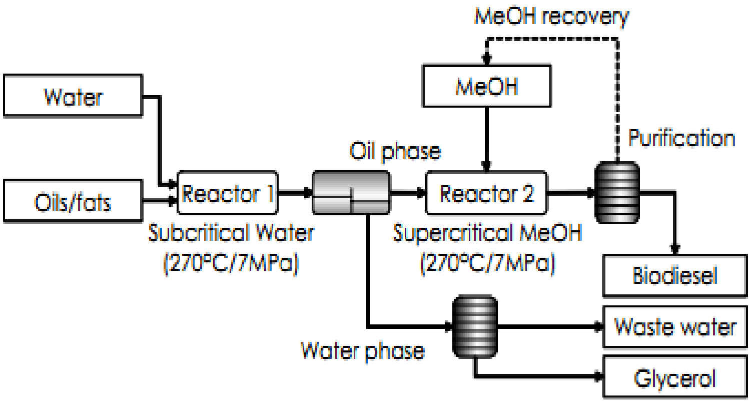

Figure 2.6: Flow diagram of two-step SCM method

First step involves hydrolysis of oils/fats with subcritical water. Products of this reaction are FA and water which are separated by decantation. Next step is mixing FA mixture and methanol at supercritical condition to produce FAME through esterification which is the primary reaction. Products of this step are unreacted methanol, water and FAME.
Comparison between the one-step SCM and the two-step SCM approaches can be seen in Table 2.6 and a comparison of catalytic and non-catalytic transesterification to produce BD is given in Table 2.7.

Table 2.6: Comparisons between one-step supercritical and two-step supercritical methods

	One-Step SCM Method	**Two-Step SCM Method**
Reaction time	9 min	20 min each step
Reaction temperature(°C)	350	270
Reaction pressure (MPa)	20	10
Reactor material	Inconel or Hastelloy	Common stainless steel
Total glycerol	0.39	0.15
Yield (%)	98.5	99.1

Table 2.7: A comparison of various approaches in BD production

Variable	**Base Catalysis**	**Acid Catalysis**	**Lipase Catalysis**	**Supercritical Alcohol**
Reaction time (min)	30-180	120-360	240-2400	3-20
Reaction temperature(°C)	60-70	55-80	30-40	240-420
FFAs in feedstock	Sponified products	Esters	Methyl esters	Esters
Water in feedstock	İntervention with rxn	İntervention with rxn	No influence	No influence
Recovery of glycerol	Difficult	Difficult	Easy	Easy
Yield of FAME	Normal	Normal	High	High
Purification of FAME	Difficult	Difficult	none	none
Production cost of catalyst	Cheap	Cheap	Expensive	none

The use of a SCM as solvent for BD production as compared to catalytic BD production is a straightforward approach and has advantages over conventional methods. In SCM method, transesterfication reaction is completed within a short period of time in the absence of any catalyst and since no catalyst exists, separation of BD from glycerol and purification processes are simpler. Even though SCM method requires high temperatures and pressures conditions for reaction, still in overall condition it has distinct advantages over conventional methods.

2.2.3 Effects of reaction parameters in biodiesel conversion

The selection of type of transesterification process highly depends on type of feedstock and its quality that is FFA and moisture contents (Meher et al., 2006). Specifically, for the base-catalyzed transesterification, the existance of FFA and water always creates negative effects since the base catalyst neutralizing the FFA reduce its effectiveness. Besides, those two produce soaps that causes difficulty in separation and purification processes (Çanakçı and Gerpen, 2003). Usually, acid catalyzed reaction takes place if, FFA content higher than 3% (Meher et al., 2006). Presence of water in oils/fats also has negative effect, because it has ability to react with catalyst and FFA which result in soap formation. Ma and Hanna (1999) reported that to be able to produce BD from beef tallow by using a base catalyst, water and FFA contents must be kept below 0.06 wt% and 0.5 wt%, respectively.

Alcohol to oils/fats molar ratio is another important parameter, and the stoichiometry of transesterification reaction shows that it should be 3:1. Some significant studies showed that this ratio should be higher than 3:1 in order to achieve high conversion. Freedman et al. (1986) conducted an investigation about the effect of molar ratios on the conversion efficiency of sunflower oil with different methanol molar ratio ranging from 1:1 to 6:1. The results showed that the best conversion that is 98% achieved with 6:1 molar ratio. On the other hand, Nouredini et al. (1998) reported that alcohol to methanol molar ratio of 8:1 provided higher conversions than 6:1. As they mentioned, higher alcohol molar ratio was increased solubility of oil by increasing the interaction surface area between the triglyceride and alcohol molecules and decreasing the reaction time.

On the contrary, Al-Widyan and Al-Shyoukh (2002) showed that the molar ratio of methanol/oil beyond 6:1 would cause an increase in BD yield, but excess amount of methanol made the ester recovery process more difficult and raised its cost.

In catalytic transesterification of oils/fats, the most important part is the selection of a proper catalyst that can be basic, acidic or enzymatic related to the quality of feedstock. FFA content of feedstock influences type of catalyst that should be chosen, if feedstock' s FFAs < 3% then homogeneous base catalyst is the best, but for feedstock's FFAs > 3%, the order of catalyst selection is as follows: homogeneous acid/base catalyst > heterogeneous acid catalyst > homogeneous base catalyst > enzyme catalyst > homogeneous acid catalyst (Sharma and Singh, 2007).

In addition to the FFA content, another factor that influences catalyst selection is the reaction time, Ma and Hanna (1999) observed that base catalyst caused faster reaction than acid catalyst and because of this feature, it could be more often used commercially. May (2004) studied the effect of different catalyst types on reaction time and concluded that base-catalyzed transesterification of refined palm oil with a low FFA content of <0.1% yielding above 98% within short reaction time (1 h max.) while acid catalysts yielding below 50% with more than 300 min reaction time. Study of Kim et al. (2004) showed that conversion of oils/fats to BD with the homogeneous catalyst was about 20 % above the heterogeneous catalyst.

The reaction temperature is related with the yield of reaction and the completion time of reaction. Increase in reaction temperature increases the BD conversion while shortening reaction time. In the study of Freedman et al. (1986), base-catalyzed transesterification of refined soybean oil was carried out at different temperatures such as 32°C, 45°C and 60°C and after 0.1 h, the corresponding conversions were 64, 87 and 94 %, respectively. Another study performed by Darnokol and Cheryan (2000), also showed that conversion of palm oil to BD using the same method was 73% and 82% for 50 and 65 °C, respectively after 4 min. Demirbas (2006) also noticed that increase in the reaction temperature caused increase in the yield of methyl ester in SCM method.

The BD yield increases with increasing reaction time. Freedman et al. (1986) found that different type of oils (soybean, cottonseed, peanut and sunflower) using similar parameters and conditions, such as methanol to oil ratio and temperature, yielded BD approximately 80 % after 1 min and 93-98 % 1 h after completion of reaction. At the same conditions, Ma and Hanna (1999) observed that even the low quality fat such as beef tallow was converted to BD within 1 h. From one to five min, the reaction proceeded very fast and beef tallow methyl esters jumped from 1 to 38. After 15 min, conversion reached its maximum value.

Similar to the reaction time, increasing rate of stirring increases the rate of reaction and its yield. Meher et al. (2006) produced BD with the same type of oil at different stirring rates as 180, 360 and 600 revolutions per minute (rpm). Their study showed that within 1 h reaction could not be completed with 180 rpm but the yield of FAME was same under 360 and 600 rpm. Sharma and Singh (2007) reported that use of magnetic stirrer (1000 rpm) instead of mechanical one (1100 rpm) increased yield of BD from 85 % to 89.5 %.

2.3 Specifications of Biodiesel

FAME is not called BD unless it meets the requirements of international standards such as ASTM, EN or national standards such as Turkish Standards (TS) in Turkey and TRNC. Properties of BD that should satisfy specifications of the standards are greatly affected by the compositional profile of BD's feedstock. Both PD and BD properties may vary due to their origins and Table 2.8 summarizes some of the critical properties of BD and PD.

Table 2.8: Typical properties of BD as compared to PD

Property	No.2 Petroleum Diesel	Biodiesel
Carbon, wt %	86.8	76.2
Hydrogen, wt %	13.2	12.6
Oxygen, wt %	0.0	11.2
Specific gravity	0.85	0.88
Cetane no.	40-45	45-55
T_{90}, °C	300-330	330-360
Viscosity at 40 °C (mm^2/s)	2-3	4-5
Energy content (LHV)(MJ/kg)	43	39
Energy –Volume basis (MJ/gal)	137	128

Main difference in properties arises from oxygen content of BD, as PD does not have any. Higher oxygen content leads to lower carbon and hydrogen contents compared to PD that results about a 10 % lower mass energy content. Although BD's energy content in terms of mass is lower, its volumetric energy content is only about 5 % below that of PD due to BD's higher fuel density. Besides, denser BD molecules result in higher distillation temperatures (as measured by T_{90}). BD's cetane number is approximately 10 % higher than that of PD's due to the content of straight chain esters. Most of BD fuels have approximately two times higher viscosity than that of PD and in BD-PD blends increasing BD portion (B-level) increases the viscosity of blend.

Related to the country where BD are being produced, there are certain standard specifications that have been established by various fuel standard-setting organizations, particularly ASTM (in the U.S.) and EN (in the European countries). Table 2.9 which is adopted from Hoekman et al. (2012) lists the major BD standards which serve as a reference for other standards are EN 14214 (Automotive Fuels) or ASTM D6751. ASTM D6751 has been assigned for pure BD fuel (B100) while ASTM D7467 is for BD blends of B6 to B20.

Table 2.9: ASTM and EN specifications for BD (B100) and BD blends

	BD blendstock (B100)				**B6-B20; BD Blends**	
Property	**U.S. (ASTM D6751-08)**		**Europe (EN 14214)**		**U.S. (ASTM D7467-08)**	
	Limits	**Method**	**Limits**	**Method**	**Limits**	**Method**
Water and sediment (vol. %, max)	0.05	D 2709	0.05	EN 12937	0.05	D 2709
Total contamination (mg/kg, max)			24	EN 12662		
Kinematic viscosity at 40 ºC (mm^2/s)	1.9-6.0	D 445	3.5-5.0	EN 3104/3105	1.9-4.1	D 445
Flash point, closed cup (ºC, min)	93	D 93	101	EN 3679	52	D 93
Methanol (wt %, max.)	0.20	EN 14110	0.20	EN 14110		
Cetane number (min)	47	D 613	51	EN 5165	40	D 613
Cloud point (ºC)	Report	D 2500			Report	D 2500
Sulfated ash (wt %, max.)	0.020	D 874	0.020	EN 3987		
Total ash (wt %, max.)					0.01	D 482
GroupI metals Na + K (mg/kg, max)	5.0	EN 14538	5.0	EN 14108/14109		
GroupII metals Ca + Mg (mg/kg, max)	5.0	EN 14538	5.0	EN 14538		
Total sulfur (ppm, max)	15	D 5453	10	EN 20846	15	D 5453
Phosphorous (ppm, max)	10	D 4951	4	EN 14107		
Acid no. (mg KOH/g, max)	0.50	D 664	0.50	EN 14104	0.30	D 664
Carbon residue (wt %, max.)	0.05	D 4530	0.30	EN 10370	0.35[e]	D 524
Free glycerin (wt %, max.)	0.02	D 6584	0.02	EN 14105/!4106		
Total glycerin (wt %, max.)	0.24	D 6584	0.25	EN 14105		
Mono glyceride (wt %, max.)			0.80	EN 14105		
Diglyceride (wt %, max.)			0.20	EN 14105		
Triglyceride (wt %, max.)			0.20	EN 14105		
Distillation (T_{90} ºC, max)	36	D 1160			343	D 86
Copper strip corrosion (3-h at 50 ºC, max)	No.3	D 130	No.1	EN 2160	No.3	D 130
Oxidation stability (h at 110 ºC, max)	3.0	EN 14112	6.0	EN 14112	6.0	EN 14112
Linolenic acid methyl esters (wt %, max.)			12.0	EN 14103		
Polyunsaturated acid methyl e. (wt ,max.)			1.0	prEN 15799		
Ester contents (wt %, max.)			96.5	EN 14103	6-20vol%	D 7371
Iodine value (g I_2 / 100 g, max)			120	EN 14111		
Density (kg / m^3)			860-900	EN 3675		
Lubricity at 60 ºC, WSD, microns, max					520	D 6079
Cold soak filterability (seconds, max)	360	D 7501				

Blends of B5 and below are permitted under the standard specifications for No. 2 PD fuel, ASTM D975. Up to date European Union has legislated only standard specifications for B100, called EN 14214, but not for any blends. The European standard specifications for No. 2 PD fuel (EN 590) permit blends of B7 and below. Full documents of specification of pure BD i.e., EN 14214 and ASTM D6751 are given in Appendix 1 and 2, respectively.

Due to its feedstock the BD properties may vary. Difference in BD properties is mainly because of the FA profile of the feedstock, BD production methods, FAME purification processes and the storage time and conditions. Total glycerol content is one of the most important specification since a number of other specifications such as viscosity, pour point, cloud point, amount of carbon residue and so on, are directly related to the amount of glycerol. High glycerol cause mainly high viscosity, injection and filter problems and high cloud and pour point. In ASTM and EU BD specification standards, the total glycerol value must be less than 0.25 and 0.24 wt %, respectively.

The most important goal in BD production is to reduce the viscosity of SVO since viscosity of fuel is directly related to engine performance and injection system. BD with low viscosity eases the fuel atomization while higher value indicates poorer. Allan and Watts (2000) showed how high viscosity BD affect the fuel injection system, such a fuel since it has larger droplet sizes it results in poorer vaporization and insufficient spray angle. Temperature is an important parameter for viscosity specification, decreasing temperature will induced an increase in BD viscosity. This relation is shown in the research of Knothe and Steidley (2007) where in cold weather and cold-start engine conditions different FAME components have high viscosity and this creates engine problems. Refaat (2009) studied the effect of molecular mass of individual FAME molecules on viscosity and the conclusion was increase in number of carbon atoms in FA makes FAME molecule heavier and increases its viscosity. He also indicated that higher SFA molecules result in high viscosity while higher unsaturation leads to low viscosity. Structure of unsaturated molecules also influenced viscosity, in the double bond the trans configuration results in higher viscosity than cis. Likely, most vegetable oils have cis double bonds, only some waste cooking oils can have substantial levels of the trans configuration that can be the reason for their higher viscosity as compared to raw oil.

Density is a critical specification of fuel that directly affects engine performance similar to viscosity. Since for fuel injection system the volume of fuel is important but not its mass, the amount of fuel being pumped depends on its density. The air–fuel ratio within the combustion chamber is metered by its volume, hence by fuel density. Densities of BD fuels are above those of PD, and increasing the B-level of BD blends increases the blend's density. Refaat (2009) studied the factors that affect FAME density (which could also be called specific gravity) which are degree of unsaturation in methyl esters and chain length. The more unsaturated FA in FAME the higher the BD fuel density and longer the chain length leading to lower density.

The tendency of a diesel fuel to gel or freeze in cold weather is well known. BD starts to gel at higher temperatures than PD and its cold flow characteristics are very poor. Determination of the flow characteristics and its improvement is a major challenge. There are three important parameters which are determined for CFP temperature characteristics of BD fuel, namely, CP (cloud point), PP (pour point) and CFPP (cold filter plugging point).

The CP is the temperature at which cloud of wax crystals first becomes visible when fuel is cooled under conditions described by ASTM D2500 or EN 23015. More sophisticated procedures have been published for cloud point measurement in recent ASTM D3117, ASTM D5771, ASTM D5772 and ASTM D5773 standards. However, these are not essential in ASTM D6751, yet. The PP is described in ASTM D97 and ISO 3016 as the temperature at which wax crystallization becomes sufficient to gel the fuel. It is not the end of solidification, but is the lowest temperature at which the fuel can flow. In ASTM D6371 and EN 116 the CFPP is defined as the temperature at which the crystals grow and begin to adhere to each other plugging the diesel filters. It directly affects the diesel engine performance in winter. The CP is the highest temperature used for characterizing cold flow and the PP is the lowest. The CFPP is usually between the CP and PP. The CP is the only cold flow property that is considered in ASTM D6751 standard whereas PP and CFPP rather than CP are taken into account in EN 14214 standard. . Full documents of ASTM D2500, ASTM D97 and ASTM D6371 are given in Appendix 3, 4 and 5, respectively.

There are some other methods to describe CFP of BD such as low temperature filterability such as the wax appearance point, those are demanded by fuel suppliers time to time. Numerous laboratory tests are commonly used to define CFP of BD (and conventional PD) listed in Table 2.10.

Table 2.10: Low temperature performance tests used for BD

Test Name	Abbreviation	Test method(s)
Cloud point	CP	EN 23015, ASTM D2500, ASTM D5773
Pour point	PP	ASTM D97, ASTM D5949
Cold filter plugging point	CFPP	EN 116, ASTM D6371
Low temp filterability test	LTFT	ASTM D4539
Wax appearance point	WAP	ASTM D3117
Cold soak filterability	-	ASTM D7501

Poor CFP is a result of long chain SFA esters present in BD. Stournas et al. (1995) reported that saturated methyl esters group with more carbon than C12 considerably increase CP and PP, even when blended with PD. In the study of both Dunn and Bagby (1995) and Refaat (2009), it was concluded that the longer the carbon chain, the higher the melting point hence poorer the CFP. Also, as Hoekman et al. (2012) indicated that degree of unsaturation has a strong effect on CFP, when unsaturated FA components are high in BD then low temperature operability of the engine is better, even though chain length of FAME components are higher.

Among all CFP specifications, only CP can be defined thermodynamically, using solid–liquid equilibrium as a function of temperature. Phase diagrams may change from one feedstock to other which BD is made up of. Related to thermodynamic properties, Lopes et al. (2008) reported that CP could be determined by knowing the type and amount of SFA components in BD and the other components have little effect. At CP temperature, the least soluble SFA crystallizes first from the solution, since SFA molecules are closely packed and highly ordered these molecules will crystallize first and degrade CP (Knothe, 2005).

Blending PD by BD results in the worsening of the low temperature performance but blending different BD components may provide positive effects. For example, Sarin et al. (2010) reported that blending palm-based biodiesel, having high SFA components and poor

CFP, with jatropha-based fuel, having better CFP, can improve low temperature performance.

Another low temperature operability problem occurs due to the formation of insoluble particles upon storage at cold weather which are identified as non-FAME impurities such as saturated monoglycerides and sterol glucosides. ASTM has adopted a new specification for this case, i.e., Cold Soak Filterability test within the biodiesel standard, D6751. (CONCAWE, 2009).

Another fuel quality characteristic is its cetane number (CN) which indicates ease in autoignition. Fuel with high CN ignited easier than with the one with low CN. The work of Knothe et al. (1997) showed that BD with long-chain hydrocarbon groups has a higher CN than PD and in BD-PD blends, increasing the B-level increases the CN of the blend. On the other hand, for a type of BD that has relatively low CN, increasing B-level induces a decrease in the CN of blend.

Hoekman et al. (2012) reported a direct relation between saturated or unsaturated FA components with CN, result was BD' feedstock rich in SFA such as tallow and palm have higher CN than one with lower SFA such as soy and rapeseed oils. Refaat (2009) studied effect of chain length on CN of BD, found that FAME molecules with longer chain length will have high CN. Another study by Dunn and Bagby (1995) showed that degree of unsaturation in FAME dictates the CN, increasing degree of unsaturation degrades CN. In a similar study, Lapuerta et al. (2009) proposed that using the number of double bonds CN could be predicted.

Iodine value describes the amount of carbon–carbon double bonds by letting them to react with I_2 (iodine); thus, it describes degree of unsaturation. Iodine value is originally included as a specification in the European BD standard, EN 14214, not in the ASTM BD standard, believing that oxidative stability could be used for similar purposes. While iodine value is a measure of total unsaturation, oxidative stability is determined by the amount of FAME molecules having multiple double bonds. While EN 14214 set their iodine value to be maximum 120 g I_2/100 g BD, the Worldwide Fuel Charter (U.S., European, and Japanese automobile manufacturer associations) allows 130 g I_2 /100 g biodiesel (WFC., 2006).

Therefore, while some BD such as soya beans-derived BD, is likely to fail by the EN iodine value specification, it would satisfy by the Worldwide Fuel Charter. Another argument for the necessity of iodine value specification application rises by Luperta et al. (2009) article which implied that there is no need for an iodine value specification because the CN specification effectively limits unsaturation.

Oxidation stability is another important fuel property in relation to in-use and storage performance of BD. Low oxidation stability indicates unstable fuel that leads to sediment and gum formation which increase viscosity. Higher degree of unsaturation in FAME causes poorer stability. Also, the structure and number of carbon atoms of unsaturated FA in feedstock of BD are important with respect to oxidative stability. Moser (2009) reported that the trans configuration in C-C double bond is more stable than cis but all natural fats and oils are dominated by cis configuration. Blending BD with different originated feedstock with each other may inherent oxidation stability, for instance, blending palm-based FAME that has high oxidation stability with less stable jatropha-based FAME makes the resultant fuel more stable (Sarin et al., 2009).

Flash point is defined as the lowest temperature at which a combustible mixture formsd above the liquid fuel and it is considered to be contrary of fuel volatility. It is dependent on both the lean air-fuel ratio and the vapor pressure of the fuel constituents. The flash point is determined by passing a flame over the surface of the preheated fuel. If the vapor above heated liquid fuel is ignited with an easily detectable flash then this temperature of vapor indicates the flash point. Low flash point in BD reveals contamination of fuel by highly volatile impurities – mainly excess methanol remaining after purification of BD.

Although it is not specified in either ASTM or EN BD standards, the energy content is a critical property of FAME. Heating value of fuels are commonly described in two ways, i.e., the higher, or gross heating value (HHV) and the lower, or net heating value (LHV). Combustion of fuel in a calorimeter gives the heat and heat gained by the calorimeter can be calculated as heating value, and this procedure is described in ASTM D 240. The difference between the HHV and the LHV described by the phase of the water that was produced at the end of combustion of the fuel. In HHV calculation, water in the products is condensed liquid while the LHV calculation, it is assumed to be in vapor. Usually the LHV is determined for engine applications and indicates the energy content of the fuel. LHV of BD is about 12 % less in weight basis than that of No. 2 PD, but in volume basis it is only 8 % less, since the BD has a higher density (Van Gerpen et al., 2004). For either HHV or LHV of blended PD-BD fuel, increasing the B-level of BD blends results in a reduction in energy content.

Demirbaş (2008) reported that the carbon chain and degree of unsaturation had strong influence on heating value. Longer carbon chain in FAME causes decrease in mass fraction of oxygen in the molecule and this leads to an increase in the heating value. Also BD with high unsaturated FA has lower energy content (MJ/kg) than that of SFA.

Lubricity refers to the reduction of friction between surfaces (fuel injector) in relative motion by forming a liquid layer (hydrodynamic lubrication) and formation of a thin, protective anti-wear layer on the surfaces (boundary lubrication) (Bacha et al., 2007). Good lubricity in diesel fuel means good protection of fuel injection systems and most of the time the fuel itself is the only lubricant. The particles (molecules/atoms) in the PD dictate lubricity. Mainly oxygen, nitrogen and sulfur in the fuel improve lubricity, but high degree of hydrotreatment processes to produce cleaner PD that is ULSD (ultra-low-sulfur-diesel) reduce its lubricity (Hoekman et al., 2012). The lubricity of ULSD can be improved by blending with BD that is excellent lubricant itself. Often, only 1-2 % B-levels provide satisfactory lubricity to ULSD (NERL, 2009).

Although B100 is not specified neither in ASTM nor in the EN BD standards, for B6–B20 blends, ASTM D7467 includes a lubricity specification. Some impurities in BD such as FFA and monoglycerides are highly effective lubricants, but reduction of them during purification process of BD reduces its lubricity nevertheless, improves low temperature properties.

CHAPTER 3

EXPERIMENTAL PRODUCTION OF BIODIESEL VIA BASE CATALYZED TRANSESTERIFICATION AND OPTIMIZATION OF PROCESS PARAMETERS USING TAGUCHI METHOD

3.1 Overview

Base-catalyzed transesterification is the most common approach for BD production from oils/fats (triglycerides). Transesterification reaction converts triglycerides into a mixture of esters of the FA that makes up the oil/fat using a short chain alcohol and a catalyst. BD is obtained from the purification of the mixture of FA methyl esters (FAME).

The transesterification reaction is represented by the general equation:

$$\text{Triglycerides} + 3\text{Monohydric Alcohol} \overset{Catalyst}{\Longleftrightarrow} 3FAME + \text{Glycerol} \qquad (3.1)$$

In the present study, four types of feedstock; namely waste frying oil (WFO), refined frying oil (RFO), refined canola oil (RCO) and waste canola oil (WCO) were transesterified in the presence of methanol. A base catalyst, i.e. NaOH, was used to speed up the reaction.

The Taguchi design of experiment (DOE) technique was implemented to optimize process parameters to ensure high BD yields. The three parameters chosen were; molar ratio of alcohol to oil, reaction temperature and reaction time which were designed in an orthogonal array to screen their effects. The three selected parameters, at two-levels, i.e. L-4 (2^3), were experimentally studied. Four experiments were conducted with selected parameters and the combination of their selected levels for the production of WFO, RFO and WCO based-BDs. RCO was converted into BD using the optimized level of control parameters to see the validation of the implemented model.

Finally, to ensure the quality of the BD produced, some of its critical properties were investigated. The properties measured were: ester content, viscosity, cloud point (CP), cold filter plugging point (CFPP), pour point (PP), free and total glycerol, calorific value and iodine value by following the ASTM and EN - ISO standards.

3.2 Materials

The four feedstock utilized in the experimental work were waste frying oil (WFO) and refined frying oil (RFO) which were with high saturated fatty acid (FA) contents whereas refined canola oil (RCO) and used canola oil (WCO) consisted of high unsaturated FA contents. RCO was purchased from a local supermarket. To obtain WCO, some part of the RCO was used in controlled frying processes. The WFO was collected from the Engineering Faculty Cafeteria of Near East University. Approximately 18 - 20 liters of WFO were accumulated in the cafeteria at the end of each day. The RFO was obtained also from the same cafeteria. Anhydrous methanol (MeOH) (99.8%) and high purity sodium hydroxide (NaOH) were purchased from Merck.

FA compositions of feedstock used were determined following the EN ISO 5508 in the TRNC- Ministry of Health-Directorate State Laboratory-Nicosia using Gas Chromatography (GC). Results of the GC analysis are tabulated in Table 3.1.

The most common FA components of BD feedstock were identified as caprylic acid (C8:0), capric acid (C10:0), lauric acid (C12:0), myristic acid (C14:0), palmitic acid (C16:0), palmitoleic acid (C16:1), stearic acid (C18:0), oleic acid (C18:1), linoleic acid (C18:2), linolenic acid (C18:3), arachidic acid (C20:0) and gondeic acid (C20:1). Trace amounts of other FA constituents like 0.001 wt % of erucic acid (C22:1) in RCO were not taken into consideration. In Cxx:y notation; while xx is the carbon atoms, y is the number of double bonds of carbon atoms in the fatty acid chain. While the WFO and RFO were found rich in saturated fatty acids (SFA) that have only single C-C bonds, the RCO and WCO were rich in unsaturated fatty acids that have double C-C bonds. Depending on number of double bonds between carbon atoms, fatty acids could be either monounsaturated fatty acids (MUFA) or polyunsaturated fatty acids (PUFA). In addition to GC analysis of raw materials, Table 3.1 also provides molecular weights and melting temperatures of the related FA and total SFA, MUFA and PUFA.

Table 3.1 FA compositions of BD feedstocks used in the current work

Fatty acid	Molecular mass (g/mol)	Melting Point (°C)	FA Composition (wt%)			
			WFO	RFO	RCO	WCO
C8:0	144.21	16.7	0.05	0.05	0.0	0.0
C10:0	172.27	31.6	0.33	0.28	0.0	0.0
C12:0	200.32	43.8	1.18	1.02	0.08	0.56
C14:0	228.38	54.4	0.10	0.08	0.0	0.0
C16:0	256.43	62.9	39.29	38.4	5.63	6.02
C16:1	254.41	-0.1	0.14	0.08	0.0	0.0
C18:0	284.48	69.3	4.04	3.52	1.57	2.01
C18:1	282.47	13.5	40.42	39.2	62.97	63.22
C18:2	280.45	-5	13.84	16.9	21.34	18.08
C18:3	278.44	-16.5	0.18	1.02	6.99	4.61
C20:0	312.54	75.5	0.0	0.0	0.46	0.49
C20:1	310.5	23.5	0.0	0.0	1.04	1.12
[1]Σ SFA			44.99	43.35	7.74	9.08
[2]Σ MUFA			40.56	39.28	64.01	64.34
[3]Σ PUFA			14.02	17.92	28.33	22.69

[1]Σ SFA = wt%(C8:0 + C10:0 + C12:0 + C14:0 + C16:0 + C18:0 + C20:0)
[2]Σ MUFA = wt%(C16:1 + C18:1 + C20:1)
[3]Σ PUFA = wt%(C18:2 + C18:3)

3.3 Experimental Set-up for Base Catalyzed Transesterification

The flowchart given in Figure 3.1 summarizes the experimental procedures followed for BD production via base-catalyzed one-step transesterification reaction.

Transesterification is the main step in BD production but, to conform international standards additional steps such as pretreatment of raw materials, separation of the reaction products and purification of the reaction products are also necassary. The steps followed in BD production will be described in details below.

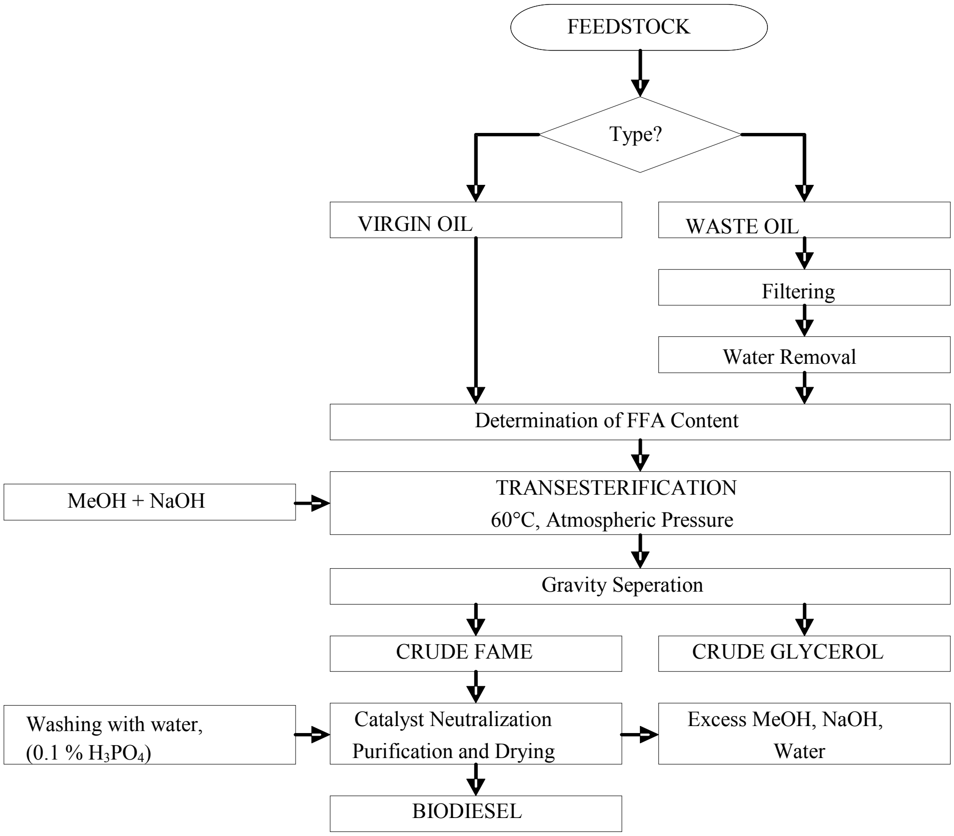

Figure 3.1 Flowchart of the experimental procedure for the BD production by base- catalyzed transesterification developed in the present study

3.3.1 Pretreatment of raw material

Raw material that initiates base catalyzed transesterification should provide certain specifications. Properties of used frying oils differ from those of virgin ones. Frying process causes hydrolysis of triglycerides by heat and water which increases the free fatty acid (FFA) content. FFA and water contents have negative effect on transesterification. Thus, triglycerides containing high amounts of water and FFA are not easily transesterified. Additional pre-processes such as filtration, water removal from WFO and WCO were performed and, also the FFA contents of all types of feedstock were determined.

Used frying oils collected were first filtered to remove food residues and then, heated up to 120 °C for 20 mins to evaporate water. After filtration and water removal, the % FFA were determined for all samples to arrange the catalyst required.

3.3.2 Determination of FFA content

For the alkaline catalyzed transesterification to take place the FFA levels in a sample should be below 3% (Sharma and Singh, 2009). Amount of catalyst and type could be arranged after determining FFA. An excess as well as insufficient amount of catalyst may cause soap formation.

% FFA is defined as the percentage by weight of free acid groups found in a sample and can be calculated using Equation 2 (Wrolstad et al., 2005) below.

$$\%\ FFA\ as\ oleic\ acid = \frac{(V_{NaOH})(N_{NaOH})(MW_{oleic\ acid})}{Weight\ of\ sample} \qquad (2)$$

where, V_{NaOH} is the volume of NaOH consumed in titration and N_{NaOH} is the normality of NaOH solution.

Titration of feedstock against a standard base solution reveals the amount of catalyst required to neutralize the FFA in feedstock during transesterification. In the titration reaction, a standard base solution is slowly added to a feedstock until the equivalence point is reached. The equivalence point is the stage where all acids completely neutralized by base and the amount of standard solution that is used in the titration could be measured hence, FFA could be calculated at this point. To understand whether the neutralization reaction completed or not an indicator should be employed. In this study, phenolphthalein was used as an indicator that changes the color (from colorless to pink) at the equivalence point. The titration procedure is described below:

- Preparation of standard solution: To prepare 1% wt NaOH solution, 1g of NaOH was dissolved in 1L of distilled water. Standard solution was poured into a 100 mL burette.

- Titration of feedstock against the standard solution; in a 500 mL flask, 1.0 mL of feedstock was dissolved in 10 mL of isopropyl alcohol and 2-3 drops of phenolphthalein were added. The resulting solution was colorless. The initial volume of standard solution was recorded.
- Standard solution was slowly added to the oil solution by swirling the flask gently until the color of solution turned into pink and stayed pink for 30 seconds.
- Volume of the standard solution used for neutralization of FFA was recorded. Then, the T value that is the difference in the volume of standard solution before and after the titration was calculated.
- Process repeated for the same feedstock for at least three times and average T was calculated.
- For each mL of NaOH used, it was found that 1 g of additional catalyst (NaOH) should be used to neutralize FFA in transesterification process.

% FFA content of feedstock was calculated using Equation 2 and the additional catalyst amount was obtained. The volume of standard solution used in titration (T), % FFA and total amount catalyst (NaOH) are tabulated in Table 3.2. The total amount of catalyst for 1000 mL of feedstock is calculated as; 1 wt % NaOH that is 3.5 g to speed up the reaction as prescribed by Freedman et al (1986) plus T amount in grams to neutralize FFA.

Table 3.2: The % FFA content of feedstocks used in the current work

	FEEDSTOCKS			
	WFO	**RFO**	**RCO**	**WCO**
***T (mL)**	2.9	1.2	0.1	2.1
% FFA	2.2	0.9	0.7	1.6
NaOH (g)	6.4	4.7	4.2	5.6

***T**= (Volume of standard solution)$_{\text{before the titration}}$ - (Volume of standard solution)$_{\text{after the titration}}$

While the % FFA content reached to a maximum in WFO, i.e., around 2.2 %, its lowest value was 0.1 % for RCO. The base-catalyzed transesterification process was preferred for all types of feedstocks since all had FFA contents less than 3 %.

3.3.3 Preparation of alcohol and catalyst solutions

NaOH and methanol were chosen as a catalyst and alcohol, respectively because of their availabilities and high purities. NaOH pellets were dissolved in methanol by agitating with magnetic stirrer at 500-600 rpm until the NaOH was completely dissolved in the alcohol.

The actual stoichiometry of transesterification reaction is 1 mole of oil for 3 moles of alcohol which results in 3 moles of FAME and 1 mole of glycerin as indicated Equation (3.1). This reaction is reversible, then usually 100 % excess alcohol is used in practice, i.e., 6 moles of alcohol for each mole of oil, thus an excess alcohol will shift the equilibrium to the right side of the equation, increasing the amount of products as may be inferred from the Le Chatelier's principle. six moles of methanol corresponds to a 1:4 alcohol-to-oil volume ratio that is 250 mL of methanol for 1000 mL of feedstock.

3.3.4 Transesterification process

Transesterification reaction was carried out in a 2.0 liter three-necked round glass flask that was coupled with a condenser, a magnetic stirrer, a T-type thermocouple and a heater as shown in Figure 3.2.

Figure 3.2: Transesterification reaction

Oil samples were poured into the reactor and heated up to a desired temperature using the heater of the magnetic stirrer at the bottom. The mixture of methanol and catalyst-NaOH was added to the reactor and all necks of the flask were closed tightly. A T-type thermocouple was fixed at the middle neck and connected a temperature controller. The mixture was agitated using magnetic stirrer at 900 rpm. Temperature of the reactor was adjusted either at 50 or 60°C and reaction time was fixed either at 60 or 90 min.

3.3.5 Separation process

The separation of reaction products was achieved by decantation, i.e., the immiscible mixture of FAME and glycerin were separated from each other by gravity. The less dense FAME was floated to the top and the denser glycerin was decanted from the bottom of the separation funnel. In the upper FAME layer, there could be the mono-, di-, and triglycerides which are indicated the incompleteness of transesterification process, while most of the catalyst and excess alcohol were concentrated in the lower glycerin layer. Impurities in the FAME prompt undesirable characteristics, for instance, increased cloud point and pour point, lower flash point. Hence, a purification process was necessary for the final product to comply with the BD standards.

Once the reaction was completed, the mixture was poured into a 2.0 L separation funnel and kept for a minimum of eight hours. Only two layers were obvious as desired for each batch. The less dense ester that is called FAME was separated by gravity and floated to the upper section of the funnel. The glycerol, excess methanol and undesired products were segregated to the bottom of the separation funnel and were decanted as shown in Figure 3.3.

Figure 3.3: FAME and glycerol mixture before gravity separation

The FAME separated was further treated with a purification processes. As well as FAME, glycerin also must be purified, nevertheless, due to the small glycerin yield, purification was not economically viable for experimental production.

3.3.6 Purification of FAME

In order to comply with the quality standards for BD, the separated impure FAME should be purified. Purification process involved washing, neutralizing and drying.

Successive washing with warm water removed the remaining impurities such as methanol, catalyst and glycerin since these contaminants were all water-soluble. Washing should be repeated until PH of the used washing water became 7.0 which was indicating all that impurities were neutralized. Only in the first washing step, acidified water used to make separation of base catalyst easier. Warm distilled water containing 0.1 wt % of H_3PO_4 and the equivalent volume of FAME were gradually mixed using a magnetic stirrer for five minutes. Then, the homogeneous mixture was transferred into the separation funnel. After the water was settled at the bottom of separation funnel as illustrated in Figure 3.4, it was decanted via a bottom-drain of the separation funnel. Two additional washing steps were made with warm distilled water hence, the removal of glycerol, catalyst, soap and excess methanol was assured.

Figure 3.4: Washing of BD with distilled water

Finally, the traces of water and alcohol must be removed by a drying step in an open container at 110°C. After drying, the purified product, i.e., the BD candidate as shown in Figure 3.5, was ready for the characterization tests following the international BD standards.

Figure 3.5: BD samples produced from four different feedstocks of the present survey

3.4 Optimization of Experimental Parameters by the Taguchi Method

Taguchi techniques were developed by Taguchi and Konishi (Taguchi and Konishi, 1987). This technique optimizes the process by determining the effect of each parameters. In the Taguchi technique, the experimental design (DOE) is used to optimize many engineering applications that is providing optimum use of process parameters. DOE via the Taguchi method uses a set of orthogonal arrays for performing of a minimum number of experimental trials. In this study, DOE was applied to obtain optimum process parameters leading to maximum BD yield during base-catalyzed transesterification process.

The Taguchi method offers a method to optimize the effect of selected parameters on process and this could be done with the minimum number of experiments. Roy (2001) summarized briefly the standard Taguchi DOE procedure as follow:

- Determination of the quality characteristic to be optimized: The quality characteristic is simply the response variable of the process or output. In this study, quality characteristic is chosen as the BD yield.

- Identification of the control parameters and their alternative levels: Control parameters affects the process directly or indirectly such as catalyst/alcohol type or amount, process temperature/pressure which are adjustable at different level.
- Design of the matrix experiment: Taguchi offers many standard orthogonal arrays to reveal the factors that degrade control parameters. Those orthogonal arrays describe the number of experiments that must be performed using different levels of control parameters chosen and the effect of the noise factors on the quality characteristic.
- Conducting the matrix experiment: Experiments are conducted by using the chosen orthogonal array and results are recorded.
- Analyzing the data and determination of the optimum levels: To analyze the results of the experiments and to determine the effect of control parameters, the Taguchi method uses a statistical measure of performance called signal to noise (S/N). S/N ratio is the ratio of the mean (signal) to the standard deviation (noise) and could be represented by different ways such as; Smaller-the-better, Nominal-the-best, Larger-the-best.

The Taguchi's DOE technique was implemented here to optimize process parameters to ensure high BD yield. The orthogonal array was designed using three control parameters, i.e., the molar ratio of alcohol to oil, reaction temperature and reaction time for the production of BD from WFO, RFO and WCO. Other parameters such as catalyst/alcohol type and catalyst concentration were used in DOE as control parameters in the previously reported studies (Kim et al., 2010, Buasri et al., 2009) therefore, in this study they were kept constant. The three selected parameters at two-levels, i.e. L-4 (2^3), are given in Table 3.3. L-4 refers to a Latin square and the experiment replication number.

Table 3.3: The DOE developed with three parameters at two levels for production of BD

Parameters	**Levels**	
	1	2
Molar ratio (oil/methanol)	1:4	1:6
Reaction temperature (°C)	50	60
Reaction time (min)	60	90

The effects of the diversity of control parameters on the BD efficiency, the orthogonal array design was performed with the experimental conditions as shown in Table 3.4. The numbers in Table 3.4 indicate the levels of the parameters.

Table 3.4: The L-4 (2^3) orthogonal array design experiment of the current work

	Parameters and their levels		
Experiment no.	Molar ratio (oil/methanol)	Reaction temp. (°C)	Reaction time (min)
1	1	1	1
2	1	2	2
3	2	1	2
4	2	2	1

Three independent variables with two level each requires 8 runs (i.e. 2^3) however, using Taguchi's DOE, the number of experiments are reduced to 4. If, one more independent variable and one more level were added i.e. L-9 ($3^4 = 81$), 9 experiments would be sufficient to determine the optimum condition instead of performing 81 experiments.

In this study, the DOE with L-4 orthogonal array was implemented for WFO, RFO and WCO to select the level of process parameters which give the maximum BD yield. To see the validation of the proposed method, RCO was converted to BD with optimum levels of the control parameters being studied those were obtained from Taguchi DOE Method.

3.5 Measurement of Biodiesel Properties

To ensure the quality of the BD produced, some of its critical properties were also investigated in addition to the cold flow properties (CFP). The properties measured were: ester content (mass %), EN 14103; viscosity at 40 ˚C (mm^2s^{-1}) (Oluwoye, 2013), ASTM D 445 or EN- ISO 3104; cloud point (CP, ˚C), ASTM D2500 or ISO 3015; cold filter plugging point (CFPP, ˚C), ASTM D6371 or EN 116; pour point (PP, ˚C), ASTM D97 or ISO 3016; free and total glycerol (mass%), TS EN 14105; calorific value (HHV, MJ/ kg) ASTM D4809; iodine value (IV, g I_2/100g) TS EN 14111. Ester content, free and total glycerol, calorific value and iodine value were determined by the Vitsan Laboratory (Dilovası, Kocaeli, Turkey) following the TS EN and ASTM standards.

3.6 Experimental set-up for CFP measurements

The experimental setup built following the ASTM D2500, ASTM D97 and ASTM D6371 standards are shown schematically in Figure 3.6.

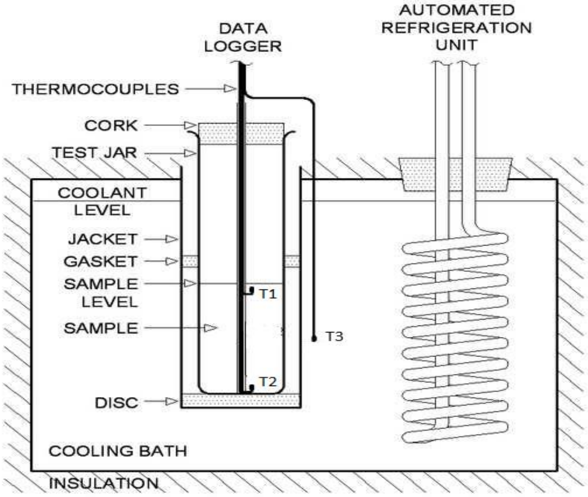

Figure 3.6: Experimental set-up for CFP measurements

An insulated cooling bath was filled with ethanol as the coolant. Ethanol was cooled down and its temperature was controlled by an automated refrigeration unit. A stirrer was used to assure the thermal homogeneity of the ethanol in the cooling bath. An aluminum cylinder jacket was placed in the middle of the cooling bath. A 6 mm thick cork disk was located at the bottom of the jacket as a thermal insulator. The glass test jar was filled with BD sample to a level of 54 mm corresponding to a sample volume of about 45 ml. The test jar was then fitted into the jacket and a uniform air gap of 5 mm in the radial direction between the test jar and the jacket was ensured by a gasket. Three T-type thermocouples for temperature readings were employed. Thermocouples T1 and T2 were used to measure the temperature of BD sample but T3 which was employed to measure the temperature of ethanol in the vicinity of the jacket close to the mid-section. Thermocouple T1 was fixed 3 mm below the surface of the sample for PP measurement whereas T2 was placed 3 mm above the inside bottom of the test jar for the determination of CP and CFPP. A vacuum system and a pipette with a filter unit were prepared in addition to the setup shown in Fig. 3.6 for CFPP measurements as described in ASTM D6371 and EN 116. The flow rate of the vacuum source was adjusted to 15 L/h, at 200 mm water of vacuum. Two layers of filters were used, each having a nominal aperture size of 160 µm and a nominal wire diameter of 80 µm as can be seen in Figure 3. 7.

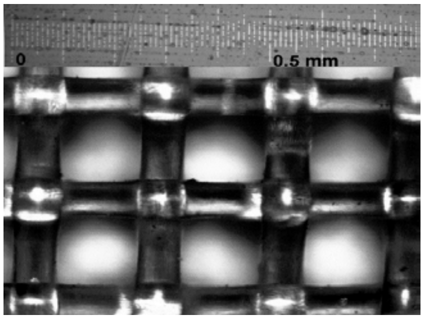

Figure 3.7: Mesh of plastic filter used in CFPP measurements

3.7 Results and Discussion

3.7.1 Determination of optimum experimental conditions using the DOE

Average percent yield of WFO based BD (WFOME), RFO based BD (RFOME), RCO based BD (RCOME) and WCO based BD (WCOME) were estimated using the Equation 3.3, 3.4 and 3.5 (Phan and Phan, 2008) and results are shown in Table 3.5 as % yield.

$$\% \, Yield = \frac{m_{ester}}{3 \times \frac{m_{oil}}{MW_{oil}} \times MW_{ester}} \tag{3.3}$$

$$MW_{oil} = 3 \times \sum_i (MW_i \times \% \, m_i) + 38 \tag{3.4}$$

$$MW_{ester} = \sum_i (MW_i \times \% \, m_i) + 14 \tag{3.5}$$

where MW_i is the molecular weight of FA_i; m_i is the mass percentage of FA_i in the feedstock that was obtained by GC analysis. MW_{oil} and MW_{ester} are the averaged molecular weight of feedstock oil and FAME produced, respectively.

The yields of WFOME, RFOME and WCOME produced using four different experimental conditions are given in Table 3.5. All experiments were performed in accordance to the conditions of control parameters that are specified in Table 3.4. The mean yield of BD produced has the highest value with 97.7 % in experiment no. 4 and seemed to be the optimal experimental conditions, whereas Experiment no. 1 has the lowest BD yield of 72.4 %. As Taguchi proposed, selecting the optimal conditions the mean yield of BD produced is not sufficient alone, also the signal-to-noise (S/N) ratio should be determined in order to describe the quality characteristics deviating from the desired value. Using the 'Larger-the-best' application, the S/N ratio were evaluated from the Equation 3.6.

$$\frac{S}{N}\, ratio = -10\, log(MSD) \qquad (3.6)$$

where *MSD* is mean squared deviation and can be calculated as,

$$MSD = \frac{1}{n}\sum_{i=1}^{n}\left(\frac{1}{y_i}\right)^2 \qquad (3.7)$$

where *n* is the number of repetitions of each experiment and y_i the yield of BD produced.

The calculated S/N ratios for the four sets of experiments are also shown in Table 3.5. The mean BD yield and the S/N ratio were 82.7 % and 38.266, respectively. Levels of control parameters of Experiment no. 4 could be chosen as optimum where the highest mean yield of BD and the largest S/N ratio was obtained.

The mean S/N ratio could also be used to show the effects of each level for each parameter. Each experimental parameter should be considered individually and the interactions at the assigned levels should be calculated by taking the average of all the S/N ratios. This can be illustrated considering one of the control parameter. If the oil/methanol molar ratio and its level 1 (1:4) are considered, the mean S/N ratio (37.328) can be calculated using the values

(37.183 and 37.472) from experiment no. 1 and 2. When its level 2 (1.6) is being considered then, the mean S/N ratio (39.204) can be calculated using the values (38.613 and 39.795) from experiment no. 3 and 4, and so on. The mean S/N ratio for each level of the three influential parameters are summarized in Table 3.6.

Table 3.5: WFOME, RFOME and WCOME yields and the S/N ratios in the four sets of experiments

Experiment no.	Yields of BD produced				
	WFOME	RFOME	WCOME	Mean	S/N Ratio
1	69.4	72.4	75.5	72.4	37.183
2	72.4	73.5	78.8	74.9	37.472
3	78.6	86.6	92.2	85.8	38.613
4	97.2	97.8	98.0	97.7	39.795

Table 3.6: Mean S/N ratio of the three influential parameters

Parameters	S/N Ratio	
	Level 1	Level 2
Molar ratio (oil/methanol)	37.328	39.204
Reaction temperature (°C)	37.898	38.634
Reaction time (min)	38.489	38.043

Magnitude of mean S/N ratio gives idea about which parameter and which level on that parameter has more impact yield of BD. The larger the S/N ratio will be the higher the BD yield. Thus, impacts order of the parameters on BD yield: molar ratio > reaction temperature > reaction time. The oil/methanol molar ratio is the most influential parameter on the yield of BD while reaction time has the smallest effect. As a result, the best reaction conditions based on the highest S/N ratio are for the first parameter (oil/methanol molar ratio) at level 2 (1:6), for the second parameter (reaction temperature) at level 2 (60°C) and the third parameter (reaction time at level 1 (60 min).

The production of BD from RCO performed under the optimum conditions to confirm their validity. The yield of RCOME was 98.1 %. Thus, yield of RCOME was very similar to that of yields of WFOME, RFOME and WCOME which were produced using optimum conditions of 1:6 oil/methanol molar ratio, 60°C as reaction temperature and 60 min as reaction time.

3.7.2 Characterization of the biodiesel produced

The BD samples produced were tested for their fuel properties following either ASTM D6751 or EN 14214 standard. The ASTM D6751 identifies that the parameters of the pure BD (B100) should fulfill before being used as a pure fuel or blended with the current diesel fuel. On the other hand, EN 14214 describes the minimum requirements for FAME. In Table 3.7 the fuel properties of the four BD samples determined are listed with the limits given in the ASTM and EN standards.

Table 3.7: The fuel properties of WFOME, RFOME, RCOME and WCOME of the present study

	Method	**Limits**	**WFOME**	**RFOME**	**RCOME**	**WCOME**
Kinematic viscosity at 40 ˚C (mm^2/s)	ASTM D 445	1.9-6.0	4.666	4.637	4.582	4.589
Higher heating value (MJ/kg)	ASTM D 4809	35.0	40.14	40.98	39.23	38.88
Free glycerin (wt %, max.)	EN 14105	0.02	0.006	0.003	0.003	0.005
Total glycerin (wt %, max.)	EN 14105	0.25	0.248	0.210	0.196	0.199
Mono glyceride (wt %, max.)	EN 14105	0.80	0.62	0.62	0.64	0.66
Diglyceride (wt %, max.)	EN 14105	0.20	0.32	0.20	0.20	0.20
Triglyceride (wt %, max.)	EN 14105	0.20	0.34	0.24	0.1	0.12
Ester contents (wt %, max.)	EN 14103	96.5	96.5	96.8	97.0	96.8
Linoleic acid methyl esters (wt %, max.)	EN 14103	12.0	0.2	1.04	6.8	4.5
Iodine value (g I_2 / 100 g, max)	EN 14111	120	110	89	66	69
Cloud point (˚C)	D 2500		15	15	-3.5	-2
Pour point (˚C)	D 97		12	11	-10	-9
Cold filter plugging point (˚C)	D 6371		14	13	-7.5	-7

The viscosities of BD produced from all of the feedstocks were greater than that of PD (2.98 mm^2/s measured at 40°C), nevertheless they were in the range of ASTM D6751. The kinematic viscosities of BD samples from frying oil and canola oil were found to be similar for both their virgin and used forms.

Iodine value is associated degree of unsaturation of FAME and included in EN 14214 specifications to fortify oxidative stability of the fuel. The higher the iodine value, lower the oxidation stability. Thus, the canola oil based BD appeared to be more stable than the frying oil based BD.

All samples accomplished the free and total glycerin requirements which are specified as 0.02 % and 0.25 %, respectively in EN 14214. It should be noted that the total glycerin level of WFOME is 0.248 that is almost the upper limit, this could be prevented by longer settling times and additional washing.

Although the calorific value is one of the critical parameters in the selection of a fuel that is not specified neither in ASTM D6751 nor EN 14214 standard, it is prescribed in EN 14213 (BD for heating purpose) with a minimum value of 35 MJ/kg which is lower than calorific value of PD i.e. 45.825 MJ/kg (Silintigo et al., 2013). This can also be seen in Table 3.7 as higher heating values of BD produced from all feedstocks were lower than PD hovewer, within the limits of the EN 14213 standard.

The CFP of BD produced from all feedstock can be considered as poor as compared with the commercial diesel no:2 fuel which has CP -16 ˚C, PP -27 ˚C and CFPP -18 ˚C. The WFOME and the RFOME showed inferior CFP as compared to the RCOME and WCOME. This behavior is attributed primarily on the large amounts of saturated fatty acid compounds present in frying oil samples and a high content of palmitic acid portions. Udomsap et al., 2008 noted that high content of palmitic acid (63 wt %) in palm stearin methyl ester caused an extreme increase in CP and PP values and reported as 18 ˚C and 19.4 ˚C, respectively.

According to the information taken from the Meteorology Department of Lefkoşa, the lowest average temperature was observed in the vicinity of 2 ˚C within last ten years in January and February in Nicosia as shown in Figure 3.8. All three CFP temperatures of the BD produced from WFO and RFO were above 2 ˚C. It appears that the pure WFOME and RFOME can be suitable from May to October, i.e. in the six months of a year in Nicosia while RCOME and WCOME can be used whole year. A common remedy to improve cold flow temperatures including CFPP is to blend commercial diesel fuel into the BD.

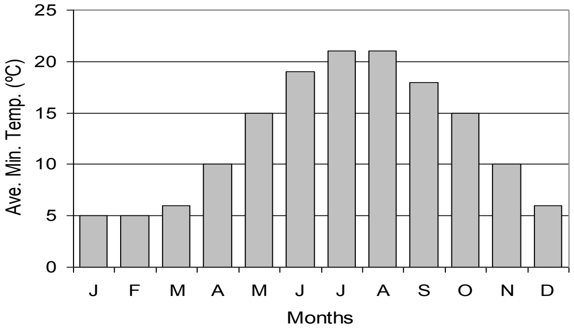

Figure 3.8: Monthly average minimum temperatures in Nicosia during a year

3.7.3 Effect of blending in improving the CFP of WFOME

To investigate the effect of blending on lowering cold flow temperatures of WFOME, three approaches were followed:

- First approach; WFO and RCO were blended in different proportions before being transesterified. Since the aim was to lower CFP of WFOME, up to 50 volume (vol) % RCO was blended with WFO. Blends were named according to their content, such as 100W0C, 90W10C and so on. In 100W0C, 100 vol % WFO was blended with 0 vol % RCO.
- In the second approach; the RCOME and the WFOME were mixed together in different vol %. WFOME was blended with 0, 25, 50, 75 and 100 vol % RCOME.
- In the third approach; WFOME was blended with a commercial diesel fuel on a volume basis. The commercial diesel fuel was the Euro diesel (EN 590:2009) that was purchased from a petrol station in Lefkoşa. Blends containing 0, 5, 10, 20, 30, 40, 50, 70, 80, 90 and 100 vol % commercial diesel were prepared.

CFP of BD produced from WFO and RCO mixtures are given in Table 3.8 and their relations are presented in Figure 3.9. All CFP temperatures tend to decrease with increasing RCO content in the BD samples.

Table 3.8: CFP temperatures of WFO and RCO blends-based BDs

	RCO content (Vol %)	CP	PP	CFPP
100W0C	0	15	12	14
90W10C	10	15	7.5	13
80W20C	20	13	4.5	11
70W30C	30	12	4	9.5
60W40C	40	10	2.5	6
50W50C	50	9	0.5	5.5
0W100C	100	-3.5	-10	-7.5

Results shows that mixing WFO with RCO before producing BD cause a decrease in CFP temperatures in the resulting BD samples. But, even up to 50 vol % of additional RCO did not provide suitable fuel to be able suitable in regional climate conditions.

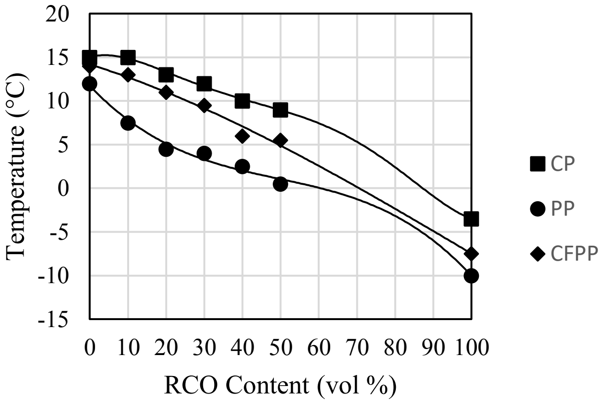

Figure 3.9: Effects of blending of WFO with RCO on the CFP temperatures of WFOME

While CP was correlated with the blend content of RCO by an empirical forth-order polynomial equation as shown in Equation 3.8. CFPP and PP were correlated with third-order polynomial equations as shown in Equation 3.9. In these equations, *X* is the RCO content in volume % and T is the temperature. The coefficients of the equations are given in Table 3.10 together with their coefficients of determination (R^2).

$$T = a + bX + cX^2 + dX^3 + eX^4 + fX^5 \tag{3.8}$$

$$T = a + bX + cX^2 + dX^3 \tag{3.9}$$

For the second approach, CFP temperatures of WFOME-RCOME mixtures are given in Table 3.9 and effect of blending are presented in Figure 3.10.

Table 3.9: CFP temperatures of WFOME and RCOME blends

	RCOME content (vol %)	CP	PP	CFPP
100WFOME0RCOME	0	15	12	14
75WFOME25RCOME	25	14	6.5	8
50WFOME50RCOME	50	9	3.5	4.5
25WFOME75RCOME	75	3	-1	0
0WFOME100RCOME	100	-3.5	-10	-7.5

Although all CFP temperatures tend to decrease with increasing RCOME content, only 25 vol % WFOME and 75 vol % RCOME mixtures could be used whole year except January and February. Other two blends which are 75WFOME-25RCOME and 50WFOME-50RCOME could be used only six months from May to October.

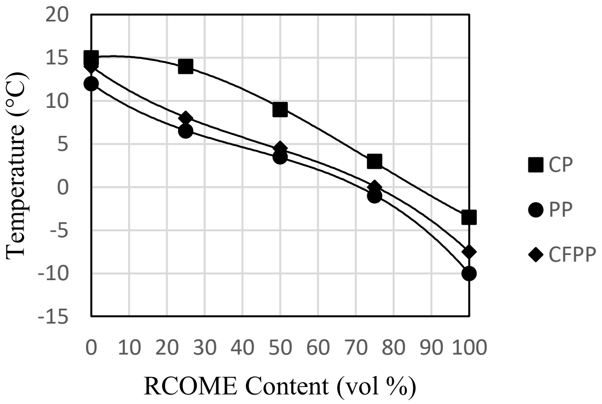

Figure 3.10: Effects of blending with RCOME on the CFP temperatures of WFOME

All three CFP temperatures, CP, CFPP and PP were correlated with the blend composition by an empirical third-order polynomial equation as shown in Equation 3.9. In this equations, *X* is the RCOME content in vol % and *T* is the temperature. The coefficients of the equations are given in Table 3.10 together with R^2.

For the third approach, CFP of WFOME BD - Commercial PD blends were determined and are presented in Figure 3.11. It can be seen that CP, CFPP and PP tend to decrease with increasing commercial diesel content. The only exception was observed in CP behavior; up to 50 % commercial diesel addition CP remained constant causing increase in difference between CP and CFPP. A rapid decrease in CP was observed when the commercial diesel concentration is kept between 70 to 90 %. The difference between CP and CFPP converges to 2°C at 100 % commercial diesel as it was initially found also for the pure BD.

The current EN 590 gives six CFPP grades for various temperate climates. They change from Grade A to Grade F covering a range of CFPP from 5°C to -20°C. After determining CFPP at -4°C for the commercial diesel, it was concluded that the diesel purchased for blending was corresponded to Grade C in the EN 590 standard.

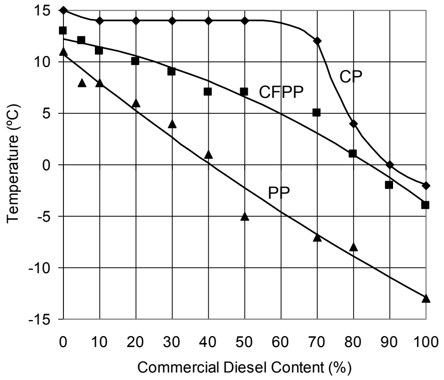

Figure 3.11: Effects of blending with EN 590:2009 commercial diesel fuel on the CP, CFPP and PP temperatures of WFOME

Tang et al, 2009, correlated the CP and PP with the blend compositions by empirical second-order polynomial equations. However, no correlation was given for CFPP. The CP curve in

Figure 3.11 can be correlated to the blend composition below 70% by an empirical fifth-order polynomial equation and by a heat capacity model above 70% commercial diesel addition which are given in Equation 3.10 and Equation 3.11, respectively. CFPP and PP were correlated with the blend composition by an empirical second-order polynomial equation as shown in Equation 3.12. In these equations, X is the commercial diesel content in % and T is the temperature. The coefficients of the equations are given in Table 3.10 together with R^2.

$$T = a + bX + cX^2 + dX^3 + eX^4 + fX^5 \qquad \text{for} \quad X \leq 70\ \% \tag{3.10}$$

$$T = a + bX + cX^{-2} \qquad X \geq 70\ \% \tag{3.11}$$

$$T = a + bX + cX^2 \tag{3.12}$$

Bhale et al, 2009, reported that crystal growth inhibitors, also known as pour point depressants, reduce PP of BD. On the contrary, they usually have no effect on CP and CFPP at low temperatures. It appears from Figure 3.11 that the commercial PD fuel can be a good PP and CFPP depressant in all blends. However, to lower the CP, blending becomes effective only above 70% concentration in the blend.

Table 3.10: Coefficients of the empirical correlations of the CP, CFPP and PP in WFOME blends

Approac	**CFP**	**Blend Content (vol %)**	**Correlation**	**Coefficients**						**R^2**
				a	***b***	***c***	***d***	***e***	***f***	
1	CP	0-100 % RCO	Eq. (3.8)	15.026	0.1173	-0.0177	0.0005	-6x10^{-6}	2x10^{-8}	0.9988
	PP	0-100 % RCO	Eq. (3.9)	11.722	-0.4576	0.074	-5x10^{-5}	--	--	0.9942
	CFPP	0-100 % RCO	Eq. (3.9)	14.184	0.1366	-0.0012	4x10^{-6}	--	--	0.9944
2	CP	0-100 % RCOME	Eq. (3.9)	15.036	0.0455	-0.042	2x10^{-5}	--	--	0.9996
	PP	0-100 % RCOME	Eq. (3.9)	11.986	-0.3095	0.0046	-4x10^{-5}	--	--	0.9999
	CFPP	0-100 % RCOME	Eq. (3.9)	13.979	-0.316	0.0039	-3x10^{-5}	--	--	0.9999
3	CP	≤ 70 % Diesel	Eq. (3.10)	14.999	-0.21131	0.01575	-0.00053	1x10^{-5}	-1x10^{-7}	0.9999
		≥ 70 % Diesel	Eq. (3.11)	-66.016	0.39324	247288	--	--	--	0.9999
	CFPP	0 -100 % Diesel	Eq. (3.12)	12.170	-0.06413	-0.00095	--	--	--	0.9890
	PP	0 -100 % Diesel	Eq. (3.12)	10.714	-0.28405	0.00048	--	--	--	0.9889

CHAPTER 4

DESIGN AND MANUFACTURE OF AN EXPERIMENTAL REACTOR FOR PRODUCTION OF BIODIESEL VIA SUPERCRITICAL METHANOL

4.1 Overview

Catalytic BD production is a time and energy consuming process due to feedstock preprocessing, product separation and purification steps. Non-catalytic BD production using supercritical alcohol may facilitate these preprocessing, separation and purification stages.

The use of a supercritical alcohol as solvent for BD production as compared to catalytic BD production is a straightforward approach (Saka and Kusdiana, 2001; Demirbas, 2006). In supercritical method, homogeneous phase between the supercritical alcohol and the triglycerides can be created at high pressures (>5 MPa) and high temperatures (>200 °C). Supercritical reaction can proceed in the absence of any catalyst and separation process of the BD from glycerol is simpler since many discrete operations such as catalyst purification are not required. Even though supercritical method requires the use of high temperatures and pressures, it could be a more advantageous choice over conventional technologies.

To be able to produce BD using supercritical fluid method a batch type of reactor was designed and manufactured to overcome extreme process conditions of high temperature and pressure. Finally, using the designed supercritical reactor, canola oil was converted into BD using the supercritical methanol.

4.2 Supercritical biodiesel production

Cengel and Boles (2008) defines critical point in their *Thermodynamics, an Engineering Approach* book as the point at which the saturated liquid and saturated vapor states are identical. Table 4.1 gives critical properties of some solvents which are used commonly in supercritical BD production.

At supercritical state that is above the critical point; the phase boundary between liquid and vapor disappears, and the substance can be considered as both liquid and vapor. The relevant phase diagram of methanol is shown in Figure 4.1. Supercritical methanol (SCM) exhibits a liquid-like density and gas-like transport properties (i.e., diffusivity and viscosity). At high temperature and pressure, density and viscosity of SCM decreases and its mass diffusivity increases. Thus, single phase characteristics makes methanol a better solvent.

Table 4.1: Critical properties of some solvents (Yaws, 1999)

Solvents	**Critical Temperature (K)**	**Critical Pressure (bar)**	**Critical Density (g/cm^3)**
Methanol	512.58	80.96	0.2720
Ethanol	516.25	63.84	0.2760
Water	647.13	220.55	0.3220

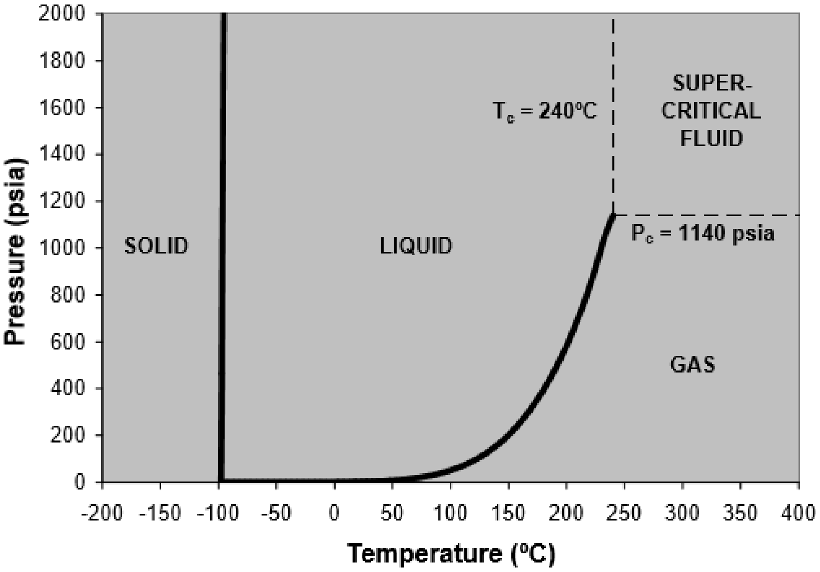

Figure 4.1: Phase diagram of methanol (Ebert, 2008)

Another property to describe the solvent strength of methanol is its solubility parameter. Solubility parameter predicts whether solute could be dissolve in the solvent or not. If both solute and solvent have similar solubility parameters, it implies that they will mix easily and homogeneously. Hansen parameters are used to predict the solubility parameter of a substances (Hansen, 1999). Table 4.2 shows Hansen solubility parameters of methanol (i.e. solvent), soybean oil that represents triglyceride (i.e. solute), oleic acid (FFA, also could be considered as solute) and water (as an example of common solvent) at atmospheric conditions (25°C and 1atm) and at supercritical conditions of methanol (300°C and 112 atm).

Table 4.2: Comparison of solubility parameters of common components of BD (Hansen, 1999)

Substance	Solubility Parameter $MPa^{0.5}$ at (25°C and 1atm)	Solubility Parameter $MPa^{0.5}$ at (300°C and 112atm)
Methanol	29.61	7.93
Soybean Oil	17.37	5.96
Oleic Acid	15.60	10.66
Water	47.90	27.56

Maximum solubility occurs, when both solute and solvent have similar solubility parameters, and this happens when their solubility parameters around 5.2 $MPa^{0.5}$ (Schulte, 2007). At atmospheric conditions, there is a big difference between solubility parameters of methanol (29.6) and that of soybean oil (17.4) and oleic acid (15.6), so they are hardly dissolve one in another and a catalyst is necessary to increase solubility. When methanol is under supercritical conditions, its solubility parameter (7.93) very close to that of soybean oil (5.96) and oleic acid (10.66) and they can dissolve easily one in another. Therefore, transesterification of triglycerides with SCM (typically above 250°C and 80 MPa or higher) due to high solubility of components occurs within few minutes (Saka and Kushdiana, 2001) while at atmospheric condition without using catalyst it takes more than ten hours (Diasakou et al., 1998) where additional catalyst increases reaction rate and completion occurs approximately within one hour in the case of a base catalyst (Freedman et al., 1986).

The shorter reaction time is not only reason in BD production by supercritical method. While base catalyzed transesterification is conventional method for BD production, there is some limitation in feedstock used such as FFA and water content, long time period for purification process of reaction products and the large amount of waste water generated (Meher et al., 2006; Sharma and Singh, 2009). To overcome such drawbacks, in 1998 Diasakou et al. developed non-catalytic transesterification using methanol. In their correspondence work, reactions occurred at subcritical temperatures (240°C, 220°C, 235°C) of methanol. And 2001, Saka and Kusdiana successfully produced first BD by SCM from rapeseed oil at 350°C and 450 bar in a 5 mL- Inconel 625 batch reactor and reaction was completed in 5 min with

95 % conversion. Later, many other researchers studied supercritical transesterification of various oils at different temperatures and pressures with different reactor sizes and also achieved high conversion within short times. Table 4.3 adopted from summary of some of these research which have reviewed by Pinnarat and Savage (2010) and Silva and Oliveria (2014). In all of these works listed in the table methanol was used as supercritical fluid.

Table 4.3: Some SCM transesterification of various vegetable oils

Temperature Pressure	**Oil type**	**Oil :Alcohol (molar ratio)**	**Reaction time**	**Reactor type**	**Conversion of methlyester**	**Reference**
350°C, 450 bar	rapeseed	1:42	4 min	5 mL,BR Inconel	>95 %	Saka and Kushidiana, 2001
350°C, Not recorded	hazelnut	1:41	5 min	100 mL, BR, SS	95 %	Demirbaş, 2002
350°C, 200 bar	sunflower	1:40	40 min	8 mL, BR, SS	96 %	Madras et al., 2004
350°C, 180 bar	coconut	1:42	7 min	TR,SS	95 %	Bunyakiat et al., 2006
280°C, 250 bar	soybean	1:42	30 min	200 mL BR	90 %	He et al., 2007
300°C, 150 bar	soybean	1:40	20 min	BR	70 %	Wang et al., 2008
350°C, Not recorded	palm oil	1:40	20 min	BR	80 %	Tan et al., 2010
350°C, 350 bar	palm olein	1:40	~15min	TR	85 %	Choi et al., 2011
270°C, 100 bar	waste canola	1:1 (mass ratio)	45 min	BR	96.4 %	Lee et al., 2012

BR: batch reactor; TR: tubular reactor; SS: stainless steel

In previous studies, while maximum operating pressure, operating temperature and reactor size were 450 bar (Saka and Kushidiana, 2001), 350°C (in many researches) and 200 mL (He et al., 2007), their minimum values were 100 bar, 270°C (Lee et al., 2012) and 5 mL (Saka and Kushidiana, 2001), respectively.

One of the aim of this thesis was to produce BD using SCM, to do so first a reactor was designed to satisfy the SCM's operating conditions then, it was manufactured. Once reactor was designed and constructed in bench scale, then it could be extended to a larger scale. Investigating the problems on construction and during operation, massive BD production will be easier.

4.3 Supercritical Reactor Design for Biodiesel Production

There are four parameters that should be decided before designing a reactor for the production of the BD using SCM.

1. Maximum operating pressure
2. Maximum operating temperature
3. Reactor size
4. Materials of construction

4.3.1 Maximum operating pressure

Reactors used for supercritical reactions are high pressure vessels. In the case of SCM, the minimum operating pressure is 78.6 bar (1140 psi) which is critical pressure of methanol as can be seen in Fig. 4.1, while maximum operating pressure that could be applied was 450 bar as in the Saka and Kushidiana’s work. Design pressure should be 5-10 % greater than that of maximum operating pressure (Moss, 2004). Since design pressure is used to assign the most severe conditions, it was chosen as 470 bar. Maximum operating pressure is the most important parameter in a reactor design because most of the calculations are based on it such as the nominal thickness of the reactor.

4.3.2 Maximum operating temperature

In high pressure and temperature operations such as supercritical transesterification in addition to the pressures temperatures are also high. For this case, since operating pressure was considered from 80 bar (that is critical pressure of methanol) to a maximum 450 bar, corresponding operation temperature could be chosen from minimum 240°C that is critical temperature of methanol to 350°C. Temperature is an important design parameter, specifically high temperature associates thermal expansion and corrosion, material selection should be concentrated on the operating temperature. Also, maximum allowable working stress is evaluated according to the maximum operating temperature.

4.3.3 Reactor size

One of the aim of the current survey was to measure fuel properties of BD after its production. Most of the devices which are designed to measure BD fuel property (such as

CP, PP, CFPP, viscosity etc.) require at least 10 mL of fuel samples. Beside this, amount of methanol used in BD production by SCM is very high that is usually 1:40 oil to alcohol mole ratio (that corresponds to approximately 1:2 oil to alcohol volume ratio). To be able to produce a minimum 100 mL of BD, the reactor should be minimum 400 mL. Reactants cannot be filled up to the brim of the reactor, since should be a space left above the ingredients to provide a required operating pressures. As a result, it was decided to design a 600 mL batch reactor, hence amount of BD produced could be 125 mL.

4.3.4 Selection of material for reactor construction

Materials for construction of high pressure vessel should satisfy strength requirements, temperature characteristics and corrosion resistance (Peters and Timmerhaus, 2003). Besides, these factors also availability, cost and ease of fabrication are other factors those must be considered during material selection.

The most common and widely used construction materials for pressure vessels are stainless steels due to their high mechanical strength, corrosion resistance, ease of availability and low cost such as Grade 304 and Grade 316 as compared to Ni alloys. While Grade 304 is the standard "18/8" stainless (18 % Cr; 8 % Ni) with excellent welding and forming characteristics, Grade 316 is the standard molybdenum-bearing grade with better overall corrosion resistant properties than Grade 304 and also it has excellent welding and forming characteristics. Other metal alloys with higher chromium, nickel and/or molybdenum content such as Incoloy™ (53 % Fe, 25 % Ni, 15 % Cr), Inconel™ (5 % Fe, 58 % Ni, 22 % Cr, 9 % Mo), Hastelloy™ (2 % Fe, 66 % Ni, 1 % Cr, 28 % Mo) with excellent corrosion resistance and high stiffness are also suitable for high pressure vessels.

Among those factors mechanical strength of the chosen material for pressure vessels is the most important design factor for safety operation. Small pressure vessels should be designed in such a way that the operating pressure still too low to cause any crack to propagate in the vessel (‘‘yield before break’’), while for large pressure vessels, their safety design allows that the smallest crack that will propagate unstably has a length greater than the thickness of the vessel wall (‘‘leak before break’’) (Ashby, 2005).

The stress in the wall of a spherical pressure vessel with radius R is given by Equation 4.1;

$$\sigma = \frac{pR_i}{2t} \tag{4.1}$$

where σ is the working stress that is less than yield strength σ_f of the wall, R_i is the inside diameter and t is the thickness of the vessel. Since maximum operating pressure was chosen as 470 bar (47 MPa) and according to the ASME Section VIII, Division 1, paragraph UG27, wall thickness of high pressure vessel should be $t > 0.5\ R_i$, then maximum σ will be 47 MPa and also minimum σ_f will be 47 MPa. Wall thickness t at pressure p without yielding can be shown in Equation 4.2

$$t \geq \frac{pR_i}{2\sigma_f} \tag{4.2}$$

Thus, the minimum wall thickness is that with the largest yield strength σ_f where $\sigma_f \gg \sigma$. In a small pressure vessel if flaw is observed that should not have a diameter greater than a_c^*; then, the stress required for the crack propagate is given below;

$$\sigma = \frac{CK_{1C}}{\sqrt{\pi a_c^*}} \tag{4.3}$$

where C is a constant near unity, a_c^* is half of the flaw length and K_{IC} is the plane-strain fracture toughness of the material. Safety can be achieved by ensuring that the working stress is less than this. When Equations 4.2 and 4.3 are combined, the resultant Equation 4.4 will indicate the largest pressure (for a given R, t and a_c^*) is carried by the material with the greatest value of K_{IC}.

$$p \leq \frac{2t}{R} \frac{K_{1C}}{\sqrt{\pi a_c^*}} \tag{4.4}$$

In the case of false inspection or if a crack length greater than a_c^* appears, Equation 4.4 cannot be fail proof. Greater safety could be achieved by requiring that the crack will not propagate even if the stress reaches the yield strength of material. This condition is expressed by setting σ equal to the yield stress σ_y as shown in Equation 4.5,

$$\pi a_c \leq C^2 \left[\frac{K_{1C}}{\sigma_f}\right]^2 \tag{4.5}$$

The tolerable crack size a_c, is maximized by choosing a material with the largest value of K_{IC}/σ_f, this is the criteria that satisfy ‘‘yield before break’’. Figure 4.2 which was developed by Ashby (2005) is showing that the material selection criterion for safe design against fracture. Two criteria were considered for material selection;

i. $M_1 = \sigma_f > 47$ MPa

ii. The largest K_{IC}/σ_f; $M_2 = K_{IC}/\sigma_f$ ''yield before break''

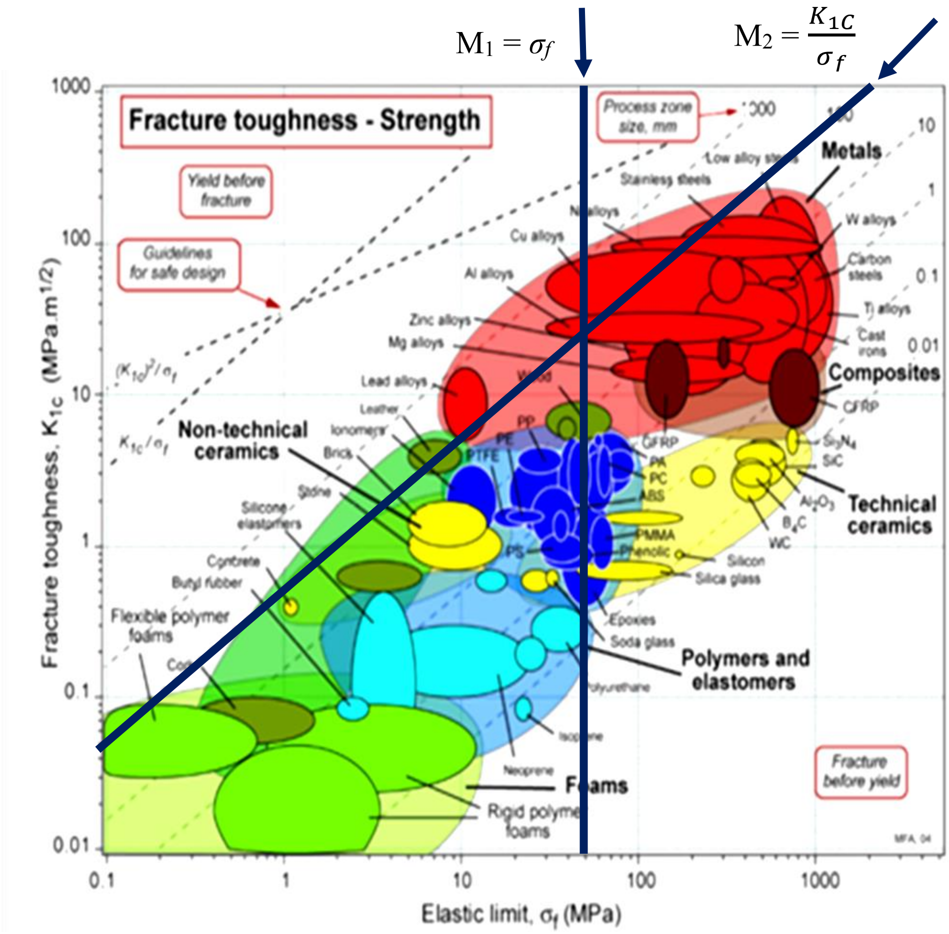

Figure 4.2: Material selection chart- fracture toughness, K_{IC} against strength, σ_f

A diagonal line corresponding to a constant value of $M_2 = K_{IC}/\sigma_f$ links materials with equal performance; those above the line are better. Stainless steels, nickel alloys, copper alloys and aluminum alloys are suitable materials for yield-before-break criteria but aluminum alloys are eliminated due to first criteria. To be able to choose the suitable material among these candidates, other factors such as corrosion resistance and cost should be evaluated.

Corrosion resistance of some common metal alloys due to transesterification medium are shown in Table 4.4 (Peters and Timmerhaus, 2003).

Table 4.4: Corrosion resistance of some constructional materials

Chemical	Iron and steel	Stainless steel Grade 304	Stainless steel Grade 316	Nickel (Inconel^{TM})	Copper (Monel^{TM})	Red brass	Aluminum
Fatty acids	C	A	A	A	A	C	A
Methanol	A	A	A	A	A	A	A
Oleic acid	C	A	A	A	A	C	A
Glycerol	A	A	A	A	A	A	A
Methyl esters	C	A	A	A	A	C	A

A= acceptable, can be used successfully, C= caution, resistance varies widely depending on conditions

Costs is another important criteria for material selection and Table 4.5 presents purchased cost for various type of metal alloys compared to that of cost of steel in plate form.

Table 4.5: Comparison of purchased cost for metal and metal alloys

Material	Ratio $= \frac{\text{cost per pound for metal}}{\text{cost per pound for steel}}$
Flanged quality steel	1
Aluminum (99 plus)	6
304 stainless steel	7
Copper (99.9 plus)	7
316 stainless steel	10
Monel	10
Nickel	12
Inconel	13
Hastelloy	15

Compare to nickel rich alloys (such as Inconel, Incoloy, Hastelloy) stainless steels (304 and 316) are more preferable due lower cost. As a result, 316 stainless steel was found to be the best choice of material for the reactor planned to be designed for supercritical BD production. Table 4.6 shows some useful material properties of 316 stainless steel that was selected from ASME Section VIII, Div. 2, Table AMG-1 and AMG-2.

4.3.5 Dimensions and minimum thickness of the reactor

The necessary wall thickness for metal vessels is a function of

i. yield point of the metal at the operating temperature,
ii. the operating pressure,
iii. the diameter of the tank and
iv. the joint or welding efficiency.

Table 4.6: Material properties of stainless steel-Grade 316

Properties	
Chemical Composition	Fe; < 0.03 C; 16-18.5 Cr; 10-14 Ni; 2-3 Mo; < 2 Mn; < 1 Si; < 0.045 P; < 0.03 S
Young' Modulus	205 GPa
Elastic Limit (σ_f)	310 MPa
Poison's Ratio	0.275
Ductility	0.51
Tensile Strength	620 MPa
Maximum Allowable Working Stress (*S*)	117 MPa
Fracture Toughness	278 MPa.m$^{1/2}$
Maximum Service Temperature	1198 K
Minimum Service Temperature	0 K
Thermal Expansion	18 µm/m.K
Minimum Specified Yield Strength (σ_y)	at 200°C: 160 MPa at 300°C: 136 MPa at 400°C: 123 MPa

Based on the ASME Boiler and Pressure Vessel Code as specified in Section VIII of Division I, minimum wall thickness t of monobloc cylindrical solid vessel could be calculated by Equation 4.6 as follows

$$t = r_i \left(\frac{SE_j+P}{SE_j-P}\right)^{1/2} - r_i + C_c \qquad \text{if } P > 0.385\,SEj \qquad (4.6)$$

where P is maximum operating pressure inside of tank (47 MPa);

S is maximum allowable working stress (117 MPa);

Ej is efficiency of joints that can be taken as 1.0 if, fully radiographed;

r_i inside radius of the shell, before corrosion allowance is added (31.5 mm)

Cc is the allowance for corrosion (could be taken as 1 mm or 0 mm- no corrosion risk)

Then, $t \geq 17.7$ mm and outside diameter of the reactor could be determined by ($2r_i+2t$) that will be equal to 115 mm. Also, length of the reactor should be equal or greater than 192 mm to satisfy the volume of the reactor volume, i.e. 600 mL.

4.3.6 Construction of the reactor

Detailed technical drawing of the reactor including vessel, hatch and clamps are shown in Figure 4.3. Dimensions of the vessel are shown in Figure 4.4 and the detailed technical drawings of hatch and clamps including their dimensions are given in Appendix 8.

Reactor manufactured by Tümtes Company, İstanbul from 316 stainless steel that was a single cylindrical block and to give desirable shape it was drilled and grinded (no welding). A photograph of the plain reactor (without equipped and accessorized) that was manufactured is shown in Figure 4.5.

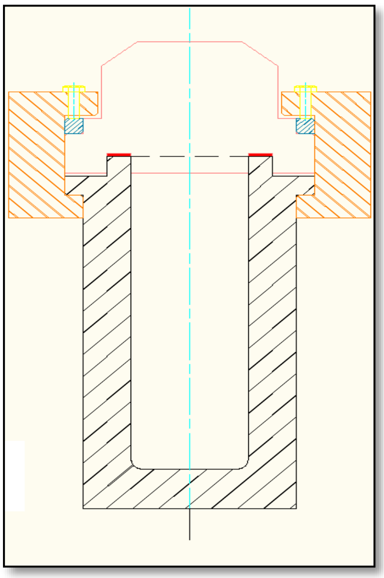

Figure 4.3: Technical drawing of designed vessel, hatch and clamps

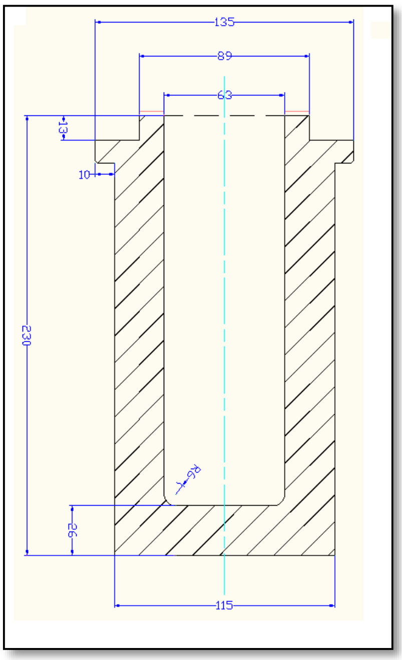

Figure 4.4: Technical drawing of pressure vessel with dimensions

Figure 4.5: Photograph of manufactured vessel, hatch and clamps

4.3.7 Equipment of the reactor

The reactor were equipped with some devices as illustrated in Figure 4.6. Their functions will be explained briefly below.

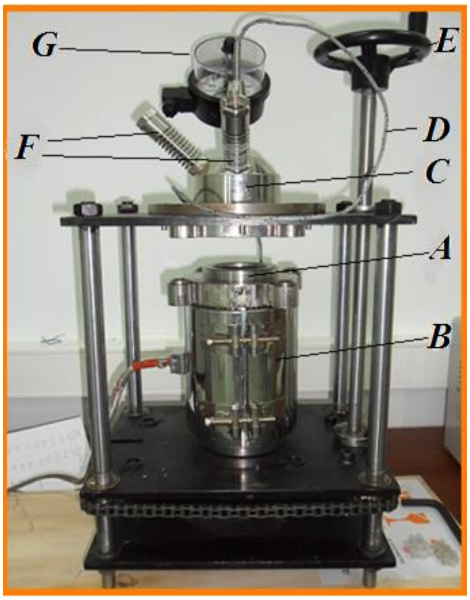

A: Pressure vessel

B: Electrical external heater

C: Hatch (vessel cover)

D: Thermocouple

E: Adjusting lever

F: Extruded fins

G: Reactor pressure gauge

Figure 4.6: The reactor manufactured for supercritical BD production

Electric heater (heating mantle) wrapped around the pressure vessel was used to reach supercritical temperatures. Heating mantles generally distribute heat evenly over the surface of the vessel and exhibit less tendency to generate harmful hotspots. The heater powered by a 3000 W power supply. During an operation, the heater was controlled manually, besides an automatic control was also available. Heat insulation outside of the heating mantle was made with an insulating material which was fire proof. Insulation helped to prevent unnecessary heat loss of the reactor.

A pressure gage, measuring 0-400 bar with a T316 stainless steel Bourdon tube, was mounted to the head with a coned adapter fitting similar to those used for the inlet/sampling valve assembly. The gage on a pressure vessel should be 150 percent of the operating pressure that was planned as 100-200 bar. This allows the gage to operate in the most accurate pressure range and prevents the gage from being stressed repeatedly to its full range, which would affect the calibration.

The gas inlet valve was connected to a dip tube that extends to a point near the bottom of the cylinder. This valve had an attached fitting which provided a socket for attaching the pressure hose furnished with the reactor. The gas release valve was installed in a port without any attachments installed on the underside of the head. Gas released from this valve would be drawn from the headspace of the vessel.

An industrial size nitrogen gas tube was used to provide pressures up to 200 bar. Nitrogen gas for transesterification reaction behaves as an inert gas that does not participate in the reaction. Regulator type STAR 50 232 was used in the experiments to regulate the pressure during the operation. A flexible high pressure hose was used to make the connection to the pressure vessel, i.e. reactor.

Flat gasket that is made of a polytetrafluoroethylene (PTFE) – fluoropolymer is used commonly as head gasket. Flat gasket closures, the gasket is held in a recess in the vessel cover. Excellent properties of PTFE materials provide a reliable closure for working temperatures up to 350 °C. In order to supply tight sealing, flat gaskets are recommended and with initial loading pressure, they develop and maintain the desired tightness. PTFE could be deformed plastically under pressure, this produces natural sealing. Another advantage of PTFE gasket is their chemical resistance.

METER PRO 04 by TÜMTES^{TM} was used as a temperature controller. Working voltage of 220 V AC is on the possibility of connecting multiple thermocouple that was chosen as Type J (Iron- Constantan) which was well suited to the operating temperature range of the vessel. These thermocouples are sealed in 1/8" diameter stainless steel sheaths and should be approximately 100 mm longer than the depth of the vessel so that a smooth bend can be made at the top to clear other head fittings. A warning alarm feature could be programmed to request the desired temperature.

For mixing purposes, the Hiedolph MR Hei-tec electromagnetic heater and stirrer was used. It was made of aluminum to provide fast heating time and thin ceramic coating made the heating plate both chemically and scratch resistant. The working voltage was 220 V AC and the mixing intensity was varies between 900-1100 rpm.

4.4 Biodiesel Production Using One-Step Supercritical Method

4.4.1 Materials

Refined canola oil (RCO) was purchased from a local supermarket which was used also in Chapter 3 to produce BD using the base catalyzed transesterication. Anhydrous methanol (MeOH) (99.8%) was purchased from Merck. The relevant properties of RCO were given in Chapter 3.

4.4.2 Experimental set-up for one-step SCM

The flowchart seen in Figure 4.7 summarizes the experimental procedures followed for BD production via one-step supercritical transesterification.

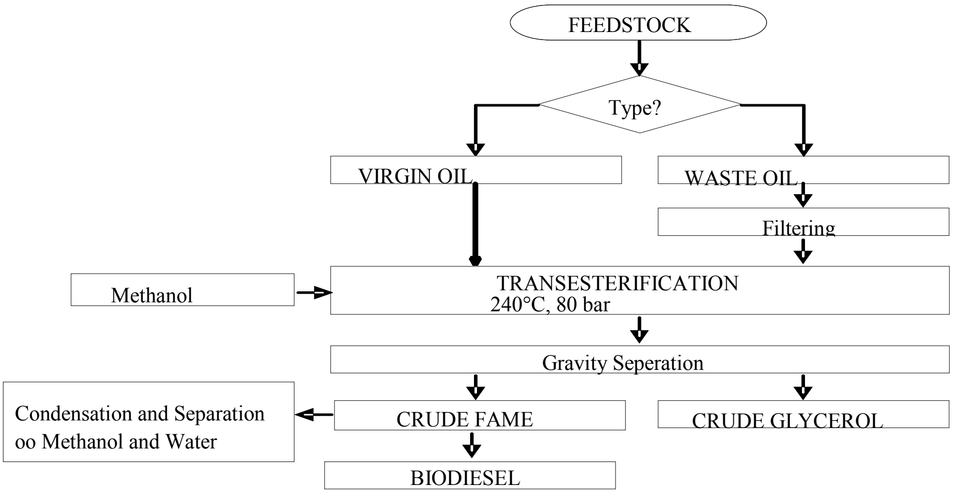

Figure 4.7: Flowchart of the experimental procedure for the BD production by one-step SCM transesterification developed in the current study

There were no pretreatment stages such as water removal or determination of FFA in non-catalytic supercritical tansesterification compared to catalytic-transesterifications in which free fatty acids and water always produced negative effects by causing soap formation and/or consuming extra catalyst and reducing its effectiveness (Demirbaş, 2006).

To perform non-catalytic transesterification, the experimental set up was used as shown in Figure 4.8.

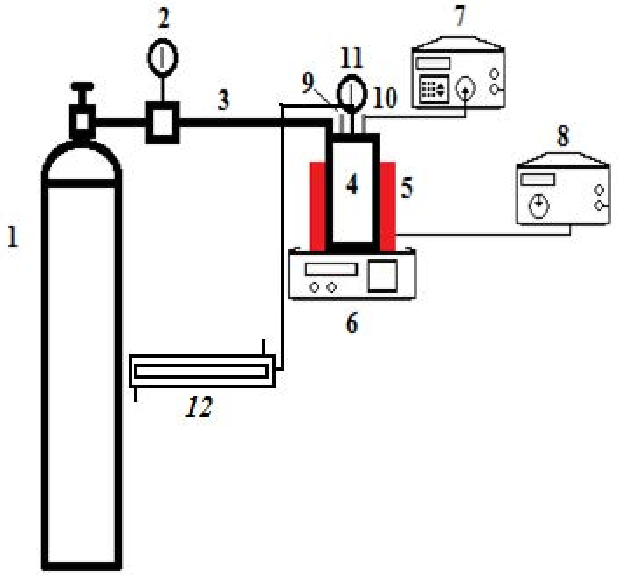

1: Nitrogen tube (200 bar)
2: Pressure regulator
3: Flexible high pressure nitrogen line
4: Supercritical reactor
5: Heater & insulating mantle
6: Magnetic stirrer
7: Electronic processes controller (display)
8: Power supply of heater
9: Release & Safety valves
10: J type thermocouple
11: Pressure gage
12: Condenser

Figure 4.8: Schematic diagram of supercritical BD production set-up

Nitrogen gas which remained inert during transesterication reaction, was supplied from the nitrogen tube (1) to provide pressure. The maximum pressure in the tube was 200 bars. The pressure was controlled by the pressure regulator (2). A flexible high pressure hose (3) was used to make the connection to the supercritical reactor (4). The external heater and insulator (5) were used to heat the contents of reactor and to minimize the heat loss to the surrounding, respectively. The heater was controlled by an AC power supply that was adjusted to 150 V (8). The electromagnetic stirrer (6) was used to mix the methanol and the oil. A safety valve (9) was used to release pressure of nitrogen from the reactor automatically if, the pressure in the reactor would exceeded the preset limits where pressure gage (11) indicated. A J-type (Iron-Constantan) thermocouple (10) was used to measure the temperature of the mixture in the vessel. The thermocouple was connected to the TUMTES™ Meter Pro 04 electronic process controller (7). The condenser (12) which was a laboratory type double pipe heat exchanger, was used to condense excess methanol and water which were evolved out at the end of the process, using tap water as a cooling fluid.

4.4.3 Experimental procedure for one-step SCM transesterication

SCM transesterification of canola oil was carried out by experimental set-up that was shown in Figure 4.8 by following the procedure listed below. Five different experiments were carried out keeping all conditions same (amount of canola oil, methanol, operating temperature and pressure) but, reaction time varied from 1 to 3 hours. Oil to alcohol molar ratio was kept constant at 1:41 that approximately corresponded to 1:2 volume ratio.

The amount of canola oil = 175 mL (= 0.197 mol)

The amount of methanol = 325 mL (= 8.024 mol)

Experimental procedure;

- Initially, RCO and methanol mixture with 1:41 oil/methanol molar ratio was charged into the supercritical reactor which corresponded to approximately 85 % of the entire volume of the reactor, the rest being occupied by air.
- Before closing the vessel, oil and methanol were mixed using a magnetic stirrer around 600 rpm until a homogeneous mixture were obtained.
- Vessel was closed using adjusting lever and the hatch tightly screwed on it.
- Pressure regulator was set to 35 bar and system was checked for all possible leakage and all leakages were fixed if, existed.
- Voltage supply was set to 150 V then, the external heater started to heat up the reactants in the vessel, meanwhile temperature was monitored via the process controller.
- Temperature and pressure were adjusted to reach the supercritical fluid region following Figure 4.1 (methanol should not be transformed to vapor phase)
- Temperature and pressure of the system were set 230-240°C and 80-85 bar, respectively then, stopwatch was started.

- The reaction time was varied from 1 to 3 hours. After the specified reaction time, the reaction vessel was removed from the heating jacket, voltage supply was switched off and cooling process took place.
- Around 85°C, excess methanol was transferred to the condenser by opening pressure valve.
- Then, reactor was opened and the product mixture was poured into a separation funnel and allowed to separate into FAME and glycerol phases. The FAME floated at the top and glycerol sank to the bottom.
- After a few hours glycerol and FAME was separated and FAME was heated 120°C to get rid of water or remaining methanol, until a steady weight was attained. The esters were weighed to determine the transesterification yield.
- CFP and viscosities of samples produced were measured.

4.4.4 Measurement of biodiesel properties

To ensure the quality of the BD produced, some of its properties such as viscosity, cloud point and pour point were measured as prescribed earlier Section 3.5. The properties measured were: viscosity at 40 ˚C (mm^2s^{-1}) (Oluwoye, 2013), ASTM D 445 or EN- ISO 3104; cloud point (CP, ˚C), ASTM D2500-09 or ISO 3015:1992; pour point (PP, ˚C), ASTM D97-05 or ISO 3016:1994.

4.5 Results and Discussion

4.5.1 Performance of the reactor

It was essential to test the reactor performance and safety before any experimental study. The supercritical reactor which was designed for high internal pressure were subjected to a hydrostatic test pressure which at every point in the vessel is at least equal to 1.3 times the working pressure, i.e. planned between 80 to 100 bar (ASME). Hydrostatic test performed at the Mechanical Engineering Laboratories of Istanbul Technical University, at 90°C and 120 bar for 1 hour and the test result is presented at Appendix 9. Test result showed that designed supercritical reactor successfully passed the hydrostatic test without showing even a minor damage.

Before BD production by SCM method, the reactor was also tested in the laboratory against leakages. For this purpose 500 mL of canola oil was placed in the reactor and its hatch was closed. It was gradually pressurized and heated up to 85 bar and 250°C, respectively. The joints were examined by water with detergent. Leaking sections were fixed by machining and/or changing the sealant. Sealing assurance was provided by keeping the reactor under the above temperature and pressure for 1 hour. Safety valve was also tested by gradually increasing the pressure to the set pressure of 90 bars. However, if the safety valve opens with an undesirable pressure increase during production at high temperatures, the pressure in the reactor may drop down below the limiting values. In such a case methanol might undergo a phase change from liquid to gas and would escape through the safety valve.

It was observed that the electrical resistance wound up on the reactor has high capacity in heating. The supplied voltage was reduced down to 150 V for better control of temperature in the reactor and not to damage the resistance in case of an overheating.

4.5.2 Efficiency of biodiesel production

Transesterification was successfully employed in the experimental work to reduce the viscosity. Five different batches were produced at 240˚C (513 K) and 83 bars (8.3 MPa) which were just above the critical temperature and pressure of methanol. These minimum values were preferred to ensure safety during production in the laboratory, even though it would result in longer reaction times. The reaction time started from 1 hour for the first batch, then, increased by half an hour for the next batch and so on.

Average percent conversions of RCO to BD was estimated using the Eqnuation 3.3 that was presented in the Chapter 3 and results are shown in Table 4.7.

Table 4.7: % Conversion of RCO to RCOME by supercritical transesterification

Batch No. (reaction time)	% Conversion of FAME produced
Batch 1 (60 min)	86.4
Batch 2 (90 min)	89.0
Batch 3 (120 min)	97.9
Batch 4 (150 min)	98.2
Batch 5 (180 min)	98.8

EN 14214 specifies that the ester content of BD must be minimum 96.5 mass %. It was noted that when the reaction time was 2 hour and more with the specified levels of conversion were achieved successfully. Lee et al. (2012) reported 96.4 % conversion at 270˚C and 100 bars (with similar condition to 240˚C and 83 bars), reaction time was 45 minutes. This shows that increases in pressure and temperature will shorten the reaction time.

4.5.3 Characterization of biodiesel produced

Only viscosity, cloud point and pour point of the BD samples were tested for their fuel properties following either ASTM D6751 or EN 14214 standard and results are given in Table 4.8. These results are compared with the reaction time and percent conversion of oil to BD. The results obtained from supercritical method are also compared with base catalyzed method.

Table 4.8: Viscosity, CP and PP test result for RCOME

	Kinematic Viscosity (mm^2/s)	**Cloud Point (˚C)**	**Pour Point (˚C)**
Base Catalyzed Transesterification *	4.582	-3.5	-10
Batch 1	5.966	4.3	-5.5
Batch 2	5.230	4.0	-6.0
Batch 3	4.760	-2.0	-8.8
Batch 4	4.592	-3.0	-9.0
Batch 5	4.580	-3.0	-9.0

*Results for RCOME from Table 3.7

The viscosity of the all samples produced from RCO falls within the acceptable range required by ASTM D446 (1.9-6.0 mm^2/s) at any reaction time. Kinematic viscosities of RCOME that was produced either by base catalyzed transesterification or supercritical transesterification showed the similar results. But, time spent for those processes would differ. Whole process of base catalyzed transesterification were taking almost 24 hours including raw material preprocesses, reaction, separation and purification which was the most time consuming part. The process of supercritical transesterification was completed within maximum 6 hours including device preparation, reaction and separation. Summary of outcomes of the two process are presented in Table 4.9.

The results showed that increasing the percent conversion of RCO to RCOME caused decrease in its kinematic viscosity. Figure 4.9 shows relation of percent conversion of

RCOME at different reaction time versus their measured kinematic viscosities. There was no significant change in kinematic viscosity and also in CP and PP in the last three batches. It shows evidence that at 240˚C and 83 bars, conversion almost completed at the end of 2 hours.

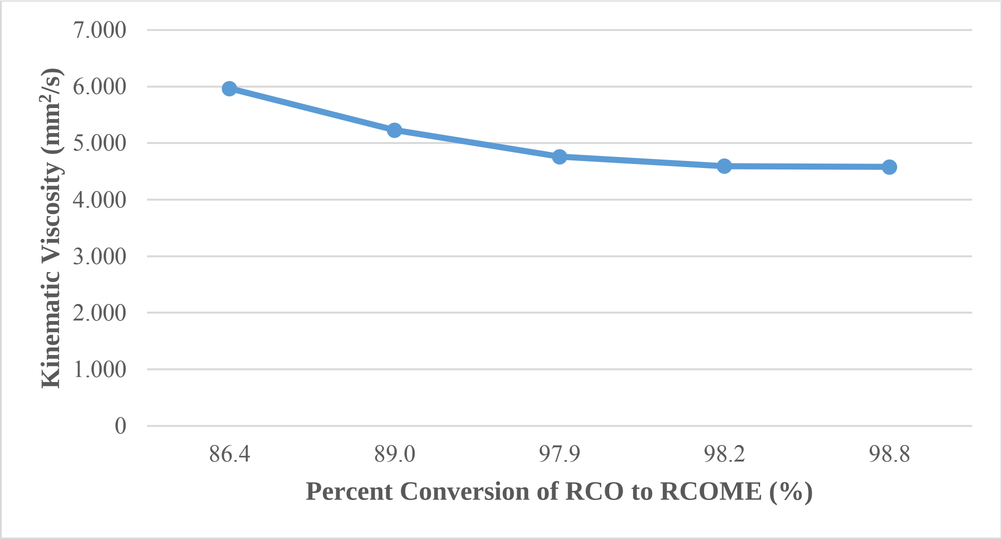

Figure 4.9 Percent conversion of RCOME vs kinematic viscosity

Table 4.9: A comparison of base-catalyzed and SCM BD production for current study

	Base-Catalyzed Transesterification	**SCM Transesterification**
Reaction time (min)	60	180
Reaction temperature(ºC)	60	240
Reaction pressure (bar)	Atmospheric pressure	83
Separation from glycerol	Need min 8 hours	10 min
FFAs in feedstock	Need to be determined	No need to determine
Water in feedstock	Need minimum 2 hours for removal	No influence
Yield of FAME (%)	98.1	98.8
Purification of FAME	Difficult –Require water washing and drying min. 6 hours	none

When SCM compared to base-catalyzed transesterification only obstacle seem high temperature and pressure conditions. Hovewer, when the systems is built then, production can be performed in higher temperature and pressure yielding high BD conversion and less reaction time. SCM method is more suitable for continuous production due to its short reaction time.

CHAPTER 5

PREDICTION OF COLD FLOW PROPERTIES OF BIODIESEL USING NEURAL NETWORKS

5.1 Overview

CFP defines the operability for diesel fuels and may be come vital cold weather. CP, PP and CFPP are used commonly to characterize CFP and all three are influenced strongly by the FA composition of the feedstock used for biodiesel production. Prediction of CFP based on the FA composition of feedstock can reduce the experimental work to produce a biodiesel suitable for a regional climate. In an attempt for this, experimental data of 103 biodiesel fuel samples were traced from the literature with their corresponding FA compositions of parent feedstock and CFP to create prediction models using multiple linear regressions (MLR) and artificial neural network (ANN). The data collected was used to evaluate correlations and empirical relations between FA composition of a feedstock and biodiesel CFP using MLR (Multiple Linear Regression) and the same data sets were employed also as input and output data for ANN prediction models. Finally, both developed prediction models were compared with the measured CFP values of RCOME and WFOME biodiesel samples those were produced experimentally at current work.

5.1.1 Relationship between FA composition and CFP

Biodiesel is a mixture of FA esters with each ester component contributing to the properties of the fuel that are related directly to FA composition of a biodiesel feedstock. Some of the physical and chemical specifications of biodiesel such as CFP, cetane number, ignition quality, heat of combustion, oxidative stability, viscosity and lubricity are directly related to FA profile of the feedstock (Knothe, 2008).

Diesel fuel has a tendency to solidify in cold weather. Biodiesel starts to crystallize at higher temperatures than diesel fuel and its cold flow characteristics are rather poor. Determination of its cold flow characteristics and its improvement is a major challenge. Poor CFP may cause fuel line, filter and pump blockage resulting in operational problems. The CFP include three important parameters for low temperature characteristics of biodiesel fuel; CP, PP and CFPP.

The FA composition of a feedstock is the main parameter determining CFP of a biodiesel. Three types of FA play vital role on CFP of biodiesel namely, SFA (saturated fatty acids) such as palmitic (C16:0) and stearic (C18:0) acids which do not have double bonds in their carbon chain, MUFA (mono-unsaturated fatty acids) such as palmitoleic (C16:1) and oleic (C18:1) acids have one double bond whereas PUFA (poly-unsaturated fatty acids) such as linoleic (C18:2) and linolenic (C18:3) acids have two or three double bonds in their carbon chain. Due to high level of saturation SFA have higher melting points when compared to MUFA and PUFA, therefore SFA will crystallize earlier at cold temperatures. As an example, palm oil-based biodiesel will exhibit higher cloud point hence, poorer CFP since it contains high mass fractions of palmitic and stearic acids (Ramos et al., 2009; Dunn, 2010). On the contrary, canola based- biodiesel exhibits relatively good CFP because of its relatively higher content of oleic acid (Hoekman et al., 2012, Giakoumis, 2013). The melting points of some common FA and their fatty acid methyl esters (FAME) are listed in Table 5.1.

Table 5.1: The melting points of some common FA and their corresponding FAME

Fatty Acid	Melting point (˚C)	Methyl ester	Melting point (˚C)
Lauric acid- C12:0	44	Methyl laurate (MeC12:0)	5
Myristic acid - C14:0	54	Methyl myristate (MeC14:0)	18.5
Palmitic acid - C16:0	63	Methyl palmitate (MeC16:0)	30.5
Stearic acid - C18:0	70	Methyl stearate (MeC18:0)	39.1
Oleic acid - C18:1	16	Methyl oleate (MeC18:1)	-20
Linoleic acid - C18:2	-5	Methyl linoleate (MeC18:2)	-35
Linolenic acid - C18:3	-11	Methyl linolenate (MeC18:3)	-52

When carbon chains are longer in an ester, the CFP of biodiesel become even worse. For instance, the peanut oil-based biodiesel revealed very poor CFP, due to its long chain SFA which are lingoceric (C22:0) and behenic (C24:0) acids (Ramos et al., 2009, Giakoumis, 2013). However, even though the SFA content of coconut oil is very high, CP of its biodiesel is lower due to, its short chain SFA contains mostly lauric and myristic acids (Dunn, 2010).

5.1.2 Prediction of CFP

Prediction of CFP of biodiesel based on the FA composition of the feedstock prior to production can lead to a way for a suitable biodiesel for the regional climate conditions. Thus, the best feedstock composition that would enhance the biodiesel quality in cold weather seems an important subject to be searched.

Sarin et al. (2009) proposed two CFP prediction models based on palmitic methyl ester content (P_{FAME}) and total unsaturated FA content (U_{FAME}) for biodiesels produced from Jatropha, Palm and Pongamia. In their model P_{FAME} content was limited to 45 % while U_{FAME} should be up to 84 %. Su et al. (2011) proposed a model based on the weighted average number of carbon atoms in FAME (Nc) and U_{FAME}, but they did not put any limitations for the U_{FAME} content. Dunn (2010) suggested a model for CFP prediction based on total SFA content (ΣSats) with limitation of 6-20 % of ΣSats. Moser's (2008) CFPP prediction model was also related to the SFA contents up to 48.2 % ΣSats limitation. The models of Ramos et al. (2009) and Wang et al. (2011) were based on SFA composition, both models claimed that CFPP was influenced only by long-chain saturated FA whereas unsaturated esters had negligible effect on it. All of these prediction models achieved above 0.90 of coefficient of determination (R^2) for a limited number of experimental data and have used statistical methods. In these models, it is essential for the user specified data points to fit the curve in order to obtain an empirical correlation. Nevertheless, the curve fitting is not necessary in soft computing methods such as artificial neural networks (ANN), fuzzy inference systems (FIS) and adaptive neuro-fuzzy inference system (ANFIS).

ANN prediction and modelling techniques identify and learn complex nonlinear or linear relations between the input and output data. In recent years, ANN has been preferred for modeling application in various disciplines such as neuroscience, mathematical and computational analysis, learning systems and engineering design applications (AlShanableh, 2005). The ANN prediction models also have been used for evaluating density, cetane number, CFP and kinematic viscosity of diesel fuels (Yang et al., 2002; Pasadakis et al., 2006; Balabin et al., 2011; Jahirul et al., 2013). Very few works have been reported for the prediction of biodiesel properties using ANN method and none of them is on CFP. In a recent work, Piloto et al., (2013) successfully predicted cetane number of biodiesel using an

ANN model and showed that ANN is superior to the other methods. Meng et al., (2014) modelled prediction of kinematic viscosity at 313 K with the highest correlation coefficient of 0.9774 as compared to other viscosity prediction methods.

5.2 Materials and Methods

For CFP prediction modelling, four types of BD (WFOME, RFOME, RCOME and WCOME) produced in Chapter 3 were used. FA compositions of their feedstock and their CFP temperatures are available in Table 3.1 and Table 3.7, respectively.

5.2.1 Data Collection

103 experimental data sets were gathered from literature which were related to biodiesel fuel samples produced from various edible or nonedible feedstock (Al-Shanableh et al., 2016). Data sets comprised chemical composition of the feedstocks and three thermophysical parameters (CP, PP and CFPP) of biodiesel produced from those feedstocks, those data sets are available in Appendix 10. The nine most common FA components of the biodiesel feedstock were chosen for modelling, namely lauric acid (C12:0), myristic acid (C14:0), palmitic acid (C16:0), stearic acid (C18:0), oleic acid (C18:1), linoleic acid (C18:2), linolenic acid (C18:3), arachidic acid (C20:0) and gadoleic acid (C20:1). The distribution of FA components in the data sets are illustrated in Figure 5.1. C16:0, C18:0, C18:1 and C18:2 are common for all feedstock.

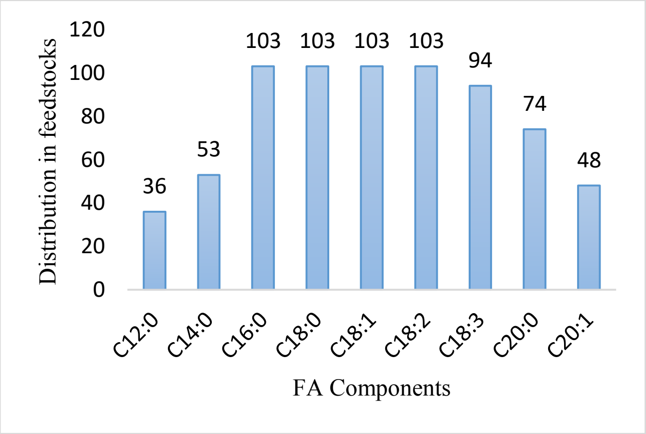

Figure 5.1: Distribution of FA components in data sets found in the literature

The maximum and the minimum values for the nine FA present in the 103 feedstock, and CFP of biodiesel fuels produced from the feedstock are given in Table 5.1. When a feedstock's FA composition falls within these ranges then, models developed here could be employed to predict the biodiesel CFP.

Table 5.2: Minimum and maximum values of FA and CFP of literature data

	Min.	Max.	Mean	Count out of 103
C12:0	0.0	49.2	8.95	36
C14:0	0.0	25.9	3.25	53
C16:0	0.9	44.1	13.0	103
C18:0	0.3	23.5	5.48	103
C18:1	1.8	92.5	38.2	103
C18:2	0.0	77.3	27.2	103
C18:3	0.0	72.3	7.77	94
C20:0	0.0	7.5	0.605	74
C20:1	0.0	66.5	2.34	48
CP (˚C)	-13.4	17.0	2.67	86
PP (˚C)	-23.0	15.0	-1.11	57
CFPP (˚C)	-13.0	17.0	-0.870	88

5.2.2 Multiple linear regression correlations

MLR creates relation between two or more explanatory variables, *x* and a response variable *y*. The population regression line for p explanatory variables is:

$$\mu_y = \beta_0 + \beta_1 x_1 + \beta_2 x_2 + \ldots\ldots + \beta_p x_p \tag{5.1}$$

Where μ_y is the mean response and directly related to the explanatory variables. The actual values for y vary about their mean μ_y. The parameters β_0, β_1, $\beta_2 \ldots \beta_p$ of the population regression line can be estimated from the fitted values b_0, $b_1 \ldots b_p$. The aim is to obtain a regression line as:

$$y = b_o + b_1 x_1 + b_2 x_2 + \ldots\ldots + b_p x_p \tag{5.2}$$

The least-squares estimates b_0, $b_1 \ldots b_p$ are usually computed using a statistical software. Here, the model was executed using the Microsoft Excel Data Analysis Add-in.

Nine FA compositions of 103 of biodiesel feedstocks (vegetable oil/animal fat) that were collected from literature were chosen as explanatory data and their measured CP, PP and

CFPP values were taken as response variables. Three empirical correlations of regression line were developed to predict CP, PP and CFPP temperatures of biodiesel samples.

5.2.3 Artificial neural network prediction

ANN is an information processing methodology that replicates the biological nervous systems. To solve specific problems, a large number of interconnected processing elements (neurons) work together.

The multilayer feed forward neural network consists of an input layer, one or more hidden layers and an output layer. The number of the nodes in the input and output layer are related to the nature of the problem (Bose and Liang, 1996). In the model developed here, the input layer is composed of 9 nodes, which are FA compositions in weight fractions of feedstock in reference data. The output layer has 3 nodes, i.e., CP, PP and CFPP temperatures of biodiesel samples. One hidden layer was chosen initially and a suitable number of nodes in the hidden layer were determined by trial and error. The nodes between each layer were connected with adaptable weights. Equation 5.3 describes how an artificial neuron or a node functions:

$$y_i = f\left(\sum_{j=1}^{n} x_j w_{ij} + b_i\right) \tag{5.3}$$

where x_j is the input from the previous node j and it is multiplied with the adapted weight w_{ij} that connects node i and node j. The total number of previous nodes connecting with node i is n. The products of all the inputs and weights are summed up and a bias b_i of node i is often added to the summation. The final summation is transferred by an activation function f to get the output of node i, y_i . The hyperbolic tangent sigmoid (tansig) function and the linear (purelin) function are commonly utilized as activation functions. The tansig function is used for a non-linear relationship approximation while the purelin function is used for a linear relationship approximation. The hidden layer activation function was chosen as sigmoid while the output layer activation function was chosen as linear (purelin) function. As mentioned in previous works (Piloto et al., 2013, Meng et al., 2014), this combination was found to be valid and accurate.

The most important step when developing ANN architecture is the training procedure, where the weights and biases are adjusted to minimize the difference between the output of the ANN and the actual value. The mean squared error (MSE) is usually applied as the performance function to interpret the difference between the output of the ANN and the actual value. The training procedure is achieved through training algorithms and the back-propagation algorithm is one of the most popular training algorithms ((Bose and Liang, 1996, Knothe, 2005). The problem in the training procedure is over-fitting, in which the ANN obtained memorizes the training examples and does not learn the ability to generalize on unseen data. To prevent over-fitting, the actual data can be divided into 3 data sets; the training set, the validation set and the test set. Both of the MSE obtained for the training set and the validation set should decrease during a training process. When the ANN starts to over fit, the error on the validation set will increase though the error on the training set continues decreasing. The training should be stopped at that stage. The test set is treated as an unseen data and will show accuracy of the trained ANN model that has been developed (Bose and Liang, 1996, Cebi 2011).

The literature data from 103 biodiesel samples were divided into 2 data sets here, 88 samples were used as training set while last 15 were used as validation set. Four BD samples produced were utilized as test data set to evaluate validity of the model developed. Each data set consisted of nine FA compositions as inputs to the model and three CFP; namely, CP, PP and CFPP as outputs. The ANN prediction system implemented using the NN-pred, a Microsoft Excel^{TM} software package. Then, data sets were loaded in the data worksheet, by filling the model parameters in the user input page, building model was initialized. A neural network model is basically a set of weights between the layers of the net. At the end of the each run, the final set of weights was saved in the Calc sheet. The output page of this file showed the values of Mean Squared Error (MSE) on the training and validation set. The ANN was trained to choose a suitable number of hidden layers starting from 1 to 12 nodes and the output should achieve the desired error goal of 0.01. In all variations learning rate, momentum and initial weights were kept constant as 0.1, 0.1 and 0.3, respectively. ANN with 6 neurons in the hidden layer appears to give the best performance, and additional nodes over 6 did not make a significant improvement in performance. Finally, an ANN model was implemented with the 9-6-3 architecture for prediction of CP, PP and CFPP temperatures as illustrated in Figure 5.2.

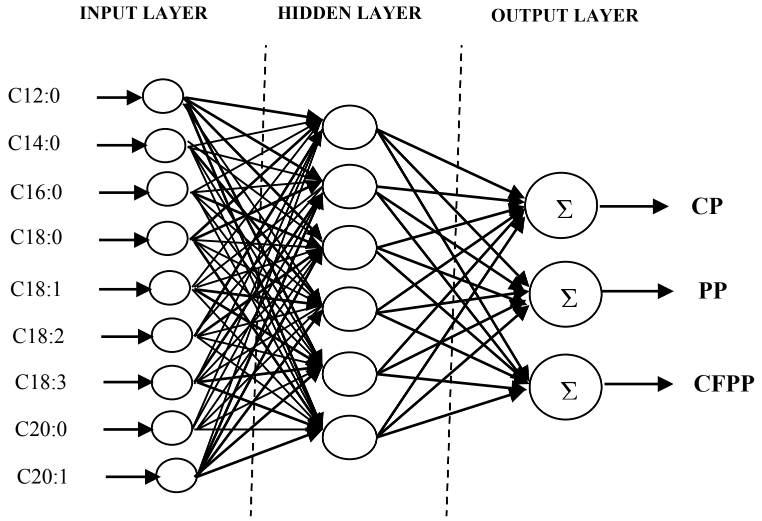

Figure 5.2: The ANN architecture implemented for prediction of CFP temperatures of BD

5.2.4 Predictive capability of the models developed

The models developed using MLR and ANN were evaluated by statistical indices in order to see their accuracies and predictive capabilities. Equations given below were used to determine the statistical indices those including standard error of prediction (*SE*), coefficient of determination (R^2), mean square error *(MSE)* and root mean square error (*RMSE*):

$$SE = \sqrt{\frac{\sum_{i=1}^{n}(y_{exp,i}-y_{p,i})^2}{n-1}} \tag{5.4}$$

$$R^2 = 1 - \frac{\sum_{i=1}^{n}(y_{exp,i}-y_{p,i})^2}{\sum_{i=1}^{n}(y_{p,i}-y_{exp,ave})^2} \tag{5.5}$$

$$MSE = \frac{1}{n}\sum_{i=1}^{n}(y_{p,i} - y_{exp,i})^2 \tag{5.6}$$

$$RMSE = \sqrt{\frac{1}{n}\sum_{i=1}^{n}(y_{p,i} - y_{exp,i})^2} \tag{5.7}$$

where n is the number of experimental data, $y_{exp,i}$ is the experimental value, $y_{p,i}$ is the predicted value, $y_{exp,ave}$ is the average experimental value and n is the number of input variables.

5.3 Results and Discussion

5.3.1 Prediction of CFP using MLR

Equation 5.8 was developed by MLR modelling to predict CP, PP and CFPP temperatures. (Cxx:y) in the correlation represents weight fraction of each FA component in the feedstock. If a feedstock did not have any of FA components then, the corresponding FA composition was taken as 0.0 wt %. The coefficients of the equation are given in Table 5.3. Using this equations the temperatures for CFP of a biodiesel could be estimated in relation to the FA composition of a feedstock.

$$CFP\ (^\circ\mathrm{C}) = a + bC12{:}0 + cC14{:}0 + dC16{:}0 + eC18{:}0 + fC18{:}1 + gC18{:}2 + hC18{:}3 + iC20{:}0 + jC20{:}1 \tag{5.8}$$

Table 5.3: Coefficients of MLR modelling for CFP calculation

CFP	**Coefficients of Equation 5.8**									
	a	***b***	***c***	***d***	***e***	***f***	***g***	***h***	***i***	***j***
CP	+11.1	-0.327	+0.238	+0.238	+0.306	-0.182	-0.182	-0.233	+2.83	-0.275
PP	+18.9	-0.401	-0.195	+0.262	+0.0570	-0.343	-0.285	-0.376	+2.81	-0.268
CFPP	-7.76	+3.68	-0.635	+0.432	+0.524	-0.0553	-0.0242	-0.0391	+3.68	-0.0171

Generally, unsaturated FA components provided a positive influence on CFP, i.e., temperatures for CP, PP and CFPP would be lower with higher UFA composition; however saturated FA components favored a negative influence. The C12:0 and C14:0 behave as outliers and gave positive effects in PP and CFPP temperatures in the MLR correlations. Low melting points of these two as compared to other SFA components resulted in positive influences on CFP values. Consequently, C12:0 and C14:0 created some nonlinearity in correlations which implies SFA increase cold flow temperatures.

The R^2 for the MLR model between FA composition and CP, PP and CFPP were found as 0.91, 0.84 and 0.88, respectively. The standard error of estimations (*SE*) for CP, PP and CPPP were 3.4, 4.1 and 3.7, respectively. The prediction performances of correlations in terms of *RMSE* were found as 2.098, 3.110 and 2.661 for CP, PP and CFPP, respectively, which indicate very low precision. The values obtained from this model were not impressive due to low R^2 values of CP, PP and CFPP. This may be due to the complexity of the reference data which varied in a wide range of biodiesel compositions related to the saturated and unsaturated portions. A comparison of the experimental (i.e. data obtained from literature) and the calculated CP, PP and CFPP values are presented in Figure 5.3 (a), (c) and (e), respectively.

5.3.2 Prediction of CFP using ANN

While implementing the ANN model, the best architecture without over fitting was chosen as 6 neurons in one hidden layer. Models with up to 6 neurons in a hidden layer could not achieve the desired MSE of 1 % neither in training nor in validation tests. Although the ANN was trained to choose a suitable number of hidden layers starting from 1 to 12 nodes, Table 5.4 summarizes the simulation results for 4, 6, 8 and 12 neurons in single hidden layer.

Table 5.4: Simulation results for CFP prediction using NN-Pred inExcel

Number of Hidden Neurons		Training Set		Validation Set	
		MSE (%)	SE (˚C)	MSE (%)	SE (˚C)
4	CP	1.023	1.6	1.584	2.0
	PP	0.997	1.9	1.102	2.3
	CFPP	0.867	1.6	1.321	2.1
6	CP	1.002	1.6	1.529	1.7
	PP	0.986	1.8	1.045	2.1
	CFPP	0.998	1.5	1.007	1.8
8	CP	1.079	1.6	1.675	1.9
	PP	0.988	1.8	1.132	2.3
	CFPP	1.001	1.8	1.122	1.9
12	CP	1.088	1.7	1.722	2.2
	PP	1.023	1.9	1.328	2.5
	CFPP	1.001	1.8	1.134	2.0

Although all models with different number of neurons were able to achieve an acceptable error goal in training phase, they failed to achieve good results in the validation phase since they were trying to obtain a very small error goal in the training phase, except the model that consists of six neurons. As a result, 9-6-3 back-propagation ANN architecture was implemented for prediction of CP, PP and CFPP of biodiesel.

Similar to the MLR modelling, the saturated FA components showed negative influences on CFP except C12:0 and C14:0 which had positive effects for all CFP. The unsaturated components provided positive influences in the ANN modelling on CFP except C20:1 which imposed a negative influence on PP and CFPP temperatures.

The R^2 from the results of ANN between FA composition and CP, PP and CFPP were found as 0.98, 0.94 and 0.96, respectively while the *SE* for over all data set of CP, PP and CPPP were 1.3, 1.6 and 1.5, respectively. The prediction performances of correlations in terms of *RMSE* were found as 0.595, 0.856 and 0.830 for CP, PP and CFPP, respectively, which indicate good precision as compared to the MLR model developed. A comparison of *SE*, *RMSE* and R^2 for ANN and MLR prediction models can be seen in Table 5.5.

A comparison of the experimental (i.e. data obtained from literature) and the predicted value using ANN model of CP, PP and CFPP are presented in Figure 5.3 (b), (d) and (f), respectively. The outcomes of MLR and ANN models are also seen in the same figures.

Table 5.5: A Comparison of *SE*, *RMSE* and R^2 values for CFP prediction models developed using MLR and ANN

	MLR prediction-model			**ANN prediction-model**		
CFP	*SE (˚C)*	*RMSE*	R^2	*SE(˚C)*	*RMSE*	R^2
CP	3.4	2.098	0.91	1.7	0.595	0.98
PP	4.1	3.110	0.84	2.1	0.856	0.94
CFPP	3.7	2.661	0.88	1.8	0.830	0.96

It can be noted that the ANN model estimated more accurate temperatures for all three CFP. Since ANN was capable to recognize patterns whether there is a linear or a nonlinear relation in the data available, the prediction of CFP via ANN models resulted in more accurate estimations than the traditional statistical MLR models.

The CP temperature of a biodiesel is more critical than the CFPP and PP temperatures both in ASTM D6751 and EN 14214 specifications due to its practical significance. The PP and CFPP are not included in those standards directly. Nevertheless, CFPP is a useful parameter for diesel engines and PP is required for storage and pipelines. Considering an error in temperature measurement as ±1.5°C (ASTM D2500) the CFP estimation with ANN can be regarded as a satisfactory assessment since they differ only about up to 8 % from the measured CFP values.

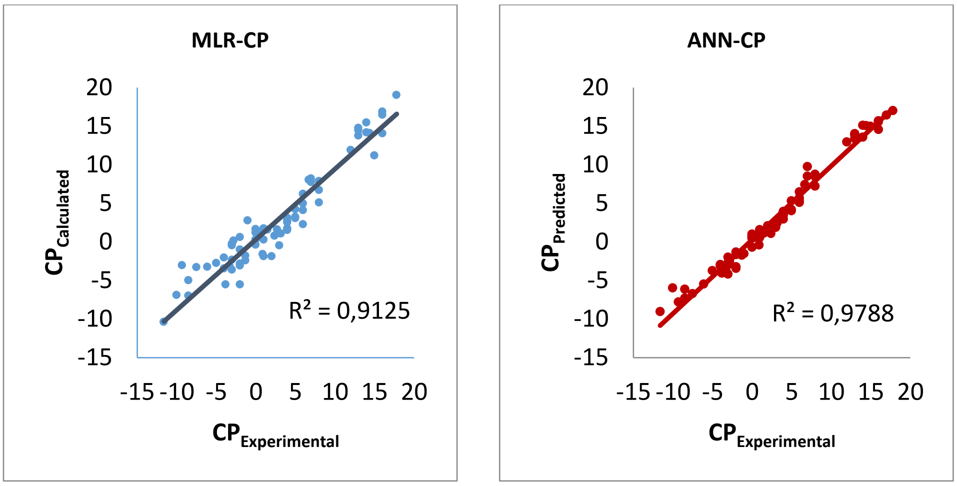

(a) MLR-CP model (b) ANN-CP model

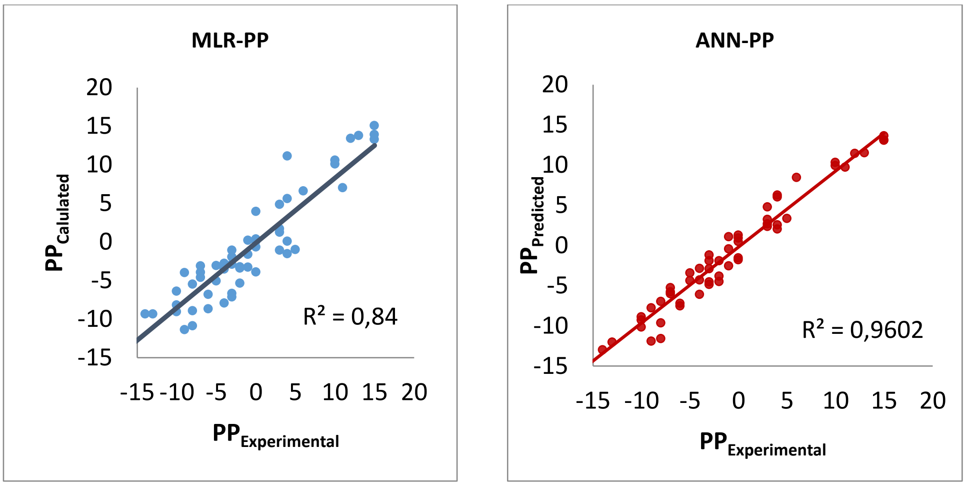

(c) MLR-PP model (d) ANN-PP model

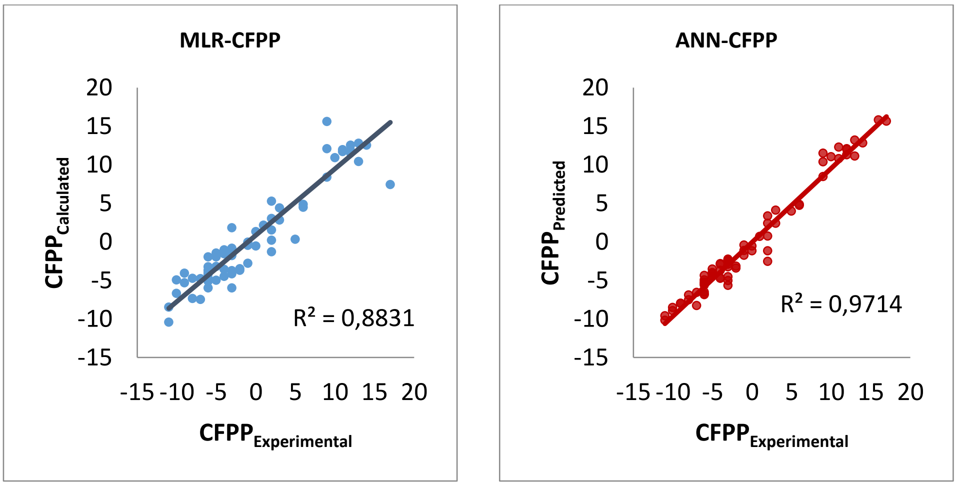

(e) MLR-CFFP model (f) ANN-CFFP model

Figure 5.3: Experimental values versus predicted values for MLR and ANN models

As a faster alternative to the time consuming experimental procedures, both models developed here may be used to estimate the temperatures of CFP of a biodiesel produced from different feedstocks with known FA compositions. It would be a challenging study to employ the two models to arrange the FA compositions of a batch of feedstock that would yield exactly the CFP temperatures needed for a regional climate.

The accuracy and predictive capability of MLR and ANN models developed here were evaluated in terms of R^2 and *RMSE*. The higher R^2 values for ANFIS models as compared to the R^2 of MLR models indicated a good fit of the model. An R^2 value approaching to unity, implied a good correlation between experimental and predicted values.

Predicted three CFP temperatures of 103 biodiesel samples by MLR and ANN models are given in Appendix 11.

5.3.3 Performances of the models developed

The prediction abilities of the ANN and MLR models generated were tested with the measured CFP values of four biodiesel samples produced in this work. In addition, the testing data set were applied to those CFP prediction models given in the literature (Su et al. 2008; Moser et al., 2008; Ramos et al., 2009; Sarin et al., 2009; Wang et al., 2011). Table 5.6 provides correlation used within those methods. A performance comparison of the CFP prediction models and the current models developed are given in Table 5.7.

Table 5.6: CFP prediction models in the literature

CFP	Method	Correlation
CP (°C)	Sarin et al.	$0.526(P_{FAME})-4.992$
	Su et al.	$18.134(N_C)-0.790(U_{FAME})$
PP (°C)	Sarin et al.	$0.571(P_{FAME})-12.24$
	Su et al.	$18.880(N_C)-(U_{FAME})$
CFPP (°C)	Moser	$0.438(\Sigma Sats)-8.93$
	Sarin et al.	$0.511(P_{FAME})-7.823$
	Su et al.	$18.019(N_C)-0.804(U_{FAME})$
	Ramos et al.	$3.1417LCSF-16.477$; $LCSF=(0.1C_{16:0})+(0.5C_{18:0})+(1C_{20:0})$
	Wang et al.	$1.7556LCSF-14.772$; $LCSF=\sum(MPn\times Cn)/100$

P_{FAME}: Palmitic acid methyl ester content (wt %); U_{FAME}: Total unsaturated FA (wt%); $\Sigma Sats$: total saturated FA content (wt%); N_C: Weighted-average number of carbon atoms; *LCSF*: The long-chain saturated factor for C16:0-C24:0; $C_{Cxx:y}$ or *Cn*: Mass fraction of saturated FA (wt %); *MPn* : Melting point of saturated FA

Table 5.7: A comparison of the measured and the predicted CFP of biodiesel samples

CFP	Method	WFOME	RFOME	RCOME	WCOME	RMSE	R^2
CP (°C)	Experimental	15	15	-3.5	-2		
	Sarin et al.	15.7	15.2	-2.0	-1.8	0.868	0.990
	Su et al.	11.6	9.4	-19.1	-17.1	11.354	0.577
	Proposed MLR	11.4	10.5	-3.1	-1.9	2.889	0.827
	Proposed ANN	13.5	14.9	-3.6	-1.7	0.768	0.992
PP (°C)	Experimental	12	11	-10	-9		
	Sarin et al.	10.2	9.7	-9.0	-8.8	1.218	0.983
	Su et al.	2.4	0.2	-36.3	-33.3	19.306	0426
	Proposed MLR	11.1	10.1	-8.5	-7.1	1.367	0.980
	Proposed ANN	11.8	9.3	-9.5	-7.8	1.181	0.989
CFPP (°C)	Experimental	14	13	-7.5	-7		
	Moser	10.8	10.1	-4.4	-4.9	2.849	0.840
	Sarin et al.	12.3	11.8	-4.9	-4.8	1.996	0.934
	Su et al.	10.5	8.8	-20.7	-18.7	9.341	0.698
	Ramos et al.	2.1	1.1	-10.8	-9.9	8.697	0.176
	Wang et al.	27.7	23.3	-6.9	-5.9	8.593	0.753
	Proposed MLR	9.6	8.9	-4.9	-4.2	3.563	0.737
	Proposed ANN	10.9	11.1	-6.8	-7.2	1.854	0.958

NR: Not reasonable

The current ANN model predicted the three CFP temperatures of biodiesel samples with higher accuracy than the other models. The Sarin et al. (2009) model appeared to be competitive with the current study. All models generated by linear regression based, since then except Sarin et al. prediction models, they did not demonstrate reasonable prediction performances.

CHAPTER 6
VARIATION OF SOLID FRACTION WITH COLD FLOW PROPERTIES OF BIODIESEL

6.1 Overview

Since the three CFP should occur at specific solid fractions during freezing, the objective was to examine in details the whole solidification history to estimate the corresponding solid fractions at these temperatures. The so-called computer-aided cooling curve analysis employed in metal casting industry was modified and applied to the current BD sample. Indications of CP, CFPP and PP were noted as slope changes on the cooling curve and also on its first derivative curve. The Newtonian thermal analysis was utilized to estimate the solid fractions in the solid-liquid mixture at CP, CFPP and PP during solidification.

6.2 Cooling curve analysis

The cooling curve recorded in a thermal analysis is a temperature versus time (T vs t) graph of a melt during freezing, hence it keeps the whole solidification history. Each phase change causes a thermal event which is displayed as a plateau on the cooling curve. It's widely employed in metal casting (Fras et al., 1993; Barlow and Stefanesou, 1997) and also for the petroleum waxes as indicated in ASTM D86. A plateau occurs in the vicinity of melting point of petroleum waxes having crystalline solids. Petroleum waxes with amorphous (non-crystalline) solids do not exhibit a plateau. A dT/dt vs t, i.e. 1st derivative, plot can disclose the small details and invisible information hidden in the T vs t graph. An analysis of the two plots can provide information about the phases evolved during liquid to solid transition. Various features of the solidified melt such as the latent heat, the type and the amounts of the phases that solidify can be found (Barlow and Stefanesou, 1997; Fras et al., 1993). The CP is considered as the temperature at which a cloud of wax crystals first becomes visible when fuel is cooled while the PP is described as the temperature at which wax crystallization becomes sufficient to gel the fuel. And also the CFPP is defined as the temperature at which the crystals grow and begin to adhere to each other plugging the diesel filters. The definitions of CP, CFPP and PP, stated above involve crystallization of BD and diesel fuels during solidification, therefore a plateau during freezing on their cooling curves should be expected.

The zero curve in a thermal analysis is an imaginary curve which is defined as the 1st derivative of a cooling curve in which the material examined does not undergo a phase change during freezing. Zero and *dT/dt* curves overlap in the fully liquid and fully solid phases but diverge from each other during liquid to solid transition period, i.e. in the two-phase region. The area enclosed by the two curves is directly related to the latent heat evolved and therefore, it can be used to determine the change of solid fraction with temperature during freezing. For the determination of the zero curve, the Newtonian approach assumes that there is no temperature change across the sample and that the heat transfer within the substance towards the casing occurs by convection. On the other side, the Fourier analysis considers the effect of temperature gradient across the sample and assumes that the heat transfer takes place by conduction. The extensive amount of data involved and dependency of variables on time and temperature necessitate computer usage for such a study and is called the computer-aided cooling curve analysis (CA-CCA). The analysis has been utilized extensively in metal casting for process and quality control (Barlow and Stefanesou, 1997; Fras et al., 1993).

Due to the absence of phase diagrams of multicomponent BD fuel, estimation of solid fractions at CP, PP and particularly at CFPP during freezing becomes a complex issue. The present study was aimed to examine the cold flow behavior of BD produced from WFO during solidification by employing the CA-CCA technique in conjunction with the Newtonian thermal analysis. Estimation of the solid fraction in the solid-liquid region of BD particularly, at the CFPP was a prime interest since the amount of crystals formed while the fuel is freezing affects directly the plugging of the filters.

6.3 Materials and Methods

The base catalyzed one step transesterification reaction method was used to produce BD from WFO which was collected from the Engineering Faculty Cafeteria in Near East University. Procedure described in Chapter 3 was followed for WFOME production. CP, PP and CFPP were determined following ASTM D2500, EN 23015, ASTM D97, ISO 3016, ASTM D6371 and EN 116 standards. Since, unlike metals, the liquid BD was transparent to light, the solidification process could be followed visually.

6.3.1 Experimental set-up for CA-CAA

The experimental setup for CA-CCA of BD sample, schematically presented in Figure 6.1 was built in accordance with the specifications given in the standards (ASTM D2500, EN 23015, ASTM D97, ISO 3016, ASTM D6371 and EN 116) referred above to assure compatibility.

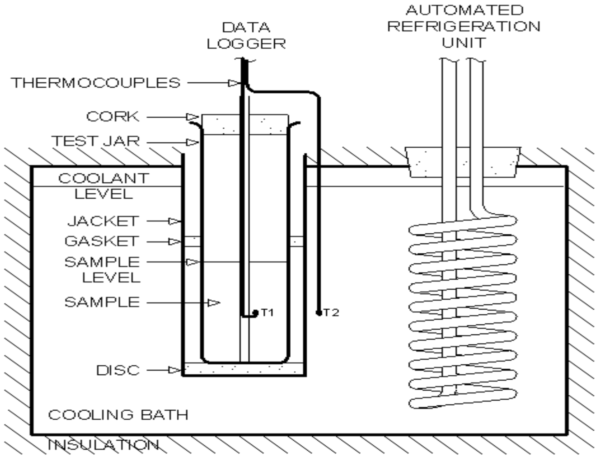

Figure 6.1: Experimental setup of CFP measurement for CA-CCA

An insulated cooling bath was filled with ethanol as the coolant. Ethanol was cooled down while its temperature was controlled by an automated refrigeration unit. A stirrer was used for thermal homogeneity of the ethanol in the cooling bath. An aluminum cylinder jacket was placed in the middle of the cooling bath. A 6 mm thick cork disk was placed at the bottom of the jacket as a thermal insulator. The glass test jar was filled with BD sample to a level of 54 mm corresponding to a sample volume of about 45 ml. The test jar was then fitted into the jacket and a uniform air gap of 5 mm in the radial direction between the test jar and the jacket was ensured by a gasket. Two T-type thermocouples for temperature readings are also shown in Figure 6.1. Thermocouple T1 was positioned 27 mm above the bottom and 3.5 mm away from the central axis of the test jar in order to measure the temperature of BD sample (T). Thermocouple T2 was placed to measure the temperature of ethanol (T_0) in the vicinity of the jacket close to the mid-section at which T1 was fixed.

6.3.2 CA-CCA and derivation of solid fraction during freezing of biodiesel sample

Prior to data collection for CA-CCA, the cooling bath was cooled down to -20 °C and the BD sample was heated up to 50 °C which was about 40 °C above the expected CP value. Temperature readings from thermocouples were recorded using a data logger with 1 second intervals and the data was stored for the analysis. The average of 30 successive measurements was calculated to smoothen the curves using Equation 6.1 below, rendering the data free of any noise.

$$T_n = \frac{\sum_{i=30(n-1)}^{30(n-1)+29} T_i}{30} \qquad t_n = \frac{\sum_{i=30(n-1)}^{30(n-1)+29} t_i}{30} \qquad n = 1,2,3,4,..... \tag{6.1}$$

where; T was temperature of the sample fuel, t was the time and n was the serial number of a data point. A similar data smoothening procedure was also described by Ul-Haq et al. (2004) during casting of an aluminum alloy.

The rate of change of temperatures with respect to time, $T_n^{'}$, and the corresponding instants, $(t_{T'})_n$, were calculated from Equation 6.2 below.

$$T_n' = \left(\frac{dT}{dt}\right)_n = \frac{T_n - T_{n+1}}{t_n - t_{n+1}} \qquad (t_{T'})_n = \frac{t_n + t_{n+1}}{2} \tag{6.2}$$

The methodology of Newtonian thermal analysis for metal casting process was described in details by Emadi et al. (2004) in which it was assumed that during metal solidification process the temperature distribution throughout the casting material is uniform, the specific heat of the metal alloy is temperature independent and does not change during solidification and also the heat transfer coefficient from the sample to the surrounding can be characterized by a unique temperature function. Hence, the heat balance equation during solidification was given as;

$$\frac{dQ}{dt} - M\,C_P \frac{dT}{dt} = U\,A(T - T_0) \tag{6.3}$$

where; M is the mass and C_P is the specific heat of the sample, U is the overall heat transfer coefficient, A is the sample surface area, T_0 is the temperature of the cooling bath and Q is the latent heat of solidification. Rearranging Equation 6.3, the cooling rate of the fuel can be determined as given in Equation 6.4. The first term on the right hand side represents the rate of change of temperature due to any phase change. The second term is the rate of change of temperature due to heat transfer from the sample to the surroundings.

$$\frac{dT}{dt} = \frac{1}{M\,C_p}\frac{dQ}{dt} - \frac{UA}{M\,C_p}(T - T_0) \tag{6.4}$$

If, no phase transformation occurs, i.e. $dQ/dt = 0$, the cooling rate of the BD sample can be written as follows where Z_N is called Newtonian zero curve or the baseline.

$$\frac{dT}{dt} = -\frac{U\,A}{M\,C_P}(T - T_0) = Z_N \tag{6.5}$$

Despite the assumptions made in the Newtonian approach for metal casting (Emadi et al., 2004), C_P value of BD, which is a mixture of fatty acid methyl esters, is a function of temperature. The variations of C_P values of 12 pure fatty acid methyl esters with respect to temperature were measured by Pauly et al. (2014) between 250 – 390 K (-23.15 – 116.85 °C). The measured values varied between 301.44 – 837.72 J/mol K. It was observed that C_P values of methyl esters were increasing functions of temperature. C_P value of methyl palmitate (MeC16:0) as one of the major compounds of BD fuel, was observed to drop from 569.49 J/mol K at 310 K (36.85 °C) in the liquid phase to 480.60 J/mol K at 295 K (21.85 °C) in the solid phase, i.e. a decrease of 15.6 % during solidification. The decrease of C_P value of methyl palmitate within the temperature range considered was 9.3 % in the liquid phase and 19.9 % in the solid phase. C_P values in solid phases of other major compounds such as methyl oleate (MeC18:1), methyl linoleate (MeC18:2) and methyl linolenate (MeC18:3) could not be measured since their pure solid phases were present below 250 K. The decrease in C_P values from 390 K (116.85 °C) to 300 K (26.85 °C) in the liquid phase were about 16 %. On average, the changes in C_P values of fatty acid methyl esters were determined as 12, 15 and 16 % in the liquid, solid and two-phase (liquid-solid) regions, respectively within the specified temperature range.

Even though the C_P value of BD sample can be determined from C_P values of fatty acid methyl esters by applying the rule of mixtures (Pauly et al., 2014), there are additional issues to be discussed while using Equation 6.5. Temperature distribution throughout the sample is not constant and *U*-value is temperature dependent. Considering that the heat transfer does not take place ideally in the radial direction and the analysis is conducted in the vicinity of the thermocouple used for temperature measurements, uncertainties may arise in the area (*A*) and mass (*M*) terms. Nevertheless, it is possible to obtain the UA/MC_p term as a function of temperature by plotting dT/dt versus $(T - T_0)$ using the data collected before and after the freezing period of BD. The dT/dt values can be calculated from Equations 6.1 and 6.2 successively. The corresponding $(T - T_0)$ values can be obtained by applying Equation 6.1 to both BD sample and cooling bath temperatures and then taking their differences. Following this, it becomes possible to plot the Newtonian zero curve from Equation 6.5.

The area between Z_N and dT/dt curves from the start to the end of freezing of BD is directly related to the total latent heat for solidification. The ratio of the incremental cumulative area, A_n, to the total area, A_{Total}, gives the incremental solid fraction $(f_s)_n$ of the sample during solidification. The Trapezoidal Rule was used for the area calculations. Equations 6.6 and 6.7 were used to estimate the solid fraction using Newtonian thermal analysis for any data point *n*. A_{Total} can also be calculated from Equation 6.7 by substituting $n = n_{Total} - 1$ where n_{Total} is the total number of data points. The new corresponding temperature $\left(T_{f_s}\right)_n$ was calculated by averaging the two successive temperatures as given in Equation 6.8, below.

$$(f_s)_n = \frac{A_n}{A_{Total}} \tag{6.6}$$

$$A_n = \sum_{i=1}^{n} \left\{ \left[\frac{1}{2}\left(T'_{i+1} + T'_i\right) - \frac{1}{2}\left(Z_{N\,i+1} + Z_{N\,i}\right) \right] \times \left(t_{i+1} - t_i\right) \right\} \tag{6.7}$$

$$\left(T_{f_s}\right)_n = \left(T_n + T_{n+1}\right)/2 \tag{6.8}$$

6.4 Results and Discussion

The dT/dt vs ($T - T_0$) curve plotted in Figure 6.2 exhibited linearity both in liquid and solid phases during freezing of BD. The curve deviated from linearity in the two-phase region in which the liquid and solid BD coexist together. The deviation is due to the latent heat of solidification which appears in the first term on the right hand side of Equation 6.4. Excluding the two-phase region, a straight line was fitted through the data points of fully liquid and fully solid regions as seen in Figure 6.2. The term UA/MC_p in Equation 6.5 remained constant and was derived from the slope of the straight line as 0.00065 s^{-1}. It should be noted that *the* UA/MC_p term can still be defined as a function of temperature and inserted into Equation 6.5.

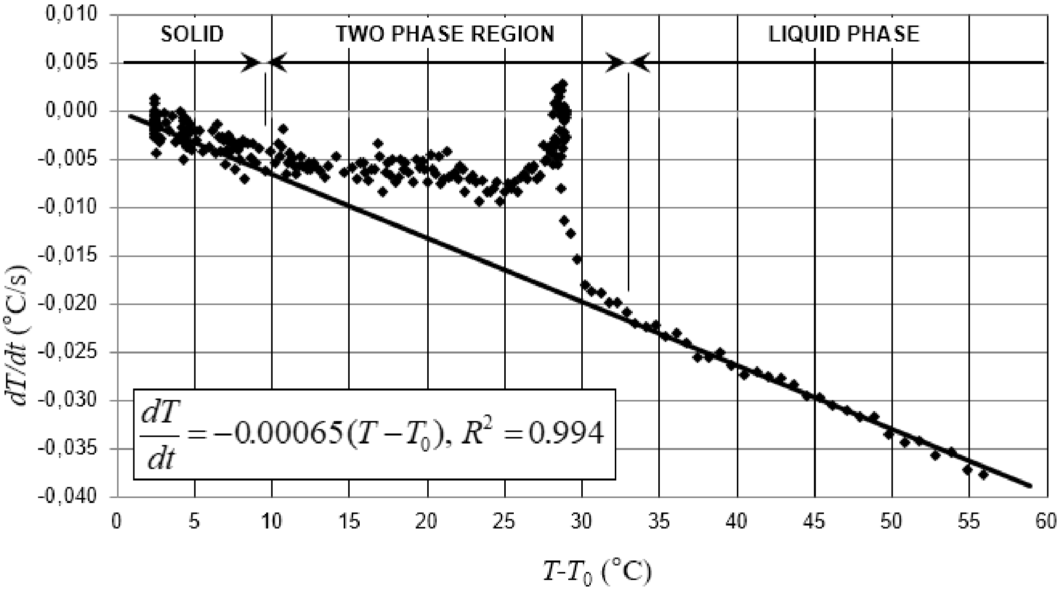

Figure 6.2: dT/dt versus ($T - T_0$) curve of BD sample during cooling

It appears that ($T - T_0$) = 32.9 °C, i.e. sample temperature T_L = 11.9 °C, indicates the end of fully liquid phase region and the beginning of two-phase region during cooling of BD. The two-phase region extends itself down to ($T - T_0$) = 9.0 °C, i.e. sample temperature T_S = -12.2 °C and then, the fully solidified BD is present at cooler temperatures. Hence, the freezing range of the BD can be noted as $\Delta T = T_L - T_S$ = 24.1 °C where T_L is the liquidous temperature at which the freezing starts and T_S is the solidus temperature revealing the end of freezing. All three CFP of BD, CP, CFPP and PP describe actually the progress of solidification in the freezing range.

Using the data collected via thermocouple T1 (Figure 6.1) and Equations 6.1 and 6.2, the cooling curve, *T* vs *t*, and *dT*/*dt* vs *t* curves were plotted and are shown in Figure 6.3. The cooling bath temperature from thermocouple T2 is also shown in the same figure. The average cooling bath temperature was fixed at -21.6 °C with a minimum of -22.9 °C and a maximum of -19.5 °C. A plateau is observed on the cooling curve (*T* vs *t*) at about 7 °C which corresponds to the experimentally determined CFPP value given in Table 6.1. The CP (9.5 °C) is located before the plateau that corresponds to a sharp change in the slope of *dT*/*dt* vs *t* curve (indicated by the letter "A") and is related with the nucleation of solid crystals in the freezing BD sample.

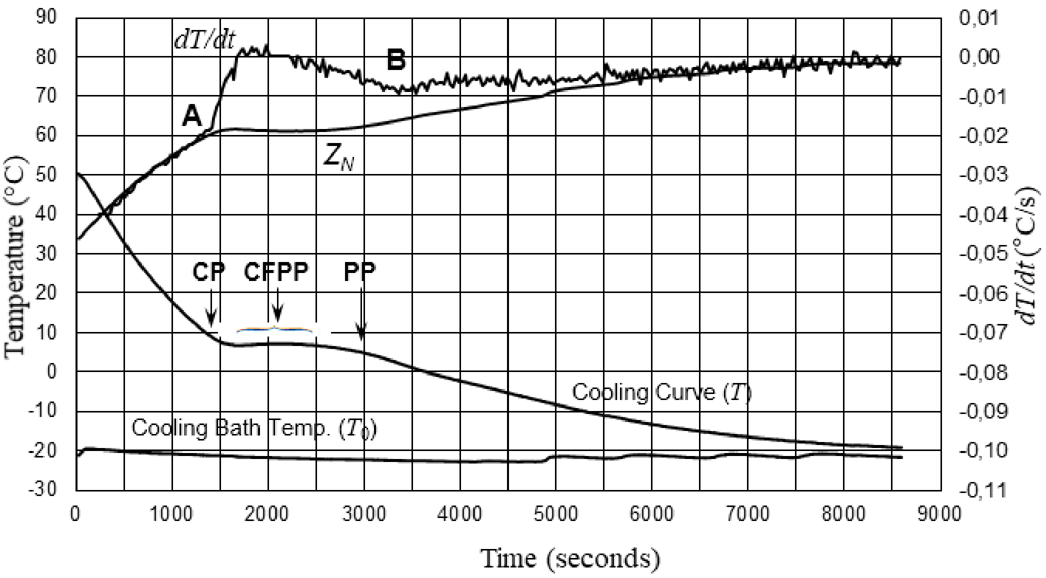

Figure 6.3: Cooling curve analysis and Newtonian zero curve of BD sample

Originally, the maximum of the *dT*/*dt* vs *t* curve and the minimum of the *T* vs *t* curve are referred as the nucleation temperature of a crystalline solid in metal casting (Flemings, 1974). PP can be considered approximately as the end of the plateau region after which the continuation of temperature drop becomes explicit. At point "B" close to the data point for

PP another remarkable change in the slope of *dT*/*dt* curve can be noticed. The change in the slope occurs at 2.5 °C which is about 2.5 °C below the experimentally determined PP value.

The Newtonian zero curve (Z_N) was determined from Equation 6.5 using all the data points and is incorporated into Figure 6.3. The Z_N and *dT*/*dt* curves overlap before and after solidification but deviate from each other during solidification, i.e. in the two phase region, since Z_N does not include latent heat during freezing.

The change of solid fraction during solidification of WFO based BD sample determined using Equations 6.6 to 6.8 is plotted in Figure 6.4. At CFPP a remarkable increase of solid fraction from 0.18 to 0.39 reveals the cause of filter plugging while the temperature drops down. Numerical values of solid fractions at CP, CFPP and PP in Figure 6.4 are listed in Table 6.1. The change in slope at point B of the *dT*/*dt* vs *t* curve in Figure 6.3 corresponds to a solid fraction of about 0.70.

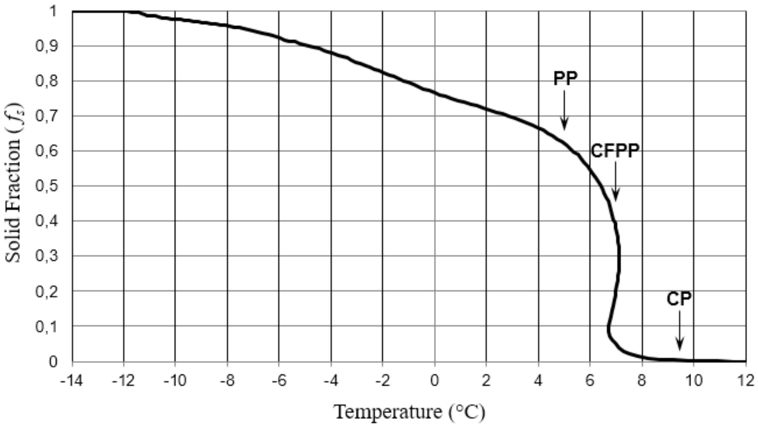

Figure 6.4: Variation of solid fraction during freezing of BD sample

Table 6.1: Solid fractions at CP, CFPP and PP while BD is freezing

	Experimental measured CFP (°C)	**Solid Fractions (f_s)**
CP	9.5	~ 0.003
CFPP	7.0	0.18 → 0.39
PP	5.0	~ 0.60

The suction times, recorded during the CFPP tests and given in Figure 6.5, increased gradually as the temperature was decreased. A jump was observed in the vicinity of 7 °C which was recorded as the CFPP of the BD sample. Below this temperature suction stopped due to the total blockage of the filter.

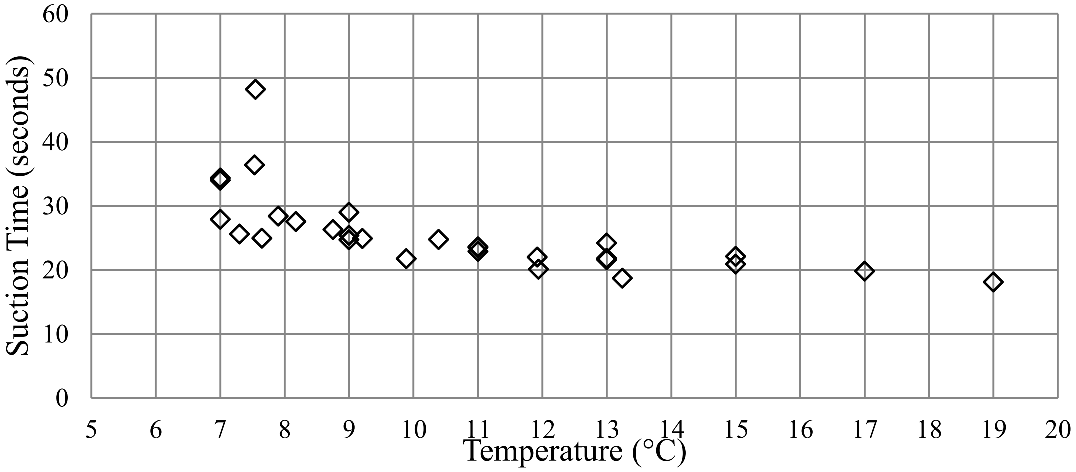

Figure 6.5: Suction times recorded during CFPP tests

A series of photographs of the freezing sample, captured during a CFPP test from 10°C down to 5 °C with 1°C intervals, are seen in Figure 6.6. The wax crystals appear as the white phase in the photographs and it is evident that no crystals were nucleated in the sample at 10°C. At 9 °C which was 0.5 °C below CP the cloud of wax crystals, i.e. solid BD, is quite visible at the bottom of the test tube. A rapid growth of solid BD which corresponds to a sudden jump of volume fraction of solid BD is followed from 7°C down to 6 °C where the CFPP was reached. The photograph at 5 °C shows the sample at its PP temperature.

Since the areal fraction can be taken as the volume fraction (Dehoff and Rhines, 1974), the volume fraction of the solid BD in the photograph at 7 °C (CFPP) can be approximated as 0.25 which is between the limits given in Table 6.1. Hence, the visual observations coincided with the solid fraction calculations given in Table 6.1 and Figure 6.4.

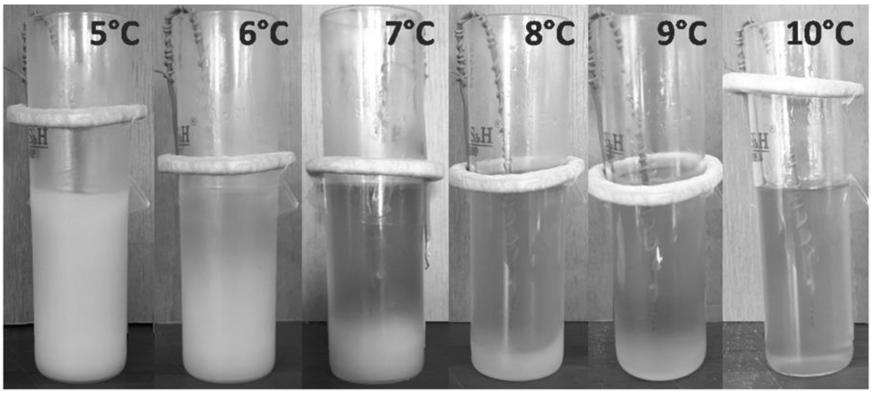

Figure 6.6: Progress of freezing observed in biodiesel during a CFPP test

It is quite challenging that all three CFP of a BD sample were determined with reasonable accuracy by conducting a single cooling curve analysis during solidification. The approach may be developed as a rapid alternative for the current ASTM and EN standards. The analysis can also be a tool to predict the solid fractions during freezing of complex systems as in the case of BD when the traditional approaches such as the lever rule and Scheil model (Marchwica et al., 2011) cannot be employed.

CHAPTER 7
CONCLUSIONS & RECOMMENDATIONS

7.1 Conclusions

BD samples utilized in the present study were produced from waste frying oil and their fresh counterparts, namely WFO, RFO, RCO and WCO. From economical point of view, waste frying oil can be a good candidate instead of virgin vegetable oil to produce BD which reduces the cost of feedstock. Furthermore, more important aspect is the environmental benefit. In addition, using WFO also helps to relieve the problem of waste oil disposal. The results of an informal survey revealed that the university cafeterias were the largest source of WFO in the TRNC whereas the smallest amount of WFO was accumulated in the kebab houses.

The BD samples of the current survey were harvested using transesterification reaction. Two different methods were applied i.e., conventional base- catalyzed and more recent supercritical methanol transesterifications. WFO appeared to have no drawbacks as a raw material in BD production in addition to its lower cost and also environmental benefits. For the base-catalyzed transesterfication, process parameters were optimized using the Taguchi technique to ensure high BD yield.

To ensure the quality of the BD produced, thirteen different properties, including CP, CFPP and PP of the FAME yield were determined and results showed that all properties were in close agreement with international standards EN 14214 and ASTM D6751. WFOME and RFOME were waxed at a higher temperature than the commercial diesel fuel and also the RCOME and WCOME, because of high palmitic and oleic acid contents of frying oil. The test results indicated that the BD produced from waste and refined oil exhibited no considerable differences in their CFP and other specifications.

Catalytic BD production is a time and energy consuming process due to feedstock preprocessing, product separation and purification steps. Therefore, non-catalytic; supercritical transesterification was also tried to yield FAME. To be able to produce BD using SCF method a batch type of reactor was design and manufactured to overcome extreme process conditions of high temperature and pressure in this technique. It appeared that the supercritical transesterification was advantageous over the base catalyzed one and eliminated the necessity for feedstock preparation and also reduced the time for reaction and purification processes.

Estimation of the three CFP temperatures based on the FA composition of a feedstock can reduce the experimental effort to produce a BD suitable for a regional climate. For this purpose, prediction models for three CFP temperatures from fatty acid compositions of BD feedstocks based on the ANN were generated. The CFP temperatures estimated by the ANN models were in close agreement with their experimental counterparts, i.e. R^2 values were found as 0.98, 0.94 and 0.96 for the CP, PP and CFPP, respectively. The prediction performances of the generated models in terms of *RMSE* were found as 0.595, 0856 and 0.830 for CP, PP and CFPP, respectively, which indicated a high accuracy. A comparison with literature confirmed that the ANN models developed here were better than the previously reported CP, PP and CFPP prediction models.

Finally, a computer-aided analysis of the cooling curve in conjunction with the Newtonian thermal analysis was carried out for cold weather characterization and also to examine the variation of solid fraction in the BD while it was freezing. It was noted that all three CFP could also be figured out in a single computer-aided cooling curve analysis instead of the three separate tests given in the EN and ASTM standards. The solid fractions were calculated as ~ 0.003, 0.18 → 0.39 and ~ 0.60, respectively at the CP, CFPP and PP temperatures. The estimations were justified with the visual observations.

7.2 Recommendations

In order to meet the energy needs of the country from renewable sources, it would be beneficial to collect the waste oils across the country and also to grow non-edible oil seed plants (such as jojoba) under a strategic plan. This will also reduce the oil imports, support economic growth, increase employment and improve environment.

Note that being an EU member it is compulsory to blend 5 % (B05) BD into the current EN 590 Eurodiesel fuel in the Greek sector of Cyprus. Likewise, it will become compulsory to blend minimum 0.5 % BD into EN 590 Eurodiesel fuel in Turkey. Hence, it is likely that production and blending of BD into EN 590 Eurodiesel may become necessary in the TRNC.

Consequently, the experience gained in the current thesis can be extended to a pilot plant for BD production and also quality tests following the EN or ASTM standards of the BD product before commercialization.

Characterization of some other specifications such as cetane number, viscosity, LHV of the FAME produced can be carried out. Those specifications can also be predicted according to a feedstock's FA composition before biodiesel production. Soft computing models such as ANN, ANFIS, and fuzzy logic can be powerful tools to develop prediction models these BD specifications.

REFERENCES

Acaroğlu, M. (2007). Alternatif Enerji Kaynakları, *Nobel Yayın Dağıtım*, 2. Basım, pp. 399-474.

Alptekin, E. & Canakci, M. (2009). Characterization of the key fuel properties of methyl ester–diesel fuel blends. *Fuel*, 88(1), 75–80.

Allan C. A.W. & Watts K.C. (2000). Comparative analysis of the atomization characteristics of fifteen biodiesel fuel types. *Transactions of the ASAE*, 43(2), 207–11.

AlShanableh F. (2005) ANN based product quality prediction for crude distillation unit. MSc Thesis, Near East University, Nicosia, Mersin10, Turkey.

AlShanableh, F., Evcil. A., Gövsa, C., Savas, M.A. (2011) A comparison of the cold flow properties of biodiesel produced from virgin and used frying oil. *Proceedings of 6th International Green Energy Conference (IGEC-VI)*. IGEC-VI-2011-103, ISBN: 978-605-89885-3-8, June 5-9, 2011, Eskisehir-Turkey.

AlShanableh, F., Evcil, A., Gövsa, C., Savas, M.A. (2012) A comparative examination of cold flow properties and acidity of biodiesel produced from virgin and waste canola oil. *Proceedings of International Conference on Energy Research and Development (ICERD5)*. April 5, 2012, Kuwait.

Al-Shanableh, F., Evcil, A., Savaş, M.A. (2016). Prediction of Cold Flow Properties of Biodiesel Fuel Using Artificial Neural Network. Procedia Computer Science 102: 273-280. doi:10.1016/j.procs.2016.09.401.

Altun, Ş., Lapuerta, M. (2014). Properties and emission indicators of biodiesel fuels obtained from waste oils from the Turkish industry. *Fuel*, 128, 288-95.

Al-Widyan, M. I., Al-Shyoukh, A.O. (2002). Experimental evaluation of the transesterification of waste palm oil into biodiesel. *Bioresources Technology*, 85, 253–6.

Amani, M.A., Davoudi, M.S., Tahvildari, K., Nabavi, S.M., Davoudi, M.S. (2013). Biodiesel production from Phoenix dactylifera as a new feedstock. *Industrial Crops and Products*, 43, 40– 43.

Anwar, A., Garforth, A. (2016). Challenges and opportunities of enhancing cold flow properties of biodiesel via heterogeneous catalysis. *Fuel*, 173, 189-208.

Araujo, V.K.W.S., Hamacher, S., Scavarda, L.F. (2010) Economic Assessment of Biodiesel Production from Waste Frying Oil. *Bioresources Technology*, 101, 4415-22.

Ashby, M.F. (2005). Material Selection in Mechanical Design. 3rd ed. Oxford: Elsevier.

ASME. (1995). Boiler and Pressure Vessel Code, Section VIII, Division 1, 1995 Edition, American Society of Mechanical Engineers.

ASTDR-Agency for Toxic Substances and Disease Registry. (1995). Toxicological profile for fuel oils. Atlanta, GA: U.S. Department of Health and Human Services, Public Health Service.

ASTM D87. (2014). Standard test method for melting point of petroleum wax (Cooling curve). West Conshohocken, PA: ASTM International.

ASTM D97. (2017). Standard test method for pour point of petroleum products. West Conshohocken, PA: ASTM international.

ASTM D2500. (2011). Standard test method for cloud point of petroleum products, ASTM, West Conshohocken.

ASTM D6371. (2016). Standard test method for cold filter plugging point of diesel and heating fuels. West Conshohocken, PA: ASTM International.

ASTM D6751. (2015). Standard specification for biodiesel fuel blend stock (B100) for middle distillate fuels. West Conshohocken, PA: ASTM international.

ASTM D 7467. (2008). Standard specification for diesel fuel oil, biodiesel blend (B6 to B20). Report no:.ASTM D 7467-08.

Bacha, J., Freel, J., Gibbs, L., Hemighaus, G., Hoekman, K., Horn, J. (2007). Diesel fuels technical review. Chevron Global Marketing.

Balabin, R.M., Lomakina, E.I., Safieva, R.Z. (2011). Neural network (ANN) approach to biodiesel analysis: analysis of biodiesel density, kinematic viscosity, methanol and water contents using near infrared (NIR) spectroscopy. *Fuel*, 90, 2007–15.

Balat, M. (2007). Production of biodiesel from vegetable oils: a survey. *Energy Sources*, 29, 895–913.

Balat, M., Balat, H. (2008). A critical review of bio-diesel as a vehicular fuel. *Energy Conversion Management*, 49, 2727–41.

Barlow, J.O., Stefanescu, D.M. (1997). Computer-aided cooling curve analysis revisited. *AFS Transactions*, 105, 349-54.

Bhale, P.V., Deshpande, N.V., Thombre, S.B. (2009). Improving the low temperature properties of biodiesel fuel. *Renewable Energy*, 34, 794-800.

Bose, N.K., Liang, P. (1996). Neural Network Fundamentals with Graphs, Algorithms and Applications. Singapore: McGraw- Hill.

Bruwer, J.J., Boshoff, B.D., Hugo, F.J.C., Du Plessis, L.M., Fuls, J., Hawkins, C., VanderWalt, A.N., Engelbert, A. (1980). The utilization of sunflower seed oil as renewable fueldiesel engines. In: *Agricultural energy*, vol. 2, biomass energy/crop production. ASAE publication 4–81. St. Joseph, MI: ASAE.

Buasri, A, Chaiyut, N., Ketlekha, P., Mongkolwatee, W., Boonrawd, S. (2009). Biodiesel Production from Crude Palm Oil with a High Content of Free Fatty Acids and Fuel Properties. *CMU Journal of Natural Sciences*, 8, 1.

Canakci, M., Gerpen, J. V. (2003). A pilot plant to produce biodiesel from high free fatty acid feedstocks. *Transaction ASAE*, 46, 945–55.

Cardoso, A.L., Nevesm, S.C.G., da Silva, M.J. (2008). Esterification of oleic acid for biodiesel production catalyzed by $SnCl_2$: a kinetic investigation. *Energies*, 1, 79–92.

Casimir, C.A., Chang, S., Lee, G., Shaw, J. (2007). Enzymatic approach to biodiesel production. *Journal of Agricultural Food Chemistry*, 55, 8995–9005.

Cebi, H. (2011). Yapay Sinir Ağları. EKİN Basım Yayın, Bursa, Turkey.

Cengel, Y. & Boles, M. (2008). Thermodynamics, an Engineering Approach. 7th ed, in SI units. McGraw-Hill.

Cetin, M., Yüksel, F. (2007). The use of hazelnut oil as a fuel in pre-chamber diesel engine. *Apply Thermal Engineering*, 27, 63–7.

CONCAWE. (2009). Special Task Force, FE/STF-24. Guidelines for handling and blending FAME. Report no.9/09.

Darnokol, D. & Cheryan, M. (2000). Kinetics of palm oil transesterification in a batch reactor. *The Journal of the American Oil Chemists' Society*, 77(12), 1263–7.

Da Silva, N.L., Batistella, C.B., Wolf Maciel, M.R., Maciel Filho, R. (2010). Biodiesel production from castor oil: optimization of alkaline ethanolysis, *Energy & Fuels*, 23, 5636-5642.

Dehoff, R.T., Rhines, F.M. (1968). Quantitative Microscopy. McGraw-Hill: New York.

Demirbas A. (2003). Biodiesel fuels from vegetable oils via catalytic and non-catalytic supercritical alcohol transesterifications and other methods: a survey. *Energy Conversion Management*, 44, 2093–109.

Demirbas, A. (2006). Biodiesel production via non-catalytic SCF method and biodiesel fuel characteristics. *Energy Conversion Management*, 47, 2271–82.

Demirbas, A. (2008). Relationships derived from physical properties of vegetable oil and biodiesel fuels. *Fuel* , 87(8–9), 1743–8.

Demirbas, A. & Kara, H. (2006). New options for conversion of vegetable oils to alternative fuels. *Energy Sources*, 28, 619–26.

Diasakou, M., Louloudi, A.,Papayannakos, N. (1998). Kinetics of the non-catalytic transesterification of soybean oil. *Fuel*, 77, 1297-1302.

Dunn, R.O. (2010). Cold flow properties of biodiesel by automatic and manual analysis methods. *Journal of ASTM International*, 7(4), 1-15.

Dunn, R.O. & Bagby, M.O. (1995). Low-temperature properties of triglyceride-based diesel fuels: transesterified methyl esters and petroleum middle distillate/ester blends. *Journal of the American Oil Chemists Society*, 72, 895–904.

Ebert, J. (2008). Supertical methanol for biodiesel production. *Biodiesel Magazine*, April 2008: 80-85.

El-Awad, M.M. & Yusaf, T.F. (2004). Performance and Exhaust Emission of a Diesel Engine Using Crude Palm Oil as Fuel Extender. *Journal of Energy &* Environment, 3, 61-68.

Emadi, D., M. Whiting, M., Djurdjevic, M, Kierkus W.T. Sokolowski, J.H. (2004) Comparison of Newtonian and Fourier thermal analysis techniques for calculation of latent heat and solidification of aluminum alloys. *Metalurgija – Journal of Metallurgy*, 91-106.

EN 116. (2015). Diesel and domestic heating fuels - Determination of cold filter plugging point.

EN 14214. (2012). Automotive fuels - Fatty acid methyl esters (FAME) - Requirements and tests.

EN 23015. (1994) Petroleum products - Determination of cloud point (ISO 3015:1992), European Standards.

Encinar, J.M., Gonzalez, J.F., Rodriguez, J.J., Tejedor, A. (2002). Biodiesel fuels from vegetable oils: transesterification of Cynara C. L. oils with ethanol. *Energy & Fuel*, 16, 443–50.

Encinar, J.M., Gonzalez, J.F., Reinares, A.R. (2007). Ethanolysis of Used Frying Oil. Biodiesel Preparation and Characterization. *Fuel Processing Technology*, 88, 513-522.

Evcil, A., AlShanableh, F., Govsa, C., Savas, M.A. (2010) Biodiesel production from waste frying oil and determination of its cold flow properties. *Proceedings of International Conference on Energy and Automotive Technologies (ICAT10)*. November 5, 2010, Istanbul-Turkey.

Flemings, M.C.. Solidification Processing. McGraw-Hill: New York, 1974.

Fernandes, M.R., Dantas Neto., A.A., Barros Neto, E.L., Castro Dantas, T.N., Moura, M.C.P.A. (2006). Combustível microemulsionado base-diesel (Diesel based microemulsion fuel). Brazilian Patent Deposit Number PI 0600616-7 A.

Fras, E., Kapturkiewicz, W., Burbielko, A., Lopez, H.F. (1993). A new concept in thermal analysis of castings. *AFS Transactions*, 131, 505-10.

Freedman, B., Butterfield, R.O., Pryde, E.H. (1986). Transesterification kinetics of soybean oil. *The Journal of the American Oil Chemists' Society*, 63(10), 1375–80.

Fukuda, H., Konda, A., Noda, N. (2001) Biodiesel fuel production by transestirification of oils. *Journal of Bioscience Bioengineering*, 92, 405–16.

Giakoumis, E.G. (2013). A statistical investigation of biodiesel physical and chemical properties, and their correlation with the degree of unsaturation. *Renewable Energy*, 50, 858-878.

Giraldo, S.Y., Rios, L.A., Suárez, N. (2013). Comparison of glycerol ketals, glycerol acetates and branched alcohol-derived fatty esters as cold-flow improvers for palm biodiesel. *Fuel*, 108, 709-14.

Goering, C.E., Schwab, A.W., Daugherty, M.J., Pryde, E.H., Heakin, A.J. (1982). Fuel properties of eleven oils. *Transaction ASAE*, 25:, 472–83.

Goff, M. J., Bauer, N.S., Lopes, S., Sutterlin, W.R., Suppes, G.J. (2004). Acid-catalyzed alcoholysis of soybean oil. *The Journal of the American Oil Chemists' Society*, 81, 415–20.

GPO (Goverment Planning Organization)(2010) KKTC, Devlet Planlama Örgütü, İzleme ve Koordinasyon Dairesi, “Ekonomik ve Sosyal Göstergeler”.

Hansen, C.M. (1999). Hansen Solubility Parameter, A User's Handbook. CRC Press.

He, H., Sun, S., Wang, T. (2007). Transesterification kinetics of soybean oil for production of biodiesel in supercritical methanol. *The Journal of the American Oil Chemists' Society*, 84, 399.

Hoekman, S.K., Broch, A., Robbins, C., Ceniceros, E., Natarajan, M. (2012) Review of biodiesel composition, properties, and specifications. *Renewable and Sustainable Energy Review*, 16, 143– 169.

Huzayyin, A.S., Bawady, A.H., Rady, M.A., Dawood, A. (1994). Experimental evaluation of Diesel engine performance and emission using blends of jojoba oil and Diesel fuel. *Energy Conversion Management*, 45:2093–112.

ISO 3016. (1994). Petroleum products - Determination of pour point.

Jahirul, M.I., Senadeera, W., Brooks, P., Brown, R.J., Situ, R., Pham, P.X., Masri, A.R. (2013). An artificial neutral network (ANN) model for predicting biodiesel kinetic viscosity as a function of temperature and chemical compositions. 20th International Congress on Modelling and Simulation, Adelaide, Australia, 1–6 December.

Jin, F., Zeng, X., Cao, J., Kawasaki, K., Kishita, A., Tohji, K., Enomoto, H. (2010). Partial hydrothermal oxidation of unsaturated high molecular weight carboxylic acids for enhancing the cold flow properties of biodiesel fuel. *Fuel*, 89, 2448-54.

Kim, H.J., Kang, B.S., Kim, M.J., Park, Y.M., Kim, D.K., Lee, J.S. (2004) Transesterification of vegetable oil to biodiesel using heterogeneous base catalyst. *Catalyst Today*, 315, 93-95.

Knothe, G., Bagby, M., and Ryan, T. (1997). Cetane Numbers of Fatty Compounds: Influence of Compound Structure and of Various Potential Cetane Improvers. *SAE Technical Paper 971681*, doi: 10.4271/971681.

Knothe, G. (2005). Dependence of biodiesel fuel properties on the structure of fatty acid alkyl esters. *Fuel Processing Technology*, 86(10), 1059–70.

Knothe G. (2008). “Designer” Biodiesel: Optimizing fatty ester composition to improve fuel properties. *Energy and Fuel*, 22, 1358-1364.

Knothe, G., Steidley, K.R. (2007). Kinematic viscosity of biodiesel components (fatty acid alkyl esters) and related compounds at low temperatures. *Fuel*, 86, 2560–7.

Korytkowska, A., Barszczewska-Rybarek, I., Gibas, M. (2001). Side-reactions in the transesterification of oligoethylene glycols by methacrylates. *Designed Monomer & Polymer*, 4, 27–37.

Krawczyk, T. (1996). Biodiesel-alternative fuel makes inroads but hurdles remain. *INFORM*, 7(8), 800-15.

Kusdiana, D., Saka, S. (2004). Two-step preparation for catalyst-free biodiesel fuel production. *Applied Biotechnology*, 115, 781-791.

Labeckas, G. & Slavinskas, S. (2006) Performance of direct-injection off-road diesel engine on rapeseed oil. *Renewable Energy*, 31, 849–63.

Lee, Y., Park, S.H., Lim, I.T., Han, K., Lee, S.Y. (2000). Preparation of alkyl (R)-(2)-3hydroxybutyrate by acidic alcoholysis of poly-(R)-(2)-3-hydroxybutyrate. *Enzyme Microbial Technology*, 27, 33–6.

Lopes, J.C. A., Boros, L., Krahenbuhl, M.A., Meirelles, A.J.A., Daridon, J.L., Pauly, J. (2008). Prediction of cloud points of biodiesel. *Energy and Fuels*, 22(2), 747–52.

Lopez, D.E., Goodwin Jr, J.G., Bruce, D.A., Lotero, E. (2005). Transesterification of triacetin with methanol on solid acid and base catalysts. *Applied Catalysis A: General*, 295, 97–105.

Luperta, M., Rodriguez-Fernandez, J., de Mora, E.F. (2009). Correlation for the estimation of the cetane number of biodiesel fuels and implications on the iodine number. *Energy Policy*, 37(11), 4337–44.

Ma, F., Hanna, M.A. (1999). Biodiesel production: a review. *Bioresources and Technology*, 70, 1–15.

Maceiras, R., Vega, M., Costa, C., Ramos, P., Marquez, M.C. (2009) Effect of Methanol Content on Enzymatic Production of Biodiesel from Waste Frying Oil. *Fuel*, 88, 2130-2134.

Marchwica, P., Sokolowski, J.H., Kierkus, W.T. (2011). Fraction solid evolution characteristics of AlSiCu alloys - Dynamic baseline approach. *Journal of Achievements in Materials and Manufacturing Engineering,* 47, 115-36.

May, C. Y. (2004). Transesterification of palm oil: effect of reaction parameters. *The Journal of Oil Palm Research*, 16, 1–11.

Meher, L.C., Kulkarni, M.G., Dalai, A.K., Naik, S.N. (2006). Transesterification of karanja (Pongamia pinnata) oil by solid basic catalysts. *European Journal of Lipid Science and Technology*, 108, 389–97.

Meng, X., Jia, M., Wang, T. (2014). Neural network prediction of biodiesel kinematic viscosity at 313 K. *Fuel*, 121, 133–140.

Moser B.R. (2008). Influence of blending canola, palm, soybean, and sunflower oil methyl esters on fuel properties of biodiesel. *Energy and Fuels*, 22(6), 4301–6.

Moser, B.R. (2009). Biodiesel production, properties and feedstocks. *In Vitro Cellular & Developmental Biology*, 45, 229–266.

Moss, D.R. (2004). Pressure Vessel Design Manual. 3rd edition. Gulf Professional Publishing, Oxford, Elsevier.

NREL. (2009). Biodiesel handling and use guide – fourth edition. *National Renewable Energy Laboratory*. Report no. NREL/ TP540-43672.

Noureddini, H., Harkey, D., Medikonduru, V. (1998). A continuous process for the conversion of vegetable oils into methyl esters of fatty acids. *Journal of Scientific and Industrial Research*, 75, 1775–83.

Noureddini, H., Gao, X., Philkana, R.S. (2005). Immobilized Pseudomonas cepacia lipase for biodiesel fuel production from soybean oil. *Bioresources Technology*, 96, 769–77.

Nwafor, O.M.I. & Rice, G. (1996). Performance of rapeseed oil blends in a diesel engine. *Applied Energy*, 54, 345–54.

Oluwoye, I. (2013). Kinematic viscosity of different biodiesel fuel at various temperatures. MSc Thesis, Near East University, Nicosia, Mersin10, Turkey.

Otera, J. (1993). Transesterication. *Chemistry Review*, 3(4), 1449-70.

Ozaktas, T. (2000). Compression ignition engine fuel properties of a used sunflower oil–diesel fuel blend. *Energy Sources*, 22, 377–82.

Öğüt, H., Oğuz H. (2006) Biyodizel. *Nobel Yayın Dağıtım*, 2. Basım.

Panoutsou, C., Namatov, I., Lychnaras V., Nikolau, A. (2008). Biodiesel Options in Greese, *Biomass and Bioenergy*, 32, 473-481.

Pasadakis, N., Sourligas, S., Foteinopoulos, C. (2006). Prediction of the distillation profile and cold properties of diesel fuels using mid-IR spectroscopy and neural networks. *Fuel*, 85, 1131–1137.

Pauly J., Kouakou, A.C., Habrioux, M., Le, Mapihan. K. (2014) Heat capacity measurements of pure fatty acid methyl esters and biodiesels from 250 to 390 K. *Fuel,* 37, 21-27.

Peters, M.S., Timmerhaus, K.D. (2003). Plant Design and Economics for Chemical Engineers. 5th ed. New York: McGraw Hill.

Phan, A.N., Phan, T.M. (2008). Biodiesel Production from Waste Cooking Oils. *Fuel*, 87, 3490-3496.

Piloto-Rodríguez, R., Sánchez-Borroto, Y., Lapuerta, M., Goyos-Pérez, L., Verhelst, S. (2013). Prediction of the cetane number of biodiesel using artificial neural networks and multiple linear regression. *Energy Conversion Management*, 65, 255–261.

Pinnarat, T., Savage, P.E. (2010). Noncatalytic esterification of oleic acid in ethanol. *The Journal of Supercritical Fluids*, 53 (1-3), 53-59.

Pramanik, K. (2003). Properties and use of Jatropha curcas oil and diesel fuel blends in compression ignition engine. *Renewable Energy*, 28, 239–48.

Qureshi, N., Saha, B.C., Hector, R.E., Hughes, S.R., Cotta, M.A. (2008). Butanol production from wheat straw by simultaneous saccharification and fermentation using Clostridium beijerinckii: Part I— Batch fermentation. *Biomass Bioenergy,* 32, 168–175.

Rakopoulos, C.D., Antonopoulos, K.A., Rakopoulos, D.C., Kakaras, E.C., Pariotis, E.G. (2007). Characteristics of the performance and emissions of a HSDI diesel engine running with cottonseed oil or its methyl ester and their blends with diesel fuel. *International Journal of Vehicle Design*, 45, 200–21.

Ramos, M.J., Fernández, C.M., Casas, A., Rodríguez, L., Pérez, A. (2009). Influence of fatty acid composition of raw materials on biodiesel properties. *Bioresources Technology*, 100, 261–268.

Rapaka, S. (2012). Reduction and Speciation of Monoglycerides to produce high quality biodiesel. MSc. University of Ottawa. Department of Chemical Engineering. Ottawa, Canada.

Rasimoglu, N., Temur, H. (2014). Cold flow properties of biodiesel obtained from corn oil. *Energy*, 68, 57-60.

Refaat A.A. (2009). Correlation between the chemical structure of biodiesel and its physical properties. *International Journal of Environmental of and Science Technology*, 6(4), 677–94.

Roy R.K. (2001). Design of experiments using the Taguchi approach: 16 steps to product and process improvement. New York: Wiley.

Royon, D., Daz, M., Ellenrieder, G., Locatelli, S. (2007). Enzymatic production of biodiesel from cotton seed oil using t-butanol as a solvent. *Bioresources Technology*, 98, 648–53.

Sabudak, T., Yıldız, M. (2010) Biodiesel Production from Waste Frying Oils and its Quality Control. *Waste Management*, 30, 799-803.

Sahoo, P.K., Das, L.M. (2009). Process optimization for biodiesel production from Jatropha, Karanja and Polanga oils. *Fuel*, 88, 1588–1594.

Saka, S., Kusdiana, D. (2001). Biodiesel fuel from rapeseed oil as prepared in supercritical methanol. *Fuel*, 80, 225–31.

Saka, S., Kusdiana, D., Minami, E. (2006) Non-catalytic biodiesel fuel production with supercritical methanol technologies. *Journal of Scientific and Industrial Research*, 65, 420-425.

Sanford, S.D., White, J.M., Shah P.S., Wee, C., Valverde, M.A., Meier, G.R. (2010). Feedstock and Biodiesel Characteristics Report. Renewable Energy Group, Inc.

Sapaun, S.M., Masjuki, H.H., Azlan, A. (1996). The use of palm oil as diesel fuel substitute. *Journal of Power Energy*, 210, 47–53.

Sarin, A., Arora, R., Singh, N.P., Sarin, R., Malhotra, R.K., Kundu, K. (2009). Effect of blends of Palm-Jatropha-Pongamia biodiesels on cloud point and pour point. *Energy*, 43, 2012-2016

Sarin, A., Arora, R., Singh, N.P., Sarin, R., Malhotra, R.K., Sarin, S. (2010). Blends of biodiesels synthesized from non-edible and edible oils: effects on the cold filter plugging point. *Energy and Fuels*, 24, 1996–2001.

Satapimonphan, S., Pengprecha, S. (2012). Improving cold flow property of biodiesel from white sesame seed oil. ICCEEI'2012) July 15-16, Singapore.

Schwab, A.W., Bagby, M.O., Freedman, B. (1987). Preparation and properties of diesel fuels from vegetable oils. *Fuel*, 66, 1372–8.

Schulte, W.B. (2007). Biodiesel production from tall oil and chicken fat via supercritical methanol treatment. University of Arkansas, Fayetteville.

Shahid, E.M., Jamal Y. (2008) A Review of Biodiesel as a Vehicular Fuel. *Renewable and Sustainable Energy Reviews*, 12, 2484-2494.

Sharma, Y.C., Singh, Y.C., Upadhyay, S.N. (2007) Advancements in Development and Characterization of Biodiesel: A Review. *Fuel*, 87, 2355-2373.

Singh, S.P., Singh, D. (2010). Biodiesel production through the use of different sources and characterization of oils and their esters as the substitute of diesel: A review. *Renewable and Sustainable Energy Reviews*, 14, 200–216.

Silitonga, A.S., Masjuki, H.H., Mahlia, T.M., Ong, H.C., Chong, W.T., Boosroh, M.H. (2013). Overview properties of biodiesel diesel blends from edible and non-edible feedstock. *Renewable and Sustainable Energy Reviews*, 22, 346–360

Silva, C., Oliveria, V. (2014). Biodiesel production through non-catalytic supercritical transesterification: current state and perspectives. *Brazilian Journal of Chemical Engineering*, 31, 271 – 285.

Srivastava, A. & Prasad, R. (2000). Triglycerides-based diesel fuels. *Renewable Sustainable Energy Review*, 4, 111–33.

Steinbach A. (2007) A Comprehensive Analysis of Biodiesel. *Biodiesel Magazine*, Nov.

Stournas, S., Lois, E., Serdari, A. (1995). Effects of fatty-acid derivatives on the ignition quality and cold flow of diesel fuel. *Journal of the American Oil Chemists Society*, 72(4), 433–7.

Stumborg, M., Wong, A., Hogan, E. (1996). Hydroprocessed vegetable oils for diesel fuel improvement. Bioresources. Technology, 56, 13–18.

Su, Y.-C., Liu, A.L., Diaz-Tovar, C.A., Gani, R. (2011). Selection of prediction methods for thermophysical properties for process modeling and product design of biodiesel manufacturing. *Industrial & Engineering Chemistry Research*, 50, 6809-6836.

Taguchi, G., Konishi, S. (1987). Taguchi methods, orthogonal arrays and linear graphs, tools for quality American supplier institute. *American Supplier Institute*, pp. 8-35.

Tang, H., Salley, S.O., Simon, K.Y. (2008). Fuel properties and precipitate formation at low temperature in soy-, cottonseed-, and poultry fat-based biodiesel blends. *Fuel,* 87, 3006–3017.

Tippayawong, N., Wongsiriamnuay, T., Jompakdee, W. (2002). Performance and emissions of a small agricultural diesel engine fueled with 100% vegetable oil: effects of fuel type and elevated inlet temperature. *Asian Journal of Energy Environment*, 3, 139–58.

TRCR (Turkish Relief Commision Report). (2012).TC Yardım Heyeti Başkanlığı- TC Lefkoşa Büyükelçiliği- KKTC 2012 Ekonomi Durum Raporu, 22-23.

Udomsap, P., Sahapatsombat, U., Puttasawat, B., Krasae, P., Chollacoop, N., Topaiboul, S. (2008). Preliminary investigation of cold flow improvers for palm-derived biodiesel blends. *Journal of the Minerals, Metals and Materials Society*, 18 (2), 99-102.

Ul-Haq, I., Shin, J.S., Lee, Z.H. Computer-aided cooling curve analysis of A356 aluminum alloy. *Metals and Materials International*, 10, 89-96.

US Patent: US7851643. (2010). Hillion G., Delford Method of Manufacturing Fatty Acid Ethyl Esters from Triglycerides and Alcohols.

Usta, N., Aydoğan, B., Çon, A.H., Uğuzdoğan, E., Özkal, S.G. (2011). Properties and quality verification of biodiesel produced from tobacco seed oil. *Energy Conversion and Management*, 52, 2031–2039.

Van Gerpen, J., Shanks, B., Pruszko, R., Clements, D., Knothe, G. (2004). Biodiesel Production Technology. National Renewable Energy Laboratory NREL/SR-510-36244.

Wang, Y.D., Al-Shemmeri, T., Eames, P., McMullan, J., Hewitt, N., Huang, Y. (2006). An experimental investigation of the performance and gaseous exhaust emissions of a diesel engine using blends of a vegetable oil. *Applied Thermal Engineering*, 26, 1684–91.

Wang, B., Li, Y.Q., Wu, N., and Lan, C.Q. (2008). CO(2) bio-mitigation using microalgae. *Journal of Applied Microbiology Biotechnology*, 79, 707–718.

Wang, J., Cao, L., Han, S. (2014). Effect of polymeric cold flow improvers on flow properties of biodiesel from waste cooking oil. *Fuel*, 117, 876-81.

Watanabe, Y., Shimada, Y., Sugihara, A., Noda, H., Fukuda, H., Tominaga, Y. (2000). Continuous production of biodiesel fuel from vegetable oil using immobilized Candida antarcticalipase. *The Journal of the American Oil Chemists' Society*, 77, 355–60.

WFC. (2006). Worldwide Fuel Charter. Report no. 4th ed. European Automobile Manufacturer’s Association.

Wrolstad, R.E., Decker, E.A., Schwartz, S.J., Sporns, P. (2005). Handbook of Food Analytical Chemistry, Wiley, 2005; 472-475.

Yang, H., Ring, Z., Briker, Y., McLean, N., Friesen, W., Fairbridge, C. (2002). Neural network prediction of cetane number and density of diesel fuel from its chemical composition determined by LC and GC–MS. *Fuel*, 81, 65–74.

Yaws, C. L. (1999). Chemical Properties Handbook. In McGraw-Hill: pp 1-29.

Zaher, F.A. (2003). Utilization of used frying oil as diesel engine fuel. *Energy Sources*, 25, 819–26.

Ziejewski, M., Kaufman, K.R., Pratt, G.L. (1983). Vegetable oil as diesel fuel. Seminar II, Northern Regional Research Center, Peoria, Illinois, 19±20 October.

Zhang, Y., Dube, M.A., McLean, D.D., Kates, M. (2003) Biodiesel production from waste cooking oil: 1. Process design and technological assessment. *Bioresource Techonology*, 89, 1–16.

Ziejewski, M., Kaufman, K.R., Pratt, G.L. (1983). Vegetable oil as diesel fuel. Seminar II, Northern Regional Research Center, Peoria, Illinois, 19-20 October.

APPENDICES

APPENDIX 1

EN 14214: AUTOMOTIVE FUELS - FATTY ACID METHYL ESTERS (FAME) FOR DIESEL ENGINES -REQUIREMENTS AND TEST METHODS

EUROPEAN STANDARD

NORME EUROPÉENNE

EUROPÄISCHE NORM

FINAL DRAFT
prEN 14214

October 2002

ICS 75.160.20

English version

Automotive fuels - Fatty acid methyl esters (FAME) for diesel engines - Requirements and test methods

Carburants pour automobiles - Esters méthyliques d'acide gras (EMAG) pour moteurs diesel - Exigences et méthodes d'essais

Kraftstoffe für Kraftfahrzeuge - Fettsäure-Methylester (FAME) für Dieselmotoren - Anforderungen und Prüfverfahren

This draft European Standard is submitted to CEN members for formal vote. It has been drawn up by the Technical Committee CEN/TC 19.

If this draft becomes a European Standard, CEN members are bound to comply with the CEN/CENELEC Internal Regulations which stipulate the conditions for giving this European Standard the status of a national standard without any alteration.

This draft European Standard was established by CEN in three official versions (English, French, German). A version in any other language made by translation under the responsibility of a CEN member into its own language and notified to the Management Centre has the same status as the official versions.

CEN members are the national standards bodies of Austria, Belgium, Czech Republic, Denmark, Finland, France, Germany, Greece, Iceland, Ireland, Italy, Luxembourg, Malta, Netherlands, Norway, Portugal, Spain, Sweden, Switzerland and United Kingdom.

Warning : This document is not a European Standard. It is distributed for review and comments. It is subject to change without notice and shall not be referred to as a European Standard.

EUROPEAN COMMITTEE FOR STANDARDIZATION
COMITÉ EUROPÉEN DE NORMALISATION
EUROPÄISCHES KOMITEE FÜR NORMUNG

Management Centre: rue de Stassart, 36 B-1050 Brussels

Ref. No. prEN 14214:2002 E

Contents

Foreword

This document (prEN 14214:2002) has been prepared by Technical Committee CEN/TC 19 "Petroleum products, lubricants and related products", the secretariat of which is held by NEN.

This document is currently submitted to the Formal Vote.

This document has been prepared under a mandate given to CEN by the European Commission and the European Free Trade Association.

This European standard exists in parallel with EN 590 “Automotive fuels - Diesel - Requirements and test methods”.

This standard gives all relevant characteristics, requirements and test methods for FAME, which are known at time to be necessary to define the product to be used as automotive diesel fuel, including iodine value. The stability characteristics of FAME are under investigation in an EU-funded research programme ‘BIOSTAB’, and suitable limits and test methods may be incorporated into an amended version of this standard upon successful conclusion of this programme, including a possible replacement for iodine value.

Many of the test methods included in this standard were the subject of inter-laboratory testing to determine the applicability of the method and its precision in relation to different sources of fatty acid methyl esters. These fatty acid methyl esters were produced from rapeseed and sunflower oil.

Annex A is normative and contains the precision data generated on the test methods which are the result of the interlaboratory testing as mentioned above, carried out by working groups of CEN/TC 19. Annex B and C, also normative, contain details on two calculations.

1 Scope

This European Standard specifies requirements and test methods for marketed and delivered fatty acid methyl esters (FAME) to be used either as automotive fuel for diesel engines at 100% concentration, or as an extender for automotive fuel for diesel engines in accordance with the requirements of EN 590. At 100% concentration it is applicable to fuel for use in diesel engine vehicles designed or subsequently adapted to run on 100% FAME.

NOTE: For the purposes of this European Standard, the terms "% (*m/m*)" and "% (*V/V*)" are used to represent respectively the mass fraction and the volume fraction.

2 Normative references

This European Standard incorporates by dated or undated reference, provisions from other publications. These normative references are cited at the appropriate places in the text and the publications are listed hereafter. For dated references, subsequent amendments to or revisions of any of these publications apply to this European Standard only when incorporated in it by amendment or revision. For undated references the latest edition of the publication referred to applies (including amendments).

EN 116:1997, *Diesel and domestic heating fuels – Determination of cold filter plugging point*

EN 590:1997, *Automotive fuels - Diesel - Requirements and test methods*

EN 12662:1998, *Liquid petroleum products - Determination of contamination in middle distillates*

prEN 14103:2001*, Fat and oil derivatives - Fatty Acid Methyl Esters (FAME) – Determination of ester and linolenic acid methyl ester contents*

prEN 14104:2001*, Fat and oil derivatives – Fatty Acid Methyl Esters (FAME) - Determination of acid value*

prEN 14105:2001, *Fat and oil derivatives – Fatty Acid Methyl Esters (FAME) – Determination of free and total glycerol and mono-, di-, triglyceride contents - Reference method*

prEN 14106:2001, *Fat and oil derivatives – Fatty Acid Methyl Esters (FAME) – Determination of free glycerol content*

prEN 14107:2001*, Fat and oil derivatives – Fatty Acid Methyl Esters (FAME) – Determination of phosphorus content by inductively coupled plasma (ICP) emission spectrometry*

prEN 14108:2001*, Fat and oil derivatives - Fatty Acid Methyl Esters (FAME) – Determination of sodium content by atomic absorption spectrometry*

prEN 14109:2001*, Fat and oil derivatives - Fatty Acid Methyl Esters (FAME) – Determination of potassium content by atomic absorption spectrometry*

prEN 14110:2001*, Fat and oil derivatives – Fatty Acid Methyl Esters (FAME) - Determination of methanol content*

prEN 14111:2001, *Fat and oil derivatives – Fatty Acid Methyl Esters (FAME) – Determination of iodine value*

prEN 14112:2001*, Fat and oil derivatives - Fatty Acid Methyl Esters (FAME) - Determination of oxidation stability (accelerated oxidation test)*

prEN 14538:2002, *Fat and oil derivatives – Fatty Acid Methyl Esters (FAME) – Determination of Ca and Mg content by optical emission spectral analysis with inductively coupled plasma (ICP OES)*

EN ISO 2160:1998, *Petroleum products - Corrosiveness to copper - Copper strip test (ISO 2160:1998)*

EN ISO 3104:3104, *Petroleum products - Transparent and opaque liquids - Determination of kinematic viscosity and calculation of dynamic viscosity (ISO 3104:1994. incl. ISO Tech. Cor. N^o 1)*

EN ISO 3170:1998, *Petroleum liquids – Manual sampling (ISO 3170:1988/A1:1998)*

EN ISO 3171:1998, *Petroleum liquids – Automatic pipeline sampling (ISO 3171:1988)*

EN ISO 3675:1998, *Crude petroleum and liquid petroleum products - Laboratory determination of density - Hydrometer method (ISO 3675:1998)*

EN ISO 4259:1995, *Petroleum products - Determination and application of precision data in relation to methods of test (ISO 4259:1992, including Cor. 1:1993)*

EN ISO 5165:1998, *Petroleum products - Determination of the ignition quality of diesel fuels - Cetane engine method (ISO 5165:1998)*

EN ISO 10370:1995, *Petroleum products - Determination of carbon residue (micro method) (ISO 10370: 1993)*

EN ISO 12185:1996/C1:2001, *Crude petroleum and petroleum products - Determination of density - Oscillating U-tube method (ISO 12185:1996, incl. ISO Tech. Cor. N^o 1)*

EN ISO 12937:2000, *Petroleum products - Determination of water - Coulometric Karl Fisher titration method (ISO 12937:2000)*

EN ISO 13759:1996, *Petroleum products – Determination of alkyl nitrate in diesel fuels – Spectrometric method (ISO 13759:1996).*

prEN ISO 20846:2002, *Petroleum products – Determination of total sulfur content of liquid petroleum products – Ultraviolet fluorescence method (ISO/DIS 20846:2002)*

prEN ISO 20884:2002, *Petroleum products – Determination of low sulfur content of automotive fuels – Wavelength-dispersive X-ray fluorescence spectrometry (ISO/DIS 20884:2002)*

ISO/DIS 3679:3679*, Petroleum products - Determination of flash point - Rapid equilibrium closed cup method*

ISO 3987:1994*, Petroleum products - Lubricating oils and additives - Determination of sulfated ash*

ASTM D 1160:1999*, Distillation of Petroleum Products at Reduced Pressure*

3 Sampling

Samples shall be taken as described in EN ISO 3170 or EN ISO 3171 and/or in accordance with the requirements of national standards or regulations for the sampling of automotive diesel fuel. The national requirements shall be set out in a national annex to this European Standard, either in detail or by reference only.

In view of the sensitivity of some of the test methods referred to in this European Standard, particular attention shall be paid to compliance with any guidance on sampling containers, which is included in the test method standard.

4 Pump marking

Information to be marked on dispensing pumps used for delivering FAME diesel fuel, and the dimensions of the mark shall be in accordance with the requirements of national standards or regulations for the marking of pumps for automotive diesel fuel. Such requirements shall be set out in detail or shall be referred to by reference in a national annex to this European Standard.

5 Requirements and test methods

5.1 Dyes and markers

The use of dyes or markers is allowed.

5.2 Additives

In order to improve the performance quality, the use of additives is allowed. Suitable fuel additives without known harmful side effects are recommended in the appropriate amount, to help to avoid deterioration of driveability and emissions control durability. Other technical means with equivalent effect may also be used.

NOTE Deposit forming tendency test methods suitable for routine control purposes have not yet been identified and developed.

5.3 Generally applicable requirements and related test methods

5.3.1 When tested by the methods indicated in Table 1, fatty acid methyl esters (FAME) shall be in accordance with the limits specified in Table 1. The test methods listed in Table 1 have been shown to be applicable to fatty acid methyl esters in an inter-laboratory test programme. Precision data from this programme are given in normative Annex A, where these were found to be different from the precision data given in the test methods for petroleum products.

5.3.2 In case of a need for identification of FAME, a recommended method based on separation and characterisation of fatty acid methyl esters by LC/GC is prEN 14331 [1].

5.3.3 In case of a need for a check upon FAME quality, iodine value of FAME may be calculated by the method presented in Annex B (normative), but this method does not constitute an alternative to the iodine value requirement of Table 1.

5.3.4 The limiting value for the carbon residue given in Table 1 is based on product prior to addition of ignition improver, if used. If a value exceeding the limit is obtained on finished fuel in the market, EN ISO 13759 shall be used as an indicator of the presence of a nitrate-containing compound. If an ignition improver is thus proved present, the limit value for the carbon residue of the product under test cannot be applied. The use of additives does not exempt the manufacturer from meeting the requirement of maximum 0,30 % (*m/m*) of carbon residue prior to addition of additives.

Table 1 - Generally applicable requirements and test methods

Property	Unit	Limits		Test method [a]
		Minimum	Maximum	
Ester content [a]	% (*m/m*)	96,5 [b]		prEN 14103
Density at 15 °C [c]	kg/m^3	860	900	EN ISO 3675 EN ISO 12185
Viscosity at 40 °C [d]	mm^2/s	3,50	5,00	EN ISO 3104
Flash point	°C	120	–	ISO/DIS 3679 [e]
Sulfur content	mg/kg	–	10,0	prEN ISO 20846 prEN-ISO 20884
Carbon residue (on 10 % distillation residue) [f]	% (m/m)	–	0,30	EN ISO 10370
Cetane number [g]		51,0		EN ISO 5165
Sulfated ash content	% (m/m)	–	0,02	ISO 3987
Water content	mg/kg	–	500	EN ISO 12937
Total contamination [h]	mg/kg	–	24	EN 12662
Copper strip corrosion (3 h at 50 °C)	Rating	Class 1		EN ISO 2160
Oxidation stability, 110 °C	Hours	6,0	–	prEN 14112
Acid value	mg KOH/g		0,50	prEN 14104
Iodine value			120	prEN 14111
Linolenic acid methyl ester	% (m/m)		12,0	prEN 14103
Polyunsaturated (>= 4 double bonds) methyl esters [i]	% (m/m)		1	
Methanol content	% (m/m		0,20	prEN 14110
Monoglyceride content	% (m/m)		0,80	prEN 14105
Diglyceride content	% (m/m)		0,20	prEN 14105
Triglyceride content [j]	% (m/m)		0,20	prEN 14105
Free glycerol [j]	% (m/m)		0,02	prEN 14105 prEN 14106
Total glycerol	% (m/m)		0,25	prEN 14105
Group I metals (Na+K) [k]	mg/kg		5,0	prEN 14108 prEN 14109
Group II metals (Ca+Mg) [l]	mg/kg		5,0	prEN 14538
Phosphorus content	mg/kg		10,0	prEN 14107

[a] See 5.5.1

[b] The addition of non-FAME components other than additives is not allowed, see 5.2.

[c] Density may be measured by EN ISO 3675 over a range of temperatures from 20 ^{0}C to 60 ^{0}C. Temperature correction shall be made according to the formula given in Annex C. See also 5.5.2

[d] If CFPP is –20 °C or lower, the viscosity measured at -20 °C shall not exceed 48 mm^2/s. In this case, EN ISO 3104 is applicable without the precision data owing to non-Newtonian behaviour in a two-phase system.

[e] A 2 ml sample and apparatus equipped with a thermal detection device shall be used

[f] ASTM D 1160 shall be used to obtain the 10% distillation residue.

[g] See 5.5.3.

[h] See 5.5.1. An improved method is under development by CEN/TC 19.

[i] Suitable test method to be developed

[j] See also 5.5.1.

[k] Method under development. See Annex A for precision data for sum of Na + K

[l] See 5.5.1. Method under development. See Annex A for precision data for sum of Ca + Mg.

5.4 Climate dependent requirements and related test methods

5.4.1 For climate-dependent requirements options are given to allow for seasonal grades to be set nationally. The options are for temperate climates six CFPP (cold filter plugging point) grades and for arctic climates five different classes. Climate-dependent requirements are given in Table 2. Table 2 is divided into two sections, one for temperate climates (table 2a) and one for arctic climates (table 2b). When tested by the methods given in tables 2a and 2b, automotive diesel fuel shall be in accordance with the limits specified in these tables.

5.4.2 In a national annex to this European Standard each country shall detail requirements for a summer and a winter grade and may include (an) intermediate and/or regional grade(s) which shall be justified by national meteorological data.

Table 2 - Climate-related requirements and test methods

Table 2a - Temperate climates

Property	Unit	Limits						Test method [a]
		Grade A	Grade B	Grade C	Grade D	Grade E	Grade F	
CFPP	°C, max.	+5	0	-5	-10	-15	-20	EN 116
[a] See also 5.5.1.								

Table 2b - Arctic climates

Property	Units	Limits					Test method [a]
		class 0	Class 1	class 2	Class 3	class 4	
CFPP	°C, max.	-20	-26	-32	-38	-44	EN 116
[a] See also 5.5.1.							

5.5 Precision and dispute

5.5.1 All test methods referred to in this European Standard include a precision statement according to EN ISO 4259. In cases of dispute, the procedures described in EN ISO 4259 shall be used for resolving the dispute, and interpretation of the results based on the test method precision shall be used. However, the methods currently available for total contamination, ester content, triglyceride content, free glycerol and alkaline metals (Na + K) do not meet the 2R requirement of EN ISO 4259 at the limit in Table 1.

5.5.2 In cases of dispute concerning density, EN ISO 3675 shall be used with the determination carried out at 15 °C.

In cases of dispute concerning free glycerol, prEN 14105 shall be used.

5.5.3 For the determination of cetane number alternative methods may also be used in cases of dispute, provided that these methods originate from a recognized method series, and have a valid precision statement, derived in accordance with EN ISO 4259, which demonstrates precision at least equal to that of the referenced method. The test result, when using an alternative method, shall also have a demonstrable relationship to the result obtained when using the reference method.

Annex A
(normative)
Details of inter-laboratory test programme

Table of precision data from inter-laboratory test programme for requirements where precision differs from ISO/TC28 precision data

Property	Test method	Unit	CEN/TC19 data for pure FAME
Viscosity at 40 °C	EN ISO 3104	mm^2/s	r 0,11% R 1,8%
Flash point	ISO/DIS 3679	deg C	r 1,9 R 15,0
Sulfur content	prEN ISO 20884	mg/kg	r 0,026X + 1,356 R 0,0567X + 1,616
Cetane number	EN ISO 5165		r 2,4 R 5,0
Sulfated ash content	ISO 3987	%(m/m)	r $0,06X^{0,85}$ R $0,142X^{0,85}$
Total contamination	EN 12662	mg/kg	not available
CFPP	EN 116	deg C	not available
Distillation	ASTM D 1160	deg C	r 2,0 R 3,0 (90% distilled)

Precision data for the sum of Na + K, measured individually by prEN 14108 and prEN 14109, are as follows:

Repeatability r $-0,017 * X + 0,512$

Reproducibility R $0,305 * X + 1,980$

Precision data for the sum of Ca + Mg, measured by prEN 14538, are as follows:

Repeatability r $0,0232X + 0,271$

Reproducibility R $0,149X + 1,186$

Annex B

(normative)

Calculation of Iodine Value

NOTE This method is adapted for biodiesel from the AOCS recommended practice Cd 1c – 85 for the determination of the iodine value of edible oil from its fatty acid composition [2].

B.1 Scope

This method describes a procedure for calculating the iodine value of neat biodiesel or biodiesel extracted from blends with diesel fuel.

B.2 Definition

This method is used to calculate the iodine value expressed in g I_2 /100 g sample from the percentage by mass of methyl esters as determined by either prEN 14103 (neat biodiesel) or prEN 14331 [1] (biodiesel extracted from blends with diesel fuel).

B.3 Procedure

The methyl ester composition of the sample is checked using the appropriate method as described in paragraph 2. The total methyl esters thus revealed should equal 100 after the deduction of the methyl ester C17 used for internal standard in prEN 14103.

The percentage by mass thus obtained is then used to calculate the sample's iodine value, being the sum of the individual contributions of each methyl ester, obtained by multiplying the methyl ester percentage by its respective factor (Table B.1), as indicated in the example in Table B.2.

The factor for each constituent of biodiesel is given in Table B.1.

Table B.1
METHYL ESTER FACTORS

Methyl ester	**Factor**
Methyl ester of saturated fatty acids	0
Methyl hexadecenoate (Methyl palmoleate) C16:1	0,950
Methyl octadecenoate (Methyl oleate) C18:1	0,860
Methyl octadecadienoate (Methyl lineolate) C18:2	1,732
Methyl octadecatrienoate (Methyl linolenate) C18:3	2,616
Methyl eicosenoate C20:1	0,785
Methyl docasenoate (Methyl erucate) C22:1	0,723

An example of the calculation of iodine value from the percentage by mass of methyl esters is given in Table B.2

Table B.2
CALCULATION EXAMPLE

Methyl ester of the following acids	Percentage % m/m	Factor	Contribution
Myristic C14:0	0,3	0	0
Palmitic C16:0	4,0	0	0
Palmitoleic C16:1	1,1	0,950	1,0
Stearic C18:0	2,0	0	0
Oleic C18:1	60,5	0,860	52,0
Linoleic C18:2	19,8	1,732	34,3
Linolenic C18:3	9,4	2,616	24,6
Eicosanoic C20:0	0,4	0	0
Eicosenoic C20:1	0,7	0,785	0,6
Docosanoic C22:0	0,7	0	0
Docosenoic C22:1	1,1	0,723	0,8
		Calculated I.V.	113,3

B.4 Expression of the result

Iodine value (calculated from the methyl ester composition) = X g I_2 /100 g (B.1)

The result shall be reported to one decimal place.

NOTE 1 In 1994 the AOCS Uniform Methods Committee reviewed the coefficients used and concluded that no changes were necessary at that time. The present procedure uses the coefficients selected in the past for use in calculating the iodine value in triglyceride blends. The reasoning behind that choice is that triple the molecular weight of a methyl ester is almost identical to the molecular weight of the corresponding triglyceride.

NOTE 2 For samples with unsaponifiable content greater than 0,5% (m/m) or those containing a significant additive content, the calculated value tends to be higher than the true value.

NOTE 3 The calculated result tends to be lower than the true value in samples with a lower iodine value.

NOTE 4 In case of dispute the iodine value should be determined by prEN 14111.

Annex C
(normative)
Correction factor for calculation of density of FAME

The conversion factor for the correction of density, determined by EN ISO 3675 over a range of temperatures from 20 ^{0}C to 60 ^{0}C, to density at 15 ^{0}C is based on data published at the International Conference on Standardization and Analysis of Biodiesel, Vienna, November 1995 [3].

The density of seven samples of FAME was measured by pyknometer at 6 temperatures over the range 20 ^{0}C to 60 ^{0}C. The mean correction factor over the range was calculated as 0,723 kg/m^3.K, with a standard deviation of 1,2 % of this value. The average density of the FAME samples at 15 ^{0}C was calculated as 886,5 kg/m^3.

The following formula shall be used for the calculation of density of FAME at a certain temperature (*T*), determined by EN ISO 3675 over the range of temperatures from 20 ^{0}C to 60 ^{0}C:

$$\text{Density at } 15\ {}^0\text{C, kg/m}^3 = \text{Density at } T\ {}^0\text{C} + 0{,}723(T - 15) \qquad \text{(C.1)}$$

Bibliography

[1] prEN 14331, Liquid petroleum products – Separation and characterisation of fatty acid methyl esters (FAME) by liquid chromatography/gas chromatography (LC/GC).

[2] *The official Methods and Recommended Practices of the AOCS*, 5th edition, 1998, Champaign, IL, USA.

[3] J. Rathbauer & A. Bachler, *Physical Properties of Vegetable Oil Methyl Esters*, International Conference on Standardization and Analysis of Biodiesel, November 6th – 7th, 1995, Vienna.

APPENDIX 2

ASTM D6751: STANDARD SPECIFICATION FOR BIODIESEL FUEL BLEND STOCK (B100) FOR MIDDLE DISTILLATE FUELS

Designation: D6751 – 09a

Standard Specification for
Biodiesel Fuel Blend Stock (B100) for Middle Distillate Fuels[1]

This standard is issued under the fixed designation D6751; the number immediately following the designation indicates the year of original adoption or, in the case of revision, the year of last revision. A number in parentheses indicates the year of last reapproval. A superscript epsilon (´) indicates an editorial change since the last revision or reapproval.

1. Scope*

1.1 This specification covers biodiesel (B100) Grades S15 and S500 for use as a blend component with middle distillate fuels.

1.2 This specification prescribes the required properties of diesel fuels at the time and place of delivery. The specification requirements may be applied at other points in the production and distribution system when provided by agreement between the purchaser and the supplier.

1.3 Nothing in this specification shall preclude observance of federal, state, or local regulations which may be more restrictive.

NOTE 1—The generation and dissipation of static electricity can create problems in the handling of distillate fuel oils with which biodiesel may be blended. For more information on the subject, see Guide D4865.

1.4 The values stated in SI units are to be regarded as standard. No other units of measurement are included in this standard.

1.4.1 *Exception*—In Annex A1, the values stated in SI units are to be regarded as the standard. The values given in parentheses are for information only.

2. Referenced Documents

2.1 *ASTM Standards:*[2]

D93 Test Methods for Flash Point by Pensky-Martens Closed Cup Tester
D130 Test Method for Corrosiveness to Copper from Petroleum Products by Copper Strip Test
D189 Test Method for Conradson Carbon Residue of Petroleum Products
D445 Test Method for Kinematic Viscosity of Transparent and Opaque Liquids (and Calculation of Dynamic Viscosity)
D524 Test Method for Ramsbottom Carbon Residue of Petroleum Products
D613 Test Method for Cetane Number of Diesel Fuel Oil
D664 Test Method for Acid Number of Petroleum Products by Potentiometric Titration
D874 Test Method for Sulfated Ash from Lubricating Oils and Additives
D974 Test Method for Acid and Base Number by Color-Indicator Titration
D975 Specification for Diesel Fuel Oils
D976 Test Method for Calculated Cetane Index of Distillate Fuels
D1160 Test Method for Distillation of Petroleum Products at Reduced Pressure
D1266 Test Method for Sulfur in Petroleum Products (Lamp Method)
D1796 Test Method for Water and Sediment in Fuel Oils by the Centrifuge Method (Laboratory Procedure)
D2274 Test Method for Oxidation Stability of Distillate Fuel Oil (Accelerated Method)
D2500 Test Method for Cloud Point of Petroleum Products
D2622 Test Method for Sulfur in Petroleum Products by Wavelength Dispersive X-ray Fluorescence Spectrometry
D2709 Test Method for Water and Sediment in Middle Distillate Fuels by Centrifuge
D2880 Specification for Gas Turbine Fuel Oils
D3117 Test Method for Wax Appearance Point of Distillate Fuels
D3120 Test Method for Trace Quantities of Sulfur in Light Liquid Petroleum Hydrocarbons by Oxidative Microcoulometry
D3242 Test Method for Acidity in Aviation Turbine Fuel
D3828 Test Methods for Flash Point by Small Scale Closed Cup Tester
D4057 Practice for Manual Sampling of Petroleum and Petroleum Products
D4177 Practice for Automatic Sampling of Petroleum and Petroleum Products

---

[1] This specification is under the jurisdiction of ASTM Committee D02 on Petroleum Products and Lubricants and is the direct responsibility of Subcommittee D02.E0 on Burner, Diesel, Non-Aviation Gas Turbine, and Marine Fuels.

Current edition approved Dec. 1, 2009. Published February 2010. Originally approved in 1999 as PS 121–99. Adopted as a standard in 2002 as D6751–02. Last previous edition approved in 2009 as D6751–09. DOI: 10.1520/D6751-09a.

[2] For referenced ASTM standards, visit the ASTM website, www.astm.org, or contact ASTM Customer Service at service@astm.org. For Annual Book of ASTM Standards volume information, refer to the standard's Document Summary page on the ASTM website.

***A Summary of Changes section appears at the end of this standard.**

D4294 Test Method for Sulfur in Petroleum and Petroleum Products by Energy Dispersive X-ray Fluorescence Spectrometry
D4530 Test Method for Determination of Carbon Residue (Micro Method)
D4737 Test Method for Calculated Cetane Index by Four Variable Equation
D4865 Guide for Generation and Dissipation of Static Electricity in Petroleum Fuel Systems
D4951 Test Method for Determination of Additive Elements in Lubricating Oils by Inductively Coupled Plasma Atomic Emission Spectrometry
D5452 Test Method for Particulate Contamination in Aviation Fuels by Laboratory Filtration
D5453 Test Method for Determination of Total Sulfur in Light Hydrocarbons, Spark Ignition Engine Fuel, Diesel Engine Fuel, and Engine Oil by Ultraviolet Fluorescence
D5771 Test Method for Cloud Point of Petroleum Products (Optical Detection Stepped Cooling Method)
D5772 Test Method for Cloud Point of Petroleum Products (Linear Cooling Rate Method)
D5773 Test Method for Cloud Point of Petroleum Products (Constant Cooling Rate Method)
D6217 Test Method for Particulate Contamination in Middle Distillate Fuels by Laboratory Filtration
D6300 Practice for Determination of Precision and Bias Data for Use in Test Methods for Petroleum Products and Lubricants
D6450 Test Method for Flash Point by Continuously Closed Cup (CCCFP) Tester
D6469 Guide for Microbial Contamination in Fuels and Fuel Systems
D6584 Test Method for Determination of Free and Total Glycerin in B-100 Biodiesel Methyl Esters by Gas Chromatography
D6890 Test Method for Determination of Ignition Delay and Derived Cetane Number (DCN) of Diesel Fuel Oils by Combustion in a Constant Volume Chamber
D7039 Test Method for Sulfur in Gasoline and Diesel Fuel by Monochromatic Wavelength Dispersive X-ray Fluorescence Spectrometry
D7397 Test Method for Cloud Point of Petroleum Products (Miniaturized Optical Method)

2.2 *Government Standard:*

40 CFR Part 79 Registration of Fuels and Fuel Additives Section 211(b) Clean Air Act[3]

2.3 *Other Documents:*[4]

UOP 389 Trace Metals in Oils by Wet Ashing and ICP-OES
UOP 391–91 Trace Metals in Petroleum Products or Organics by AAS
EN 14112 Fat and oil derivatives—Fatty acid methyl esters (FAME)—Determination of oxidation stability (Accelerated oxidation test)[5]
EN 14110 Fat and oil derivatives—Fatty acid methyl esters (FAME)—Determination of methanol content[5]
EN 14538 Fat and oil derivatives—Fatty acid methyl esters (FAME)—Determination of Ca, K, Mg and Na content by optical emission spectral analysis with inductively coupled plasma (ICP OES)[5]

3. Terminology

3.1 *Definitions:*

3.1.1 *biodiesel, n*—fuel comprised of mono-alkyl esters of long chain fatty acids derived from vegetable oils or animal fats, designated B100.

3.1.1.1 *Discussion—biodiesel*, as defined above, is registered with the U.S. EPA as a fuel and a fuel additive under Section 211(b) of the Clean Air Act. There is, however, other usage of the term biodiesel in the marketplace. Due to its EPA registration and the widespread commercial use of the term biodiesel in the U.S. marketplace, the term biodiesel will be maintained for this specification.

3.1.1.2 *Discussion*—Biodiesel is typically produced by a reaction of a vegetable oil or animal fat with an alcohol such as methanol or ethanol in the presence of a catalyst to yield mono-alkyl esters and glycerin, which is removed. The finished biodiesel derives approximately 10 % of its mass from the reacted alcohol. The alcohol used in the reaction may or may not come from renewable resources.

3.1.2 *biodiesel blend (BXX), n*—blend of biodiesel fuel with diesel fuel oils.

3.1.2.1 *Discussion*—In the abbreviation BXX, the XX represents the volume percentage of biodiesel fuel in the blend.

3.1.3 *biodiesel fuel, n*—synonym for *biodiesel.*

3.1.4 *diesel fuel, n*—middle petroleum distillate fuel.

3.1.5 *free glycerin, n*—a measure of the amount of glycerin remaining in the fuel.

3.1.6 *Grade S15 B100, n*—a grade of biodiesel meeting ASTM Specification D6751 and having a sulfur specification of 15 ppm maximum.

3.1.7 *Grade S500 B100, n*—a grade of biodiesel meeting ASTM Specification D6751 and having a sulfur specification of 500 ppm maximum.

3.1.8 *middle distillate fuel, n*—kerosines and gas oils boiling between approximately 150°C and 400°C at normal atmospheric pressure and having a closed-cup flash point above 38°C.

3.1.9 *total glycerin, n*—the sum of the free glycerin and the glycerin portion of any unreacted or partially reacted oil or fat.

4. Requirements

4.1 The biodiesel specified shall be mono-alkyl esters of long chain fatty acids derived from vegetable oils and animal fats.

4.2 Unless otherwise specified, samples for analysis shall be taken by the procedure described in Practices D4057 or D4177.

---

[3] Available from U.S. Government Printing Office Superintendent of Documents, 732 N. Capitol St., NW, Mail Stop: SDE, Washington, DC 20401.

[4] Available from ASTM International, 100 Barr Harbor Drive, PO Box C700, West Conshohocken, PA. Visit the ASTM website, www.astm.org, or contact ASTM Customer Service at service@astm.org.

[5] Available from the National CEN Members listed on the CEN website (www.cenorm.be) or from the CEN/TC19 secretariat (astm@nen.nl).

4.3 The biodiesel specified shall conform to the detailed requirements shown in Table 1.

NOTE 2—A considerable amount of experience exists in the U.S. with a 20 % blend of biodiesel, primarily produced from soybean oil, with 80 % diesel fuel (B20). Experience with biodiesel produced from animal fat and other oils is similar. Experience with B20 and lower blends in other applications is not as prevalent. Although biodiesel (B100) can be used, blends of over 20 % biodiesel with diesel fuel (B20) should be evaluated on a case by case basis until further experience is available.

NOTE 3—The user should consult the equipment manufacturer or owner's manual regarding the suitability of using biodiesel or biodiesel blends in a particular engine or application.

5. Test Methods

5.1 The requirements enumerated in this specification shall be determined in accordance with the following methods.

5.1.1 *Flash Point*—Test Methods D93, except where other methods are prescribed by law. Test Methods D3828 or D6450 can also be used. The precision and bias of Test Methods D3828 and D6450 with biodiesel is not known and is currently under investigation. Test Methods D93 shall be the referee method.

5.1.2 *Water and Sediment*—Test Method D2709. Test Method D1796 may also be used. Test Method D2709 shall be the referee method. The precision and bias of these test methods with biodiesel is not known and is currently under investigation.

5.1.3 *Viscosity*—Test Method D445.

5.1.4 *Sulfated Ash*—Test Method D874.

5.1.5 *Oxidation Stability*—Test Method EN 14112.

5.1.6 *Sulfur*—Test Method D5453. Test Method D7039 may also be used. Other test methods may also be suitable for determining up to 0.05 % (500 ppm) sulfur in biodiesel fuels such as Test Methods D1266, D2622, D3120 and D4294 but may provide falsely high results (see X1.5) although their precision and bias with biodiesel is unknown. Test Method D5453 shall be the referee test method.

5.1.7 *Corrosion*—Test Method D130, 3 h test at 50°C.

5.1.8 *Cetane Number*—Test Method D613. Test Method D6890 may also be used. Test Method D613 shall be the referee method.

5.1.9 *Cloud Point*—Test Method D2500. Test Method D5771, D5772, D5773, or D7397 may also be used. Test Method D3117 may also be used because it is closely related. Test Method D2500 shall be the referee test method. The precision and bias of Test Method D3117 for biodiesel is not known and is currently under investigation.

5.1.10 *Acid Number*—Test Method D664. Test Methods D3242 or D974 may also be used. Test Method D664 shall be the referee test method.

5.1.11 *Carbon Residue*—Test Method D4530. A100 % sample shall replace the 10 % residual, with percent residue in the original sample reported using the 10 % residual calculation (see X1.9.1). Test Methods D189 or D524 may also be used. Test Method D4530 shall be the referee method.

5.1.12 *Total Glycerin*—Test Method D6584.

5.1.13 *Free Glycerin*—Test Method D6584.

5.1.14 *Phosphorus Content*—Test Method D4951.

5.1.15 *Distillation Temperature, Reduced Pressure*—Test Method D1160.

5.1.16 *Calcium and Magnesium, combined*—Test Method EN 14538. Test Method UOP 389 may also be used. Test Method EN 14538 shall be the referee test method.

TABLE 1 Detailed Requirements for Biodiesel (B100) (All Sulfur Levels)

Property	Test Method[A]	Grade S15 Limits	Grade S500 Limits	Units
Calcium and Magnesium, combined	EN 14538	5 max	5 max	ppm (µg/g)
Flash point (closed cup)	D93	93 min	93 min	°C
Alcohol control				
One of the following must be met:				
1. Methanol content	EN 14110	0.2 max	0.2 max	mass %
2. Flash point	D93	130 min	130 min	°C
Water and sediment	D2709	0.050 max	0.050 max	% volume
Kinematic viscosity, 40°C	D445	1.9-6.0[B]	1.9–6.0[B]	mm^2/s
Sulfated ash	D874	0.020 max	0.020 max	% mass
Sulfur[C]	D5453	0.0015 max (15)	0.05 max (500)	% mass (ppm)
Copper strip corrosion	D130	No. 3 max	No. 3 max	
Cetane number	D613	47 min	47 min	
Cloud point	D2500	Report[D]	Report[D]	°C
Carbon residue[E]	D4530	0.050 max	0.050 max	% mass
Acid number	D664	0.50 max	0.50 max	mg KOH/g
Cold soak filterability	Annex A1	360 max[F]	360 max[F]	seconds
Free glycerin	D6584	0.020 max	0.020 max	% mass
Total glycerin	D6584	0.240 max	0.240 max	% mass
Phosphorus content	D4951	0.001 max	0.001 max	% mass
Distillation temperature, Atmospheric equivalent temperature, 90 % recovered	D1160	360 max	360 max	°C
Sodium and Potassium, combined	EN 14538	5 max	5 max	ppm (µg/g)
Oxidation stability	EN 14112	3 minimum	3 minimum	hours

[A] The test methods indicated are the approved referee methods. Other acceptable methods are indicated in 5.1.

[B] See X1.3.1. The 6.0 mm^2/s upper viscosity limit is higher than petroleum based diesel fuel and should be taken into consideration when blending.

[C] Other sulfur limits can apply in selected areas in the United States and in other countries.

[D] The cloud point of biodiesel is generally higher than petroleum based diesel fuel and should be taken into consideration when blending.

[E] Carbon residue shall be run on the 100 % sample (see 5.1.11).

[F] B100 intended for blending into diesel fuel that is expected to give satisfactory vehicle performance at fuel temperatures at or below –12°C shall comply with a cold soak filterability limit of 200 s maximum.

5.1.17 *Sodium and Potassium, combined*—Test Method EN 14538. Test Method UOP 391 may also be used. Test Method EN 14538 shall be the referee test method.

5.1.18 *Cold Soak Filterability*—The test method in Annex A1 shall be used to determine the cold soak filterability. B100 intended for blending into diesel fuels that is expected to give satisfactory vehicle performance at fuel temperatures at or below –12°C shall comply with a cold soak filtration limit of 200 s maximum. A cold soak filterability standard test method is under development.

NOTE 4—Interim precision information is provided in Annex A1 for the cold soak filterability test to give the user some indication of the repeatability and reproducibility expected.

6. Workmanship

6.1 The biodiesel fuel shall be visually free of undissolved water, sediment, and suspended matter.

7. Keywords

7.1 alternative fuel; biodiesel fuel; diesel fuel oil; fuel oil; renewable resource

ANNEX

(Mandatory Information)

A1. DETERMINATION OF FUEL FILTER BLOCKING POTENTIAL OF BIODIESEL (B100) BLEND STOCK BY COLD SOAK LABORATORY FILTRATION

A1.1 Scope

A1.1.1 This test method covers the determination by filtration time after cold soak of the suitability for a Biodiesel (B100) Blend Stock for blending with middle distillates to provide adequate low temperature operability performance to at least the cloud point of the finished blend.

A1.1.2 The interim precision of this test method has been determined.

A1.1.3 The values stated in SI units are to be regarded as the standard. The values given in parentheses are for information only.

A1.1.4 *This standard does not purport to address all of the safety concerns, if any, associated with its use. It is the responsibility of the user of this standard to establish appropriate safety and health practices and determine the applicability of regulatory limitations prior to use.*

A1.2 Referenced Documents

A1.2.1 *ASTM Standards*:[2]

D4057 Practice for Manual Sampling of Petroleum and Petroleum Products

D4865 Guide for Generation and Dissipation of Static Electricity in Petroleum Fuel Systems

D5452 Test Method for Particulate Contamination in Aviation Fuels by Laboratory Filtration

A1.3 Terminology

A1.3.1 *Definitions*:

A1.3.1.1 *biodiesel, n*—fuel comprised of mono-alkyl esters of long chain fatty acids derived from vegetable oils or animal fats, designated B100.

A1.3.1.2 *bond, v*—to connect two parts of a system electrically by means of a conductive wire to eliminate voltage differences.

A1.3.1.3 *ground, v*—to connect electrically with earth.

A1.3.2 *Definitions of Terms Specific to this Standard*:

A1.3.2.1 *filtered flushing fluids, n*—either of two solvents, heptane or 2,2, 4–trimethylpentane, filtered through a nominal 0.45 µm glass fiber filter.

A1.3.2.2 *glass fiber filter, n*—the 0.7 µm glass fiber filters used in this test method.

A1.3.3 *Abbreviations*:

A1.3.3.1 *CSFT*—cold soak filtration test.

A1.4 Summary of Test Method

A1.4.1 In this test method, 300 mL of biodiesel (B100) is stored at 4.4°C (40°F) for 16 h, allowed to warm to 20 to 22°C (68 to 72°F), and vacuum filtered through a single 0.7 µm glass fiber filter.

A1.4.2 In this test method, the filtration time is reported in seconds.

A1.5 Significance and Use

A1.5.1 Some substances that are soluble or appear to be soluble in biodiesel at room temperature will, upon cooling or standing at room temperature for extended periods, come out of solution. These substances can cause filter plugging. This test method provides an accelerated means of assessing the propensity for these substances to plug filters.

A1.5.1.1 Fuels that give short filtration times are expected to give satisfactory operation down to the cloud point of biodiesel blends.

A1.5.2 The test method can be used in specifications as a means of controlling levels of minor filter plugging components in biodiesel and biodiesel blends.

A1.6 Apparatus

A1.6.1 *Filtration System*—Arrange the following components as shown in Fig. A1.1.

A1.6.1.1 *Funnel and Funnel Base*, with a stainless steel filter support for a 47–mm diameter glass fiber filter and a locking ring or spring action clip capable of receiving 300 mL.

NOTE A1.1—Sintered glass supports were found to give much higher filtration times during initial studies and should not be used.

A1.6.1.2 *Ground/Bond Wire*, 0.912 to 2.59 mm (No. 10 through No. 19) bare-stranded flexible stainless steel or copper installed in the flasks and grounded as shown in Fig. A1.1.

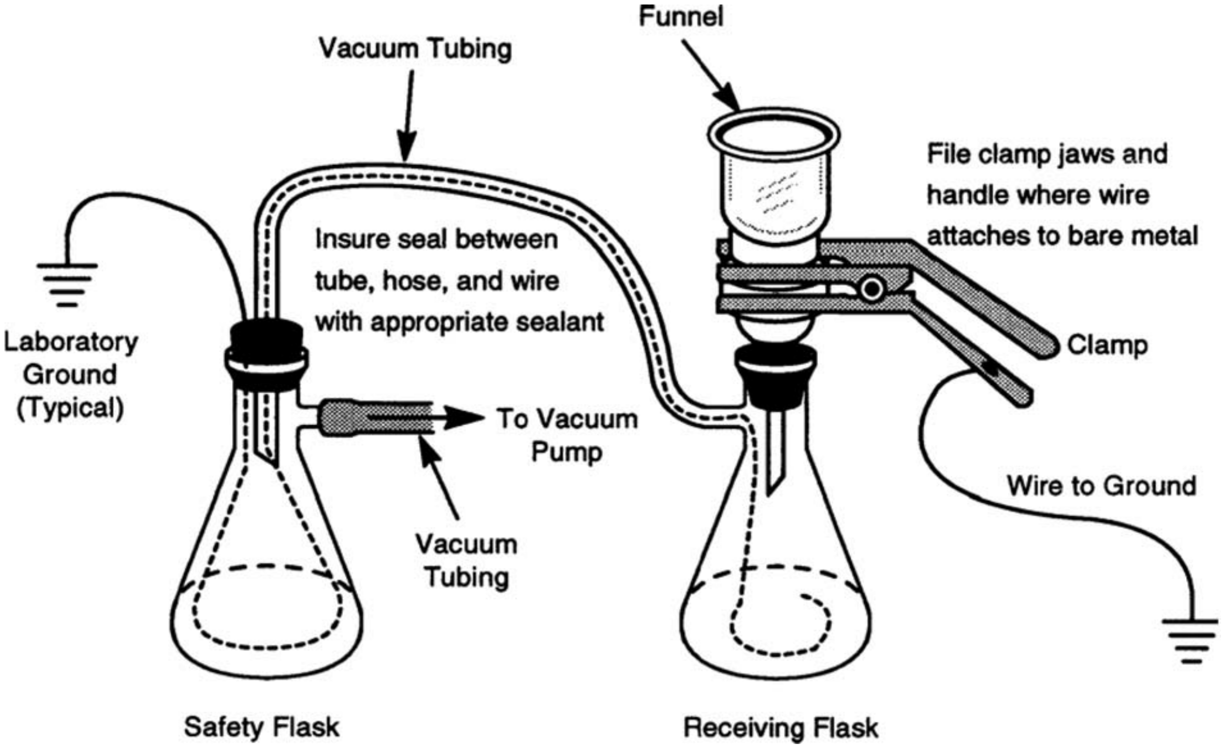

FIG. A1.1 Schematic of Filtration System

NOTE A1.2—The electrical bonding apparatus described in Test Method D5452 or other suitable means of electrical grounding which ensure safe operation of the filtration apparatus and flask can be used. If the filtrate is to be subsequently tested for stability it is advisable not to use copper as copper ions catalyze gum formation during the stability test.

A1.6.1.3 *Receiving Flask*, 1-L borosilicate glass vacuum filter flask, into which the filtration apparatus fits, equipped with a sidearm to connect to the safety flask.

A1.6.1.4 *Safety Flask*, 1-L borosilicate glass vacuum filter flask equipped with a sidearm to connect the vacuum system. A fuel and solvent resistant rubber hose, through which the grounding wire passes, shall connect the sidearm of the receiving flask to the tube passing through the rubber stopper in the top of the safety flask.

A1.6.1.5 *Vacuum System*, a vacuum system capable of producing a vacuum of 70 to 100 kPa below atmospheric pressure when measured at the receiving flask. A mechanical vacuum pump may be used if it has this capability.

NOTE A1.3—Water aspirated vacuum will not provide relative vacuum within the prescribed range.

A1.6.2 *Other Apparatus*:

A1.6.2.1 *Forceps*, approximately 12-cm long, flat-bladed, with non-serrated, non-pointed tips.

A1.6.2.2 *Graduated Cylinders*, to contain at least 0.5 L of fluid and marked at 10-mL intervals. Graduated cylinders, 100-mL, may be required for samples which filter slowly.

A1.6.2.3 *Petri Dishes*, approximately 12.5 cm in diameter, with removable glass supports for glass fiber filters.

NOTE A1.4—Small watch glasses, approximately 5 to 7 cm in diameter, have also been found suitable to support the glass fiber filters.

NOTE A1.5—B100 will dissolve some plastics. This can cause the filters to adhere to the plastic.

A1.6.2.4 *Glass Fiber Filters*, plain, 47-mm diameter, nominal pore size 0.7-µm.

A1.6.2.5 *Protective Cover*, polyethylene film or clean aluminum foil.

A1.6.2.6 *Liquid or Air Bath or Chamber*, capable of sustaining a temperature of 4.4 ± 1.1°C (40 ± 2°F) for 16 h.

A1.6.2.7 *Timer*, capable of displaying elapsed times of at least 900 s to the nearest 0.1 s.

A1.7 Reagents and Materials

A1.7.1 *Purity of Reagents*—Reagent grade chemicals shall be used in all tests. Unless otherwise indicated, it is intended that all reagents shall conform to the specifications of the Committee on Analytical Reagents of the American Chemical Society, where such specifications are available.[6] Other grades may be used, provided it is first ascertained that the reagent is of sufficient purity to permit its use without lessening the accuracy of the determination.

A1.7.2 *Flushing Fluids*—Flushing fluids are not required for the test as the filter is not weighed. However, heptane or isooctane may be used to wash the apparatus after filtration to remove any residue. Alternatively soap and water may be used in accordance with A1.7.3.

---

[6] *Reagent Chemicals, American Chemical Society Specifications*, American Chemical Society, Washington, DC. For Suggestions on the testing of reagents not listed by the American Chemical Society, see *Annual Standards for Laboratory Chemicals*, BDH Ltd., Poole, Dorset, U.K., and the *United States Pharmacopeia and National Formulary*, U.S. Pharmacopeial Convention, Inc. (USPC), Rockville, MD.

A1.7.2.1 *Heptane*, (**Warning**—Flammable).

A1.7.2.2 *2,2,4-trimethylpentane (isooctane)*, (**Warning**—Flammable).

A1.7.3 *Liquid or Powder Detergent*, water-soluble, for cleaning glassware.

A1.8 Preparation of Apparatus and Sample Containers

A1.8.1 Clean all components of the filtration apparatus using the reagents described in A1.7.2 and A1.7.3.

A1.8.1.1 Remove any labels, tags, and so forth.

A1.9 Sampling

A1.9.1 The sample container should be 500 ± 15 mL in volume and have a screw-on cap with an inert liner. Glass containers are preferred to facilitate a visual inspection of the contents and the container before and after filling. Glass containers also allow for visual inspection of the container, after the sample is emptied, to confirm complete emptying of the container. Epoxy-lined sample cans, polytetrafluoroethylene (PTFE) bottles, and high density linear polyethylene bottles have also been found suitable as sample containers but are less desirable since visual inspection of the interior of the container is more difficult.

A1.9.2 Precautions to avoid sample contamination shall include selection of an appropriate sampling point. It is preferred to obtain samples dynamically from a sampling loop in a distribution line, or from the flushing line of a field sampling kit. Ensure that the line to be sampled is flushed with fuel before collecting the sample.

A1.9.2.1 Use clean sample containers.

A1.9.2.2 Keep a clean protective cover over the top of the sample container until the cap is installed. Similarly protect the funnel opening of the assembled filtration apparatus with a clean protective cover until ready for use.

A1.9.2.3 Where it is desirable or only possible to obtain samples from static storage, follow the procedures given in Practice D4057 or equivalent, taking precautions for cleanliness of all equipment used. The sample should pass through a minimum number of intermediate containers prior to placement in the prepared container.

A1.9.2.4 Samples obtained from static storage can give results that are not representative of the bulk contents of the tank because of particulate matter settling. Where possible, the contents of the tank should be circulated or agitated before sampling, or the sampling should be performed shortly after a tank has been filled.

A1.9.3 Visually inspect the sample container before taking the samples to verify that there are no visible particles present inside the container. Fill the sample container to contain 300 mL. Protect the fuel sample from prolonged exposure to light by wrapping the container in aluminum foil or storing it in the dark to reduce the possibility of particulate formation by light-promoted reactions. Do not transfer the fuel sample from its original sample container into an intermediate storage container. If the original sample container is damaged or leaking, then a new sample shall be obtained.

A1.9.3.1 If a 500-mL bottle is not available, or the sample has already been received in a container not suitable for this test, follow A1.9.5.

A1.9.4 Analyze fuel samples as soon as possible after sampling.

A1.9.4.1 Upon receipt of a Biodiesel Blend Stock (B100) sample, the entire sample shall be heated to 40°C for at least 3 h under an inert atmosphere to erase any thermal history and to dissolve any solids that might have precipitated during transit unless it is known that the sample has never been cooled below 20°C. If the sample has never been exposed to temperatures below 20°C then proceed to A1.9.5.

A1.9.4.2 After heating for the required time, allow the sample to sit for 24 h at a temperature no lower than 20°C.

A1.9.5 Shake the sample vigorously for 1 min, and transfer 300 mL to a clean fresh 500 ± 15 mL bottle.

A1.10 Preparation of Glass Fiber Filter

A1.10.1 Each filtration uses one filter. The glass fiber filter used for each individual test shall be identified by marking the petri dishes used to hold and transport the filters.

A1.10.2 Clean all glassware used in preparation of glass fiber filter as described in A1.8.1.

A1.10.3 Using forceps, place the filters on clean glass support rods or watch glasses in petri dish.

A1.10.4 Place the petri dish with its lid slightly ajar in a drying oven at 90 ± 5°C, and leave it for 30 min.

A1.10.5 Remove the petri dish from the drying oven. Keep the petri dish cover ajar, such that the filter is protected from contamination from the atmosphere. Allow 30 min for the filter to come to equilibrium with room air temperature and humidity.

A1.10.6 Using clean forceps, place the filter centrally on the filter support of the filtration apparatus (see Fig. A1.1). Install the funnel and secure with locking ring or spring clip. Do not remove the plastic film from the funnel opening until ready to start filtration.

A1.11 Procedure

A1.11.1 Place 300 mL of sample in a glass 500–mL bottle, and set in a liquid or air bath or chamber at 4.4 ± 1.1°C (40 ± 2°F) for 16 ± 0.5 h.

A1.11.2 After the 16-h cold soak is completed, allow the sample to come back to room temperature at 20 to 22°C (68 to 72°F) on its own without external heating. The sample shall be completely liquid before filtration. The sample shall be filtered within 1 h after reaching 20 to 22°C (68 to 72°F).

A1.11.3 Complete assembly of the receiving flask, 0.7 µm glass fiber filter and funnel as a unit (see Fig. A1.1) before swirling the sample. To minimize operator exposure to fumes, the filtering procedure should be performed in a fume hood.

A1.11.4 Start the vacuum system. Record the pressure in the system after 1 min of filtration. The vacuum shall be between 71.1 and 84.7 kPa (21 and 25 in. Hg) below atmospheric pressure. If the vacuum is not within the specified range, make adjustments to the vacuum system.

A1.11.5 Thoroughly clean the outside of the sample container in the region of the cap by wiping it with a damp, lint-free cloth. Swirl the container vigorously for about 2 to 3 s to dislodge any particles that may have adhered to the walls of the container.

A1.11.6 Immediately after swirling, pour the entire contents of the sample container into the filtration funnel and simultaneously start the timer. The entire contents of the sample container shall be filtered through the glass fiber filter to ensure a correct measure of the contamination in the sample.

NOTE A1.6—Take care not to shake the sample vigorously, as this could cause some of the solids to go back into solution.

A1.11.7 If the filtration is not complete when 720 s (12 min) has elapsed, turn off the vacuum system and record the duration of the filtration to the nearest second. Record the pressure in the system and the volume filtered just before the termination of the filtration.

A1.12 Reporting

A1.12.1 Report the time for the 300–mL B100 to be completely filtered as B100 filtration time in seconds.

A1.12.2 If the filtration of the 300 mL failed to be completed after 720 s, report the volume that was filtered after 720 s.

A1.13 Precision and Bias

A1.13.1 *Precision*—The precision of this test method for B100 filtration has not yet been determined.

A1.13.1.1 *Repeatability*—The difference between successive test results, obtained by the same operator using the same apparatus under constant operating conditions on identical test material for B100 filtration has not yet been determined.

A1.13.1.2 *Reproducibility*—The difference between the two single and independent results obtained by different operators working in different laboratories on identical test material for B100 filtration has not yet been determined.

A1.13.1.3 *Interim Precision*—Repeatability and reproducibility determinations were made using data from the ASTM Biodiesel Low Temperature Operability Task Force. The analysis of the data is the subject of a research report, RR:D02-1649.[7] The report is an attempt to supply such an analysis based on well-established methodologies. Subsequent to test method publication a more thorough round robin is planned.

	200 s	360 s
Repeatability	34.0	61.0
Reproducibility	115.9	208.1

NOTE A1.7—The degree of freedom associated with the repeatability estimate from this round robin study is 25 for repeatability which is below 30 but acceptable. The degree of freedom associated with the reproducibility estimate from this round robin study is 10 and below acceptable limits. For that reason only the repeatability is included in A1.13.1.4. Since the minimum requirement of 30 (in accordance with Practice D6300) is not met, users are cautioned that the actual repeatability/reproducibility may be significantly different than these estimates. An ASTM ILS will be conducted in the future.

A1.13.1.4 The difference between successive test results, obtained by the same operator using the same apparatus under constant operating conditions on identical test material for B100 filtration would in the long run, in the normal and correct operation of this test method, exceed 0.1689(X + 1.2018) time(s) only in one case in twenty.

A1.13.2 *Bias*—The procedure given for the determination of B100 filtration time has no bias because the value of the filtration time is defined in terms of this test method.

A1.14 Keywords

A1.14.1 biodiesel; diesel fuel; glass fiber filter; biodiesel; filter blocking potential, cold soak filtration test, CSFT, biodiesel blend; laboratory filtration; glass fiber filter; low temperature operability, middle distillate fuel.

---

[7] Supporting data have been filed at ASTM International Headquarters and may be obtained by requesting Research Report RR:D02-1649.

APPENDIXES

(Nonmandatory Information)

X1. SIGNIFICANCE OF PROPERTIES SPECIFIED FOR BIODIESEL FUEL

X1.1 Introduction

X1.1.1 The properties of commercial biodiesel fuel depends upon the refining practices employed and the nature of the renewable lipids from which it is produced. Biodiesel, for example, can be produced from a variety of vegetable oils or animal fats which produce similar volatility characteristics and combustion emissions with varying cold flow properties.

X1.1.2 The significance of the properties in this appendix are based primarily on the commercial use of biodiesel in on-road and off-road diesel engine applications. Some of the properties may take on other significance if biodiesel is used as a fuel or blending component in other applications. See the respective finished product specifications for additional information on significance of properties of those applications.

X1.2 Flash Point

X1.2.1 The flash point, as specified, is not directly related to engine performance. It is, however, of importance in connection with legal requirements and safety precautions involved in fuel handling and storage that are normally specified to meet insurance and fire regulations.

X1.2.2 The flash point for biodiesel has been set at 93°C (200°F) minimum, so biodiesel falls under the non-hazardous category under National Fire Protection Association codes.

X1.3 Viscosity

X1.3.1 For some engines it may be advantageous to specify a minimum viscosity because of power loss due to injection pump and injector leakage. Maximum allowable viscosity, on the other hand, is limited by considerations involved in engine design and size, and the characteristics of the injection system. The upper limit for the viscosity of biodiesel (6.0 mm^2/s at 40°C) is higher than the maximum allowable viscosity in Specification D975 Grade 2-D and 2-D low sulfur (4.1 mm/s at 40°C). Blending biodiesel with diesel fuel close to its upper limit could result in a biodiesel blend with viscosity above the upper limits contained in Specification D975.

X1.4 Sulfated Ash

X1.4.1 Ash-forming materials may be present in biodiesel in three forms: (*1*) abrasive solids, (*2*) soluble metallic soaps, and (*3*) unremoved catalysts. Abrasive solids and unremoved catalysts can contribute to injector, fuel pump, piston and ring wear, and also to engine deposits. Soluble metallic soaps have little effect on wear but may contribute to filter plugging and engine deposits.

X1.5 Sulfur

X1.5.1 The effect of sulfur content on engine wear and deposits appears to vary considerably in importance and depends largely on operating conditions. Fuel sulfur can also affect emissions control systems performance and various limits on sulfur have been imposed for environmental reasons. B100 is essentially sulfur-free.

NOTE X1.1—Test Method D5453 should be used with biodiesel. Use of other test methods may provide falsely high results when analyzing B100 with extremely low sulfur levels (less than 5 ppm). Biodiesel sulfur analysis from RR:D02-1480[8], *Biodiesel Fuel Cetane Number Testing Program, January-April, 1999*, using Test Method D2622 yielded falsely high results due to the presence of the oxygen in the biodiesel. Sulfur results using Test Method D2622 were more accurate with B20 than with B100 due to the lower oxygen content of B20. Potential improvements to Test Method D2622 may provide more accurate values in the future.

X1.6 Copper Strip Corrosion

X1.6.1 This test serves as a measure of possible difficulties with copper and brass or bronze parts of the fuel system. The presence of acids or sulfur-containing compounds can tarnish the copper strip, thus indicating the possibility for corrosion.

X1.7 Cetane Number

X1.7.1 Cetane number is a measure of the ignition quality of the fuel and influences white smoke and combustion roughness. The cetane number requirements depend on engine design, size, nature of speed and load variations, and on starting and atmospheric conditions.

X1.7.2 The calculated cetane index, Test Methods D976 or D4737, may not be used to approximate the cetane number with biodiesel or its blends. There is no substantiating data to support the calculation of cetane index with biodiesel or biodiesel blends.

X1.8 Cloud Point

X1.8.1 Cloud point is of importance in that it defines the temperature at which a cloud or haze of crystals appears in the fuel under prescribed test conditions which generally relates to the temperature at which crystals begin to precipitate from the fuel in use. Biodiesel generally has a higher cloud point than petroleum based diesel fuel. The cloud point of biodiesel and its impact on the cold flow properties of the resulting blend should be monitored by the user to ensure trouble-free operation in cold climates. For further information, consult Appendix X4 of Specification D975.

X1.9 Carbon Residue

X1.9.1 Carbon residue gives a measure of the carbon depositing tendencies of a fuel oil. While not directly correlating with engine deposits, this property is considered an approximation. Although biodiesel is in the distillate boiling range, most biodiesels boil at approximately the same temperature and it is difficult to leave a 10 % residual upon distillation. Thus, a 100 % sample is used to replace the 10 % residual sample, with the calculation executed as if it were the 10 % residual. Parameter E (final weight flask charge/original weight flask charge) in 8.1.2 of Test Method D4530-93 is a constant 20/200.

X1.10 Acid Number

X1.10.1 The acid number is used to determine the level of free fatty acids or processing acids that may be present in biodiesel. Biodiesel with a high acid number has been shown to increase fueling system deposits and may increase the likelihood for corrosion.

NOTE X1.2—Acid number measures a different phenomenon for biodiesel than petroleum based diesel fuel. The acid number for biodiesel measures free fatty acids or degradation by-products not found in petroleum based diesel fuel. Increased recycle temperatures in new fuel system designs may accelerate fuel degradation which could result in high acid values and increased filter plugging potential.

X1.11 Free Glycerin

X1.11.1 The free glycerin method is used to determine the level of glycerin in the fuel. High levels of free glycerin can cause injector deposits, as well as clogged fueling systems, and result in a buildup of free glycerin in the bottom of storage and fueling systems.

X1.12 Total Glycerin

X1.12.1 The total glycerin method is used to determine the level of glycerin in the fuel and includes the free glycerin and the glycerine portion of any unreacted or partially reacted oil or fat. Low levels of total glycerin ensure that high conversion of the oil or fat into its mono-alkyl esters has taken place. High levels of mono-, di-, and triglycerides can cause injector deposits and may adversely affect cold weather operation and filter plugging.

X1.13 Phosphorus Content

X1.13.1 Phosphorus can damage catalytic converters used in emissions control systems and its level must be kept low. Catalytic converters are becoming more common on diesel-powered equipment as emissions standards are tightened, so low phosphorus levels will be of increasing importance. Biodiesel produced from U.S. sources has been shown to have

---

[8] Supporting data have been filed at ASTM International Headquarters and may be obtained by requesting Research Report RR:D02-1480.

low phosphorus content (below 1 ppm) and the specification value of 10 ppm maximum is not problematic. Biodiesel from other sources may or may not contain higher levels of phosphorus and this specification was added to ensure that all biodiesel, regardless of the source, has low phosphorus content.

X1.14 Reduced Pressure Distillation

X1.14.1 Biodiesel exhibits a boiling point rather than a distillation curve. The fatty acids chains in the raw oils and fats from which biodiesel is produced are mainly comprised of straight chain hydrocarbons with 16 to 18 carbons that have similar boiling temperatures. The atmospheric boiling point of biodiesel generally ranges from 330 to 357°C, thus the specification value of 360°C is not problematic. This specification was incorporated as an added precaution to ensure the fuel has not been adulterated with high boiling contaminants.

NOTE X1.3—The density of biodiesel meeting the specifications in Table 1 falls between 0.86 and 0.90, with typical values falling between 0.88 and 0.89. Since biodiesel density falls between 0.86 and 0.90, a separate specification is not needed. The density of raw oils and fats is similar to biodiesel, therefore use of density as an expedient check of fuel quality may not be as useful for biodiesel as it is for petroleum based diesel fuel. This section has been added to provide users and engine interests with this information.

NOTE X1.4—In certain items of fuel injection equipment in compression ignition engines, such as rotary/distributor fuel pumps and injectors, the fuel functions as a lubricant as well as a source for combustion. Blending biodiesel fuel with petroleum based compression-ignition fuel typically improves fuel lubricity.

X1.15 Alcohol Control

X1.15.1 Alcohol control is to limit the level of unreacted alcohol remaining in the finished fuel. This can be measured directly by the volume percent alcohol or indirectly through a high flash point value.

X1.15.2 The flash point specification, when used for alcohol control for biodiesel, is intended to be 100°C minimum, which has been correlated to 0.2 vol % alcohol. Typical values are over 160°C. Due to high variability with Test Method D93 as the flash point approaches 100°C, the flash point specification has been set at 130°C minimum to ensure an actual value of 100°C minimum. Improvements and alternatives to Test Method D93 are being investigated. Once complete, the specification of 100°C minimum may be reevaluated for alcohol control.

X1.16 Calcium and Magnesium

X1.16.1 Calcium and magnesium may be present in biodiesel as abrasive solids or soluble metallic soaps. Abrasive solids can contribute to injector, fuel pump, piston, and ring wear, as well as to engine deposits. Soluble metallic soaps have little effect on wear, but they may contribute to filter plugging and engine deposits. High levels of calcium and magnesium compounds may also be collected in exhaust particulate removal devices, are not typically removed during passive or active regeneration, and can create increased back pressure and reduced time to service maintenance.

X1.17 Sodium and Potassium

X1.17.1 Sodium and potassium may be present in biodiesel as abrasive solids or soluble metallic soaps. Abrasive solids can contribute to injector, fuel pump, piston and ring wear, and also to engine deposits. Soluble metallic soaps have little effect on wear, but they may contribute to filter plugging and engine deposits. High levels of sodium or potassium compounds may also be collected in exhaust particulate removal devices, are not typically removed during passive or active regeneration, and they can create increased back pressure and reduced period to service maintenance.

X1.18 Oxidation Stability

X1.18.1 Products of oxidation in biodiesel can take the form of various acids or polymers, which, if in high enough concentration, can cause fuel system deposits and lead to filter clogging and fuel system malfunctions. Additives designed to retard the formation of acids and polymers can significantly improve the oxidation stability performance of biodiesel. See Appendix X2 for additional information on long-term storage.

X2. LONG-TERM STORAGE OF BIODIESEL

X2.1 Scope

X2.1.1 This appendix provides guidance for consumers of biodiesel (B100) who may wish to store quantities of fuels for extended periods. Consistently successful long-term fuel storage requires attention to fuel selection, storage conditions, and monitoring of properties prior to and during storage. This appendix is directed toward biodiesel (B100) and may be more or less applicable to blends of biodiesel with petroleum based diesel fuel.

X2.1.2 Normally produced biodiesel has adequate stability properties to withstand normal storage without the formation of troublesome amounts of insoluble degradation products, although data suggests some biodiesel may degrade faster than petroleum based diesel fuel. Biodiesel that is to be stored for prolonged periods should be selected to avoid formation of sediments, high acid numbers, and high viscosities that can clog filters, affect fuel pump operation or plug combustor nozzles or injectors. The selection of biodiesel should result from supplier-user discussions.

X2.1.3 These suggested practices are general in nature and should not be considered substitutes for any requirement imposed by the warranty of the distillate fuel equipment manufacturers or by federal, state, or local government regulations. Although they cannot replace knowledge of local conditions or good engineering and scientific judgment, these suggested practices do provide guidance in developing an individual fuel management system for the biodiesel fuel user. They include suggestions in the operation and maintenance of existing fuel storage and handling facilities and for identifying where, when, and how fuel quality should be monitored.

X2.2 Terminology

X2.2.1 *bulk fuel*—fuel in the storage facility in quantities over 50 gallons.

X2.2.2 *combustor fuel*—fuel entering the combustion zone of the burner or engine after filtration or other treatment of bulk fuel.

X2.2.3 *fuel contaminants*—foreign materials that make fuel less suitable or unsuitable for the intended use. Fuel contaminants include materials introduced subsequent to the manufacture of fuel and fuel degradation products.

X2.2.4 *fuel-degradation products*—those materials formed in fuel after it is produced. Insoluble degradation products may combine with other fuel contaminants to reinforce deleterious effects. Soluble degradation products (acids and gums) may be more or less volatile than the fuel and may cause an increase in injector and nozzle deposits. The formation of degradation products may be catalyzed by contact with metals, especially those containing copper and, to a lesser extent, iron.

X2.2.5 *long-term storage*—storage of fuel for longer than 6 months after it is received by the user.

X2.3 Fuel Selection

X2.3.1 The stability properties of biodiesel are not fully understood and appear to depend on the vegetable oil and animal fat sources, severity of processing, and whether additional production plant treatment has been carried out or stability additives are present.

X2.3.2 The composition and stability properties of biodiesel produced at specific production plants may be different. Any special requirements of the user, such as long-term storage, should be discussed with the supplier.

X2.4 Fuel Additives

X2.4.1 Available fuel additives appear to improve the long term storage of biodiesel. Most additives should be added as close to the production site as possible to obtain maximum benefits.

X2.4.2 Biocides or biostats destroy or inhibit the growth of fungi and bacteria which can grow at fuel-water interfaces to give high particulate concentrations in the fuel. Available biocides are soluble in the fuel phase or the water phase, or both. Refer to Guide D6469 for a more complete discussion.

X2.5 Tests for Fuel Quality

X2.5.1 Test methods for estimating the storage stability of biodiesel (B100) are being developed. Modifications of Test Method D2274 to use glass fiber filters, varying times and temperatures, and the measurement of pre-test and post-test acid number and viscosity appear promising. However, correlation of this test with actual storage stability is unknown, and may depend upon field conditions and fuel composition.

X2.5.2 Performance criteria for accelerated stability tests that ensure satisfactory long-term storage of biodiesel (B100) have not been established.

X2.6 Fuel Monitoring

X2.6.1 A plan for monitoring the quality of bulk fuel during prolonged storage is an integral part of a successful monitoring program. A plan to replace aged fuel with fresh product at established intervals is also desirable.

X2.6.2 Stored fuel should be periodically sampled and its quality assessed. Practice D4057 provides guidance for sampling. Fuel contaminants and degradation products may settle to the bottom of a quiescent tank although detrimental changes to biodiesel can occur (rising acid value) without causing sediment formation. A *Bottom* or *Clearance* sample, as defined in Practice D4057, should be included in the evaluation along with an *All Level* sample.

X2.6.3 The quantity of insoluble fuel contaminants present in biodiesel can be determined using Test Method D6217 with glass fiber filters and abundant washing although no precision or bias testing has been performed with biodiesel using Test Method D6217.

X2.6.4 The acid value of biodiesel appears to exceed its specified maximum before other deleterious fuel property changes occur. A conscientious program of measuring the acid value of biodiesel may be sufficient for monitoring biodiesel stability.

X2.7 Fuel Storage Conditions

X2.7.1 Contamination levels in fuel can be reduced by storage in tanks kept free of water, and tankage should have provisions for water draining on a scheduled basis. Water promotes corrosion, and microbiological growth may occur at a fuel-water interface. Refer to Guide D6469 for a more complete discussion. Underground or isothermal storage is preferred to avoid temperature extremes; above-ground storage tanks should be sheltered or painted with reflective paint. High storage temperatures accelerate fuel degradation. Fixed roof tanks should be kept full to limit oxygen supply and tank breathing. The use of airtight sealed containers, such as drums or totes, can enhance the storage life of biodiesel.

X2.7.2 Copper and copper-containing alloys should be avoided with biodiesel due to increased sediment and deposit formation. Contact with lead, tin, and zinc can also cause increased sediment levels that can rapidly plug filters and should be avoided.

X2.7.3 Appendix X3 of Specification D2880 discusses fuel contaminants as a general topic. The discussion in Specification D2880 pertains to gas turbine combustion which may or may not be applicable to diesel engine combustion.

SUMMARY OF CHANGES

Subcommittee D02.E0 has identified the location of selected changes to this standard since the last issue (D6751–09) that may impact the use of this standard. (Approved Dec. 1, 2009.)

(*1*) Added Test Method D5771 and D5772 to 5.1.9 and to the Referenced Documents.

Subcommittee D02.E0 has identified the location of selected changes to this standard since the last issue (D6751–08) that may impact the use of this standard. (Approved April 15, 2009.)

(*1*) Added Test Method D7397 cloud point as an option to Test Method D2500 in 5.1.9 and to the Referenced Documents.

Subcommittee D02.E0 has identified the location of selected changes to this standard since the last issue (D6751–07b$^{\epsilon 1}$) that may impact the use of this standard. (Approved Oct. 1, 2008.)

(1) Added Annex A1.
(2) Revised Table 1.
(3) Added 5.1.18.
(4) Added Note 4.

APPENDIX 3

ASTM D2500: STANDARD TEST METHOD FOR CLOUD POINT OF PETROLEUM PRODUCTS

An American National Standard
British Standard 4458

Designation: D 2500 – 09

Designation: 219/82

Standard Test Method for Cloud Point of Petroleum Products[1]

This standard is issued under the fixed designation D 2500; the number immediately following the designation indicates the year of original adoption or, in the case of revision, the year of last revision. A number in parentheses indicates the year of last reapproval. A superscript epsilon (´) indicates an editorial change since the last revision or reapproval.

This standard has been approved for use by agencies of the Department of Defense.

1. Scope*

1.1 This test method covers only petroleum products and biodiesel fuels that are transparent in layers 40 mm in thickness, and with a cloud point below 49°C.

NOTE 1—The interlaboratory program consisted of petroleum products of Test Method D 1500 color of 3.5 and lower. The precisions stated in this test method may not apply to samples with ASTM color higher than 3.5.

1.2 The values stated in SI units are to be regarded as standard. No other units of measurement are included in this standard.

1.3 *This standard does not purport to address all of the safety concerns, if any, associated with its use. It is the responsibility of the user of this standard to establish appropriate safety and health practices and determine the applicability of regulatory limitations prior to use.* For specific hazard statements, see Section 7.

2. Referenced Documents

2.1 *ASTM Standards:*[2]

D 1500 Test Method for ASTM Color of Petroleum Products (ASTM Color Scale)

E 1 Specification for ASTM Liquid-in-Glass Thermometers

2.2 *Energy Institute Standard:*[3]

Specifications for IP Standard Thermometers

3. Terminology

3.1 *Definitions of Terms Specific to This Standard:*

3.1.1 *biodiesel*, *n*—a fuel comprised of mono-alkyl esters of long chain fatty acids derived from vegetable oils or animal fats, designated B100.

3.1.1.1 *Discussion*—Biodiesel is typically produced by a reaction of vegetable oil or animal fat with an alcohol such as methanol or ethanol in the presence of a catalyst to yield mono-esters and glycerin. The fuel typically may contain up to 14 different types of fatty acids that are chemically transformed into fatty acid methyl esters (FAME).

3.1.2 *biodiesel blend*, *n*—a blend of biodiesel fuel with petroleum-based diesel fuel designated BXX, where XX is the volume % of biodiesel.

3.1.3 *cloud point*, *n*—*in petroleum products and biodiesel fuels,* the temperature of a liquid specimen when the smallest observable cluster of hydrocarbon crystals first occurs upon cooling under prescribed conditions.

3.1.3.1 *Discussion*—To many observers, the cluster of wax crystals looks like a patch of whitish or milky cloud, hence the name of the test method. The cloud appears when the temperature of the specimen is low enough to cause wax crystals to form. For many specimens, the crystals first form at the lower circumferential wall of the test jar where the temperature is lowest. The size and position of the cloud or cluster at the cloud point varies depending on the nature of the specimen. Some samples will form large, easily observable, clusters, while others are barely perceptible.

3.1.3.2 *Discussion*—Upon cooling to temperatures lower than the cloud point, clusters of crystals will grow in multiple directions; for example, around the lower circumference of the test jar, towards the center of the jar, or vertically upwards. The crystals can develop into a ring of cloud along the bottom circumference, followed by extensive crystallization across the bottom of the test jar as temperature decreases. Nevertheless, the cloud point is defined as the temperature at which the crystals first appear, not when an entire ring or full layer of wax has been formed at the bottom of the test jar.

3.1.3.3 *Discussion*—In general, it is easier to detect the cloud point of samples with large clusters that form quickly, such as paraffinic samples. The contrast between the opacity of the cluster and the liquid is also sharper. In addition, small brightly-reflective spots can sometimes be observed inside the cluster when the specimen is well illuminated. For other more difficult samples, such as naphthenic, hydrocracked, and those samples whose cold flow behavior have been chemically

---

[1] This test method is under the jurisdiction of ASTM Committee D02 on Petroleum Products and Lubricants and is the direct responsibility of Subcommittee D02.07 on Flow Properties.

Current edition approved April 15, 2009. Published April 2009. Originally approved in 1966. Last previous edition approved in 2005 as D 2500–05.

[2] For referenced ASTM standards, visit the ASTM website, www.astm.org, or contact ASTM Customer Service at service@astm.org. For *Annual Book of ASTM Standards* volume information, refer to the standard's Document Summary page on the ASTM website.

[3] Available from Energy Institute, 61 New Cavendish St., London, WIG 7AR, U.K., http://www.energyinst.org.uk.

***A Summary of Changes section appears at the end of this standard.**

altered, the appearance of the first cloud can be less distinct. The rate of crystal growth is slow, the opacity contrast is weak, and the boundary of the cluster is more diffuse. As the temperature of these specimens decrease below the cloud point, the diffuse cluster will increase in size and can form a general haze throughout. A slight haze throughout the entire sample, which slowly becomes more apparent as the temperature of the specimen decreases, can also be caused by traces of water in the specimen instead of crystal formation (see Note 3). With these difficult samples, drying the sample prior to testing can eliminate this type of interference.

3.1.3.4 *Discussion*—The purpose of the cloud point method is to detect the presence of the wax crystals in the specimen; however trace amounts of water and inorganic compounds may also be present. The intent of the cloud point method is to capture the temperature at which the liquids in the specimen begin to change from a single liquid phase to a two-phase system containing solid and liquid. It is not the intent of this test method to monitor the phase transition of the trace components, such as water.

4. Summary of Test Method

4.1 The specimen is cooled at a specified rate and examined periodically. The temperature at which a cloud is first observed at the bottom of the test jar is recorded as the cloud point.

5. Significance and Use

5.1 For petroleum products and biodiesel fuels, cloud point of a petroleum product is an index of the lowest temperature of their utility for certain applications.

6. Apparatus (see Fig. 1)

6.1 *Test Jar*, clear, cylindrical glass, flat bottom, 33.2 to 34.8-mm outside diameter and 115 and 125-mm height. The inside diameter of the jar may range from 30 to 32.4 mm within the constraint that the wall thickness be no greater than 1.6 mm. The jar should be marked with a line to indicate sample height 54 6 3 mm above the inside bottom.

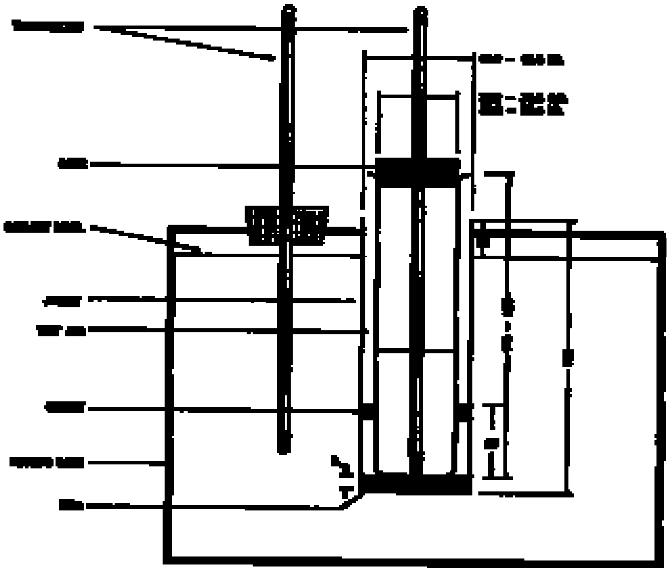

NOTE—All dimensions are in milllimetres.

FIG. 1 Apparatus for Cloud Point Test

6.2 *Thermometers*, having ranges shown below and conforming to the requirements as prescribed in Specification E 1 or Specifications for IP Standard Thermometers.

		Thermometer Number	
Thermometer	Temperature Range	ASTM	IP
High cloud and pour	−38 to +50°C	5C	1C
Low cloud and pour	−80 to +20°C	6C	2C

6.3 *Cork*, to fit the test jar, bored centrally for the test thermometer.

6.4 *Jacket*, metal or glass, watertight, cylindrical, flat bottom, about 115 mm in depth, with an inside diameter of 44.2 to 45.8 mm. It shall be supported free of excessive vibration and firmly in a vertical position in the cooling bath of 6.7 so that not more than 25 mm projects out of the cooling medium.

6.5 *Disk*, cork or felt, 6-mm thick to fit loosely inside the jacket.

6.6 *Gasket*, ring form, about 5 mm in thickness, to fit snugly around the outside of the test jar and loosely inside the jacket. The gasket may be made of rubber, leather, or other material that is elastic enough to cling to the test jar and hard enough to hold its shape. Its purpose is to prevent the test jar from touching the jacket.

6.7 *Bath or Baths*, maintained at prescribed temperatures with a firm support to hold the jacket vertical. The required bath temperatures may be maintained by refrigeration if available, otherwise by suitable cooling mixtures. Cooling mixtures commonly used for bath temperatures shown are in Table 1.

7. Reagents and Materials

7.1 *Acetone*—Technical grade acetone is suitable for the cooling bath, provided it does not leave a residue on drying. (**Warning—**Extremely flammable.)

7.2 *Carbon Dioxide (Solid) or Dry Ice*—A commercial grade of dry ice is suitable for use in the cooling bath.

7.3 *Petroleum Naphtha*—A commercial or technical grade of petroleum naphtha is suitable for the cooling bath. (**Warning—**Combustible. Vapor harmful.)

7.4 *Sodium Chloride Crystals*—Commercial or technical grade sodium chloride is suitable.

7.5 *Sodium Sulfate*—A reagent grade of anhydrous sodium sulfate should be used when required (see Note 3).

TABLE 1 Cooling Mixtures and Bath Temperatures

	Bath Temperature
Ice and water	0 6 1.5°C
Crushed ice and sodium chloride crystals, or acetone or petroleum naptha (see 7) with solid carbon dioxide added to give the desired temperature	–18 6 1.5°C
Acetone or petroleum naptha (see 7) with solid carbon dioxide added to give the desired temperature	–33 6 1.5°C
Acetone or petroleum naptha (see 7) with solid carbon dioxide added to give the desired temperature	–51 6 1.5°C
Acetone or petroleum naptha (see 7) with solid carbon dioxide added to give the desired temperature	–69 6 1. 5°C

8. Procedure

8.1 Bring the sample to be tested to a temperature at least 14°C above the expected cloud point. Remove any moisture present by a method such as filtration through dry lintless filter paper until the oil is perfectly clear, but make such filtration at a temperature of at least 14°C above the approximate cloud point.

8.2 Pour the sample into the test jar to the level mark.

8.3 Close the test jar tightly by the cork carrying the test thermometer. Use the high cloud and pour thermometer if the expected cloud point is above −36°C and the low cloud and pour thermometer if the expected cloud point is below −36°C. Adjust the position of the cork and the thermometer so that the cork fits tightly, the thermometer and the jar are coaxial, and the thermometer bulb is resting on the bottom of the jar.

NOTE 2—Liquid column separation of thermometers occasionally occurs and may escape detection. Thermometers should be checked periodically and used only if their ice points are 0 ± 1°C, when the thermometer is immersed to the immersion line in an ice bath, and when the emergent column temperature does not differ significantly from 21°C. Alternatively, immerse the thermometer to a reading and correct for the resultant cooler stem temperature.

8.4 See that the disk, gasket, and the inside of the jacket are clean and dry. Place the disk in the bottom of the jacket. The disk and jacket shall have been placed in the cooling medium a minimum of 10 min before the test jar is inserted. The use of a jacket cover while the empty jacket is cooling is permitted. Place the gasket around the test jar, 25 mm from the bottom. Insert the test jar in the jacket. Never place a jar directly into the cooling medium.

NOTE 3—Failure to keep the disk, gasket, and the inside of the jacket clean and dry may lead to frost formation, which may cause erroneous results.

8.5 Maintain the temperature of the cooling bath at 0 ± 1.5°C.

8.6 At each test thermometer reading that is a multiple of 1°C, remove the test jar from the jacket quickly but without disturbing the specimen, inspect for cloud, and replace in the jacket. This complete operation shall require not more than 3 s. If the oil does not show a cloud when it has been cooled to 9°C, transfer the test jar to a jacket in a second bath maintained at a temperature of −18 ± 1.5°C (see Table 2). Do not transfer the jacket. If the specimen does not show a cloud when it has been cooled to −6°C, transfer the test jar to a jacket in a third bath maintained at a temperature of −33 ± 1.5°C. For the determination of very low cloud points, additional baths are required, each bath to be maintained in accordance with Table 2. In each case, transfer the jar to the next bath, if the specimen does not exhibit cloud point and the temperature of the specimen reaches the lowest specimen temperature in the range identified for the current bath in use, based on the ranges stated in Table 2.

TABLE 2 Bath and Sample Temperature Ranges

Bath	Bath Temperature Setting, °C	Sample Temperature Range, °C
1	0 ± 1.5	Start to 9
2	−18 ± 1.5	9 to −6
3	−33 ± 1.5	−6 to −24
4	−51 ± 1.5	−24 to −42
5	−69 ± 1.5	−42 to −60

8.7 Report the cloud point, to the nearest 1°C, at which any cloud is observed at the bottom of the test jar, which is confirmed by continued cooling.

NOTE 4—A wax cloud or haze is always noted first at the bottom of the test jar where the temperature is lowest. A slight haze throughout the entire sample, which slowly becomes more apparent as the temperature is lowered, is usually due to traces of water in the oil. Generally this water haze will not interfere with the determination of the wax cloud point. In most cases of interference, filtration through dry lintless filter papers, such as described in 8.1, is sufficient. In the case of diesel fuels, however, if the haze is very dense, a fresh portion of the sample should be dried by shaking 100 mL with 5 g of anhydrous sodium sulfate for at least 5 min and then filtering through dry lintless filter paper. Given sufficient contact time, this procedure will remove or sufficiently reduce the water haze so that the wax cloud can be readily discerned. Drying and filtering should be done always at a temperature at least 14°C above the approximate cloud point but otherwise not in excess of 49°C.

9. Report

9.1 Report the temperature recorded in 8.7 as the cloud point, Test Method D 2500.

10. Precision and Bias

10.1 The precision of this test method as determined by statistical examination of interlaboratory results is as follows:

10.1.1 *Repeatability*—The difference between two test results, obtained by the same operator with the same apparatus under constant operating conditions on identical test material, would in the long run, in the normal and correct operation of this test method, exceed 2°C only in 1 case in 20.

10.1.2 *Reproducibility*—The difference between two single and independent results obtained by different operators working in different laboratories on identical test material, would in the long run, in the normal and correct operation of this test method, exceed 4°C only in 1 case in 20.

10.1.3 The precision statements were derived from a 1990 interlaboratory cooperative test program.[4] Participants analyzed 13 sample sets comprised of various distillate fuels and lubricating oils with temperature range from -1 to -37°C. Eight laboratories participated with the manual D 2500/IP219 test method. Information on the type of samples and their average cloud points are in the research report.

10.2 *Bias*—The procedure in this test method has no bias, because the value of cloud point can be defined only in terms of a test method.

10.3 *Precision for Biodiesel Products*[5]—The precision of this test method as determined by statistical examination of interlaboratory results is as follows:

10.3.1 *Repeatability for Blends of Biodiesel in Diesel*—The difference between successive test results obtained by the same operator, using the same apparatus, under constant operating

---

[4] Supporting data have been filed at ASTM International Headquarters and may be obtained by requesting Research Report RR: D02–1444.

[5] Supporting data (the results of the 2001 interlaboratory cooperative test program) have been filed at ASTM International Headquarters and may be obtained by requesting Research Report RR: D02–1524.

conditions, on identical test material would, in the long run, in the normal and correct operation of this test method, exceed 2°C only in 1 case in 20.

10.3.2 *Reproducibility for Blends of Biodiesel in Diesel*—The difference between two single and independent test results obtained by different operators, working in different laboratories, on identical test material would, in the long run, in the normal and correct operation of this test method, exceed 3°C only in 1 case in 20.

NOTE 5—The precision for blends of biodiesel in diesel samples comprised cloud points from about −2 to +10°C.

10.3.3 The precision statements were derived from a 2001 interlaboratory cooperative test program.[5] Participants analyzed eleven sample sets comprised of different blends of two petroleum distillate fuels, diesel and kerosene, with various biodiesel fuels with temperature range from +10 to −45°C. Ten laboratories participated with the manual D 2500/IP219 test method. Information on the type of samples and their average cloud points are in the research report.

NOTE 6—One of the outcomes of the interlaboratory study was the selection of the sample types, since the ones used in the study contributed to a difficulty in determining the precision statement. Kerosene is a sufficiently different fuel type from biodiesel to cause some slight separation of phases upon cooling when in B20 blends. Also, the particular kerosene sample used was atypical, which complicated the study further. Therefore, data from the blends of kerosene in biodiesel were not used in the precision statement. In addition, the diesel fuel used in the research report was high cloud point material. Due to the cloud point of the base diesel material, this temperature range in the precision statement was limited.

NOTE 7—A future interlaboratory cloud study will be done to include a wider range of base biodiesel fuels with various distillate blend stocks.

10.4 *Bias for Biodiesel Products*[5]—The procedure in this test method has no bias, because the value of cloud point can be defined only in terms of a test method.

11. Keywords

11.1 cloud point; petroleum products; wax crystals

SUMMARY OF CHANGES

Subcommittee D02.07 has identified the location of selected changes to this standard since the last issue (D 2500–05) that may impact the use of this standard.

(1) Revised 6.7.
(2) Revised 7.
(3) Added Table 1.
(4) Deleted original Note 2.

APPENDIX 4

ASTM D97: STANDARD TEST METHOD FOR POUR POINT OF PETROLEUM PRODUCTS

Designation: D 97 – 05

An American National Standard

Designation: 15/95

Standard Test Method for Pour Point of Petroleum Products[1]

This standard is issued under the fixed designation D 97; the number immediately following the designation indicates the year of original adoption or, in the case of revision, the year of last revision. A number in parentheses indicates the year of last reapproval. A superscript epsilon (ϵ) indicates an editorial change since the last revision or reapproval.

This standard has been approved for use by agencies of the Department of Defense.

1. Scope*

1.1 This test method is intended for use on any petroleum product.[2] A procedure suitable for black specimens, cylinder stock, and nondistillate fuel oil is described in 8.8. A procedure for testing the fluidity of a residual fuel oil at a specified temperature is described in Appendix X1.

1.2 Several ASTM test methods offering alternative procedures for determining pour points using automatic apparatus are available. None of them share the same designation number as Test Method D 97. When an automatic instrument is used, the ASTM test method designation number specific to the technique shall be reported with the results. A procedure for testing the pour point of crude oils is described in Test Method D 5853.

1.3 *This standard does not purport to address all of the safety concerns, if any, associated with its use. It is the responsibility of the user of this standard to establish appropriate safety and health practices and determine the applicability of regulatory limitations prior to use.*

2. Referenced Documents

2.1 *ASTM Standards:* [3]

D 117 Guide for Sampling, Test Methods, and Specifications for Electrical Insulating Oils of Petroleum Origin
D 396 Specification for Fuel Oils
D 1659 Test Method for Maximum Fluidity Temperature of Residual Fuel Oil[4]
D 2500 Test Method for Cloud Point of Petroleum Products
D 3245 Test Method for Pumpability of Industrial Fuel Oils
D 5853 Test Method for Pour Point of Crude Oils
E 1 Specification for ASTM Liquid-in-Glass Thermometers

2.2 *Energy Institute Standards:*

Specifications for IP Standard Thermometers [5]

3. Terminology

3.1 *Definitions:*

3.1.1 *black oil*, *n*—lubricant containing asphaltic materials. Black oils are used in heavy-duty equipment applications, such as mining and quarrying, where extra adhesiveness is desired.

3.1.2 *cylinder stock*, *n*—lubricant for independently lubricated engine cylinders, such as those of steam engines and air compressors. Cylinder stock are also used for lubrication of valves and other elements in the cylinder area.

3.1.3 *pour point*, *n—in petroleum products*, the lowest temperature at which movement of the test specimen is observed under prescribed conditions of test.

3.1.4 *residual fuel*, *n*—a liquid fuel containing bottoms remaining from crude distillation or thermal cracking; sometimes referred to as heavy fuel oil.

3.1.4.1 *Discussion*—Residual fuels comprise Grades 4, 5, and 6 fuel oils, as defined in Specification D 396.

4. Summary of Test Method

4.1 After preliminary heating, the sample is cooled at a specified rate and examined at intervals of 3°C for flow characteristics. The lowest temperature at which movement of the specimen is observed is recorded as the pour point.

---

[1] This test method is under the jurisdiction of ASTM Committee D02 on Petroleum Products and Lubricants and is the direct responsibility of Subcommittee D02.07 on Flow Properties.

Current edition approved June 1, 2005. Published July 2005. Originally approved in 1927, replacing D 47. Last previous edition approved in 2004 as D 97–04.

In the IP, this test method is under the jurisdiction of the Standardization Committee. This test method was adopted as a joint ASTM-IP Standard in 1965.

[2] Statements defining this test and its significance when applied to electrical insulating oils of mineral origin will be found in Guide D 117.

[3] *Reagent Chemicals, American Chemical Society Specifications,* American Chemical Society, Washington, DC. For suggestions on the testing of reagents not listed by the American Chemical Society, see *Annual Standards for Laboratory Chemicals,* BDH Ltd., Poole, Dorset, U.K., and the *United States Pharmacopeia and National Formulary,* U.S. Pharmacopeial Convention, Inc. (USPC), Rockville, MD.

[4] Withdrawn.

[5] Methods for Analysis and Testing, *IP Standards for Petroleum and its Products*, Part I, Vol 2.

***A Summary of Changes section appears at the end of this standard.**

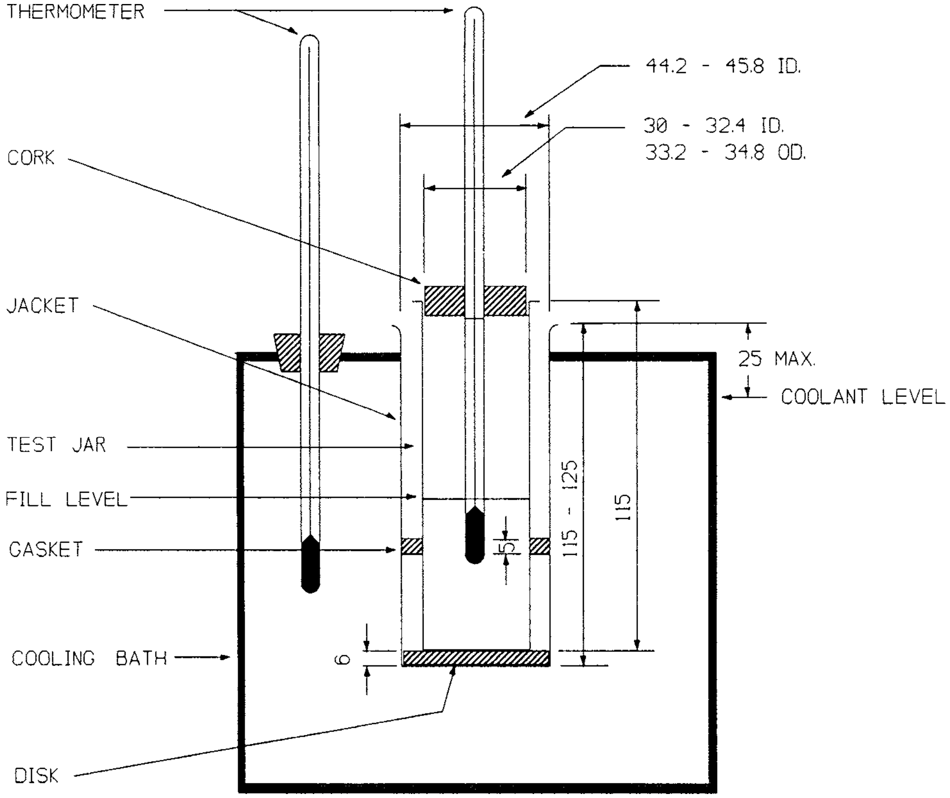

NOTE—Dimensions are in millimetres (not to scale).

FIG. 1 Apparatus for Pour Point Test

5. Significance and Use

5.1 The pour point of a petroleum specimen is an index of the lowest temperature of its utility for certain applications.

6. Apparatus

6.1 *Test Jar*, cylindrical, of clear glass, flat bottom, 33.2 to 34.8-mm outside diameter, and 115 to 125 mm in height. The inside diameter of the jar can range from 30.0 to 32.4 mm, within the constraint that the wall thickness be no greater than 1.6 mm. The jar shall have a line to indicate a sample height 54 ± 3 mm above the inside bottom. See Fig. 1.

6.2 *Thermometers*, having the following ranges and conforming to the requirements prescribed in Specification E 1 for thermometers:

	Temperature	Thermometer Number	
Thermometer	Range	ASTM	IP
High cloud and pour	−38 to +50°C	5C	1C
Low cloud and pour	−80 to +20°C	6C	2C
Melting point	+32 to +127°C	61C	63C

6.2.1 Since separation of liquid column thermometers occasionally occurs and may escape detection, thermometers should be checked immediately prior to the test and used only if they prove accurate within ±1°C (for example ice point).

6.3 *Cork*, to fit the test jar, bored centrally for the test thermometer.

6.4 *Jacket*, watertight, cylindrical, metal, flat-bottomed, 115 ± 3-mm depth, with inside diameter of 44.2 to 45.8 mm. It shall be supported in a vertical position in the cooling bath (see 6.7) so that not more than 25 mm projects out of the cooling medium, and shall be capable of being cleaned.

6.5 *Disk*, cork or felt, 6 mm thick to fit loosely inside the jacket.

6.6 *Gasket*, to fit snugly around the outside of the test jar and loosely inside the jacket. The gasket may be made of rubber, leather, or other material that is elastic enough to cling to the test jar and hard enough to hold its shape. Its purpose is to prevent the test jar from touching the jacket.

6.7 *Bath or Baths*, maintained at prescribed temperatures with a firm support to hold the jacket vertical. The required bath temperatures may be obtained by refrigeration if available, otherwise by suitable freezing mixtures. Freezing mixtures commonly used for temperatures down to those shown are as follows:

	For Temperatures Down
Ice and water	9°C
Crushed ice and sodium chloride crystals	−12°C
Crushed ice and calcium chloride crystals	−27°C
Acetone or petroleum naphtha (see Section 6) chilled in a covered metal beaker with an ice-salt mixture to −12°C then with enough solid carbon dioxide to give the desired temperature.	−57°C

7. Reagents and Materials

7.1 The following solvents of technical grade are appropriate for low-temperature bath media.

7.1.1 *Acetone*, (**Warning**—Extremely flammable).

7.1.2 *Alcohol, Ethanol* (**Warning**—Flammable).

7.1.3 *Alcohol*, *Methanol* (**Warning**—Flammable. Vapor harmful).

7.1.4 *Petroleum Naphtha*, (**Warning**—Combustible. Vapor harmful).

7.1.5 *Solid Carbon Dioxide*, (**Warning**—Extremely cold −78.5°C).

8. Procedure

8.1 Pour the specimen into the test jar to the level mark. When necessary, heat the specimen in a water bath until it is just sufficiently fluid to pour into the test jar.

NOTE 1—It is known that some materials, when heated to a temperature higher than 45°C during the preceding 24 h, do not yield the same pour point results as when they are kept at room temperature for 24 h prior to testing. Examples of materials which are known to show sensitivity to thermal history are residual fuels, black oils, and cylinder stocks.

8.1.1 Samples of residual fuels, black oils, and cylinder stocks which have been heated to a temperature higher than 45°C during the preceding 24 h, or when the thermal history of these sample types is not known, shall be kept at room temperature for 24 h before testing. Samples which are known by the operator not to be sensitive to thermal history need not be kept at room temperature for 24 h before testing.

8.1.2 Experimental evidence supporting elimination of the 24-h waiting period for some sample types is contained in a research report.[6]

8.2 Close the test jar with the cork carrying the high-pour thermometer (5.2). In the case of pour points above 36°C, use a higher range thermometer such as IP 63C or ASTM 61C. Adjust the position of the cork and thermometer so the cork fits tightly, the thermometer and the jar are coaxial, and the thermometer bulb is immersed so the beginning of the capillary is 3 mm below the surface of the specimen.

8.3 For the measurement of pour point, subject the specimen in the test jar to the following preliminary treatment:

8.3.1 *Specimens Having Pour Points Above −33°C*—Heat the specimen without stirring to 9°C above the expected pour point, but to at least 45°C, in a bath maintained at 12°C above the expected pour point, but at least 48°C. Transfer the test jar to a water bath maintained at 24°C and commence observations for pour point.

8.3.2 *Specimens Having Pour Points of −33°C and Below*—Heat the specimen without stirring to 45°C in a bath maintained at 48°C and cool to 15°C in a water bath maintained at 6°C. Remove the high cloud and pour thermometer, and place the low cloud and pour thermometer in position.

8.4 See that the disk, gasket, and the inside of the jacket are clean and dry. Place the disk in the bottom of the jacket. Place the gasket around the test jar, 25 mm from the bottom. Insert the test jar in the jacket. Never place a jar directly into the cooling medium.

8.5 After the specimen has cooled to allow the formation of paraffin wax crystals, take great care not to disturb the mass of specimen nor permit the thermometer to shift in the specimen; any disturbance of the spongy network of wax crystals will lead to low and erroneous results.

8.6 Pour points are expressed in integers that are positive or negative multiples of 3°C. Begin to examine the appearance of the specimen when the temperature of the specimen is 9°C above the expected pour point (estimated as a multiple of 3°C). At each test thermometer reading that is a multiple of 3°C below the starting temperature remove the test jar from the jacket. To remove condensed moisture that limits visibility wipe the surface with a clean cloth moistened in alcohol (ethanol or methanol). Tilt the jar just enough to ascertain whether there is a movement of the specimen in the test jar. The complete operation of removal, wiping, and replacement shall require not more than 3 s.

8.6.1 If the specimen has not ceased to flow when its temperature has reached 27°C, transfer the test jar to the next lower temperature bath in accordance with the following schedule:

Specimen is at +27°C, move to 0°C bath
Specimen is at +9°C, move to −18°C bath
Specimen is at −6°C, move to −33°C bath
Specimen is at −24°C, move to −51°C bath
Specimen is at −42°C, move to −69°C bath

8.6.2 As soon as the specimen in the jar does not flow when tilted, hold the jar in a horizontal position for 5 s, as noted by an accurate timing device and observe carefully. If the specimen shows any movement, replace the test jar immediately in the jacket and repeat a test for flow at the next temperature, 3°C lower.

8.7 Continue in this manner until a point is reached at which the specimen shows no movement when the test jar is held in a horizontal position for 5 s. Record the observed reading of the test thermometer.

8.8 For black specimen, cylinder stock, and nondistillate fuel specimen, the result obtained by the procedure described in 8.1 through 8.7 is the upper (maximum) pour point. If required, determine the lower (minimum) pour point by heating the sample while stirring, to 105°C, pouring it into the jar, and determining the pour point as described in 8.4 through 8.7.

8.9 Some specifications allow for a pass/fail test or have pour point limits at temperatures not divisible by 3°C. In these cases, it is acceptable practice to conduct the pour point measurement according to the following schedule: Begin to examine the appearance of the specimen when the temperature of the specimen is 9°C above the specification pour point. Continue observations at 3°C intervals as described in 8.6 and 8.7 until the specification temperature is reached. Report the sample as passing or failing the specification limit.

9. Calculation and Report

9.1 Add 3°C to the temperature recorded in 8.7 and report the result as the Pour Point, ASTM D 97. For black oil, and so forth, add 3°C to the temperature recorded in 8.7 and report the

---

[6] Supporting data have been filed at ASTM International Headquarters and may be obtained by requesting Research Report RR: D02-1377.

result as Upper Pour Point, ASTM D 97, or Lower Pour Point, ASTM D 97, as required.

10. Precision and Bias

10.1 *Lubricating Oil and Distillate and Residual Fuel Oil.* [7]

10.1.1 *Repeatability*—The difference between successive test results, obtained by the same operator using the same apparatus under constant operating conditions on identical test material, would in the long run, in the normal and correct operation of this test method, exceed 3°C only in one case in twenty. Differences greater than this should be considered suspect.

10.1.2 *Reproducibility*—The difference between two single and independent test results, obtained by different operators working in different laboratories on identical test material, would in the long run, in the normal and correct operation of this test method, exceed 6°C only in one case in twenty. Differences greater than this should be considered suspect.

10.2 *Bias*—There being no criteria for measuring bias in these test-product combinations, no statement of bias can be made.

10.3 The precision statements were prepared with data on ten new (unused) mineral oil-based lubricants and sixteen assorted fuel oils tested by twelve cooperators. The mineral oil-based lubricants had pour points ranging from −48 to −6°C while the fuel oils had pour points ranging from −33 to +51°C. The following precision data were obtained:

	Mineral Oil Lubricants	Fuel Oils
95 % Confidence		
Repeatability, °C	2.87	2.52
Reproducibility, °C	6.43	6.59

APPENDIX

(Nonmandatory Information)

X1. TEST FOR FLUIDITY OF A RESIDUAL FUEL OIL AT A SPECIFIED TEMPERATURE

X1.1 General

X1.1.1 The low-temperature flow properties of a waxy fuel oil depend on handling and storage conditions. Thus, they may not be truly indicated by pour point. The pour point test does not indicate what happens when an oil has a considerable head of pressure behind it, such as when gravitating from a storage tank or being pumped along a pipeline. Failure to flow at the pour point is normally attributed to the separation of wax from the fuel; however, it can also be due to the effect of viscosity in the case of very viscous fuel oils. In addition pour points of residual fuels are influenced by the previous thermal history of the specimens. A loosely knit wax structure built up on cooling of the oil can be normally broken by the application of relatively little pressure.

X1.1.2 The usefulness of the pour point test in relation to residual fuel oils is open to question, and the tendency to regard the pour point as the limiting temperature at which a fuel will flow can be misleading. The problem of accurately specifying the handling behavior of fuel oil is important, and because of the technical limitations of the pour point test, various pumpability tests have been devised to assess the low-temperature flow characteristics of heavy residual fuel oils. Test Method D 3245 is one such method. However, most alternative methods tend to be time-consuming and as such do not find ready acceptance as routine control tests for determining low-temperature flow properties. One method which is relatively quick and easy to perform and has found limited acceptance as a "go-no-go" method is based on the appendix method to the former Test Method D 1659–65. The method is described as follows.

X1.2 Scope

X1.2.1 This method covers the determination of the fluidity of a residual fuel oil at a specified temperature in an as-received condition.

X1.3 Definition

X1.3.1 *fluidity temperature*—the sample when tested in an as-received condition is considered "fluid at the temperature of the test" if it will flow 2 mm in 1 min in a 12.5 mm U-tube under a maximum pressure of 152 mm of mercury.

X1.4 Summary of Test Method

X1.4.1 A sample of fuel in its as-received condition is cooled at the specified temperature for 30 min in the standard U-tube and is tested for movement under prescribed pressure conditions.

X1.5 Significance and Use

X1.5.1 This method may be used as a "go-no-go" procedure for operational situations where it is necessary to ascertain the fluidity of a residual oil under prescribed conditions in an as-received condition. The conditions of this method simulate those of a pumping situation where the oil is expected to flow through a 12-mm pipe under slight pressure at a specified temperature. Fluidity, like Test Method D 97, is used to define cold flow properties. It differs from D 97, however, in that (*1*) it is restricted to residual fuel oil and (*2*) a prescribed pressure is applied to the sample. The latter represents an attempt to overcome the technical limitations of the Pour Point Method where gravity-induced flow is the criterion. Test Method

---

[7] The cloud point procedure formerly part of this test method now appears as Test Method D 2500.

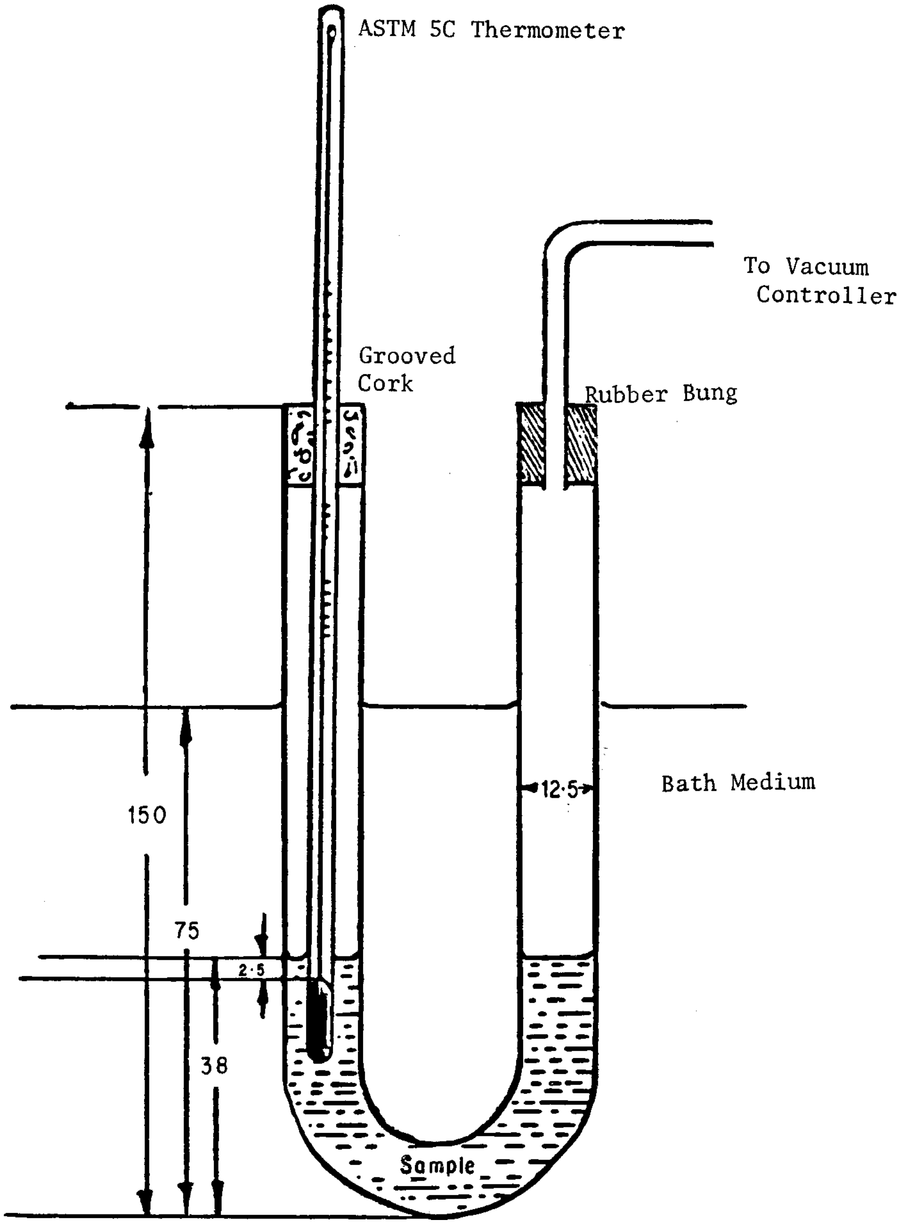

NOTE—All dimensions are in millimetres

FIG. X1.1 Disposition of U-tube in Fluidity Temperature Test Bath

D 3245, represents another method for predicting field performance in cold flow conditions. Test Method D 3245, however, does have limitations and may not be suitable for use with very waxy fuel oils which solidify so rapidly in the chilling bath that a reading cannot be obtained under the conditions of the test. It is also a time-consuming test and therefore not suitable for routine control testing.

X1.6 Apparatus

X1.6.1 *Glass U-Tubes*, 150 mm high, having a uniform internal diameter of 12.5 ± 1 mm and a radius of curvature, measured to the outside curve of the tube of 35 mm (Fig. X1.1).

X1.6.2 *Thermometers*—Thermometers having a range from −38 to +50°C and conforming to the requirements of Thermometer 5C as prescribed in Specification E 1, shall be used for insertion in the glass U-tubes and for measuring the temperatures of the baths.

X1.6.3 *Fluidity Temperature Test Bath,*[8] consists of a reservoir, a stirrer, and a motor and pump to circulate coolant through the coils of the tubing placed in the bottom of the test bath and passing through the cold bath. The flow of coolant through these coils can be controlled by a thermostat and a solenoid valve. It is possible that, where justified by the quantity of work, more than one such bath could be utilized to permit concurrent testing at more than one temperature (Fig. X1.2).

---

[8] A kinematic viscosity bath is usually satisfactory.

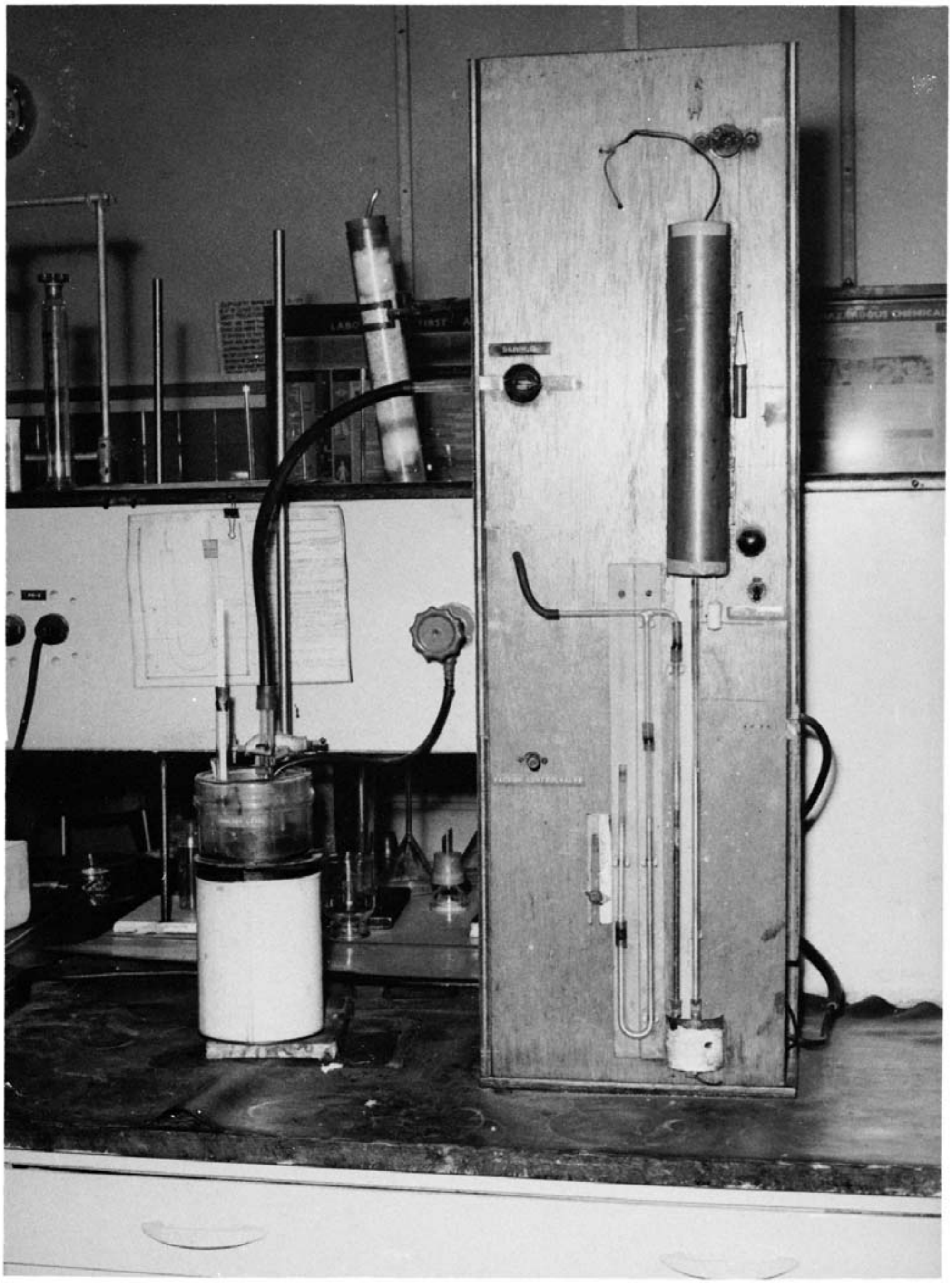

FIG. X1.2 Fluidity Temperature Apparatus

X1.6.4 *Mercury Manometer* calibrated in 10-mm divisions with a distinguishing mark at 152 mm (equivalent to 20.3 kPa).

X1.6.5 *Automatic Vacuum Controller*[9] *(as shown in Fig. X1.3 and Fig. X1.4)*—A device that gradually increased the vacuum applied to one end of the U-tube at the specified rate of 10 mm/4S.

X1.7 Preparation of Apparatus

X1.7.1 Adjust the automatic vacuum controller as follows: close the stopcock on the tube connecting the automatic vacuum controller to the fluidity tester. A pinchcock on the rubber tube will serve as well as a stopcock. Wind the thread attached to the steel rod around the pulley on the synchronous motor until the end of the rod is about 15 mm above the zero level of the mercury in the control manometer. Turn on the power switch. The thread will begin to unwind, lowering the steel rod. When the rod contacts the mercury, the relay will

---

[9] This apparatus may be shop fabricated. Details of special parts are indicated in Figs. X1.3 and X1.4. Alternatively the apparatus can be purchased.

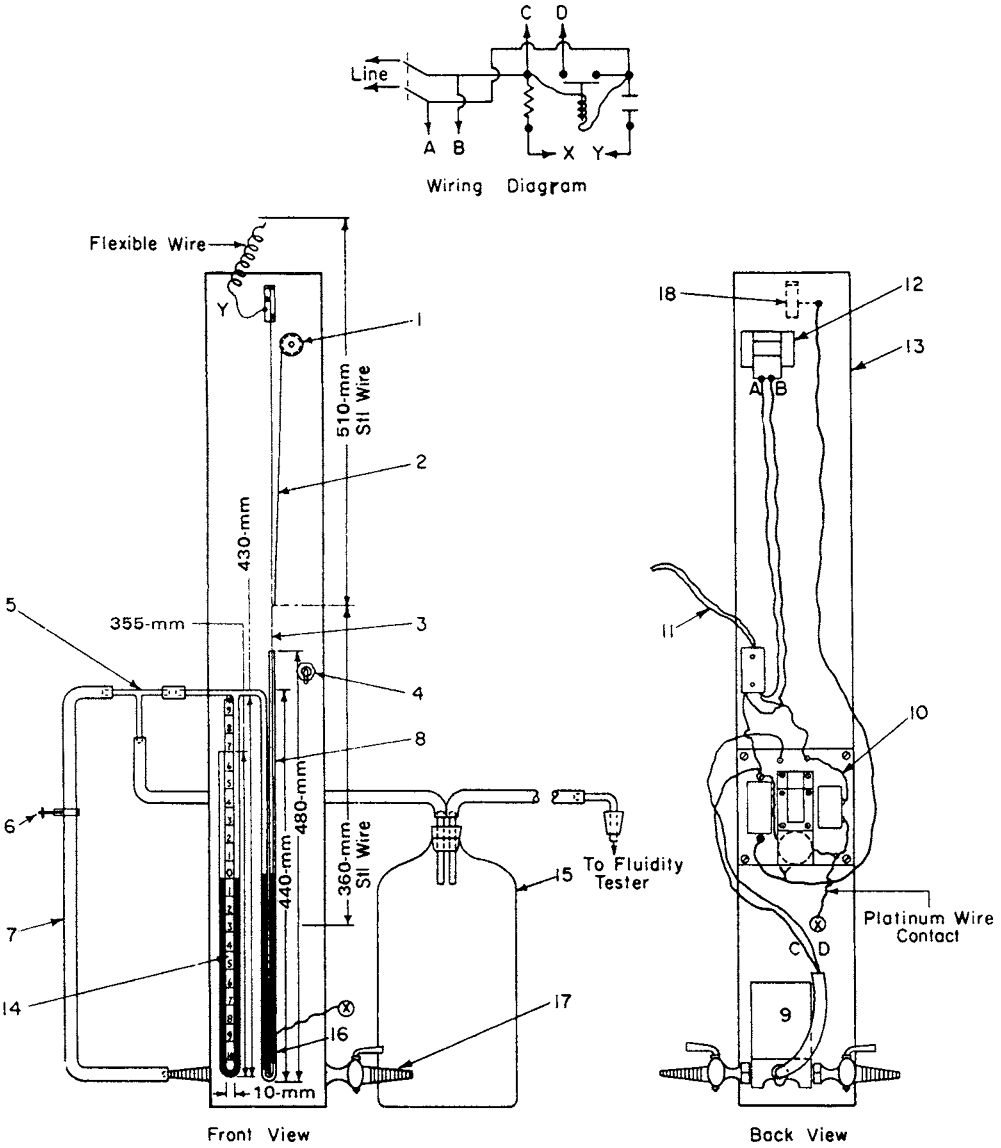

1—26-mm diameter face pulley
2—Thread
3—Steel rod
4—Switch-DPST
5—Tee, 90-mm long
6—Needle valve
7—Rubber or plastic tubing
8—6-mm heat-resistant glass tube
9—Solenoid valve
10—Electric relay
11—Electric cord to outlet
12—Synchronous motor
13—Plywood of approximately 10-mm thickness
14—Millimeter scale
15—4-L bottle
16—0.5-mm heat-resistant glass capillary
17—To vacuum line
18—Rod holder

FIG. X1.3 Assembly Automatic Vacuum Controller Apparatus

open the solenoid valve in the vacuum line and air will be pumped from the system at a rate limited by the needle valve. Adjust this needle valve until the descending mercury in the control manometer just leads the rod, reducing the relay operation to a minimum. When properly adjusted, the pulsations caused by the opening and closing of the solenoid valve should not exceed ±1 mm. In this manner the pressure in the system will be reduced gradually at a rate governed by the descent of the steel rod.

X1.8 Procedure

X1.8.1 Pour the sample as received into a thoroughly cleaned and dry standard fluidity U-tube, without contacting the upper walls of the tube, until the vertical height of the

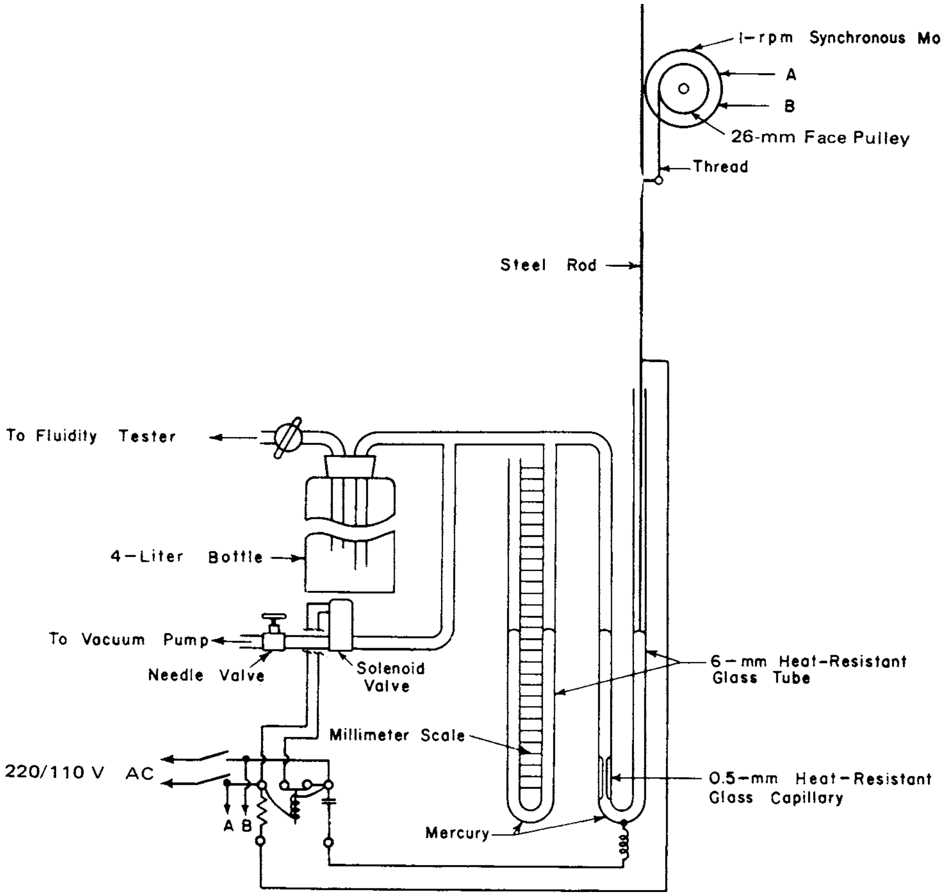

FIG. X1.4 Detail of Automatic Vacuum Controller

sample in the U-tube is 38 mm. Insert in one leg of each U-tube an ASTM Thermometer 5C in a cork that has been grooved to permit the passage of air. The thermometer must be placed in the center of the tube and its bulb immersed so that the beginning of the capillary is 3 mm below the surface of the specimen.

X1.8.2 Fix the tube in the bath set at the specific temperature, immersed to a depth of approximately 75 mm. Control the bath and sample temperatures within ±1°C and ±0.5°C, respectively, of the specified temperature of the test.

X1.8.3 Maintain the sample at the specified temperature for 30 min ± 30 s, with the U-tube connected to the automatic vacuum controller, and the stopcock or pinch-clamp open. Wind the thread on the pulley attached to the synchronous motor. Turn the power switch to the ON position. Apply suction automatically to the U-tube at the prescribed rate. Observe any movement of the specimen during a one-minute interval which is the time required to apply 152-mm Hg vacuum to the specimen in the U-tube. Immediately disconnect the U-tube from the automatic vacuum controller, turn off the power switch and rewind the thread. If the specimen has moved 2 mm or more during the time (1 min) the suction was applied, the specimen is considered fluid at the temperature of the test.

X1.9 Report

X1.9.1 Report the fluidity of the sample at a specified temperature as follows:

X1.9.1.1 If the sample fulfills the conditions of flow, as defined in X1.3.1, report fluidity: “Fluid at (temperature of test)” or fluidity at (temperature of test): “Pass.”

X1.9.1.2 If the sample does not fulfill the conditions of flow, as defined in X1.3.1, report fluidity: “Not fluid at (temperature of test)” or fluidity at (temperature of test): “Fail.”

X1.10 Precision and Bias

X1.10.1 As in the case of pass-fail data, no statement is made about either the precision or the bias of this method for measuring the fluidity of a residual fuel specimen since the result merely states whether there is conformance to the criteria for success specified in the procedure.

SUMMARY OF CHANGES

Subcommittee D02.07 has identified the location of selected changes to this standard since the last issue (D 97–04) that may impact the use of this standard.

(*1*) Added Test Method D 5853 to the Scope and Referenced Documents sections.

APPENDIX 5

ASTM D6371: STANDARD TEST METHOD FOR COLD FILTER PLUGGING POINT OF DIESEL AND HEATING FUELS

Designation: D 6371 – 05

An American National Standard

Standard Test Method for
Cold Filter Plugging Point of Diesel and Heating Fuels[1]

This standard is issued under the fixed designation D 6371; the number immediately following the designation indicates the year of original adoption or, in the case of revision, the year of last revision. A number in parentheses indicates the year of last reapproval. A superscript epsilon (e) indicates an editorial change since the last revision or reapproval.

1. Scope*

1.1 This test method covers the determination of the cold filter plugging point (CFPP) temperature of diesel and domestic heating fuels using either manual or automated apparatus.

NOTE 1—This test method is technically equivalent to test methods IP 309 and EN 116.

1.2 The manual apparatus and automated apparatus are both suitable for referee purposes.

1.3 This test method is applicable to distillate fuels, including those containing a flow-improving or other additive, intended for use in diesel engines and domestic heating installations.

1.4 The values stated in SI units are to be regarded as standard. No other units of measurement are included in this standard.

1.5 *This standard does not purport to address all of the safety concerns, if any, associated with its use. It is the responsibility of the user of this standard to establish appropriate safety and health practices and determine the applicability of regulatory limitations prior to use.* For specific hazard statements, see Section 7.

2. Referenced Documents

2.1 *ASTM Standards:* [2]

D 2500 Test Method for Cloud Point of Petroleum Products
D 4057 Practice for Manual Sampling of Petroleum and Petroleum Products
D 4177 Practice for Automatic Sampling of Petroleum and Petroleum Products
D 5771 Test Method for Cloud Point of Petroleum Products (Optical Detection Stepped Cooling Method)
D 5772 Test Method for Cloud Point of Petroleum Products (Linear Cooling Rate Method)
D 5773 Test Method for Cloud Point of Petroleum Products (Constant Cooling Rate Method)
E 1 Specification for ASTM Liquid-in-Glass Thermometers

2.2 *IP Standards:*[3]

IP 309 Diesel and domestic heating fuels - Determination of cold filter plugging point
Specifications for IP Standard Thermometers

2.3 *ISO Standards:*[4]

IP 3310 Test sieves - Technical requirements and testing - Part 1: Metal cloth

2.4 *European Standards:*[5]

EN 116 Diesel and domestic heating fuels - Determination of cold filter plugging point

3. Terminology

3.1 *Definitions of Terms Specific to This Standard:*

3.1.1 *certified reference material*, *n*—a stable petroleum product with a method-specific nominal CFPP value established by a method-specific interlaboratory study following RR:D02-1007[6] guidelines or ISO Guides 34 and 35.[4]

3.1.2 *cold filter plugging point*, *n*—highest temperature, expressed in multiples of 1°C, at which a given volume of fuel fails to pass through a standardized filtration device in a specified time when cooled under the conditions prescribed in this test method.

4. Summary of Test Method

4.1 A specimen of the sample is cooled under specified conditions and, at intervals of 1°C, is drawn into a pipet under a controlled vacuum through a standardized wire mesh filter. The procedure is repeated, as the specimen continues to cool, for each 1°C below the first test temperature. Testing is continued until the amount of wax crystals that have separated out of solution is sufficient to stop or slow down the flow so that the time taken to fill the pipet exceeds 60 s or the fuel fails to return completely to the test jar before the fuel has cooled by a further 1°C.

4.2 The indicated temperature at which the last filtration was commenced is recorded as the CFPP.

---

[1] This test method is under the jurisdiction of ASTM Committee D02 on Petroleum Products and Lubricants and is the direct responsibility of Subcommittee D02.07 on Flow Properties.

Current edition approved May 1, 2005. Published May 2005. Originally approved in 1999. Last previous edition approved in 1999 as D 6371–99.

[2] For referenced ASTM standards, visit the ASTM website, www.astm.org, or contact ASTM Customer Service at service@astm.org. For *Annual Book of ASTM Standards* volume information, refer to the standard's Document Summary page on the ASTM website.

[3] Available from Energy Institute, 61 New Cavendish St., London, WIG 7AR, U.K.

[4] Available from American National Standards Institute (ANSI), 25 W. 43rd St., 4th Floor, New York, NY 10036.

[5] Available from European Committee for Standardization, Central Secretariat, Rue Bréderode 2, B-1000, Brussels, Belgium.

[6] Supporting data have been filed at ASTM International Headquarters and may be obtained by requesting Research Report RR:D02-1007.

***A Summary of Changes section appears at the end of this standard.**

5. Significance and Use

5.1 The CFPP of a fuel is suitable for estimating the lowest temperature at which a fuel will give trouble-free flow in certain fuel systems.

5.2 In the case of diesel fuel used in European light duty trucks, the results are usually close to the temperature of failure in service except when the fuel system contains, for example, a paper filter installed in a location exposed to the weather or if the filter plugging temperature is more than 12°C below the cloud point value in accordance with Test Method D 2500, D 5771, D 5772, or D 5773. Domestic heating installations are usually less critical and often operate satisfactorily at temperatures somewhat lower than those indicated by the test results.

5.3 The difference in results obtained from the sample *as received* and after heat treatment at 45°C for 30 min can be used to investigate complaints of unsatisfactory performance under low temperature conditions.

6. Apparatus

6.1 *Manual Apparatus*:

6.1.1 The apparatus, as detailed in 6.1.2-6.1.13, shall be arranged as shown in Fig. 1.

6.1.2 *Test Jar*, cylindrical, of clear glass, flat bottomed, with an internal diameter of 31.5 6 0.5 mm, a wall thickness of 1.25 60.25 mm and a height of 120 6 5 mm. The jar shall have a permanent mark at the 45 6 1 mL level.

NOTE 2—Test jars of the required dimensions may be obtained by selection from jars conforming to Test Method D 2500, which specifies a wider diameter tolerance.

6.1.3 *Jacket*, brass, watertight, cylindrical, flat bottomed, to be used as an air bath. It shall have an inside diameter of 45 60.25 mm, outside diameter of 48 6 0.25 mm, and a height of 115 6 3 mm (see Fig. 2).

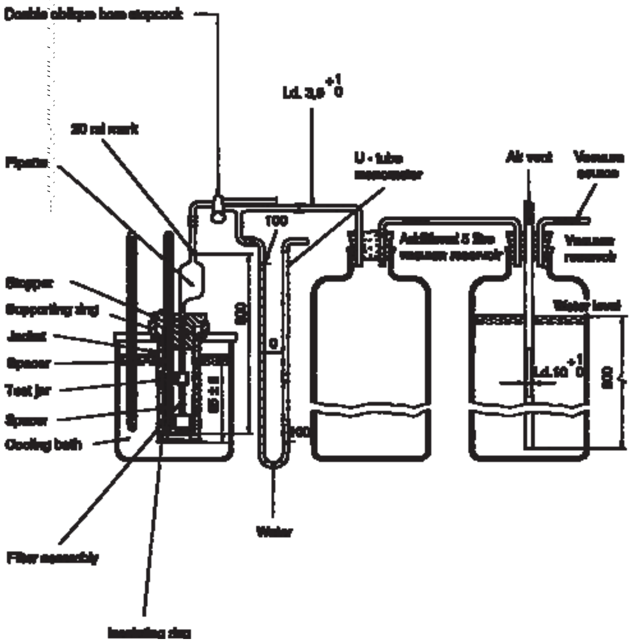

NOTE—All dimensions are in millimetres, and the comma (,) is used as the decimal point.

FIG. 1 Arrangement of Manual CFPP Apparatus

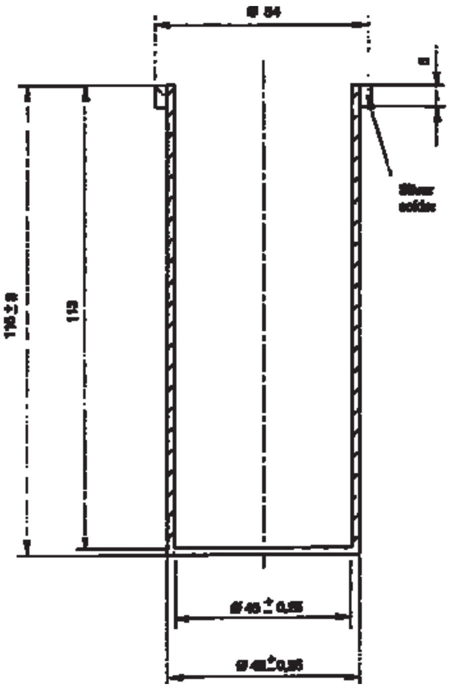

NOTE—All dimensions are in millimetres, and the comma (,) is used as the decimal point.

FIG. 2 Watertight Brass Jacket

6.1.4 *Insulating Ring*, made from oil-resistant plastics or other suitable material, to be placed in the bottom of the jacket (see 6.1.3) to provide insulation for the bottom of the test jar. It shall fit closely inside the jacket and have a thickness of 6 + 0.3 - 0.0 mm.

6.1.5 *Spacers (two)*, approximately 5-mm thick, made of oil-resistant plastics or other suitable material, to be placed as shown in Fig. 1 around the test jar (see 6.1.2) to provide insulation for the test jar from the sides of the jacket. The spacers shall fit closely to the test jar and closely inside the jacket. The use of incomplete rings, each with a 2-mm circumferential gap, will accommodate variations in test jar diameter. The spacers and insulating ring may be made as a single part as shown in Fig. 3.

6.1.6 *Supporting Ring*, of oil resistant plastics or other suitable non-metallic, non-absorbent, oil-resistant material, used to suspend the jacket (see 6.1.3) in a stable and upright position in the cooling bath and to provide a concentric location for the stopper (see 6.1.7). A design is shown in Fig. 4 for guidance, but this design may be modified to suit the cooling bath.

6.1.7 *Stopper*, of oil-resistant plastics or other suitable nonmetallic, nonabsorbent, oil-resistant material, to fit the test jar and the support ring as shown in Fig. 5. It shall have three holes to accommodate the pipet (see 6.1.8) and the thermometer (see 6.1.9) and to allow venting of the system. If necessary, when using the high-range thermometer (see 6.1.9), the upper part of the stopper shall have an indentation to permit the thermometer (see 6.1.9) to be read down to a temperature of -30°C. A pointer shall be fitted to the upper surface of the stopper to facilitate location of the thermometer in relation to

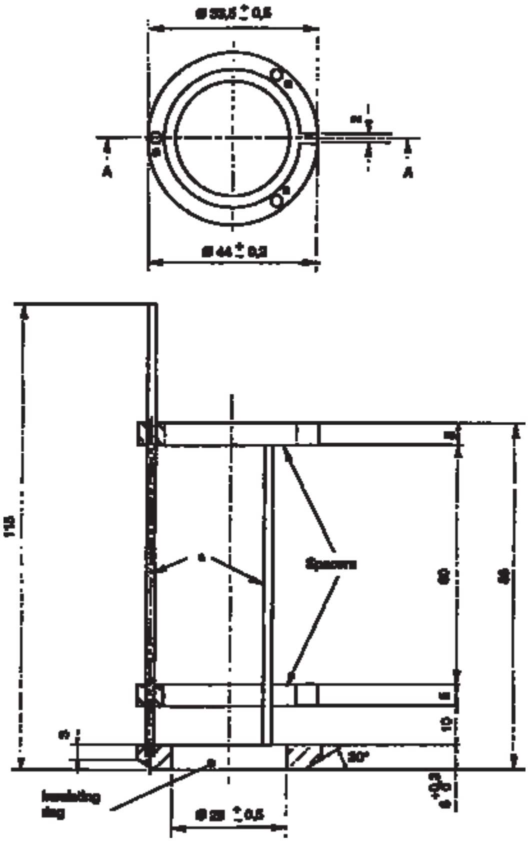

NOTE—All dimensions are in millimetres, and the comma (,) is used as the decimal point.

FIG. 3 Spacers

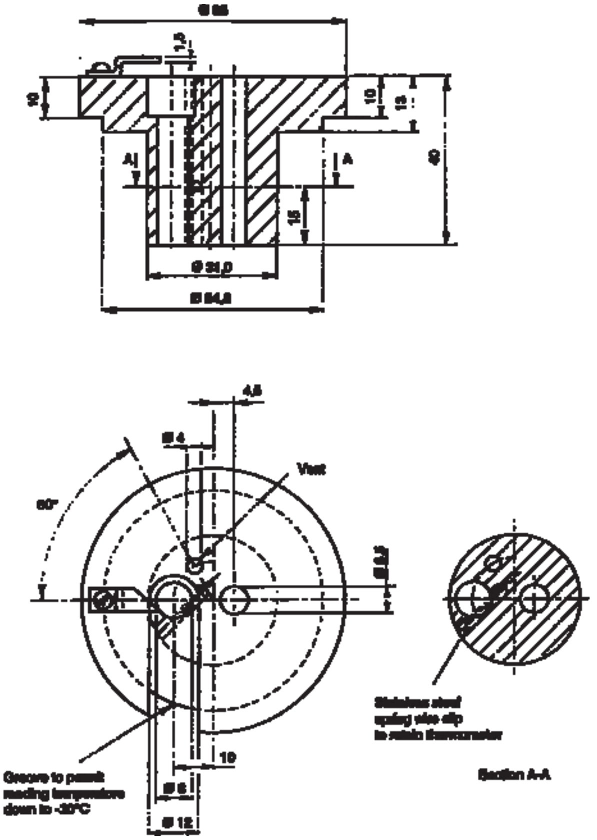

NOTE—All dimensions are in millimetres, and the comma (,) is used as the decimal point.

FIG. 5 Stopper with Holes for Thermometer, Pipet, and Vent

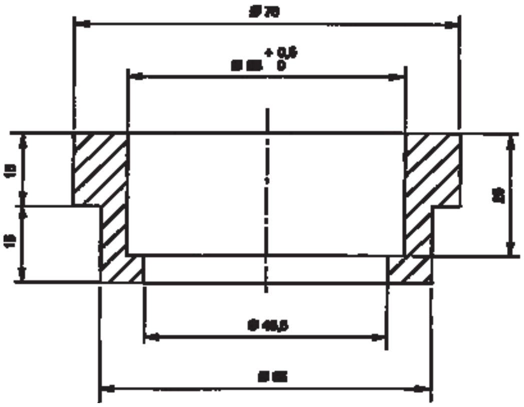

NOTE—All dimensions are in millimetres, and the comma (,) is used as the decimal point.

FIG. 4 Supporting Ring

the bottom of the test jar. A spring wire clip shall be used to retain the thermometer in the correct position.

6.1.8 *Pipet with Filter Unit*:

6.1.8.1 *Pipet*, of clear glass with a calibration mark corresponding to a contained volume of 20 ± 0.2 mL at a point 149 ± 0.5 mm from the bottom of the pipet (see Fig. 6). It shall be connected to the filter unit (see 6.1.8.2).

6.1.8.2 *Filter Unit (see* Fig. 7*)*, containing the following elements:

(1) Brass Body, with a threaded cavity that houses the wire mesh holder. The cavity shall be fitted with an O-ring of oil-resistant plastics. The internal diameter of the central tube shall be 4 ± 0.1 mm.

(2) Brass Screw Cap, to connect the upper part of the body of the filter unit (see 6.1.8.2) to the lower part of the pipet (see 6.1.8.1) to ensure a leak-free joint. An example of satisfactory connection is shown in Fig. 7.

(3) Disc, 15 ± 0.1-mm diameter, of plain weave stainless steel wire mesh gauze with a nominal aperture size of 45 µm. The nominal diameter of the wire shall be 32 µm, and the tolerance for the size of an individual aperture shall be as follows:

No aperture size shall exceed the nominal size by more than 22 µm.

The average aperture size shall be within ± 3.1 µm of the nominal size.

Not more than 6 % of the apertures shall be above the nominal size by more than 13 µm.

(4) Filter Holder of Brass, in which the disc of wire mesh gauze (see 6.1.8.2 (*3*)) is firmly clamped by a retaining ring pressed into the filter holder. The diameter of the exposed part of the gauze shall be 12 + 0.1 - 0.0 mm (see Fig. 8).

(5) Brass Cylinder, threaded on the outside, that can be screwed into the cavity of the body (see 6.1.8.2 (*1*)) to clamp the filter holder (see 6.1.8.2 (*4*)) against the O-ring (6.1.8.2

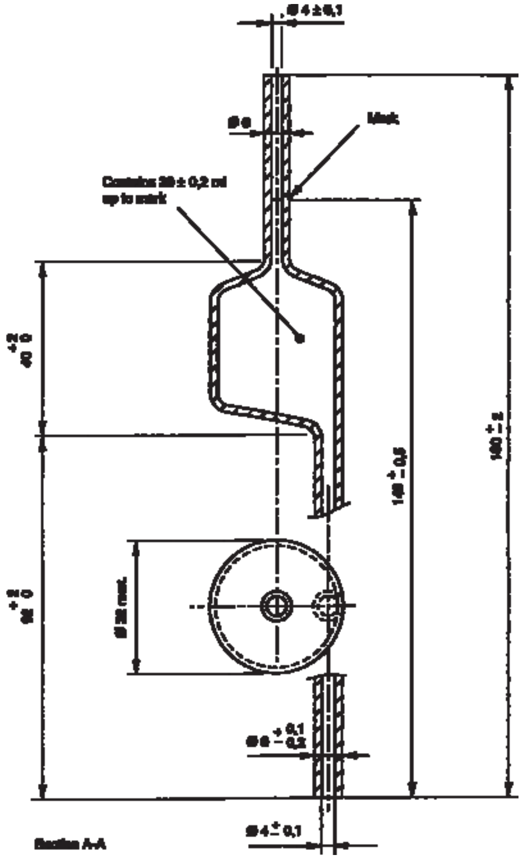

NOTE—All dimensions are in millimetres, and the comma (,) is used as the decimal point.

FIG. 6 Pipet

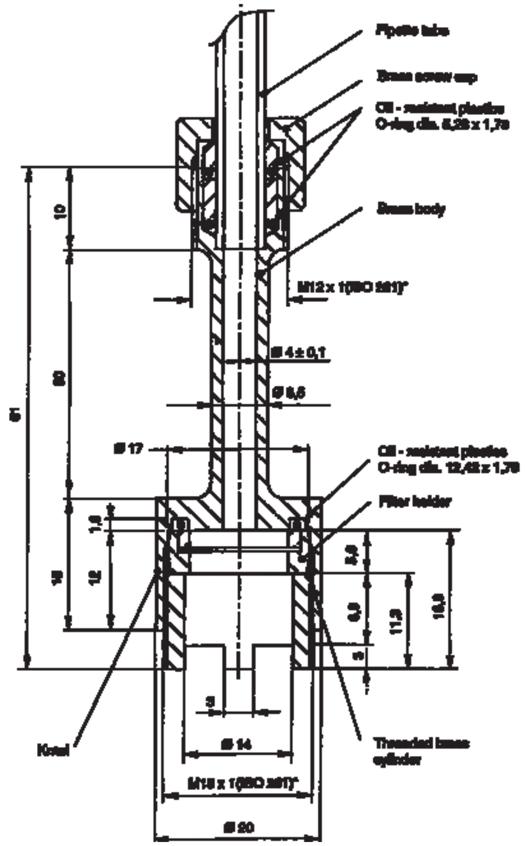

NOTE—All dimensions are in millimetres, and the comma (,) is used as the decimal point.

FIG. 7 Filter Unit

(*1*)), The lower end shall have four slots to allow the specimen to flow into the filter unit.

NOTE 3—The requirements for the wire mesh are taken from ISO 3310, to which reference may be made for methods for testing the gauze.

6.1.9 *Thermometers*, having ranges shown below and conforming to the requirements prescribed in Specification E 1 or Specifications for IP Standard Thermometers.

Thermometer	Temperature Range	Thermometer Number ASTM	IP
High-range for CFPP down to −30°C	−38°C to +50°C	5C	1C
Low-range from CFPP below −30°C	–80°C to +20°C	6C	2C
Cooling bath	−80°C to +20°C	6C	2C

6.1.10 *Cooling Bath*:

6.1.10.1 The type of cooling bath is optional, but it shall be of a shape and size suitable for containing the jacket (see 6.1.3) in a stable and upright position at the required depth.

6.1.10.2 The bath shall be fitted with a cover with one or more holes in it to accommodate the supporting ring (see 6.1.6). The jacket (see 6.1.3) may be permanently mounted in the cover.

6.1.10.3 The bath temperature shall be maintained at the required value and tolerance by a refrigeration unit or by the use of suitable freezing mixtures, ensuring a homogenous temperature in the bath by stirring or other means of agitation.

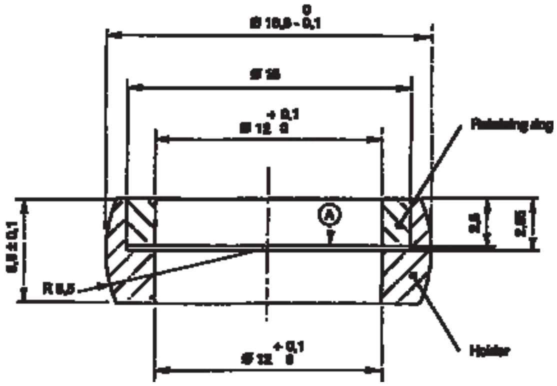

NOTE—All dimensions are in millimetres, and the comma (,) is used as the decimal point.

FIG. 8 Brass Filter Holder

Table 1 lists the bath temperature set-points required in the CFPP procedure. If only one bath is utilized, it must have the

TABLE 1 Cooling Bath Temperatures

Expected CFPP	Required Cooling Bath Temperature(s)
Down to −20°C	−34 ± 0.5°C
Between −20°C and −35°C	−34 ± 0.5°C then −51 ± 1°C
Below −35°C	−34 ± 0.5°C then −51 ± 1°C then −67 ± 2°C

ability to change down to the next lower set-point temperature in a time period not exceeding 2 min 30 s.

6.1.11 *Stopcock*, glass, with double oblique bore of 3-mm diameter.

6.1.12 *Vacuum Source*, vacuum pump or water pump powerful enough to ensure an air flow rate in the vacuum regulator of 15 ± 1 L/h for the duration of the test.

6.1.13 *Vacuum Regulator*, consisting of a glass bottle, at least 350-mm high, not less than 5 L capacity, partially filled with water. It shall be closed by a stopper with three holes of convenient diameters for glass tubes. Two tubes shall be short and shall not go below the water level. The third tube, with an internal diameter of 10 ± 1 mm, shall be long enough for one end to be approximately 200 mm beneath the surface of the water while the other end reaches a few centimetres above the stopper. The depth of the immersed part shall then be adjusted to obtain a depression of 200 ± 1 mm of water (2 ± 0.05 kPa) on the manometer, which shall contain water. A second empty 5 L bottle shall be fitted in the line to serve as a vacuum reservoir to ensure a constant depression. The arrangement is shown in Fig. 1.

6.1.14 *Stopwatch*, with a graduation or reading of 0.2 s or lower, with an accuracy of 0.1 % over a period of 10 min.

6.2 *Automated Apparatus*:

6.2.1 The automated apparatus shall include elements conforming to 6.1.1-6.1.8, platinum resistance thermometers, cooling bath(s), vacuum pump, and suitable electronic control and measurement devices.

6.2.2 *Cooling Bath*, a refrigeration unit capable of maintaining the cooling bath at the required temperature and also of automatically changing the bath temperature within 2 min 30 s at the appropriate stage (see 12.2.5).

6.2.3 *Vacuum Pump*, powerful enough to ensure an air flow rate in the vacuum regulator of a minimum of 15 ± 1 L/h, and to maintain a constant vacuum of 200 ± 1 mm (2 ± 0.05 kPa) for the duration of the test. For multi-position testers using the same vacuum pump, the flow rate shall be checked when several positions are operating simultaneously.

7. Reagents and Materials

7.1 *Heptane*, clean commercial or reagent grade. (**Warning**—Flammable. Harmful if inhaled.)

7.2 *Acetone*, clean commercial or reagent grade. (**Warning**—Extremely flammable.)

7.3 *Filter Paper*, (approximately 4 to 6 μm retention).

7.4 *Certified Reference Materials*.

8. Sampling

8.1 Unless otherwise specified in the commodity specification, samples shall be taken as described in Practice D 4057 or D 4177 in accordance with the requirements of national standards or regulation for the sampling of the product under test, or both.

9. Preparation of Test Specimen

9.1 Filter approximately 50 mL of the sample (see 8.1) at laboratory ambient temperature, but in any case not at a temperature less than 15°C, through dry filter paper (see 7.3).

10. Preparation of Apparatus

10.1 Prepare the manual apparatus or the automated apparatus for operation in accordance with the manufacturer's instructions for calibrating, checking, and operating the equipment. See Fig. 1 for manual apparatus.

10.2 Before each test, dismantle the filter unit (see 6.1.8.2) and wash the pieces and the test jar (see 6.1.2), the pipet (see 6.1.8.1) and the thermometer (see 6.1.9 for manual apparatus and 6.2 for platinum resistance used in automated equipment) with heptane (see 7.1), then rinse with acetone (see 7.2) and dry in a stream of filtered air. Check the cleanliness and dryness of all elements, including the jacket (see 6.1.3). Examine the wire mesh (see 6.1.8.2(*3*)) and the joints (see 6.1.8.2(*1*) and 6.1.8.2(*2*) for damage; if necessary renew them.

10.3 Check that the screw cap (see 6.1.8.2(*2*) is tight enough to prevent leakage.

11. Calibration and Standardization

11.1 Adjust the automated CFPP apparatus (when used) in accordance with the manufacturer's instructions.

11.2 Calibrate the temperature measuring device in accordance with the manufacturer's instructions.

11.3 Periodically verify the correct functioning of manual and automated apparatus using a certified reference material or in-house secondary reference material, such as fuel of known CFPP value.

NOTE 4—It is preferable that verification be carried out at least two times a year, where possible, using certified reference materials. The apparatus should be checked more frequently (for example, weekly) using a secondary verification material.

11.4 When the CFPP values obtained using a verification material deviate by more than the test repeatability (see 15.2), or an unacceptable statistical quality control bias is observed, check the condition and operation of the apparatus to ensure conformity with the specification as stated in this test method. The manufacturer's instruction manual should provide guidance on ensuring that the apparatus is correctly set up and calibrated.

12. Procedure

12.1 *Manual Apparatus*:

12.1.1 Establish the cooling bath temperature at –34 ± 0.5°C

12.1.2 Place the insulating ring (see 6.1.4) on the bottom of the jacket (see 6.1.3). If spacers (see 6.1.5) are not mounted on the insulating ring (see 6.1.4), position them approximately 15 and 75 mm above the bottom of the test jar (see 6.1.2).

12.1.3 Pour the filtered specimen (see Section 9) into the clean and dry test jar to the mark (45 mL).

12.1.4 Close the test jar with the stopper (see 6.1.7) carrying the pipet with filter unit (see 6.1.8) and the appropriate thermometer (see 6.1.9). Use a low-range thermometer if the expected CFPP is below –30°C. Thermometers shall not be changed during the test. Adjust the apparatus in such a way that the bottom of the filter unit (see 6.1.8.2(*5*)) rests on the bottom of the test jar, and position the thermometer so that its lower end is 1.5 ± 0.2 mm above the bottom of the test jar. Take care to ensure that no part of the thermometer is not in contact with the side of the test jar or the filter body.

NOTE 5—The precise positioning of the thermometer in the test jar is a critical parameter of this test method. The position of the lower end of the thermometer above the bottom of the test jar can be indirectly measured by marking the stem of the thermometer flush with the stopper (see 6.1.7) when the lower end of the thermometer is just touching the bottom of the test jar, and then pulling the thermometer up such that the reference line is 1.5 6 0.2 mm above the top of the stopper.

12.1.5 If the jacket is not an integral part of the cooling bath, place the jacket vertically to a depth of 85 6 2 mm in the cooling bath (see 6.1.10), which is maintained at the temperature of –34 6 0.5°C.

12.1.6 Insert the test jar assembly in a stable vertical position into the jacket.

12.1.7 With the stopcock (see 6.1.11) open to atmosphere, connect the pipet to the vacuum system (see 6.1.12 and 6.1.13) by means of flexible tubing attached to the stopcock (see Fig. 1). Switch on the vacuum source and regulate to ensure an air flow rate of 15 L/h in the vacuum regulator (see 6.1.13). Before starting a test, check that the U-tube manometer indicates a 200 6 1 mm of water depression (2 6 0.05 kPa).

12.1.8 Start the test immediately after inserting the test jar assembly into the jacket, but if the cloud point of the sample is known, it is permitted to wait until the specimen has cooled to a temperature of not less than 5°C above its cloud point.

12.1.9 When the specimen temperature reaches a suitable integer value, turn the stopcock (see 6.1.11) so that the filter assembly is connected to the vacuum source, causing the specimen to be drawn through the wire mesh into the pipet; simultaneously start the stopwatch.

12.1.10 When the specimen reaches the mark on the pipet, stop the stopwatch and turn the stopcock to its initial position to vent the pipet and so allow the specimen to return to the test jar.

12.1.11 If the time taken to reach the mark exceeds 60 s on the first filtration, abandon the test and repeat it on a fresh portion, starting at a higher temperature.

12.1.12 Repeat the operations (see 12.1.9 to 12.1.10) for each 1°C decrease of the specimen temperature until the temperature is reached at which the pipet is not filled to the 20 mL mark within 60 s. Record the temperature at which this last filtration was commenced as CFPP (see Section 13).

NOTE 6—A small minority of samples may exhibit anomalous aspiration behavior, which can be detected by examining the observed aspiration times. This behavior is marked by an unexpected reduction in the time taken to fill the pipet, after which aspiration time again continues to increase progressively, until the failure limit of 60 s is reached.

12.1.13 If the filter has not plugged when the temperature of the specimen reaches –20°C, continue the test by using a second cooling bath maintained at –51 6 1°C, quickly transferring the test jar and filtration assembly to a new jacket placed on the second cooling bath. Alternatively, for single bath apparatus, adjust the refrigeration unit to –51 6 1°C. The new temperature must be reached within 2 min 30 s of the adjustment. Repeat the operations 12.1.9 to 12.1.10 to each 1°C decrease of the specimen temperature.

12.1.14 If the filter has not plugged when the temperature of the specimen reaches –35°C, continue the test by using a third cooling bath maintained at –67 6 2°C by quickly transferring the test jar and filtration assembly to a new jacket placed on the second cooling bath. Alternatively, for single bath apparatus, adjust the refrigeration unit to –67 6 2°C. The new temperature must be reached within 2 min 30 s of the adjustment. Repeat the operations 12.1.9 to 12.1.10 at each 1°C decrease of the specimen temperature.

12.1.15 If the filter has not plugged when the temperature of the specimen reaches –51°C, discontinue the test (see Section 13).

12.1.16 If, after cooling in accordance with 12.1.12, 12.1.13, and 12.1.14, the specimen fills the pipet to the mark in less than 60 s, but does not flow back completely into the test jar when the pipet is vented to atmosphere through the stopcock (see 6.1.11) before the start of the next aspiration, record the temperature at the commencement of the filtration as the CFPP (see Section 13).

12.2 *Automated Apparatus*:

12.2.1 Check that the cooling bath is operating and has reached the temperature required as specified in the manufacturer's instructions.

12.2.2 Pour the filtered specimen (see Section 9) into the clean and dry test jar to the 45 mL mark.

12.2.3 Close the test jar with the stopper (see 6.1.7) carrying the pipet with filter unit (see 6.1.8) and the platinum resistance thermometer. Adjust the apparatus in such a way that the bottom of the filter unit (see 6.1.8.2(*5*)) rests on the bottom of the test jar, and position the thermometer so that its lower end is 1.5 6 0.2 mm above the bottom of the test jar. Take care to ensure that no part of the thermometer is in contact with the side of the test jar or the filter body.

NOTE 7—The precise positioning of the thermometer in the test jar is a critical parameter of this test method. The position of the lower end of the thermometer above the bottom of the test jar can be indirectly measured by marking the stem of the thermometer flush with the stopper (see 6.1.7) when the lower end of the thermometer is just touching the bottom of the test jar, and then pulling the thermometer up such that the reference line is 1.5 6 0.2 mm above the top of the stopper.

12.2.4 If necessary, reconnect the pipet to the vacuum system. Switch on the vacuum source and regulate to ensure an air flow rate of 15 L/h in the vacuum regulator. Check that the U-tube manometer (if used) indicates a 200 6 1 mm depression (2 6 0.05 kPa) or that the electronic vacuum regulator indicates a pressure of 2 6 0.05 kPa.

12.2.5 Press the start button immediately after insertion of the test jar assembly. If the cloud point is known, aspiration of the specimen through the filter may be set to start when it has cooled to a temperature not less than 5°C above the cloud point. The apparatus will carry out the test procedure filtering the specimen at each 1°C decrease if temperature and measuring the filtering time. If the time to reach the 20 mL mark exceeds 60 s on the first filtration, the test is to be abandoned and repeated on a fresh specimen starting at a higher temperature. The apparatus will record the first temperature at which the specimen fails to reach the 20 mL mark in less than 60 s or fails to flow back into the test jar when the vacuum is cut off as CFPP (see Section 13). The test will be discontinued if the specimen reaches −51°C without plugging (see Section 13). During the procedure, the apparatus will automatically change the cooling bath temperature as indicated below.

	Bath Temperature
Start of test	−34 ± 0.5°C
When (if) specimen reaches −20°C	−51 ± 1°C
When (if) specimen reaches −35°C	−67 ± 2°C

NOTE 8—A small minority of samples may exhibit anomalous aspiration behavior, which can be detected by examining the aspiration times recorded in the test printout for signs of an unexpected reduction in the time taken to fill the pipet, after which aspiration time again continues to increase progressively until the failure limit of 60 s is reached.

12.2.6 If the automated CFPP apparatus used does not incorporate a lower light sensor, it shall only be used if the test sequence is observed as in the manual procedure (see 12.1.16), so that any fuels not flowing back into the test jar as described are detected and reported accordingly.

13. Report

13.1 Report the temperature read or indicated at the beginning of the last filtration to the nearest 1°C (see 12.1.12, 12.1.16, and 12.2.5) as the CFPP.

13.2 If the specimen has reached −51°C without plugging (see 12.1.15 and 12.2.5) report as “Not plugged at −51°C.”

13.3 The report shall contain at least the following information:

13.3.1 The type and identification of the product under test;

13.3.2 A reference to this test method;

13.3.3 The sampling procedure used (see Section 8);

13.3.4 The result of the test (13.1 or 13.2);

13.3.5 Any deviation from the procedure described (see Note 6 and Note 8); and

13.3.6 the date of the test.

14. Precision and Bias

14.1 The precision of this procedure as determined by the statistical examination of the interlaboratory test results is as follows:

14.2 *Repeatability*—The difference between results obtained on the same day by the same operator with the same apparatus under constant operating conditions on identical test material, would in the long run, with normal and correct operation of the test method, exceed 1.76°C only in one case in twenty.

14.3 *Reproducibility*—The difference between two single and independent results obtained by different operators working in different laboratories on identical test material, would in the long run, in the normal and correct operation of the test method, exceed the values indicated by the formula:

$$0.102\ (25-X)°\mathrm{C}$$

where: X is the average of the two results being compared, only in one case in twenty.

NOTE 9—The interlaboratory test program used to determine the precision of this test method was carried out in 1988 by the IP. The program involved 46 laboratories and 5 samples, ranging in CFPP values from 0°C to −33°C. Extrapolations to measurements more than a few degrees outside this range are unsupported by the data. The raw data from the 1988 program was reanalyzed in 1997 using the ASTM D2PP program.[7] The report of the reevaluation is available from ASTM Headquarters.

14.4 *Bias*—The procedure in this test method has no bias because the value of CFPP can be defined only in terms of a test method.

14.5 *Relative Bias*—The current interlaboratory tests confirm that there is no relative bias between the manual and automated apparatuses. Both apparatuses are suitable for reference purposes.

15. Keywords

15.1 automated cold filter plugging point; cold filter plugging point (CFPP); diesel; domestic heating fuels; filterability; manual cold filter plugging point

---

[7] Supporting data have been filed at ASTM International Headquarters and may be obtained by requesting Research Report RR:D02-1452.

SUMMARY OF CHANGES

Subcommittee D02.07 has identified the location of selected changes to this standard since the last issue (D 6371–99) that may impact the use of this standard.

(1) Modified 7.3 to remove the reference to “lintless.”

APPENDIX 6

THE DETAILED TECHNICAL DRAWINGS AND PICTURES OF SUPERCRITICAL REACTOR, HATCH AND CLAMPS

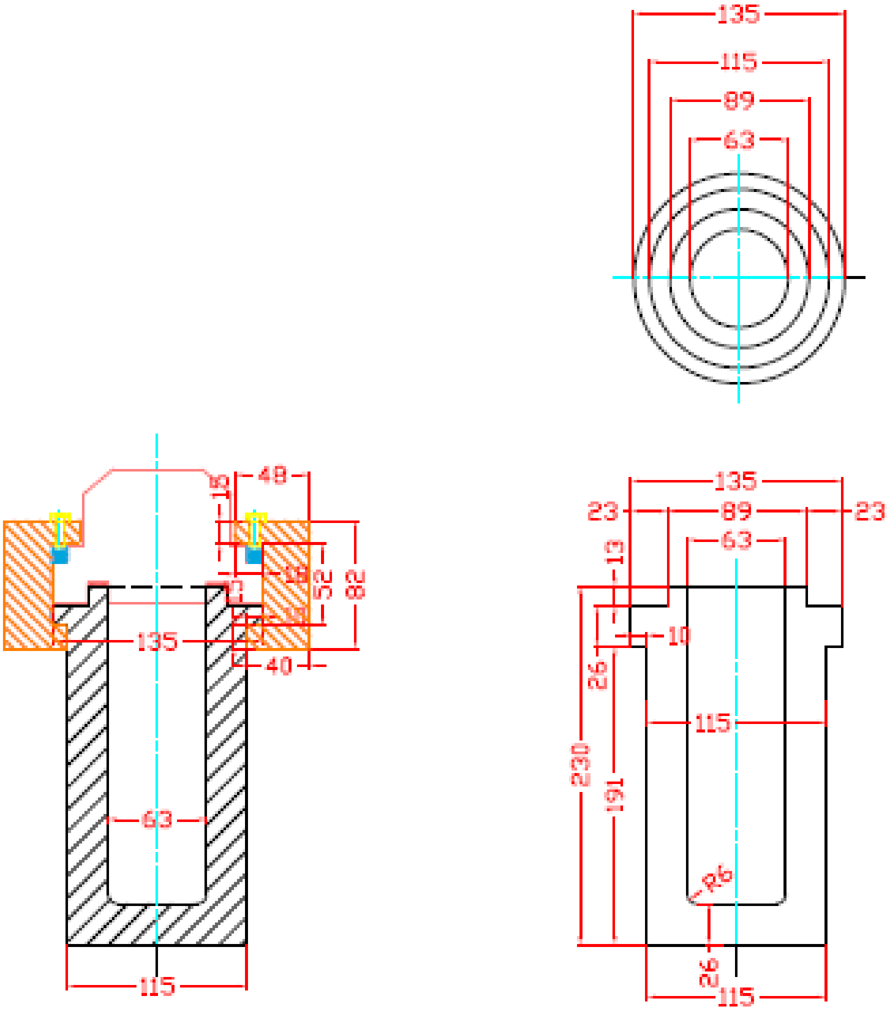

REAKTÖR KARIŞTIRICI

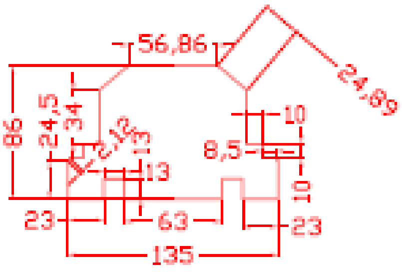

KAPAK ÖLÇÜLERİ

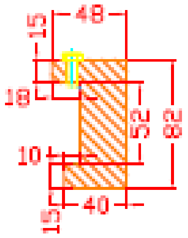

KELEPÇE ÖLÇÜLERİ

APPENDIX 7

PERFORMANCE AND SAFETY TESTS OF SUPERCRITICAL REACTOR DESIGNED

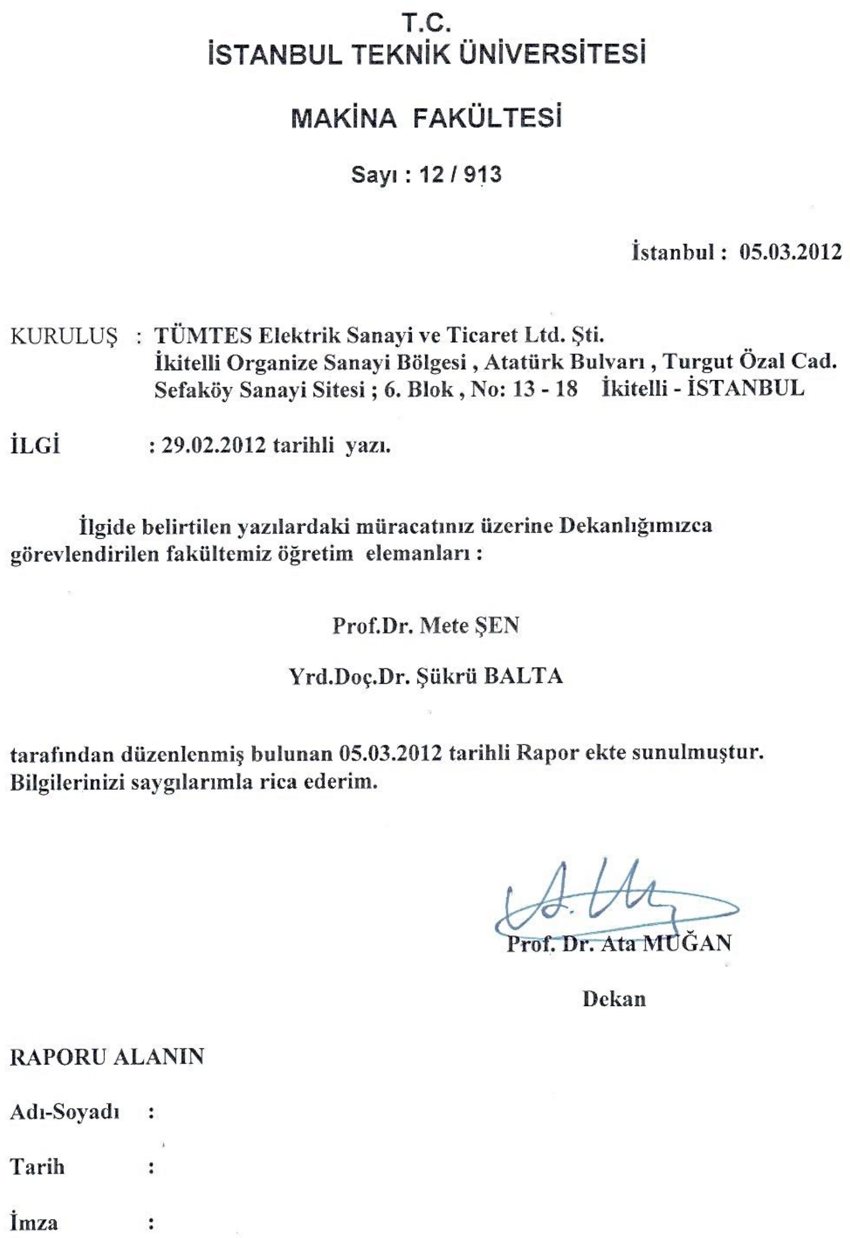

T.C.
İSTANBUL TEKNİK ÜNİVERSİTESİ

MAKİNA FAKÜLTESİ

Sayı : 12 / 913

İstanbul : 05.03.2012

KURULUŞ : **TÜMTES Elektrik Sanayi ve Ticaret Ltd. Şti.**
İkitelli Organize Sanayi Bölgesi , Atatürk Bulvarı , Turgut Özal Cad.
Sefaköy Sanayi Sitesi ; 6. Blok , No: 13 - 18 İkitelli - İSTANBUL

İLGİ : 29.02.2012 tarihli yazı.

İlgide belirtilen yazılardaki müracatınız üzerine Dekanlığımızca görevlendirilen fakültemiz öğretim elemanları :

Prof.Dr. Mete ŞEN

Yrd.Doç.Dr. Şükrü BALTA

tarafından düzenlenmiş bulunan 05.03.2012 tarihli Rapor ekte sunulmuştur. Bilgilerinizi saygılarımla rica ederim.

Prof. Dr. Ata MUĞAN

Dekan

RAPORU ALANIN

Adı-Soyadı :

Tarih :

İmza :

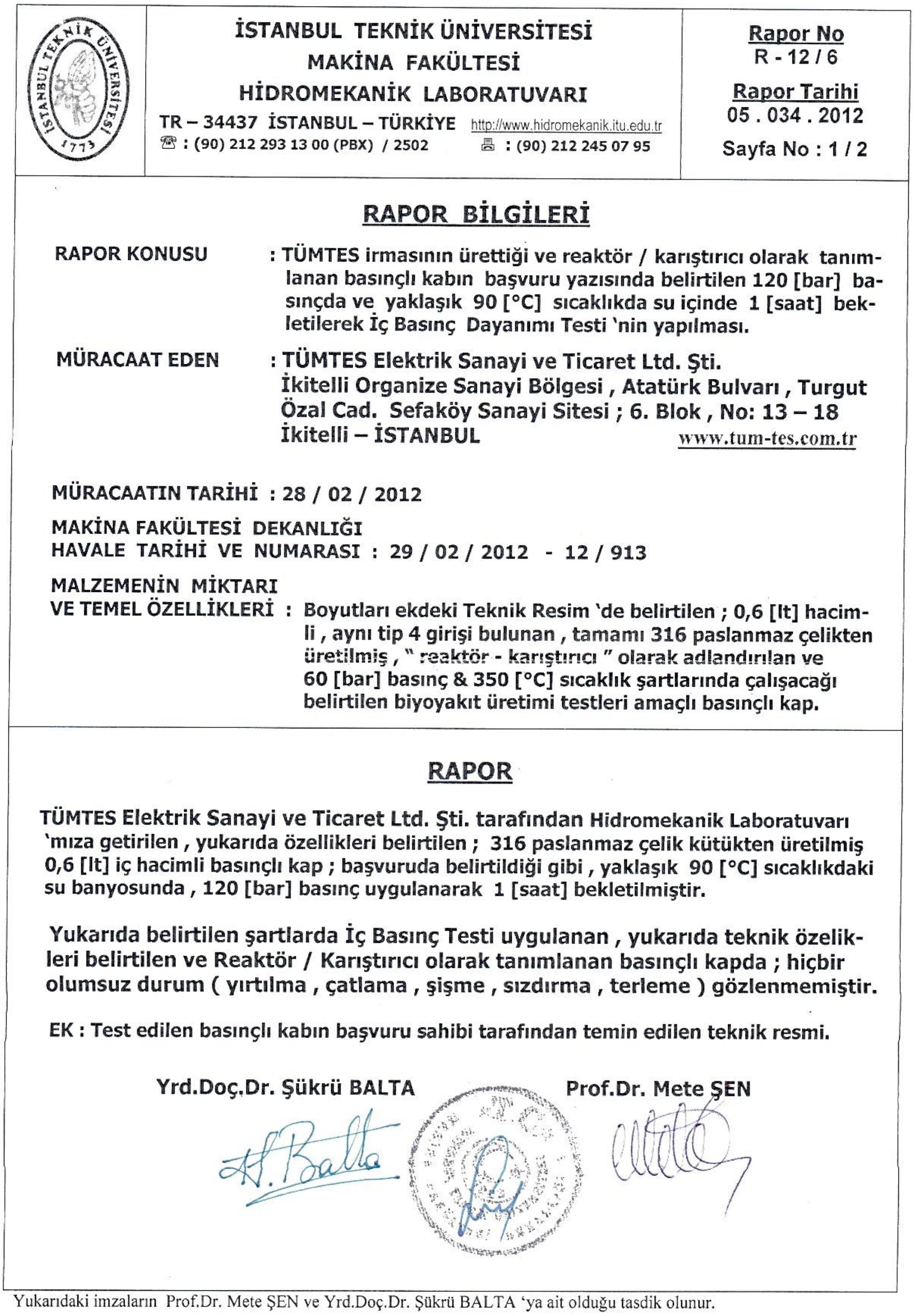

İSTANBUL TEKNİK ÜNİVERSİTESİ
MAKİNA FAKÜLTESİ
HİDROMEKANİK LABORATUVARI
TR – 34437 İSTANBUL – TÜRKİYE http://www.hidromekanik.itu.edu.tr
☎ : (90) 212 293 13 00 (PBX) / 2502 🖷 : (90) 212 245 07 95

Rapor No
R - 12 / 6
Rapor Tarihi
05 . 034 . 2012
Sayfa No : 1 / 2

RAPOR BİLGİLERİ

RAPOR KONUSU : TÜMTES irmasının ürettiği ve reaktör / karıştırıcı olarak tanımlanan basınçlı kabın başvuru yazısında belirtilen 120 [bar] basınçda ve yaklaşık 90 [°C] sıcaklıkda su içinde 1 [saat] bekletilerek İç Basınç Dayanımı Testi 'nin yapılması.

MÜRACAAT EDEN : TÜMTES Elektrik Sanayi ve Ticaret Ltd. Şti.
İkitelli Organize Sanayi Bölgesi , Atatürk Bulvarı , Turgut
Özal Cad. Sefaköy Sanayi Sitesi ; 6. Blok , No: 13 – 18
İkitelli – İSTANBUL www.tum-tes.com.tr

MÜRACAATIN TARİHİ : 28 / 02 / 2012

MAKİNA FAKÜLTESİ DEKANLIĞI
HAVALE TARİHİ VE NUMARASI : 29 / 02 / 2012 - 12 / 913

MALZEMENİN MİKTARI
VE TEMEL ÖZELLİKLERİ : Boyutları ekdeki Teknik Resim 'de belirtilen ; 0,6 [lt] hacimli , aynı tip 4 girişi bulunan , tamamı 316 paslanmaz çelikten üretilmiş , " reaktör - karıştırıcı " olarak adlandırılan ve 60 [bar] basınç & 350 [°C] sıcaklık şartlarında çalışacağı belirtilen biyoyakıt üretimi testleri amaçlı basınçlı kap.

RAPOR

TÜMTES Elektrik Sanayi ve Ticaret Ltd. Şti. tarafından Hidromekanik Laboratuvarı 'mıza getirilen , yukarıda özellikleri belirtilen ; 316 paslanmaz çelik kütükten üretilmiş 0,6 [lt] iç hacimli basınçlı kap ; başvuruda belirtildiği gibi , yaklaşık 90 [°C] sıcaklıkdaki su banyosunda , 120 [bar] basınç uygulanarak 1 [saat] bekletilmiştir.

Yukarıda belirtilen şartlarda İç Basınç Testi uygulanan , yukarıda teknik özelikleri belirtilen ve Reaktör / Karıştırıcı olarak tanımlanan basınçlı kapda ; hiçbir olumsuz durum (yırtılma , çatlama , şişme , sızdırma , terleme) gözlenmemiştir.

EK : Test edilen basınçlı kabın başvuru sahibi tarafından temin edilen teknik resmi.

Yrd.Doç.Dr. Şükrü BALTA **Prof.Dr. Mete ŞEN**

H. Balta

Yukarıdaki imzaların Prof.Dr. Mete ŞEN ve Yrd.Doç.Dr. Şükrü BALTA 'ya ait olduğu tasdik olunur.

EK : Test edilen Reaktör / Karıştırıcı 'nın Teknik Resmi.

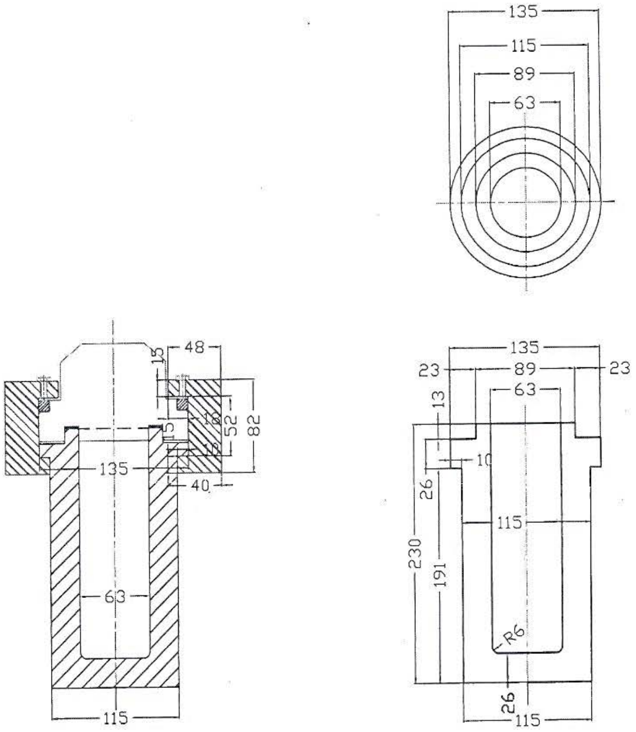

REAKTÖR KARIŞTIRICI

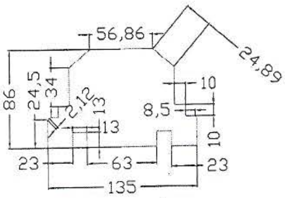

KAPAK ÖLÇÜLERİ

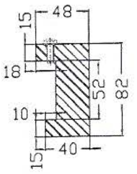

KELEPÇE ÖLÇÜLERİ

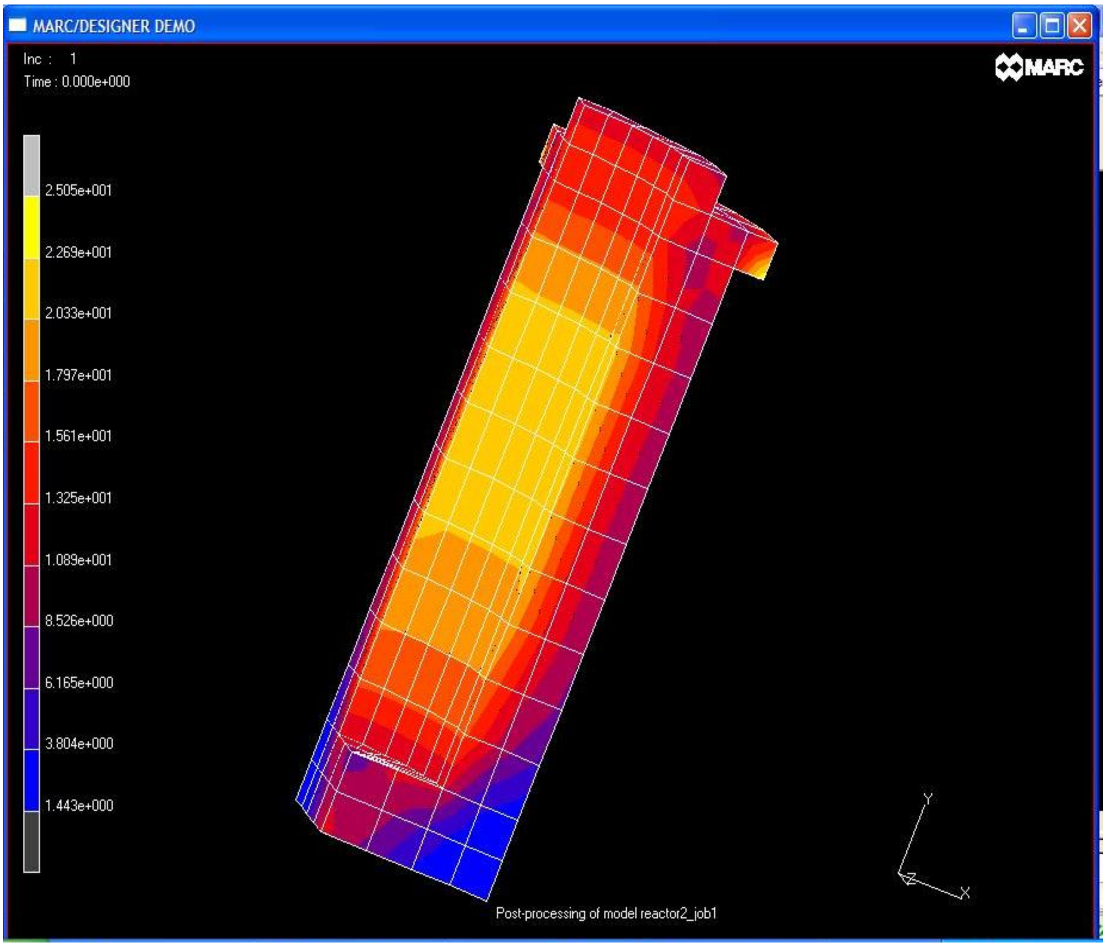
MARC/DESIGNER DEMO
Inc : 1
Time : 0.000e+000
MARC
2.505e+001
2.269e+001
2.033e+001
1.797e+001
1.561e+001
1.325e+001
1.089e+001
8.526e+000
6.165e+000
3.804e+000
1.443e+000
Y
Z
X
Post-processing of model reactor2_job1

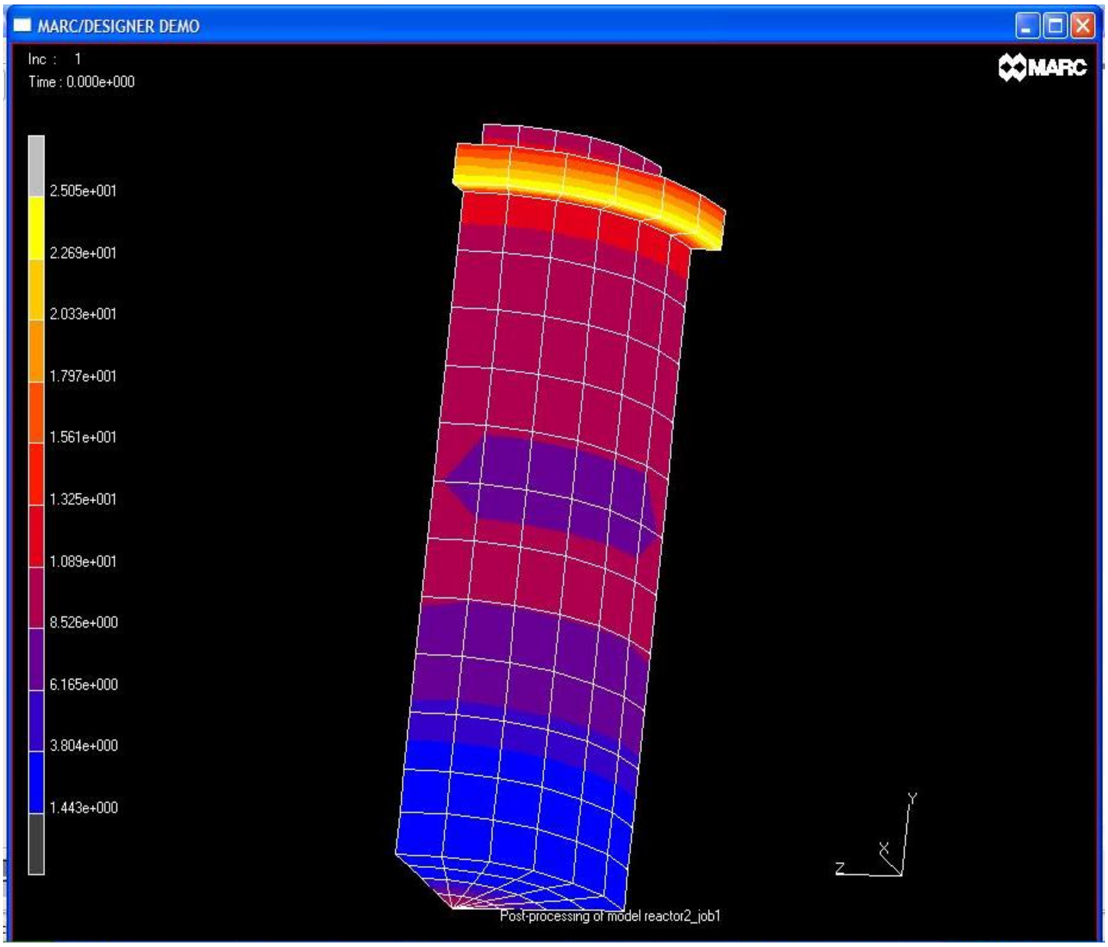
MARC/DESIGNER DEMO
Inc : 1
Time : 0.000e+000
MARC
2.505e+001
2.269e+001
2.033e+001
1.797e+001
1.561e+001
1.325e+001
1.089e+001
8.526e+000
6.165e+000
3.804e+000
1.443e+000
Y
X
Z
Post-processing of model reactor2_job1

APPENDIX 8

EXPERIMENTAL DATA SETS OF BIODIESEL FUEL SAMPLES TRACED FROM THE LITERATURE WITH THEIR FATTY ACID COMPOSITION AND CFP TEMPERATURES

Oil/ Fat	C 12:0	C 14:0	C 16:0	C 18:0	C 18:1	C 18:2	C 18:3	C 20:0	C 20:1	CP	PP	CFPP	References
Almond			10.4	2.9	77.1	7.6	0.8	0.3				-6	Ramos et al.. 2009
Animal fat	0	2.1	24	23.5	45.8	0	2.6	0	0				Da Silva et al.. 2010
Babassu	45.8	17.2	9.7	4	14.2	1.8				4		10	Sanford et al.. 2010
Beef tallow	0.2	2.4	24.4	19.1	41.7	5.9	0.7	0.4	0.5	14	10	12	Giakoumis. 2013
Beef tallow	0.2	2.9	24.3	22.8	40.2	3.3	0.7	0.2	0.6	16		14	Sanford et al. 2010
Borage			9.3	3.8	17.1	38.7	26.1			-1.3		-4	Sanford et al.. 2010
Camelina			5	2.2	17.7	18	37.9	1.4		1.5		-1	Sanford et al.. 2010
Camelina	0.4	2.7	6.1	2.8	16.8	17	35.6	1.4	14.4	3	-7	-3	Hoekman et al.. 2012
Canola			3.6	1.5	61.6	21.7	9.6		1.4	0	-9	-7	Dunn. 2010
Canola			4.5	2	60.7	21.2	9.5	0.6	1.5	-2	-8	-7	Giakoumis. 2013
Canola			4.2	2	60.4	21.2	9.6	0.7	1.5	-2	-6	-9	Hoekman et al.. 2012
Canola			3.8	1.9	63.9	19	9.7	0.6		-3.3		-13	Sanford et al. 2010
Castor			1.4	1.1	91.5	4.8	0.6	0.3	0.4	-15	-23	-1	Giakoumis. 2013
Castor			0.9	1.1	90.3	4	0.6			-13.4		7	Sanford et al. 2010
Castor			1.6	0.9	92.5	3.7		0.3					Da Silva et al.. 2010
Chichen	0.1	0.7	24.1	6.4	41.4	18.8	1.1	0.1	0.4	8	4	3	Giakoumis. 2013
Coconut	48.6	19.7	8.5	3	7.5	2	0.2	0.2	9.2	5	-3		Dunn. 2010
Coconut	47.7	18.5	9.1	2.7	6.8	2.1	0.1	0.1		-3	-9	-5	Hoekman et al.. 2012
Coconut	46.9	18.7	9.7	2.8	6.8	2.2		0.1		-1	-4	-4	Giakoumis. 2013
Coconut	49.2	18.5	9.1	2.7	6.5	1.7				0		-4	Sanford et al. 2010
Coconut	45.8	25.9	12.3	2.7	10.2	3.1							Da Silva et al.. 2010
Coffee			11	3.4	70	12.7	0.8	0.6		0		-4	Sanford et al. 2010
Corn			11.8	2.1	27.4	57.7	0.6	0.34	0.3	-3	-5	-5	Giakoumis. 2013
Corn			12.1	1.8	27.2	56.2	1.3	0.4		-2.8		-3	Sanford et al. 2010
Corn			11.5	1.9	26.6	58.7	0.6	0.3	0.1	-3	-2	-8	Hoekman et al.. 2012
Corn			6.5	1.4	65.6	25.2	0.1	0.1	0.1			-12	Ramos et al.. 2009
Cottonseed		0.7	25.9		1.7	16	55.1	0.16	0.22	1	0	5	Giakoumis. 2013
Cottonseed		0.8	24.7	2.7	18.5	53	0			6	0	3	Tang et al.. 2008
Croton		0.1	7.3	3.4	10.8	77.3	5.4		0.1	-4	-6	11	Giakoumis. 2013
Date seed	24	13	17.44	0.3	36.8	7	0			4	-1		Amani et al. 2013
Evening primrose			6	1.8	6.6	76.3	9	0.3		-7.5		-10	Sanford et al. 2010
Frying oil			12	5	25	52	6						Da Silva et al.. 2010
Grapeseed		0.1	6.9	4	19	69.1	0.3	0.3				-6	Ramos et al.. 2009

Hazelnut			6.3	3.7	79.4	10.8	0.2	0.1	0.1	-12	-14	-13	Giakoumis. 2013
Hazelnut			5.1	2.1	76.9	13.1	0.2	0.2	0.3	-9.3	-13	-12.7	Moser. 2012
Hemp			5.2	2.4	13.1	57.1	20	0.7		-1.3		-6	Sanford et al. 2010
Hepar. high IV	0.1	1.5	28	20.2	36.1	9.7	0.3	0.2		16		13	Sanford et al. 2010
Hepar. low IV	0.2	1	20.7	8.9	46.7	15.6	0.5	0.2		6.7		6	Sanford et al. 2010
High Oleic Sunflower			4.6	3.4	62.8	27.5	0.1	0.3				-6	Ramos et al.. 2009
Jatropa		0.2	14.4	5.8	42.8	35.4	0.2	0.1	0.1	6	-1	-1	Giakoumis. 2013
Jatropha			12.7	5.5	39.1	41.6	0.2	0.2		2.7		0	Sanford et al. 2010
Jatropha		0.1	14.5	7	39.5	37	0.2			4	3	2	Dunn. 2010
Jatropha			16	6.5	43.5	34.4	0.8			10	4		Sahoo and Das. 2009
Jatropha	0.1	0.3	14.9	6.1	40.4	36.2	0.3	0.2	0.1	5	0		Hoekman et al.. 2012
Karanja			11.7	7.5	51.6	16.5	2.7			15	5		Sahoo and Das. 2009
Karanja			10.9	7.9	53.6	21.3	2.1	1.8	1.2	8	3	-7	Giakoumis. 2013
Lard	0.3	1.6	25.1	13.2	44.4	12.1	1.2	0.2	0.9	15	11	9	Giakoumis. 2013
Lesquerella		0.1	0.9	1.7	13	5.8	10.6	0.7	66.5	-11.6		-6	Sanford et al. 2010
Linseed			5.2	3.3	19	16.1	54.5	0.1	0.1	-2	-8	-8	Giakoumis. 2013
Linseed			4.4	3.8	20.7	15.9	54.6	0.2		-3.8		-8	Sanford et al. 2010
Mahua		0.2	22.2	22.5	39	14.9	0.1	1		4	4		Giakoumis. 2013
Maringa			5.5	5.8	76.3	0.7		3.1		13.3		13	Sanford et a.. 2010
Mustard			2.6	1.2	20.6	20.6	13.3	0.9	10.7	3.2		-5	Sanford et al. 2010
Neem			14.9	20.6	43.9	17.9	0.4	1.6		14.4		11	Sanford et al. 2010
Neem	0.4	0.2	17.6	16.6	45.8	17.8	0.7	1.2		12	6		Giakoumis. 2013
Olive			10.5	2.6	76.9	7.5				-2	-3	-6	Dunn. 2010
Olive			11.6	3.1	75	7.8	0.6	0.3				-6	Ramos et al.. 2009
Olive		0.1	11.5	2.8	74.5	9.5	0.5	0.5	0.3	-2	-5	-5	Giakoumis. 2013
Palm	0.1	0.7	36.7	6.6	46.1	8.6	0.3	0.4	0.2			10	Ramos et al.. 2009
Palm	0.4	1.1	42.4	4.2	40.9	10	0.3	0.2	0.2	13	12	11	Giakoumis. 2013
Palm	0.2	0.5	43.4	4.6	41.9	8.6	0.3	0.3		13		12	Sanford et al. 2010
Palm	0.3	1.1	42.5	4.2	41.3	9.5	0.3	0.3	0.1	14	13	9	Hoekman et al.. 2012
Palm	0.2	1.1	44.1	4.4	39	10.6	0.3			16	15	12	Dunn. 2010
Palm	0.3	1.5	40	5	40	11	0.3	0.8					Da Silva et al.. 2010
Peanut		0.1	8	1.8	1.8	53.3	28.4	3.9	2.4			17	Ramos et al.. 2009
Peanut			10.3	2.8	47.6	31.5	0.6	1.1	1.5	4	-3	16	Giakoumis. 2013
Peanut			6.7	2.3	78.2	4.4		7.5	1.9	17.8	15	16	Moser.. 2012

Perilla			5.3	2.2	16.6	13.7	62.1			-8.5		-11	Sanford et al. 2010
Polanga			12	12.9	34.1	38.3	0.3			13	4		Sahoo and Das. 2009
Poultary fat	0.1	1	19.6	7.5	36.8	28.4	2	0.1		6		2	Sanford et al. 2010
Poultary fat		1.1	25.5	7.6	36.7	27	1.8			7	3	2	Tang et al.. 2008
Rapeseed			4.9	1.6	33	20.4	7.9		9.3			-10	Ramos et al.. 2009
Rapeseed			4.1	1.6	62.2	20.6	8.7	0.9	1.1	-3	-10	-9	Giakoumis. 2013
Rapeseed	0.1		4.2	1.6	59.5	21.5	8.4	0.4	2.1	-3	-10	-12	Hoekman et al.. 2012
Ricebran		0.3	12.5	2.1	47.5	35.4	1.1	0.6		0.3		-3	Sanford et al. 2010
Ricebran	0.1	0.5	18.1	2.2	42.4	34.8	0.9	0.5	0.2	5	-1	0	Giakoumis. 2013
Rubberseed		0.5	9.4	9.4	24.2	38.1	17.5	0.3	0.1	4	-7	-1	Giakoumis. 2013
Safflower		0.1	7.4	2.4	14.4	75.3	0.1			-5	-8	-8	Giakoumis. 2013
Safflower		0.1	8.2	2.5	14.2	74.3	0.1	0.1		-4	-7	-6	Hoekman et al.. 2012
Sesame			9.8	5.2	40.1	43.1	0.6	0.2		1	0		Satapimonphan 2012
Soy	0.1	0.1	11.6	3.9	23.7	53.8	5.9	0.3	0.3	0	-4	-4	Hoekman et al.. 2012
Soybean			8.5	4.9	22.7	51.2	6.5			0	-2	-2	Dunn. 2010
Soybean			11.3	3.6	24.9	53	6.1	0.3	0.3			-5	Ramos et al.. 2009
Soybean	0.1	0.1	11.4	4.2	23.5	53.5	6.6	0.3	0.2	0	-3	-4	Giakoumis. 2013
Soybean			14.1	5.2	25.3	48.7	6.1			3	-3	-3	Tang et al.. 2008
Soybean			9.4	4.1	22	55.3	8.9			0.9		-4	Sanford et al. 2010
Soybean			11	5.1	27	51.3	5.4						Da Silva et al.. 2010
Stillinga	0.4	0.1	7.5	2.3	16.7	31.5	41.5			-8.5		-12	Sanford et al. 2010
Sunflower			4.2	3.3	63.6	27.6	0.2			3.4		-3	Sanford et al. 2010
Sunflower			6.3	3.9	67.8	20.8	0.2	0.2	0.1	1	-4	-3	Giakoumis. 2013
Sunflower	0.1	0.1	6.4	3.6	21.7	66.3	1.5	0.3	0.2	2	-2	-2	Hoekman et al.. 2012
Sunflower			6.2	3.7	25.2	63.1	0.2	0.3	0.2			-3	Ramos et al.. 2009
Tallow		3.4	29.5	26	34.9	1.5				17	15	9	Dunn. 2010
Tallow	0.2	2.6	24.3	18.2	42.2	4.4	0.9	0.2	0.6	13	10	13	Hoekman et al.. 2012
Tobacco		0.14	8.2	3.6	12.1	73	0.8	0.2	0.1			-5	Usta et al.. 2011
Tung			1.8	2.1	5.3	6.8	72.2			-10		-11	Sanford et al. 2010
Used cooking oil	0.1	0.1	11.8	4.4	25.3	49.5	7.1	0.3		2.4		2	Sanford et al. 2010
Walnut			7.2	2.6	15.1	60.7	12.8		0.2	-6.1	-10	-9	Moser.. 2012
Waste Cooking	0.2	0.7	15.9	6.2	42.8	29.4	2	0.4	0.6	5	0	-3	Giakoumis. 2013
White Grease		1.3	21.6	9	50.4	12.2	1.2	0.2		7		6	Sanford et al. 2010
Yellow grease	0.1	0.5	14.3	8	35.6	35	4	0.3		6		2	Sanford et al. 2010
Yellow grease	0.2	0.8	16.5	7.1	44.6	25.1	1.1	0.3	0.5	8	3	1	Hoekman et al.. 2012

APPENDIX 9

PREDICTED AND CALCULATED CFP TEMPERATURES OF REFENCE DATA SETS

APPENDIX 9- A: Predicted and calculated CP temperatures of refence data sets

Oil/ Fat	CP_{EXP}	CP_{MLR}	CP_{ANN}
Babassu	4	1.5	3.7402
Beef tallow	14	15.5	14.121
Beef tallow	16	16.9	15.6919
Borage	-1.3	-1.8	-1.7291
Camelina	3	-0.5	2.998
Camelina	1.5	1.5	1.1223
Canola	-2	-2.9	-2.2602
Canola	-2	-3.1	-2.4282
Canola	-3.3	-3.1	-3.6267
Chichen	8	7.9	8.7689
Coconut	-1	2.8	-1.5353
Coconut	0	1.6	0.7297
Coffee	0	1.2	1.001
Corn	-3	-0.5	-2.9932
Corn	-3	-0.2	-2.7203
Corn	-2.8	0.1	-2.5349
Cottonseed	1	1.7	1.1776
Cottonseed	6	5.0	5.3452
Croton	-4	-3.5	-3.715
Date seed	4	3.1	3.4152
Evening primrose	-7.5	-3.3	-6.722
Hazelnut	-9.3	-3.0	-8.7782
Hemp	-1.3	-2.4	-1.6645
Hepar. high IV	16	16.4	15.5678
Hepar. low IV	6.7	8.0	7.4269
Jatropa	6	2.3	5.4089
Jatropha	5	3.0	4.01
Jatropha	4	2.7	3.9148
Jatropha	2.7	1.6	2.2593
Karanja	8	6.7	8.4785
Lard	15	11.2	14.9736
Lesquerella	-11.6	-10.4	-11.0399
Linseed	-2	-5.5	-3.2488
Linseed	-3.8	-5.6	-4.0598
Mustard	3.2	1.0	3.4991
Neem	12	11.9	12.9381
Neem	14.4	14.1	15.0621
Olive	-2	-1.0	-1.674
Olive	-2	0.6	-1.827
Palm	14	14.2	13.5872
Palm	16	14.0	15.5724
Palm	13	13.8	13.4095
Palm	13	14.4	13.8738

Peanut	4	2.5	3.9514
Peanut	17.8	19.0	16.9975
Perilla	-8.5	-7.0	-8.2902
Poultary fat	7	7.7	7.5307
Poultary fat	6	6.2	6.4831
Rapeseed	-3	-3.6	-4.1807
Rapeseed	-3	-2.3	-2.9847
Ricebran	5	3.2	4.1769
Ricebran	0.3	1.1	0.5859
Rubberseed	4	1.7	3.9473
Safflower	-4	-2.1	-3.9583
Safflower	-5	-2.8	-4.7446
Sesame	1	0.3	0.8564
Soy	0	0.3	0.4757
Soybean	0	-0.4	-0.7034
Soybean	0	0.3	0.6035
Soybean	3	1.1	2.8725
Soybean	0.9	-1.6	0
Stillinga	-8.5	-5.0	-8.144
Sunflower	2	-1.9	2
Sunflower	1	-1.9	1.1147
Tallow	13	14.8	14.0481
Tallow	17	20.4	16.8178
Tung	-10	-6.9	-7.9715
Used cooking oil	2.4	0.8	2.0812
Walnut	-6.1	-3.3	-6.4796
Waste Cooking	5	4.2	5.2994
White Grease	7	8.2	7.7465
Yellow grease	8	5.1	7.2305
Yellow grease	6	4.1	5.6867
WFOME	**15**	**11.4**	**13.5488**
RFOME	**15**	**10.5**	**14.9254**
RCOME	**-3.5**	**-3.1**	**-3.5671**
WCOME	**-2**	**-1.9**	**-1.7005**

APPENDIX 9-B: Predicted and calculated PP temperatures of refence data sets

Oil/ Fat	PP_{EXP}	PP_{MLR}	PP_{ANN}
Beef tallow	10	10.6	10.3132
Camelina	-7	-3.9	-6.8031
Canola	-6	-8.7	-6.5312
Canola	-9	-11.4	-9.9302
Canola	-8	-9.0	-8.6367
Castor	-23	-12.9	-21.987
Chichen	4	5.6	4.2318
Coconut	-9	-4.0	-8.7765
Coconut	-3	-7.2	-3.8732
Coconut	-4	-3.5	-4.3292
Corn	-2	-3.2	-2.8227
Corn	-5	-3.1	-4.4157
Cottonseed	0	0.1	1.257
Cottonseed	0	3.9	0.912
Croton	-6	-6.8	-6.205
Date seed	-1	-3.3	-1.5663
Hazelnut	-14	-9.4	-14.9787
Hazelnut	-13	-9.3	-12.522
Jatropa	-1	-1.6	-0.4577
Jatropha	0	-0.7	0.4538
Jatropha	3	-1.1	3.2002
Jatropha	4	-1.6	3.5237
Karanja	3	1.7	2.6508
Karanja	5	-1.0	4.3217
Lard	11	7.0	10.7018
Linseed	-8	-10.9	-9.6163
Mahua	4	11.1	5.9908
Neem	6	6.6	7.4236
Olive	-3	-6.7	-4.5627
Olive	-5	-5.1	-4.3771
Palm	13	13.8	12.4919
Palm	15	13.9	14.603
Palm	12	13.4	11.4031
Peanut	-3	-1.1	-1.921
Peanut	15	13.3	14.04
Polanga	4	0.1	3.005
Poultary fat	3	4.8	4.7525
Rapeseed	-10	-9.1	-10.1824
Rapeseed	-10	-8.2	-9.2811
Ricebran	-1	0.2	1.0803

Rubberseed	-7	-3.1	-6.2591
Safflower	-7	-4.6	-6.0166
Safflower	-8	-5.5	-6.97
Sesame	0	-3.9	-0.8179
Soy	-4	-2.8	-3.8725
Soybean	-2	-3.4	-1.9173
Soybean	-3	-2.9	-2.9252
Soybean	-3	-2.0	-2.2185
Sunflower	-2	-5.4	-2.5268
Sunflower	-4	-8.0	-5.0858
Tallow	10	10.1	9.9165
Tallow	15	15.0	14.0814
Walnut	-10	-6.4	-9.8745
Waste Cooking	0	0.4	-0.5779
Yellow grease	3	1.2	2.359
WFOME	**12**	**11.1**	**11.1287**
RFOME	**11**	**10.1**	**9.3338**
RCOME	**-10**	**-8.5**	**-9.5411**
WCOME	**-9**	**-7.1**	**-7.7885**

APPENDIX 9-C: Predicted and calculated CFPP temperatures of refence data sets

Oil/ Fat	$CFPP_{EXP}$	$CFPP_{MLR}$	$CFPP_{ANN}$
Almond	-6	-5.1	-5.585
Beef tallow	12	11.5	12.0878
Beef tallow	14	12.5	13.8105
Borage	-4	-4.5	-4.5222
Camelina	-3	-1.5	-2.4351
Camelina	-1	-2.8	-1.1158
Canola	-7	-7.4	-7.2511
Canola	-7	-4.8	-6.5705
Chichen	3	4.4	3.1236
Coffee	-4	-1.0	-3.6972
Corn	-5	-1.9	-4.531
Corn	-3	-1.8	-3.2503
Cottonseed	5	0.4	4.9836
Cottonseed	3	2.8	2.3977
Evening primrose	-10	-4.9	-9.4996
Grapeseed	-6	-3.2	-5.4205
Hemp	-6	-4.2	-5.357
Hepar. high IV	13	12.8	13.1863
Hepar. low IV	6	4.5	5.8767
High Oleic Sunflower	-6	-4.7	-6.7668
Jatropa	-1	0.0	-0.7413
Jatropha	2	0.2	-1.1803
Jatropha	0	-0.6	-0.1414
Lard	9	8.4	8.4675
Lesquerella	-6	-6.0	-6.8487
Linseed	-8	-7.4	-7.4917
Mustard	-5	-5.0	-4.4633
Neem	11	12.0	11.2785
Olive	-6	-3.7	-6.4958
Olive	-5	-1.4	-4.4322
Olive	-6	-2.0	-5.9406
Palm	9	12.1	10.3646
Palm	12	11.8	11.3088
Palm	11	11.7	10.8069
Palm	12	12.5	11.9958
Palm	10	10.9	11.0247
Peanut	16	20.3	15.8169
Peanut	17	7.4	16.6559
Perilla	-11	-8.5	-10.1569
Poultary fat	2	5.3	2.3803
Poultary fat	2	3.0	2.4049
Rapeseed	-9	-4.1	-8.9857
Rapeseed	-10	-6.7	-9.9284
Ricebran	0	1.3	-0.538
Ricebran	-3	-0.8	-2.9099
Rubberseed	-1	-0.5	-0.4128
Safflower	-6	-4.0	-5.2071

Safflower	-8	-4.7	-7.8788
Soy	-4	-1.5	-3.8963
Soybean	-2	-3.5	-2.4169
Soybean	-4	-1.5	-3.8202
Soybean	-3	-1.0	-3.4133
Soybean	-4	-3.6	-4.6981
Soybean	-5	-1.8	-4.9987
Sunflower	-2	-3.7	-2.1562
Sunflower	-3	-4.2	-3.5164
Sunflower	-3	-6.0	-3.629
Sunflower	-3	-3.7	-4.0288
Tallow	13	10.4	12.1345
Tallow	9	15.6	9.5117
Tobacco	-5	-3.2	-5.1685
Tung	-11	-10.4	-10.587
Used cooking oil	2	-1.3	-2.5225
Walnut	-9	-5.3	-8.9626
Waste Cooking	-3	1.8	-2.2261
White Grease	6	4.9	5.7253
Yellow grease	1	2.2	0.6951
Yellow grease	2	1.5	1.7632
WFOME	**14**	**9.6**	**10.9388**
RFOME	**13**	**8.9**	**11.1207**
RCOME	**-7.5**	**-4.9**	**-6.7885**
WCOME	**-7**	**-4.2**	**-7.2217**

APPENDIX 10

CURRICULUM VITAE

CURRICULUM VITAE

PERSONAL INFORMATION

Surname, Name	: Al Shanableh, Filiz
Nationality	: Turkish, Cypriot
Date and Place of Birth	: 31 August 1965, Ordu
Marital Status	: Married
Phone	: +90 392 223 64 64 (ext.243)
Fax	: +90 392 223 66 24
E-mail	: filiz.shanableh@neu.edu.tr

EDUCATION

Degree	Institution	Year of Graduation
BSc	Middle East Technical University – Turkey Department of Chemical Engineering	1992
MA	Near East University– TRNC Department of International Relations	1996
MSc	NEU, Department of Electrical and Electronic Engineering	2005
PhD	NEU, Department of Mechanical Engineering	2017

WORK EXPERIENCE

Year	Place	Enrollment
Oct, 1992-present	Member of the Teaching Staff Faculty of Engineering	Senior Lecturer

PUBLICATIONS IN INTERNATIONAL REFEREED JOURNALS (IN COVERAGE OF SSCI/SCI-EXPANDED AND AHCI):

- Evcil, A., Al-Shanableh, F., Savaş, M. A. (2018) Variation of solid fraction with cold flow properties of biodiesel produced from waste frying oil. Fuel, Vol. 215C, pp 522-527.

PUBLICATIONS IN INTERNATIONAL REFEREED JOURNALS (IN COVERAGE OF British Education Index, ERIC, Science Direct, Scopus, IEEE):

- Al-Shanableh, F., Evcil, A., Savaş, M.A. (2017). Fuzzy logic model for prediction of cold filter plugging point of biodiesel from various feedstock. *Procedia Computer Science*, 120: 245-252.

- Al-Shanableh, F., Evcil, A., Savaş, M.A. (2016). Prediction of Cold Flow Properties of Biodiesel Fuel Using Artificial Neural Network. *Procedia Computer* Science, 102: 273-280. doi:10.1016/j.procs.2016.09.401.

BULLETING PRESENTED IN INTERNATIONAL ACADEMIC MEETINGS AND PUBLISHED IN PROCEEDINGS BOOKS:

- Al-Shanableh, F., Evcil, A., Savaş, M.A. (2017). Fuzzy logic model for prediction of cold filter plugging point of biodiesel from various feedstock . *9th International Conference on Theory and Application of Soft Computing, Computing with Words and Perception, ICSCCW 2017,* 24-25 August 2017, Budapest, Hungary.

- Al-Shanableh, F., Evcil, A., Savaş, M.A. (2016). Prediction of Cold Flow Properties of Biodiesel Fuel Using Artificial Neural Network. *12th International Conference on Application of Fuzzy Systems and Soft Computing, ICAFS 2016,* 29-30 August 2016, Vienna, Austria.

- F. Al-Shanableh, A. Evcil, C. Gövsa, M. A. Savaş, "A Comparative Examination of Cold Flow Properties and Acidity of Biodiesel Produced from Virgin and Waste Canola Oil*", International Conference on Energy Research and Development (ICERD5)*, Kuwait, April 5, 2012.

- AlShanableh Filiz, Evcil Ali, Gövsa Cemal, Savas Mahmut A., "A Comparison of Cold Flow Properties of Biodiesel Produced from Virgin and Used Frying Oil", *6th International Green Energy Conference (IGEC-6)*, Eskişehir, Turkey, June 5-9, 2011.

- Evcil Ali, AlShanableh Filiz, Govsa Cemal, Savas Mahmut A., "Biodiesel Production from Waste Frying Oil and Determination of Its Cold Flow Properties", *International Conference on Energy and Automotive Technologies (ICAT'10)*, Istanbul, Turkey, November 5, 2010.

BULLETING PRESENTED IN NATIONAL ACADEMIC MEETINGS AND PUBLISHED IN PROCEEDINGS BOOKS:

- Ali EVCIL, Filiz ALSHANABLEH, Cemal GÖVSA, Mahmut A. SAVAS, *Atık Kızartma Yağından Biyodizel Üretimi ve Soğuk Akış Özelliklerinin KKTC İklim Koşullarına Uyarlanması*, YEKSEM 2013: Yenilenebilir Enerji Kaynakları Sempozyumu, 4-6 Ekim 2013, Girne, KKTC, http://yeksem2013.org.

- Ali Evcil, Filiz Alshableh, Cemal Gövsa, Mahmut A. Savaş,"*Taze ve Atık Kanola Yağlarından Biyodizel Üretimi ve Soğuk Akış Özelliklerinin KKTC Koşulları*

Açısından Değerlendirilmesi", 9. Ulusal Temiz Enerji Sempozyumu, 25-28 Aralık 2013, Selçuk Üniversitesi, Konya, Bildiriler Kitabı, s. 1-11

BOOKS-

COURSES GIVEN *(from 2010 to 2017)*

Master	***Undergraduate***
Biofuels	Engineering Materials
	Thermodynamics I
	Thermodynamics II
	Biofuels
	Mass Transfer
	Electrical Materials
	Unit Operations for Food Eng. III
	Material and Energy Balances for Food Eng.
	General Chemistry

UNDERTAKEN PROJECTS

- 2010-2012- Project Member- This research is supported by the Near East University Research Fund under the project no: YDÜ 2010-2-21. Production of biodiesel from waste frying oil and characterization of its cold flow properties. TR / TRNC Scientific Research Project –December, 2010- January, 2012

CONFERENCE ORGANIZATION-

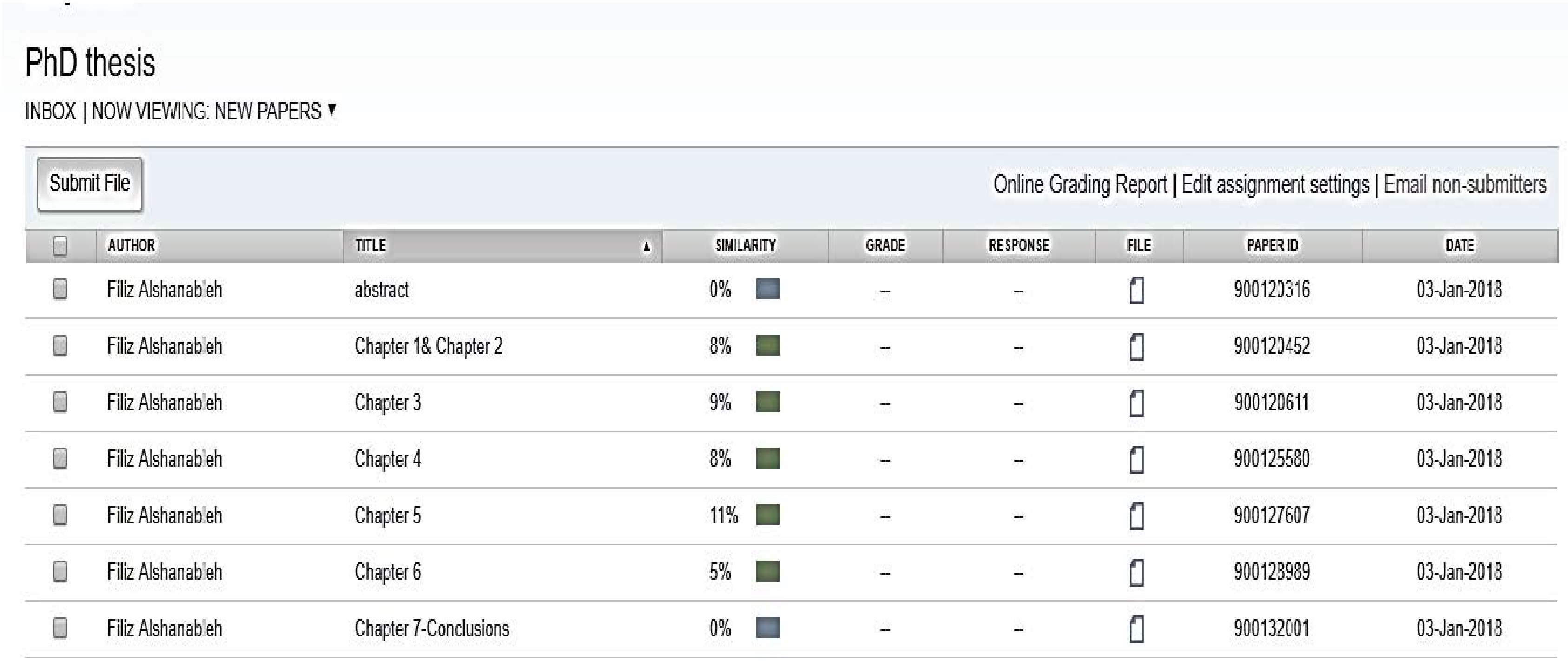

PhD thesis

INBOX | NOW VIEWING: NEW PAPERS ▾

☐	AUTHOR	TITLE ▲	SIMILARITY	GRADE	RESPONSE	FILE	PAPER ID	DATE
☐	Filiz Alshanableh	abstract	0% 🟦	–	–	🗋	900120316	03-Jan-2018
☐	Filiz Alshanableh	Chapter 1& Chapter 2	8% 🟩	–	–	🗋	900120452	03-Jan-2018
☐	Filiz Alshanableh	Chapter 3	9% 🟩	–	–	🗋	900120611	03-Jan-2018
☐	Filiz Alshanableh	Chapter 4	8% 🟩	–	–	🗋	900125580	03-Jan-2018
☐	Filiz Alshanableh	Chapter 5	11% 🟩	–	–	🗋	900127607	03-Jan-2018
☐	Filiz Alshanableh	Chapter 6	5% 🟩	–	–	🗋	900128989	03-Jan-2018
☐	Filiz Alshanableh	Chapter 7-Conclusions	0% 🟦	–	–	🗋	900132001	03-Jan-2018